Universitat de Lleida

Phenological adaptation and its genetic mechanisms in barley (Hordeum vulgare L.)

Arantxa Monteagudo Gálvez
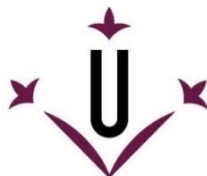
http://hdl.handle.net/10803/669235

Universitat de Lleida

TESI DOCTORAL

Phenological adaptation and its genetic mechanisms in barley (*Hordeum vulgare* L.)

Arantxa Monteagudo Gálvez

Memòria presentada per optar al grau de Doctor per la Universitat de Lleida
Programa de Doctorat en Ciencia y Tecnología Agraria y Agroalimentaria

This work has been done at Estación Experimental de Aula Dei (EEAD), belonging to Consejo Superior de Investigaciones Científicas (CSIC), in Zaragoza

Directores:
Dr. Ernesto Igartua Arregui
Dra. Ana María Casas Cendoya

Tutor:
Dr. Ignacio Romagosa Clariana

Agradecimientos / Acknowledgements

Quiero dar las gracias a mis directores de tesis, Dr. Ernesto Igartua y Dra. Ana Casas. Estaré siempre agradecida por esta oportunidad y por todo lo que he aprendido, no sólo sobre ciencia. A mi tutor en la Universidad, Dr. Ignacio Romagosa, que me ha asistido pacientemente en tantas ocasiones con los trámites de la universidad, y siempre tiene la solución.

To Dr. Ildikó Karsai and Dr. Ben Trevaskis, for letting me to learn and experience science from a wide perspective. Al Dr. Bruno Contreras, por su infinita paciencia. Al Dr. Javier Ramos, por transmitirme que la historia siempre es importante. A la Dra. Pilar Gracia, por hacerme un huequito en su despacho.

A mis compañeros Asun, Blanca, Javier, Julia, Manasés, Pili, Tere, Toni y Vanesa, porque la experiencia de la cosecha sabe mejor con un café de Tere y torto de Peñaflor.

To my Friends in Hungary (Mariann, Anna, Jutus, Tibor, Szilvi) and in Australia (Kerrie, Jose, María, Aitana, Sol, Jess, Brett). For opening my eyes to these wonderful countries and let me learn from the best teams. Hope to see you soon!

A Isabel, Francisco y Pierre por escucharme, por hacerlo todo mucho más fácil, y porque en las comidas se soluciona todo.

Al Dr. Carlos P. Cantalapiedra por enseñarme y por hacer que la sala de becarios de Genética nunca fuera aburrida. A las futuras Dras. Miriam Fernández y Alejandra Cabeza por permitirme enseñarles y por contagiarme su positivismo. A Álvaro Rodríguez, Chesco Montardit y Najla Ksouri por sus consejos, asistencias técnicas y correcciones, por las que os debo mucho. Quiero ser como vosotros.

En estos cuatro años han pasado muchas cosas, he aprendido muchísimo y me ha dado tiempo para perderme a mí misma. Las dudas, los triunfos, las derrotas, … un torbellino de emociones constante. Y en ese tiempo, a veces oscuro, las personas más cercanas te sorprenden de maneras insospechadas. Por todo ese apoyo, nadie se merece más tu dedicación y amor que las personas que siempre te han querido. Gran parte de este logro os pertenece. A mi Pilar, por protegerme con sus Santos cada vez que salía de casa. A la familia Nieto-Soria porque con ellos siempre se

aprende y por su infinita comprensión. Mi agradecimiento y reconocimiento a Raquel Serrano por el diseño de la portada. A Ana, Isa, Roberto y Mario, porque son un ejemplo y por esas conversaciones de salvar el mundo desde la cocina. A Jorge, Paula y Ainara, porque el tiempo de juegos no es opcional. A mi madre, por ser mi guía. A mi padre, por su coraje y por transmitirme su pasión por la agricultura. Y especialmente a Fran, por su paciencia e incondicionalidad, día sí y día también ...

A todos ellos ...

Gracias

A Fran, Varis, Lucía y Pilar,

mis grandes pilares

Resumen

Tanto en la comunidad científica como entre mejoradores de variedades existe una creciente preocupación sobre cómo influirá el cambio climático en la duración de los ciclos de los cultivos y sobre sus fechas de floración, debido a sus implicaciones en el rendimiento. En la región mediterránea, la cebada es un cereal de importancia que tiene además potencial adaptativo a una gran cantidad de ambientes. En este cultivo, las señales de temperatura y luz controlan la floración, mediante la interacción de los genes de vernalización (*HvVRN1*, *HvVRN2* y *HvFT1*) y fotoperiodo (*PPD-H1* y *HvFT3*).

El objetivo principal de la tesis ha sido profundizar en el control genético de la floración en cebada, tratando de descifrar cómo afectan la temperatura y diferentes parámetros de la luz, como el fotoperiodo y la calidad del espectro lumínico, a la fenología y a la respuesta de los genes de floración. Se han realizado estudios para: i) determinar el umbral de longitud de día que marca el momento para la inducción de la expresión de *HvVRN2*; ii) caracterizar el papel de otros posibles inductores y represores de floración en condiciones no inductivas de invierno; iii) entender cómo es la respuesta inmediata a cambios en el fotoperiodo, y si la variación natural en la sensibilidad al fotoperiodo (marcada por diferentes alelos de *PPD-H1*) afecta al reloj circadiano; iv) estudiar la influencia de la calidad de luz en el desarrollo y en la expresión de genes de floración y del genoma de cebada.

El uso de diferentes fechas de siembra en condiciones de fotoperiodo natural y creciente permitió concluir que *HvVRN2* se expresa siempre en ausencia de vernalización y su expresión aumenta notablemente a partir de días con 12 h 30 min de luz. La expresión de *HvFT3* necesita de una cierta acumulación de frío, es dependiente de la edad, y su expresión está asociada con floraciones más tempranas. Además, se ha aportado evidencia de variantes genéticas que retrasan el desarrollo, como las encontradas en la secuencia del represor de floración y posible actor en el proceso de vernalización, *HvOS2*.

Para estudiar la respuesta a los cambios de longitud de día, se evaluó la expresión de genes del reloj y de floración a lo largo de 3 días desde la transición entre fotoperiodos. Se observó una respuesta rápida y estable en los genes del reloj que, en algunos de ellos, estuvo condicionada por la variante de *PPD-H1*, como la rapidez de respuesta de *HvTOC1*. También el ritmo de la expresión de los genes de floración estuvo sujeto a la variación en *PPD-H1*.

Finalmente, se realizó un estudio exhaustivo del desarrollo de cebada en diferentes condiciones de calidad de luz. Las mayores diferencias se debieron a un retraso promovido por bombillas de tipo fluorescente, especialmente en las fases de aparición de primer nudo y el tiempo hasta el comienzo de la elongación del tallo.

Sin embargo, no todas las variedades respondieron igual, y se clasificaron en sensibles e insensibles a la calidad de luz. El análisis de RNA-seq reveló diferencias en la expresión de tres genotipos con diferente sensibilidad, sugiriendo que la mayor diversidad podría residir en factores de transcripción y fotorreceptores específicos, como los fitocromos y criptocromos.

En este trabajo se han encontrado diferencias genotípicas y se han propuesto mecanismos genéticos que pueden ser de utilidad en el diseño de variedades de cebada mejor adaptadas a condiciones climáticas futuras.

Abstract

In the scientific community and among plant breeders, there is an increasing concern about how the climate change will affect crop season duration and flowering time of crops, due to their implications on yield. In the Mediterranean region, barley is an important cereal that also has adaptive potential to diverse environments. In this crop, temperature and light cues control flowering through the interaction between vernalization (*HvVRN1*, *HvVRN2* and *HvFT1*) and photoperiod genes (*PPD-H1* and *HvFT3*).

The main objective of this thesis is to increase our knowledge on the genetic control of flowering time in barley, focusing on how temperature and different light attributes, as photoperiod and spectral quality, affect to phenology and to the response of the main flowering time genes. The studies carried out aimed at: i) determining the day-length threshold that marks the moment for the induction of the *HvVRN2* expression; ii) characterizing the role of other possible promoters and repressors of flowering under non-inductive conditions for winter barleys; iii) understanding the immediate response to photoperiod changes, and whether natural variation in photoperiod sensitivity (determined by *PPD-H1* alleles) affects the functioning of the circadian clock; iv) studying the influence of light quality on barley development and on the expression of flowering time genes and barley genome.

The use of different sowing times under natural and increasing photoperiod conditions led to conclude that, although *HvVRN2* is always expressed in absence of vernalization, its expression increases markedly after day-length reaches 12 h 30 min. *HvFT3* expression occurs after some cold accumulation, is age-dependent, and its expression is associated with early flowering. Also, there is evidence of genotypic variants that can be associated with a developmental delay, as those found in the sequence of *HvOS2*, a flowering repressor and possible actor in the vernalization process.

To study the response to day-length shifts, expression of circadian clock and flowering time genes was evaluated for 3 days from the transition between photoperiods. A rapid and stable response of the clock genes was observed, in some cases conditioned to the *PPD-H1* variant, as the rapid response of *HvTOC1*. Also, the rhythmicity of the expression of the flowering time genes was subjected to variation at *PPD-H1*.

Finally, an exhaustive study of barley development under different light quality conditions was carried out. The greatest differences were due to a delay promoted by fluorescent light bulbs, especially in the time to first node appearance and until the onset of stem elongation. However, not every variety responded equally, and

they could be classified in sensitive and insensitive to light quality. The RNA-seq analysis revealed differences in gene expression of three genotypes with different sensitivity to light quality, suggesting that the greatest diversity could be found in transcription factors and specific photoreceptors, as phytochromes and cryptochromes.

The genotypic differences found and the genetic mechanisms proposed in this work can be useful tools for the design of barley ideotypes better adapted for future climatic conditions.

Resum

Tant en la comunitat científica com entre milloradors de varietats existeix una creixent preocupació sobre com influirà el canvi climàtic en la durada dels cicles dels cultius i sobre les seves dates de floració, per les seves implicacions en el rendiment. A la regió mediterrània, l'ordi és un cereal d'importància que també té potencial adaptatiu a una gran quantitat d'ambients. En aquest cultiu, els senyals de temperatura i llum controlen la floració, mitjançant la interacció dels gens de vernalització (*HvVRN1*, *HvVRN2* i *HvFT1*) i fotoperíode (*PPD-H1* i *HvFT3*).

L'objectiu principal de la tesi ha estat aprofundir en el control genètic de la floració en ordi, intentant desxifrar com afecten la temperatura i diferents paràmetres de la llum, com el fotoperíode i la qualitat de l'espectre lumínic, a la fenologia i a la resposta dels gens de floració. S'han realitzat estudis per a: i) determinar el llindar de longitud de dia que marca el moment per a la inducció de l'expressió de *HvVRN2*; ii) caracteritzar el paper d'altres possibles inductors i repressors de floració en condicions no inductives d'hivern; iii) entendre com és la resposta immediata a canvis en el fotoperíode, i si la variació natural en la sensibilitat al fotoperíode (marcada per diferents al·lels de *PPD-H1*) afecta el rellotge circadià; iv) estudiar la influència de la qualitat de llum en el desenvolupament i en l'expressió de gens de floració i del genoma d'ordi.

L'ús de diferents dates de sembra en condicions de fotoperíode natural i creixent va permetre concloure que *HvVRN2* s'expressa sempre en absència de vernalització i la seva expressió augmenta notablement a partir de dies amb 12 h 30 min de llum. L'expressió de HvFT3 necessita d'una certa acumulació de fred, és depenent de l'edat i la seva expressió està associada amb floracions més primerenques. A més a més, s'ha aportat evidència de variants genètiques que retarden el desenvolupament, com les trobades en la seqüència del repressor de floració i possible actor en el procés de vernalització, *HvOS2*.

Per estudiar la resposta als canvis de longitud de dia, es va avaluar l'expressió de gens del rellotge i de floració al llarg de 3 dies des de la transició entre fotoperíodes. Es va observar una resposta ràpida i estable en els gens del rellotge que, en alguns d'ells, va estar condicionada per la variant de *PPD-H1*, com la rapidesa de resposta de *HvTOC1*. També el ritme de l'expressió dels gens de floració va estar subjecte a la variació en *PPD-H1*.

Finalment, es va realitzar un estudi exhaustiu del desenvolupament d'ordi en diferents condicions de qualitat de llum. Les majors diferències es van deure a un retard promogut per bombetes de tipus fluorescent, especialment en les fases d'aparició de primer nus i el temps fins al començament de l'elongació de la tija. No obstant això, no totes les varietats van respondre igual, i es van classificar en

sensibles i insensibles a la qualitat de llum. L'anàlisi de RNA-seq va revelar diferències en l'expressió de tres genotips amb diferent sensibilitat, suggerint que la major diversitat podria residir en factors de transcripció i fotoreceptors específics, com els fitocroms i criptocroms.

En aquest treball s'han trobat diferències genotípiques i s'han proposat mecanismes genètics que poden ser d'utilitat en el disseny de varietats d'ordi millor adaptades a condicions climàtiques futures.

● ● ●
x

Table of contents

• • •

xii

List of figures

Chapter 1

Chapter 2

Chapter 3

Chapter 4

Chapter 5

List of tables

Abbreviations

B: Blue region of the light spectrum.

CCA1: *CIRCADIAN CLOCK ASSOCIATED 1*.

DE: Differentially expressed.

DEV: plant developmental stage.

EC: *EVENING COMPLEX*.

F: Fluorescent light bulbs.

FLC: *FLOWERING LOCUS C*.

FM: Shift from fluorescent to metal halide light bulbs.

FR: Far red region of the light spectrum.

GI: *GIGANTEA*.

GY: green-yellow regions of the light spectrum.

HvFT1: *FLOWERING LOCUS T 1*.

HvOS2: *ODDSOC2* (*SUPPRESSOR OF OVER-EXPRESSION OF CONSTANS*).

HvVRN1: *VERNALIZATION 1*.

HvVRN2: *VERNALIZATION 2*.

M: Metal halide light bulbs.

MF: Shift from metal halide to fluorescent light bulbs.

MSA: Main shoot apex.

LD: long day.

LD-SD: Shift from long to short days.

PAR: Photosynthetically active radiation.

PEBP: phosphatidylethanolamine-binding protein.

PPD-H1: *PHOTOPERIOD 1*.

PPD-H2: *PHOTOPERIOD 2*

PRR: pseudo response regulator.

qRT-PCR: Quantitative Real-Time Polymerase Chain Reaction.

R: Red region of the light spectrum.

SD: short day.

SD-LD: Shift from short to long days.

Syn: Synonymous.

TOC1: *TIMING OF CAB EXPRESSION1*.

VER: Vernalization.

W: Waddington stage.

Chapter 1

General introduction

Chapter 1. General Introduction

1.1. Barley (*Hordeum vulgare*, L.)

1.1.1. Origin and classification

Cultivated and wild barleys are classified in the genus *Hordeum*, tribe Triticeae (syn. Hordeae, Hordeeae), family Poaceae (formerly Gramineae). All *Hordeum* species share the same karyotype (large chromosomes, diploid, 2n = 14). The species *H. vulgare*, which encompasses all the cultivated barley, has lax and pendulous ears, known as spikes, with one or three grains per rachis node, giving two or six rowed spikes (Briggs, 1978).

Barley is an ancient crop that was first domesticated around 10,000 years ago in the Fertile Crescent, an area including part of current Iraq, Turkey, Jordan, Syria, Palestine, and Lebanon (Dai and Zhang, 2016). The wild barley form, *Hordeum vulgare* ssp. *spontaneum*, consists of a wide range of races of varying degrees of leaf size, grain size, grain colour, disease resistance, dormancy and rachis fragility; spring and winter forms are known, and even hooded samples have been found. This crop is highly adaptable, thus is not strange to see that barley is linked to the early human civilization history and their movements (Langridge, 2018). It is one of the first domesticated plants, as traces of barley have been found at the oldest archaeological sites. Indeed, there exist archaeological evidence of consumption of barley 17,000 years BC, revealing the use of the pre-domesticated wild barley (*Hordeum vulgare* subsp. *spontaneum*) (reviewed by Komatsuda, 2014). The spread of barley out of the Fertile Crescent followed eastward and westward routes, along which domestication continued as a protracted process, and recent studies have shown that there were several domestication events (Morrell and Clegg, 2007; Dai *et al.*, 2012). Certainly, barley distribution and adaptation to diverse and harsh

conditions produced a diversification that has become a precious resource for breeding.

1.1.2.   Importance of the crop

From an agricultural and economic point of view, barley is a relevant crop at global scale. In 2017, almost 150 million tonnes of barley were produced on 47.5 million ha, yielding on average ~ 3.1 tonnes ha^{-1} (FAOSTAT, 2019). With these data, barley is currently the fourth most cultivated crop in the world, only behind maize, rice and wheat.

Globally, barley is mainly used for animal feeding, as grain and also as forage, due to its high content in starch, fibre and protein. In addition, barley malt is the base of the production of brewed and distilled beverages as beer and whisky, which confers an added value to the crop, acquiring economic relevance in several countries (Verstegen *et al.*, 2014). Although barley remains a staple crop in several areas and has important spiritual, nutritional, and cultural significance (Meints *et al.*, 2015), currently only a small part of barley production is dedicated to human food. However, the use as a functional food is gaining importance due to its benefits for human health.

Compared to wheat, barley is often seen as an inferior food staple, being described as the 'poor man's bread' (Langridge, 2018). Despite this limitation, barley has always been considered the most resilient amongst the winter cereals, with a range of possible uses that is still unexplored (Ceccarelli *et al.*, 2010). The adaptability of this crop allowed its wide dispersion on our globe, reaching a wide range of environments, including higher altitudes and latitudes, and harsher semi-arid areas than other crop species (Graner *et al.*, 2003). Compared to wheat, its closest related cereal, barley has a hardier profile, which makes it a good choice for vulnerable and/or extreme areas, where wheat would struggle to produce acceptable yield. In

the last decade, area cultivated with barley decreased, but its production was maintained (Figure 1.1), indicating successful breeding and management efforts for this crop. However, improvement in this period has been small compared to the rapid increase of barley production observed between 1960 and mid-1980s. Recently, barley was pushed out of some productive regions, and its production moved to low rainfall and stressed environments (Langridge, 2018), making the overall gain for the crop lower than expected. With this historical overview in mind, current research and breeding strategies are addressed to improve the knowledge of key genes for environmental adaptation, and introduce a relatively small number of these known genes into diverse germplasms. Hence, this replacement would produce new gene pools for evaluation or inclusion in breeding programs (Langridge and Waugh, 2019).

Production/Yield quantities of Barley in World + (Total)
1961 - 2017

Source: FAOSTAT (Jul 31, 2019)
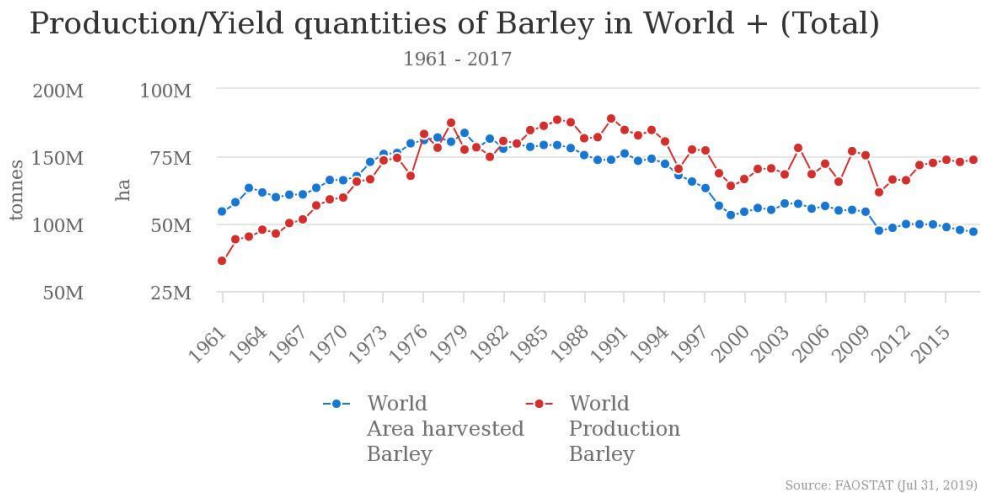
Figure 1.1. Production and harvested area in the world from 1961 to 2017.

It is important to consider that adequate timing of plant development is crucial to maximize yield formation under harsh environmental conditions (Wiegmann *et al.*, 2019). Hence, the knowledge of the factors involved in the adaptability of barley is a demand to cope with the increased stresses derived from the climate change, the

reduced arable land available and the future ability to feed an ever-growing population (Godfray *et al.*, 2010; Powell *et al.*, 2012; FAOSTAT, 2019). Thus, a main goal for plant breeding is to make crops more productive.

Yield is determined by the growth and developmental processes that occur during the crop cycle. Such processes determine to a large extent the adaptability of the crop. The duration of each growth stage varies depending on the environment (photoperiod, temperature, drought, diseases and pests), area of cultivation, time of sowing and genetic factors (i.e., spring sown barleys develop faster than autumn sown barleys).

Specifically, in those regions where water is a limited source, as in those affected by the Mediterranean climate, the main factor of a successful adaptation is the phenology. Variability in the flowering date depends on environmental effects and interaction between genes that control the transition from the vegetative to the reproductive state. In barley, flowering date must fit with the growth habit to optimize the access to water and flower in the most adequate conditions, with a large impact on final yield (van Oosterom and Acevedo, 1992).

1.1.3.   Barley genome

Barley is a diploid, self-fertile specie, with a low number of large chromosomes (2n = 2x = 14). The total length of the barley genome is 5.1 Gb. It is a large and complex genome with a high number of repeated sequences (over 80%). These features were a great challenge to develop a high-quality genome sequence. The International Barley Sequencing Consortium (IBSC) released a first draft of the gene space sequence in 2012, using the cultivar 'Morex' as reference (Mayer *et al.*, 2012). A dense genetic map was anchored to it (Comadran *et al.*, 2012), which facilitated the association between resources. Resources like a population based-sequencing (POPSEQ, Mascher *et al.*, 2013), a set of sequenced BAC contigs (Ariyadasa *et al.*,

2014), and *de novo* assemblies from other barley cultivars ('Barke' and 'Bowman', Mayer *et al.*, 2012; 'Haruna Nijo', Sato *et al.*, 2016; 'Zangquin320', Dai *et al.*, 2018) enriched the information of the barley genome. The first version of a barley reference sequence was developed five years later (Mascher *et al.*, 2017). The progress on this reference is ongoing, and it is expected that the second version of the 'Morex' genome sequence assembly (Mascher, 2019; Monat *et al.*, 2019), will improve the previous one.

The study of barley genome is important in itself, and also for its contribution to research in other crops. Its diploid genome and the close relation between barley and wheat, has made barley a natural model for monocot crops.

Barley has been relevant in research on metabolism, genetics and physiology, and in several cases, it has served as a starting point for works in other species, notably in wheat (Langridge, 2018). The development of genomic tools in this crop has renewed the interest in mutants that are used to elucidate a range of developmental and metabolic pathways in plants (Druka *et al.*, 2011). Specifically, studies in flowering time control in barley and the involvement of vernalization and photoperiod genes has been useful in the equivalent work in wheat and other cereals (Turner *et al.*, 2005; Beales *et al.*, 2007). Also, as a robust and widely-spread crop, barley has emerged as a model for investigating and responding to biotic and abiotic stresses, and for studying adaptation for future climate conditions (Newton *et al.*, 2011; Dawson *et al.*, 2015).

1.2. Development

Barley (*Hordeum vulgare* L.) is a long day plant that flowers earlier under increasing day-lengths, similarly to other cereals as wheat (*Triticum* spp.). Attending to growth habit, barley varieties are classified as winter and spring cultivars. Winter barleys are sown in autumn, benefiting from the warmth of the

soils and the humidity from autumn rains, which are essential at the beginning of the cycle. In the Mediterranean region, autumn sown barley has to survive a range of mild to harsh winters, and then flower sufficiently early in the spring to avoid the heat and drought of late spring or early summer. Spring types, on the other hand, are sown commonly in late winter or the beginning of spring, avoiding the damage caused by cold winters. This is a simple agronomic distinction, useful to classify the varieties. However, the existing variation is more complex, being affected by several environmental and genetic factors that will be detailed in the following sections of this thesis.

1.2.1. Developmental phases

Several scales have been proposed with the objective of recording the progress of the entire plant and the apex through its different stages. Plant developmental stages are usually defined checking for first node appearance (plant developmental stage 31, or DEV31) and appearance of the awns just visible above the last leaf sheath (DEV49). Taking into account other parameters such as leaf number, plant height and number of tillers, it is possible to dissect the development into phenophases non-destructively (Kiss *et al.*, 2011). In this thesis, we follow the Waddington scale (Waddington *et al.*, 1983) for determining the stages of the apex, and the Zadok's scale (Zadoks *et al.*, 1974), following the description of Tottman *et al.* (1979), for the development of the whole plant.

(Next page)
Figure 1.2. Summary of development in barley.
From early phases (left) to heading and embryo formation (right). From the upper to the lower part, morphological changes occurring from a wide to a microscopic perspective. LP, leaf primordium; DR, double ridge; Le, lemma; Co, collar; Gi, glume initials; Fi, floret initials; Ap, awn primordium; Sp, stamen primordium; Op, ovary primordium.
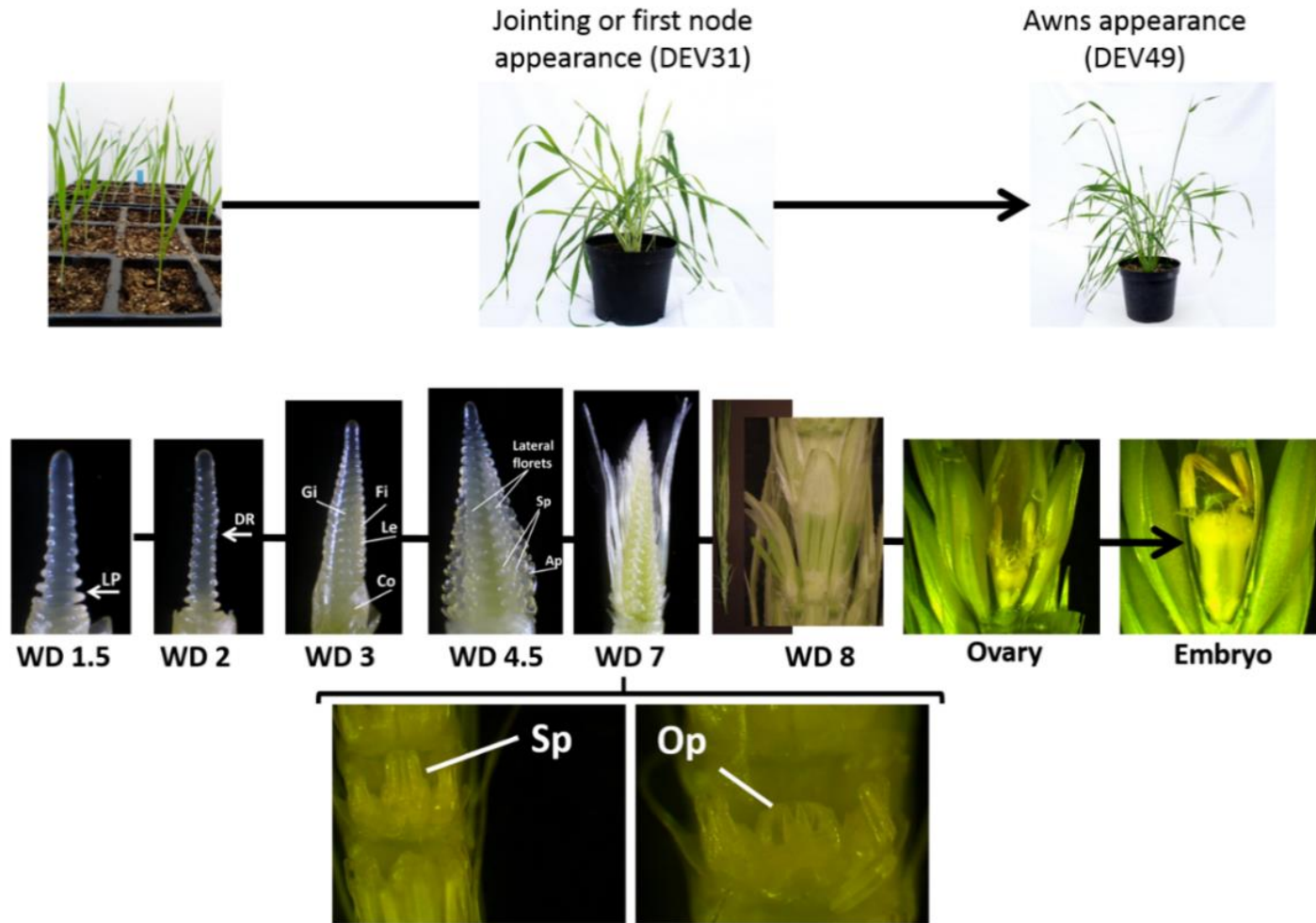
One of the most important changes in the development of the plant is the transition from the *vegetative* to the *reproductive* phase. The *vegetative* stage occurs from the seedling emergence up until floral initiation. During development, the plant reaches a point in which the apical primordia cease producing leaf primordia and start to produce floral organs, as detailed in Figure 1.2. In this moment, the apical primordia transit to the *reproductive* stage, which involves several morphological and genetic changes that mark a no-return point. A crucial step is the development of double ridges in the apex (W 2.0, Waddington *et al.*, 1983), that marks the initiation of floral primordia (Figure 1.2).

When plant reaches 3-4 expanded leaves, tillering starts. At this moment, cultivars already present a prostrate or an erect growth habit, a highly heritable trait, which partially depends on environmental conditions, culture management and sowing density (Molina-Cano, 1989). Then, the stem becomes differentiated into nodes, which is the "jointing" phase or first node appearance (DEV31). This phase can coincide with the onset of the stem elongation phase (DEV30, Borràs et al., 2009). Although, depending on the variety and the environmental conditions, DEV30 can follow, with various lags, DEV31 (Karsai et al., 2013). When the stem starts to elongate, internodal regions become hollow. At this time, all the spikelets are formed. These processes are relevant agronomically, as the period from triple mound (W 2.25) to heading, strongly influences barley yield through the number of fertile florets (Miralles et al., 2000).

Development continues with the upwards advancement of the apex as the stem grows. Eventually the last leaf, named 'flag leaf', emerges (DEV 37). The flag leaf sheath is bulged, because it contains the developing ear, a moment described as "booting". Then, the shoot's terminal node lengthens enough to push out the awns. That moment is the 'awn appearance' (DEV 49) stage. Then, anthesis occurs in the newly-emerged ear, starting in the middle of the ear and progressing upwards and

downwards. During flowering, leaves initiate senescence, starting by the older basal leaves, losing the green color and becoming yellow. Gradually, the plant dries until full maturity, when the grain ripens.

Barley development is controlled by genetic factors. The precise timing of flowering requires the coordination of at least three pathways, which respond to the length of the daily light period (photoperiodic pathway), prolonged low temperatures (vernalization) and high temperatures (ambient-temperature pathway) (Andrés and Coupland, 2012; Casal and Qüesta, 2018). The genetic control of the vernalization and photoperiod responses has been studied in depth, deciphering major factors controlling flowering time. Those factors have strong interactions among them and with the environment, which will be described in the next sections.

1.2.2.   Vernalization

In winter cereals, experiencing a period of cold previous to the spring is needed for normal promotion of flowering (Laurie *et al.*, 1995; Trevaskis *et al.*, 2003). This process is called **vernalization** and prepares the plant for the arrival of the optimum conditions to flower (Trevaskis, 2010). The vernalization treatment must be fully completed before the induction of flowering by long days.

In winter cereals, vernalization and photoperiod are the main environmental signals that coordinate the flowering date. It is known that temperature and photoperiod are coordinated to reach flowering in the right moment through the major flowering genes. Genes *HvVRN1* and *HvVRN2* interact to regulate cold temperature response, and *HvFT1* (syn. *HvVRN3*) integrates their signal with those coming from photoperiod response genes, *HvFT3* (*PPD-H2*) and *PPD-H1*, to allow flowering in the right moment.

HvVRN1 encodes an AP1-like MADS-box transcription factor. Several alleles are known, as result of deletions or insertions in the first intron, which are associated

with different degrees of vernalization requirement (Hemming *et al.*, 2009). Induction of *HvVRN1* is related to changes in the pattern of histone methylation, which provides a memory of cold exposure in winter barley plants (Oliver *et al.*, 2009). The VRN1 protein directly binds to the promoter regions of the repressor genes *HvVRN2* and *HvOS2*, downregulating their expression, and also to the *HvFT1* promoter, enhancing its expression (Deng *et al.*, 2015*a*). These results explain why vernalization is a pre-requisite to promote flowering under LD in temperate cereals.

HvVRN2 encodes a transcription factor, *ZCCT-H*, with a zinc-finger and a CCT domain, that belongs to the *CONSTANS*-like family. This gene delays flowering in plants that have not been vernalized (Yan *et al.*, 2004). There are two allelic variants for this gene, that consist on presence/absence variation (Karsai *et al.*, 2005). In winter barleys, that present the dominant variants, the expression of the genes is highly dependent on day-length, being induced in long days (Karsai *et al.*, 2005; Trevaskis *et al.*, 2006). Commonly, the *ZCCT-H* genes are absent in spring varieties, and also in a third class of varieties, called facultative, that have a winter *HvVRN1* allele, and are suited to both autumn and spring sowings.

The accepted gene model establishes that cold upregulates the floral promoter *HvVRN1*, which is required to downregulate the flowering repressor *HvVRN2* (Figure 1.3). Then, *HvVRN1* allows the expression of the flowering inducer *HvFT1* in leaves. *HvVRN2* delays flowering until plants have satisfied their cold needs. Winter barleys carry a combination of an allele with full length first intron at *HvVRN1* (called a "winter" allele) and a present *HvVRN2* allele.
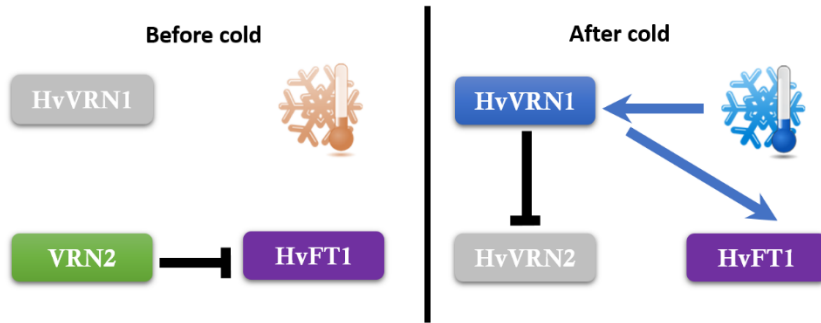
Figure 1.3. Scheme of the flowering gene model proposed in barley.

Recently, other repressors of flowering have been identified, although their relevance is still unknown. One of them is *ODDSOC2* (in barley *HvOS2*), that acts in the vernalization pathway (Greenup *et al.*, 2010; Ruelens *et al.*, 2013; Sharma *et al.*, 2017). *HvOS2* is a MADS-box gene, orthologue of the Arabidopsis *FLOWERING LOCUS C* (*AtFLC*). In barley, this gene is downregulated by cold (Greenup *et al.*, 2010), affected by photoperiod and induced by high temperatures (Hemming *et al.*, 2012).

1.2.3.   Light responses

Day-length and diurnal changes in the spectral composition of light are two aspects of the seasonal light regime that work as phenological cues, either individually or in combination (Linkosalo and Lechowicz, 2006). The effect of photoperiod on cereal processes is well established, whereas the influence of qualitative changes in light conditions has received less attention (Ugarte *et al.*, 2010).

1.2.3.1.   Photoperiod

Changes in photoperiod constitute an environmental cue that plants use to detect changes in the seasons, and optimize the time to flower. The interaction of vernalization and photoperiod genes in temperate grasses is well-known (Campoli and von Korff, 2014; Song *et al.*, 2015). The two most important genes related to

photoperiod response are *PHOTOPERIOD1* (*PPD-H1*) and *PHOTOPERIOD2* (*PPD-H2,* syn. *HvFT3*).

PPD-H1 determines the sensitivity to long days (Laurie *et al.*, 1995), regulating flowering through the induction of *HvFT1* (Turner *et al.*, 2005). Its candidate gene is *HvPRR37*, *pseudo-response regulator 37*, which encodes a pseudo-receiver domain, involved in signal transduction, and a CCT domain. This gene belongs to the family of PSEUDO RESPONSE REGULATORS (PRR), involved in the feedback loops that constitute the circadian clock. Two allelic variants characterize the different sensitivity to long days. The natural (recessive, *ppd-H1*) mutation in the CCT domain of the gene causes photoperiod insensitivity and late flowering in spring barleys. Contrary, the photoperiod sensitive allele carried by most winter types produces early flowering (Turner *et al.*, 2005). The mutated *ppd-H1* allele was selected in Central European spring barley genotypes, whereas the dominant wild-type *PPD-H1* allele is prevalent in wild and Mediterranean winter barleys (Jones *et al.*, 2008). Besides its role in the photoperiod requirement of plants, *PPD-1* is involved in the control of leaf and spike morphology in barley and wheat (Boden *et al.*, 2015; Digel *et al.*, 2016; Alqudah *et al.*, 2018). Mulki and von Korff (2016) identified interactions between *PPD-H1*, *HvCO1*/*HvCO2* and *HvVRN2* that could determine different regulation of flowering time before and after vernalization, highlighting the complexity of the model, that integrates signals of vernalization and photoperiod pathways (Figure 1.4).

PPD-H2 was identified as the locus responsible of the sensitivity to short days in winter x spring crosses (Laurie *et al.*, 1995; Cuesta-Marcos *et al.*, 2008). The candidate gene behind this locus is *HvFT3*, a FT-like member of the PEBP family. Two allelic variants for this gene are known: a dominant one, with a functional copy of the gene, and a recessive allele, with most of the gene missing and non-functional (Faure *et al.*, 2007; Kikuchi *et al.*, 2009). Most works that have studied the role of

this gene were carried out in spring types (Faure *et al.*, 2007; Kikuchi *et al.*, 2009). Casao *et al.* (2011) studied the presence of this gene exclusively in winter barley. They found that the dominant allele is frequent in varieties cultivated in low latitudes (< 44ºN), and in a high number of Spanish landraces (35-44ºN), but not in varieties grown in more northern latitudes. *HvFT3* has acquired particular relevance in autumn sowings in Mediterranean regions, being associated with flowering time QTL and grain yield QTL x environment in different populations (Cuesta-Marcos *et al.*, 2008, 2009; Karsai *et al.*, 2008; Francia *et al.*, 2011; Tondelli *et al.*, 2014). It seems to have a role in adaptation, interacting with vernalization genes, with a proposed role as promoter of flowering in winter cultivars that have not satisfied their cold needs (Casao *et al.*, 2011). Recently, Mulki *et al.* (2018), working with mutants, reported a specific biological role of this gene controlling spikelet initiation but not floral development.

Vernalization and photoperiod signals converge to promote flowering through the regulation of the central flowering gene, *HvFT1* (candidate of *VRN-H3*), homologue of *FLOWERING LOCUS T* of *Arabidopsis*. *HvFT1* encodes a phosphatidylethanolamine-binding protein (PEBP) (Kobayashi *et al.*, 1999), involved in signalling. In wheat and barley, *HvFT1* is induced by long days, promoting flowering. In *Arabidopsis*, *FT* expression is induced in leaves when plants are exposed to long days, and the *FT* protein moves to the shoot apex to promote flowering (Corbesier *et al.*, 2007). A similar mechanism is probably to be acting in cereals (Trevaskis *et al.*, 2007).
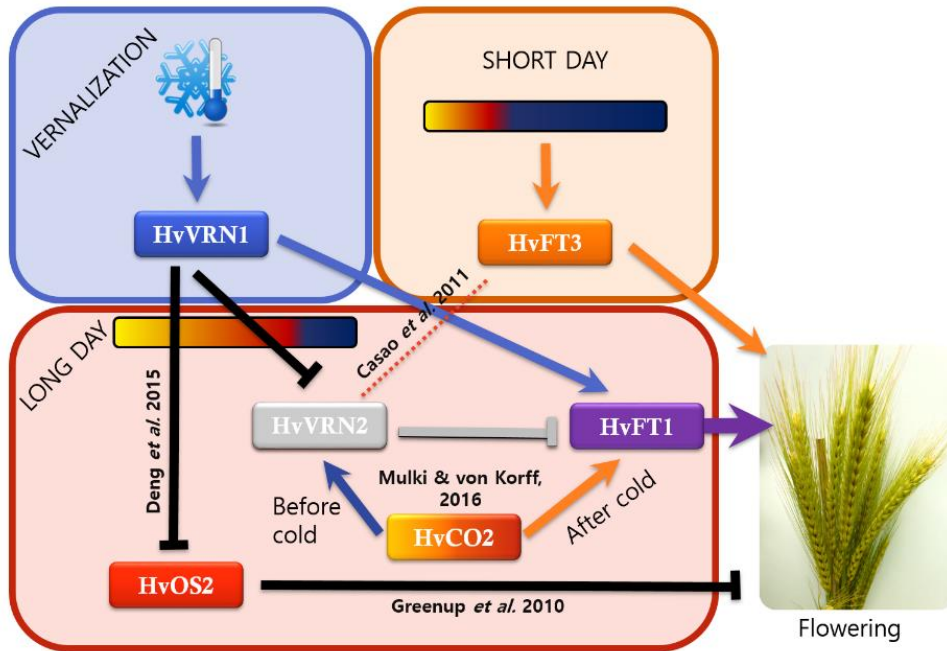
Figure 1.4. Scheme of the interaction between photoperiod and vernalization pathways in barley to trigger flowering.

1.2.3.2. Circadian rhythms

Circadian clock is the inner control of an organism to keep track of the time of the day, depending on the environmental cues received. All the living creatures (cyanobacteria, mammals, higher plants) have a mechanism controlling the rhythmicity. The circadian rhythm influences a variety of functions like cell cycle, metabolism, and sleep-wake cycle. The circadian clock may be altered or disrupted under various conditions. As an example, jet-lag, the well-known disruption of human sleep patterns that occurs after travelling across different time zones is the result of an alteration of the circadian clock.

In general, circadian rhythm is self-sustained (the rhythm is maintained continuously), entrainable (can be shifted and synchronized by environmental cues), it is temperature compensated (shows slight modifications with temperature),

and transmits a signal to other oscillators (Fuhr *et al.*, 2015). A biological clock comprises three main elements: clock input, core oscillator and clock output. Clock input transmits the environmental signals, as photoperiod and temperature, to the oscillator module, which marks the rhythmicity to the output genes, controlling diverse physiological responses (Más, 2005). Some of them are associated with metabolism, growth and development, indicating that the clock has a widespread control of the transcriptome (McClung, 2013). Actually, around one third of the transcriptome of *Arabidopsis* is under circadian control. It is clear that the circadian clock controls many different aspects of plant biology and is essential for optimum plant performance (reviewed in Hubbard and Dodd, 2016).

The functioning of the clock is well-known in *Arabidopsis*. It consists on self-regulatory loops that maintain a rhythm of peaks and valleys in each day-night cycle. In the established model, *CCA1* (*CIRCADIAN CLOCK ASSOCIATED 1*) and *LHY* (*LATE ELONGATED HYPOCOTYL*) peak before dawn, and their products repress *TIMING OF CAB EXPRESSION1* (*TOC1*) (Gendron *et al.*, 2012; Huang *et al.*, 2012; Fung-Uceda *et al.*, 2018). In the evening, TOC1 suppresses the expression of *CCA1* and *LHY* (Figure 1.5). Those genes compose the central loop of the clock. In addition, CCA1 and LHY participate in another loop promoting *PRR7* and *PRR9*. These PRR genes also repress *CCA1* and *LHY* sequentially during the day. In the evening, *EARLY FLOWERING 3* (*ELF3*), *EARLY FLOWERING 4* (*ELF4*) and *LUX ARRHYTHMO* (*LUX*, also known as *PHYTOCLOCK1*, *PCL1*) conform the "evening complex" (EC) that represses the *PRR* genes early at night (reviewed by Johansson and Staiger, 2015). In addition, *GIGANTEA* (*GI*) is also involved in the evening control of the clock, repressing indirectly *TOC1* in the evening. The cycle ends with the maintained repression of *TOC1* at night by CCA1/LHY.
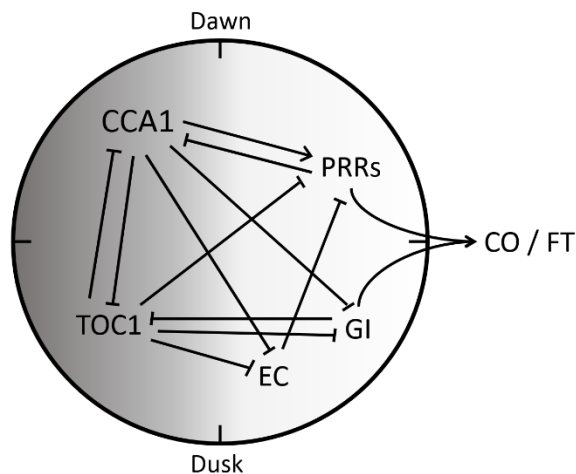
Figure 1.5. Simple scheme of the feedback loops that conform the circadian clock in *Arabidopsis thaliana*.
Based on the snapshot of the Flowering Interactive database, FLOR-ID (http://www.phytosystems.ulg.ac.be/florid/, last visited 02 August 2019; Bouché *et al.*, 2015).

Some of the clock genes in *Arabidopsis* and rice (*Oryza sativa*) have a homologue in barley (Campoli *et al.*, 2012; Calixto *et al.*, 2015). Similarities in sequence and expression pattern suggest that most of them could have a conserved function. Some of the differences between *Arabidopsis* and barley clock are:

- There is no clear homologue of *AtELF4* in barley, although there exist two *ELF4*-like genes (Calixto *et al.*, 2015).

- The morning loop seems to be governed by one gene in barley instead of two in *Arabidopsis*. The barley gene seems to be more related to *LHY* than *CCA* (Calixto *et al.*, 2015).

- Barley clock starts to have a robust rhythm after having some lights-on and lights-off signals (Deng *et al.*, 2015*b*), whereas *Arabidopsis*' rhythm starts free-running oscillations in absence of light-dark cues (Zhong *et al.*, 1998; Salome *et al.*, 2008).

The implications of these differences in a system that is internally driven have not been fully explored in barley, although could be determinant in the adaptive mechanism of the species (Webb *et al.*, 2019), as the circadian clock allows the organism to anticipate and prepare for changes (Inoue *et al.*, 2018). Some studies have reported that mutations in the clock genes could contribute to adaptation to local environments, optimizing among others, flowering time. Polymorphism in circadian clock genes may contribute to local adaptations over a wide range of latitudes in many plant species. The study of circadian rhythms in wild barleys showed variability for circadian traits, being period lengths associated to temperature and ecogeographical origin of the plants, and the amplitudes with soil composition (Dakhiya *et al.*, 2017). Thus, a robust fitness to an environment, governed by the circadian rhythms could be a part of the adaptive response to that particular environment and could be exploited for breeding purposes in the future.

1.2.3.3. Light quality

Plants synchronize their physiological and developmental phases with daily and seasonal cues in the environment through the circadian clock. To respond to photoperiod cues, the plant must discern between day and night (darkness is detected as low photon flux), measure the duration of one or both, to coordinate downstream processes. Wavelength, intensity, direction, duration (as seen before), and other attributes of light are used by plants to predict imminent seasonal change and to determine when to initiate physiological and developmental processes (Franklin, 2009; Ugarte *et al.*, 2010). In general, plants depend on ambient light conditions to regulate their development, and to be able of adapt to changing environments. Nowadays, these responses are used to control and optimize plant development under controlled conditions. The wide use of controlled-environments to promote plant growth and development, together with the advent of new methods as "speed breeding" (Watson *et al.*, 2018) have raised the interest on the study of

responses of plants to controlled conditions. However, crop responses to light quality and intensity are not fully understood. What is known is that biological processes such as seed germination, circadian rhythm, shade avoidance and flowering development are all under influence of light spectrum (Smith, 2000).

The genetic control of light quality responses and its effect on flowering have been studied mostly in horticultural (Gómez and Izzo, 2018) and ornamental (Meng and Runkle, 2014) species, and in *Arabidopsis thaliana* (Thomas, 2006; Adams *et al.*, 2009). In this model plant, the genes involved in the shade avoidance response are well-known. Shade avoidance is a set of processes that plants initiate, triggered by the reduction of light that reaches the plant due to the shading usually by neighbouring organisms, to better compete for light harvesting (Ballaré and Pierik, 2017). Phytochrome light receptors are central to the perception of variation of light quality, and regulate the developmental plasticity of plants, having effect on stem elongation and branching (Franklin, 2009; Trevaskis, 2018). Other receptors active in light sensing are cryptochromes (Cry1a, Cry1b and Cry2) that mediate the blue and UV-A light-induced gene expression through different mechanisms (Casal, 2013). These photoreceptors partially differ in their function and target processes and absorb different wavelengths of light to regulate genome expression and plant development.

Spectral composition is involved in several responses of the plants: end-of-day, shade avoidance, and also in adaptation to natural conditions (Smith, 1982). Variation of spectral composition of daylight under natural conditions is particularly relevant from the agronomic point of view. Zenit angle, altitude, climatic and atmospheric factors influence the spectral energy distribution of the solar light (Holmes and Smith, 1977). Also, during the day, the relative levels of blue, red and far-red wavelengths change, i.e. radiation in the blue and far-red regions change while sun approaches the horizon, and after sunset. In general, time

• • •

and duration of the red and far-red parts of the spectrum vary with altitude, latitude and time of year, whereas some specific-of-location parameters, as atmospheric turbidity and cloud cover, affect the rate and magnitude of the changes in the spectrum. In a climate change scenario, where latitudinal shifts of cultivated varieties are expected, these physical factors might influence in the failure or success of the crop in a different environment. Hence, understanding the biological mechanisms affecting development in response to specific parts of the light spectrum can contribute to design future breeding strategies.

1.3.   Objectives

This work aims to deepen in the knowledge of light and temperature effects on the genetic control of flowering time in barley. The main purpose was to shed light on the complex functioning of the molecular mechanisms involved in barley flowering, focusing on the behaviour of major flowering time genes under different conditions, to explore their role in adaptation. In the course of this work, new information about the possible function of less-known genes has opened new questions.

The specific objectives were:

- To find out the threshold of day-length that induces the expression of *HvVRN2* and other possibly-related genes. This timepoint would mark the moment at which a winter barley would need to have fulfilled its cold needs.

- To characterize further the role of other possible inducers and repressors of flowering under non-optimum conditions for winter barley flowering, as incomplete or null vernalization.

- To deepen in the knowledge on clock modulation in barley when day-length is altered, focusing on the role of *PPD-H1*, through the study of *PPD-H1* dependent relationships between the day-length, circadian rhythms and florigen induction.

- To find out whether there are genetic differences in the responses triggered by light quality (spectrum) in barley development. Also, to identify genes involved in light-response pathways that could explain the different sensitivity to light quality.

1.4. References

Adams S, Allen T, Whitelam GC. 2009. Interaction between the light quality and flowering time pathways in *Arabidopsis*. Plant Journal **60**, 257–267.

Alqudah AM, Youssef HM, Graner A, Schnurbusch T. 2018. Natural variation and genetic make-up of leaf blade area in spring barley. Theoretical and Applied Genetics **131**, 873–886.

Andrés F, Coupland G. 2012. The genetic basis of flowering responses to seasonal cues. Nature Reviews Genetics **13**, 627–639.

Ariyadasa R, Mascher M, Nussbaumer T, *et al.* 2014. A Sequence-Ready Physical Map of Barley Anchored Genetically by Two Million Single-Nucleotide Polymorphisms. Plant Physiology **164**, 412–423.

Ballaré CL, Pierik R. 2017. The shade-avoidance syndrome: Multiple signals and ecological consequences. Plant, Cell & Environment **40**, 2530–2543.

Beales J, Turner A, Griffiths S, Snape JW, Laurie DA. 2007. A *Pseudo-Response Regulator* is misexpressed in the photoperiod insensitive *Ppd-D1a* mutant of wheat (*Triticum aestivum* L.). Theoretical and Applied Genetics **115**, 721–733.

Boden S, Cavanagh C, Cullis BR, Ramm K, Greenwood J, Jean Finnegan E, Trevaskis B, Swain SM. 2015. *Ppd-1* is a key regulator of inflorescence architecture and paired spikelet development in wheat. Nature Plants **1**, 14016.

Borràs G, Romagosa I, van Eeuwijk F, Slafer GA. 2009. Genetic variability in duration of pre-heading phases and relationships with leaf appearance and tillering dynamics in a barley population. Field Crops Research **113**, 95–104.

Bouché F, Lobet G, Tocquin P, Périlleux C. 2015. FLOR-ID: an interactive database of flowering-time gene networks in *Arabidopsis thaliana*. Nucleic Acids Research **44**, D1167–D1171.

Briggs DE. 1978. *Barley*. Springer Netherlands.

Calixto CPG, Waugh R, Brown JWS. 2015. Evolutionary Relationships Among Barley and *Arabidopsis* Core Circadian Clock and Clock-Associated Genes. Journal of Molecular Evolution **80**, 108–119.

Campoli C, von Korff M. 2014. Genetic control of reproductive development in temperate cereals. In: Fornara F, ed. Advances in botanical research: Vol. 72. The molecular genetics of floral transition and flower development. New York: Academic Press, 131–158.

Campoli C, Shtaya M, Davis SJ, von Korff M. 2012. Expression conservation within the circadian clock of a monocot: natural variation at barley *Ppd-H1* affects circadian expression of flowering time genes, but not clock orthologs. BMC Plant Biology **12**, 97.

Casal JJ. 2013. Photoreceptor signaling networks in plant responses to shade. Annual Review of Plant Biology **64**, 403–427.

Casal JJ, Qüesta JI. 2018. Light and temperature cues : multitasking receptors and transcriptional integrators. New Phytologist **217**, 1029–1034.

Casao MC, Karsai I, Igartua E, Gracia MP, Veisz O, Casas AM. 2011. Adaptation of barley to mild winters: A role for *PPDH2*. BMC Plant Biology **11**, 164.

Ceccarelli S, Grando S, Maatougui M, *et al.* 2010. Plant breeding and climate changes. The Journal of Agricultural Science **148**, 627–637.

Comadran J, Kilian B, Russell J, *et al.* 2012. Natural variation in a homolog of *Antirrhinum CENTRORADIALIS* contributed to spring growth habit and environmental adaptation in cultivated barley. Nature genetics **44**, 1388–1392.

Corbesier L, Vincent C, Jang S, *et al.* 2007. FT Protein Movement Contributes to Long-Distance Signaling in Floral Induction of Arabidopsis. Science **316**, 1030–1033.

Cuesta-Marcos A, Casas AM, Hayes PM, Gracia MP, Lasa JM, Ciudad F, Codesal P, Molina-Cano JL, Igartua E. 2009. Yield QTL affected by heading date in Mediterranean grown barley. Plant Breeding **128**, 46–53.

Cuesta-Marcos A, Igartua E, Ciudad FJ, *et al.* 2008. Heading date QTL in a spring × winter barley cross evaluated in Mediterranean environments. Molecular Breeding **21**, 455–471.

Dai F, Nevo E, Wu D, Comadran J, Zhou M, Qiu L, Chen Z, Beiles A, Chen G, Zhang G. 2012. Tibet is one of the centers of domestication of cultivated barley. Proceedings of the National Academy of Sciences of the United States of America **109**, 16969–16973.

Dai F, Wang X, Zhang XQ, Chen Z, Nevo E, Jin G, Wu D, Li C, Zhang G. 2018. Assembly and analysis of a *qingke* reference genome demonstrate its close genetic relation to modern cultivated barley. Plant Biotechnology Journal **16**, 760–770.

Dai F, Zhang G. 2016. 1 – Domestication and Improvement of Cultivated Barley. In: Zhang G and Li C, eds. Exploration, Identification and Utilization of Barley Germplasm. Academic Press, 1–26.

Dakhiya Y, Hussien D, Fridman E, Kiflawi M, Green R. 2017. Correlations between Circadian Rhythms and Growth in Challenging Environments. Plant Physiology **173**, 1724–1734.

Dawson IK, Russell J, Powell W, Steffenson B, Thomas WTB, Waugh R. 2015. Barley: a translational model for adaptation to climate change. New Phytologist **206**, 913–931.

Deng W, Casao MC, Wang P, Sato K, Hayes PM, Finnegan EJ, Trevaskis B. 2015*a*. Direct links between the vernalization response and other key traits of cereal crops. Nature Communications **6**, 5882.

Deng W, Clausen J, Boden S, Oliver SN, Casao MC, Ford B, Anderssen RS, Trevaskis B. 2015*b*. Dawn and Dusk Set States of the Circadian Oscillator in Sprouting Barley (*Hordeum vulgare*) Seedlings. PLOS ONE **10**, e0129781.

Digel B, Tavakol E, Verderio G, Tondelli A, Xu X, Cattivelli L, Rossini L, von Korff M. 2016. Photoperiod-H1 (Ppd-H1) Controls Leaf Size. Plant Physiology **172**, 405–415.

Druka A, Franckowiak J, Lundqvist U, *et al.* 2011. Genetic Dissection of Barley Morphology and Development. Plant Physiology **155**, 617–627.

FAOSTAT. 2019. *FAOSTAT Database*. http://faostat.fao.org. Last accessed: 31/07/2019.

Faure S, Higgins J, Turner A, Laurie DA. 2007. The *FLOWERING LOCUS T*-like gene family in barley (*Hordeum vulgare*). Genetics **176**, 599–609.

Francia E, Tondelli A, Rizza F, *et al.* 2011. Determinants of barley grain yield in a wide range of Mediterranean environments. Field Crops Research **120**, 169–178.

Franklin KA. 2009. Light and temperature signal crosstalk in plant development. Current Opinion in Plant Biology **12**, 63–68.

Fuhr L, Abreu M, Pett P, Relógio A. 2015. Circadian systems biology: When time matters. Computational and Structural Biotechnology Journal **13**, 417–426.

Fung-Uceda J, Lee K, Seo PJ, Polyn S, De Veylder L, Mas P. 2018. The Circadian Clock Sets the Time of DNA Replication Licensing to Regulate Growth in *Arabidopsis*. Developmental Cell **45**, 101-113.e4.

Gendron JM, Pruneda-Paz JL, Doherty CJ, Gross AM, Kang SE, Kay SA. 2012. *Arabidopsis* circadian clock protein, TOC1, is a DNA-binding transcription factor. Proceedings of the National Academy of Sciences of the United States of America **109**, 3167–3172.

Godfray HCJ, Beddington JR, Crute IR, Haddad L, Lawrence D, Muir JF, Pretty J, Robinson S, Thomas SM, Toulmin C. 2010. Food Security: The Challenge of Feeding 9 Billion People. Science **327**, 812–819.

Gómez C, Izzo LG. 2018. Increasing efficiency of crop production with LEDs. AIMS agriculture and food **3**, 135–153.

Graner A, Bjørnstad S, Konishi T, Ordon F. 2003. Molecular diversity of the barley genome. In: Bothmer R von, Hintum T van, Kntipffer H and Sato K, eds. Diversity in barley (*Hordeum vulgare*). Elsevier Science B.V., Amsterdam, The Netherlands, 121–141.

Greenup AG, Sasani S, Oliver SN, Talbot MJ, Dennis ES, Hemming MN, Trevaskis B. 2010. *ODDSOC2* Is a MADS Box Floral Repressor That Is Down-Regulated by Vernalization in Temperate Cereals. Plant Physiology **153**, 1062–1073.

Hemming MN, Fieg S, James Peacock W, Dennis ES, Trevaskis B. 2009. Regions associated with repression of the barley (*Hordeum vulgare*) *VERNALIZATION1* gene are not required for cold induction. Molecular Genetics and Genomics **282**, 107–117.

Hemming MN, Walford SA, Fieg S, Dennis ES, Trevaskis B. 2012. Identification of High-Temperature-Responsive Genes in Cereals. Plant Physiology **158**, 1439–1450.

Holmes MG, Smith H. 1977. The function of phytochrome in the natural environment - I. Characterization of daylight for studies in photomorphogenesis and photoperiodism. Photochemistry and Photobiology **25**, 533–538.

Huang W, Pérez-García P, Pokhilko A, Millar AJ, Antoshechkin I, Riechmann JL, Mas P. 2012. Mapping the Core of Arabidopsis Circadian Clack defines the network

structure of the oscillator. Science **338**, 75–79.

Hubbard K, Dodd A. 2016. Rhythms of Life: The Plant Circadian Clock. The Plant Cell **28**, 1–10.

Inoue K, Araki T, Endo M. 2018. Circadian clock during plant development. Journal of Plant Research **131**, 59–66.

Johansson M, Staiger D. 2015. Time to flower: Interplay between photoperiod and the circadian clock. Journal of Experimental Botany **66**, 719–730.

Jones H, Leigh FJ, Mackay I, Bower MA, Smith LMJ, Charles MP, Jones G, Jones MK, Brown TA, Powell W. 2008. Population-Based Resequencing Reveals That the Flowering Time Adaptation of Cultivated Barley Originated East of the Fertile Crescent. Molecular Biology and Evolution **25**, 2211–2219.

Karsai I, Igartua E, Casas AM, Kiss T, Soós V, Balla K, Bedo Z, Veisz O. 2013. Developmental patterns of a large set of barley (Hordeum vulgare) cultivars in response to ambient temperature. Annals of Applied Biology **162**, 309–323.

Karsai I, Szucs P, Koszegi B, Hayes PM, Casas AM, Bedo Z, Veisz O. 2008. Effects of photo and thermo cycles on flowering time in barley: A genetical phenomics approach. Journal of Experimental Botany **59**, 2707–2715.

Karsai I, Szucs P, Mészáros K, Filichkina T, Hayes PM, Skinner JS, Láng L, Bedo Z. 2005. The *Vrn-H2* locus is a major determinant of flowering time in a facultative x winter growth habit barley (*Hordeum vulgare* L.) mapping population. Theoretical and Applied Genetics **110**, 1458–1466.

Kikuchi R, Kawahigashi H, Ando T, Tonooka T, Handa H. 2009. Molecular and Functional Characterization of PEBP Genes in Barley Reveal the Diversification of Their Roles in Flowering. Plant Physiology **149**, 1341–1353.

Kiss T, Balla K, Veisz O, Karsai I. 2011. Elaboration of a non-destructive methodology for establishing plant developmental patterns in cereals. Acta Agronomica Hungarica **59**, 293–301.

Kobayashi Y, Kaya H, Goto K, Iwabuchi M, Araki T. 1999. A Pair of Related Genes with Antagonistic Roles in Mediating Flowering Signals. Science **286**, 1960–1962.

Komatsuda T. 2014. Chapter 3. Domestication. In: Kumlehn J and Stein N, eds. Biotechnological Approaches to Barley Improvement. Springer-Verlag Berlin Heidelberg, 37–54.

Langridge P. 2018. Economic and Academic Importance of Barley. In: Stein N and Muehlbauer GJ, eds. The Barley Genome, Compendium of Plant Genomes. Springer, Cham, 1–10.

Langridge P, Waugh R. 2019. Harnessing the potential of germplasm collections. Nature Genetics **51**, 200–201.

Laurie DA, Pratchett N, Snape JW, Bezant JH. 1995. RFLP mapping of five major genes and eight quantitative trait loci controlling flowering time in a winter × spring barley

(*Hordeum vulgare* L.) cross. Genome **38**, 575–585.

Linkosalo T, Lechowicz MJ. 2006. Twilight far-red treatment advances leaf bud burst of silver birch (*Betula pendula*). Tree physiology **26**, 1249–1256.

Más P. 2005. Circadian clock signaling in Arabidopsis thaliana: From gene expression to physiology and development. International Journal of Developmental Biology **49**, 491–500.

Mascher M. 2019. Pseudomolecules and annotation of the second version of the reference genome sequence assembly of barley cv. Morex [Morex V2]. DOI:10.5447/IPK/2019/8

Mascher M, Gundlach H, Himmelbach A, *et al.* 2017. A chromosome conformation capture ordered sequence of the barley genome. Nature **544**, 427–433.

Mascher M, Muehlbauer GJ, Rokhsar DS, *et al.* 2013. Anchoring and ordering NGS contig assemblies by population sequencing (POPSEQ). Plant Journal **76**, 718–727.

Mayer KFX, Waugh R, Langridge P, *et al.* 2012. A physical, genetic and functional sequence assembly of the barley genome. Nature **491**, 711–717.

McClung CR. 2013. Beyond *Arabidopsis*: The circadian clock in non-model plant species. Seminars in Cell and Developmental Biology **24**, 430–436.

Meints B, Cuesta-Marcos A, Fisk S, Ross A, Hayes P. 2016. 3 – Food Barley Quality Improvement and Germoplasm Utilization. In: Zhang G and Li C, eds. Exploration, Identification and Utilization of Barley Germplasm. Academic Press, 41 – 73.

Meng Q, Runkle ES. 2014. Controlling Flowering of Photoperiodic Ornamental Crops with Light-emitting Diode Lamps: A Coordinated Grower Trial. HortTechnology **24**, 702–711.

Miralles DJ, Richards RA, Slafer GA. 2000. Duration of the stem elongation period influences the number of fertile florets in wheat and barley. Australian Journal of Plant Physiology **27**, 931–940.

Molina-Cano JL. 1989. *La cebada. Morfología, fisiología, genética, agronomía y usos industriales*. Ediciones Mundi-Prensa, Madrid.

Monat C, Padmarasu S, Lux T, *et al.* 2019. TRITEX: chromosome-scale sequence assembly of Triticeae genomes with open-source tools. bioRxiv **2**, 631648.

Morrell PL, Clegg MT. 2007. Genetic evidence for a second domestication of barley (*Hordeum vulgare*) east of the Fertile Crescent. Proceedings of the National Academy of Sciences of the United States of America **104**, 3289–3294.

Mulki MA, Bi X, von Korff M. 2018. FLOWERING LOCUS T3 Controls Spikelet Initiation But Not Floral Development. Plant Physiology **178**, 1170-1186.

Mulki MA, von Korff M. 2016. *CONSTANS* Controls Floral Repression by Up-Regulating *VERNALIZATION2* (*VRN-H2*) in Barley. Plant Physiology **170**, 325–337.

Newton AC, Flavell AJ, George TS, *et al.* 2011. Crops that feed the world 4. Barley: a resilient crop? Strengths and weaknesses in the context of food security. Food Security **3**,

141–178.

Oliver SN, Finnegan EJ, Dennis ES, Peacock WJ, Trevaskis B. 2009. Vernalization-induced flowering in cereals is associated with changes in histone methylation at the *VERNALIZATION1* gene. Proceedings of the National Academy of Sciences of the United States of America **106**, 8386–8391.

van Oosterom EJ, Acevedo E. 1992. Adaptation of barley (*Hordeum vulgare* L.) to harsh Mediterranean environments - I. Morphological traits. Euphytica **62**, 1–14.

Powell N, Ji X, Ravash R, Edlington J, Dolferus R. 2012. Yield stability for cereals in a changing climate. Functional Plant Biology **39**, 539–552.

Ruelens P, de Maagd RA, Proost S, Theißen G, Geuten K, Kaufmann K. 2013. FLOWERING LOCUS C in monocots and the tandem origin of angiosperm-specific MADS-box genes. Nature Communications **4**, 2280.

Salome PA, Xie Q, McClung CR. 2008. Circadian timekeeping during early *Arabidopsis* development. Plant Physiology **147**, 1110–1125.

Sato K, Tanaka T, Shigenobu S, Motoi Y, Wu J, Itoh T. 2016. Improvement of barley genome annotations by deciphering the Haruna Nijo genome. DNA Research **23**, 21–28.

Sharma N, Ruelens P, Dhauw M, Maggen T, Dochy N, Torfs S, Kaufmann K, Rohde A, Geuten K. 2017. A Flowering Locus C Homolog Is a Vernalization-Regulated Repressor in *Brachypodium* and Is Cold-Regulated in Wheat. Plant Physiology **173**, 1301–1315.

Smith H. 1982. Light quality, photoperiod, and plant strategy. Annual Review of Plant Physiology **33**, 481–518.

Smith H. 2000. Phytochromes and light signal perception. Nature **407**, 585.

Song YH, Shim JS, Kinmonth-Schultz HA, Imaizumi T. 2015. Photoperiodic Flowering: Time Measurement Mechanisms in Leaves. Annual Review of Plant Biology **66**, 441–464.

Thomas B. 2006. Light signals and flowering. Journal of Experimental Botany **57**, 3387–3393.

Tondelli A, Francia E, Visioni A, *et al.* 2014. QTLs for barley yield adaptation to Mediterranean environments in the 'Nure' × 'Tremois' biparental population. Euphytica **197**, 73–86.

Tottman DR, Makepeace RJ, Broad H. 1979. An explanation of the decimal code for the growth stages of cereals, with illustrations. Annals of Applied Biology **93**, 221–234.

Trevaskis B. 2010. The central role of the *VERNALIZATION1* gene in the vernalization response of cereals. Functional Plant Biology **37**, 479–487.

Trevaskis B. 2018. Developmental Pathways Are Blueprints for Designing Successful Crops. Frontiers in Plant Science **9**, 745.

Trevaskis B, Bagnall DJ, Ellis MH, Peacock WJ, Dennis ES. 2003. MADS box genes

control vernalization-induced flowering in cereals. Proceedings of the National Academy of Sciences of the United States of America **100**, 13099–13104.

Trevaskis B, Hemming MN, Dennis ES, Peacock WJ. 2007. The molecular basis of vernalization-induced flowering in cereals. Trends in Plant Science **12**, 352–357.

Trevaskis B, Hemming MN, Peacock WJ, Dennis ES. 2006. *HvVRN2* responds to day-length, whereas *HvVRN1* is regulated by vernalization and developmental status. Plant Physiology **140**, 1397–1405.

Turner A, Beales J, Faure S, Dunford RP, Laurie DA. 2005. The Pseudo-Response Regulator *Ppd-H1* Provides Adaptation to Photoperiod in Barley. Science **310**, 1031–1034.

Ugarte CC, Trupkin SA, Ghiglione H, Slafer G, Casal JJ. 2010. Low red/far-red ratios delay spike and stem growth in wheat. Journal of Experimental Botany **61**, 3151–3162.

Verstegen H, Köneke O, Korzun V, von Broock R. 2014. The World Importance of Barley and Challenges to Further Improvements. In: Kumlehn J and Stein N eds. Biotechnological Approaches to Barley Improvement. Springer, Berlin, Heidelberg, 3–19.

Waddington SR, Cartwright PM, Wall PC. 1983. A quantitative Scale of Spike Initial and Pistil Development in Barley and Wheat. Annals of Botany **51**, 119–130.

Watson A, Ghosh S, Williams MJ, *et al.* 2018. Speed breeding is a powerful tool to accelerate crop research and breeding. Nature Plants **4**, 23–29.

Webb AAR, Seki M, Satake A, Caldana C. 2019. Continuous dynamic adjustment of the plant circadian oscillator. Nature Communications **10**, 4–9.

Wiegmann M, Maurer A, Pham A, *et al.* 2019. Barley yield formation under abiotic stress depends on the interplay between flowering time genes and environmental cues. Scientific Reports **9**, 6397.

Yan L, Loukoianov A, Blechl A, Tranquilli G, Ramakrishna W, SanMiguel P, Bennetzen JL, Echenique V, Dubcovsky J. 2004. The wheat *VRN2* gene is a flowering repressor down-regulated by vernalization. Science **303**, 1640–1644.

Zadoks JC, Chang TT, Konzak CF. 1974. A Decimal Code for the Growth Stages of Cereals. Weed Research **14**, 415–421.

Zhong HH, Painter JE, Salome PA, Straume M, McClung CR. 1998. Imbibition, but not release from stratification, sets the circadian clock in Arabidopsis seedlings. The Plant cell **10**, 2005–2017.

Chapter

2

FINE-TUNING OF THE FLOWERING TIME CONTROL IN WINTER BARLEY: THE IMPORTANCE OF *HvOS2* AND *HvVRN2* IN NON-INDUCTIVE CONDITIONS

Chapter 2. Fine-tuning of the flowering time control in winter barley: the importance of *HvOS2* and *HvVRN2* in non-inductive conditions

2.1.   Introduction

Tight coordination of flowering time to environmental conditions is crucial for crop reproductive success and has a major impact on yield (Campoli and von Korff, 2014; Digel *et al.*, 2015). Barley (*Hordeum vulgare* L.) and wheat (*Triticum* spp.) are long-day (LD) plants, flowering earlier under increasing day-lengths. Depending on their growth habit, cereals are classified as winter or spring. Winter cereals need a period of exposure to low temperature (vernalization), which must be completed in a timely manner so the plant is prepared to take full advantage of the induction of flowering by long days (Trevaskis, 2010). This requirement could make winter cereals more susceptible to climate change, since the probability of accumulating enough cold hours will likely decrease in warming winters. Winter barley varieties are sown in autumn, benefiting from the warmth of the soils and the humidity from autumn rains, which are essential at the beginning of the cycle. In the Mediterranean region, they have to survive a range of mild to harsh winters, and then flower sufficiently early in the spring to avoid the heat and drought of late spring or early summer. Barley ideotypes for future climatic conditions in Europe must present combinations of vernalization requirement and photoperiod responses tuned to the needs of each specific region (Tao *et al.*, 2017). For this reason, plant breeding for upcoming conditions demands comprehensive studies on the effect of photoperiod on major flowering genes, and their interaction with the vernalization pathway. In this regard, special emphasis should be given to environmental conditions closer to natural ones, as it is not known "whether the current model of photoperiodic flowering regulation can recapitulate the seasonal flowering mechanisms in complicated natural LD environments" (Song *et al.*, 2018).

The accepted gene model for vernalization-responsive varieties establishes that, during winter, cold exposure upregulates the floral promoter *HvVRN1*, which is required to downregulate the flowering repressor *HvVRN2*, allowing expression of the flowering inducer *HvFT1* in leaves (Distelfeld *et al.*, 2009). *HvVRN2,* a *ZCCT-H* gene, is member of the *CONSTANS*-like gene family, which delays flowering until plants have satisfied their cold needs (Yan *et al.*, 2004). Winter barleys have the dominant variant, whose expression is highly dependent on day-length, being induced in long days (Karsai *et al.*, 2005; Trevaskis *et al.*, 2006). *HvVRN1* encodes an *AP1*-like MADS-box transcription factor (Danyluk *et al.*, 2003; Trevaskis *et al.*, 2003; Yan *et al.*, 2003). It presents several alleles as a result of deletions or insertions in the first intron, associated with different degrees of vernalization requirement (Hemming *et al.*, 2009). In winter barley, *HvVRN1* is expressed after exposure to low-temperatures (Von Zitzewitz *et al.*, 2005; Sasani *et al.*, 2009), although it can be activated by other pathways such as the developmental pathway, with a marked delay compared with induction by vernalization (Trevaskis *et al.*, 2006). Induction of *HvVRN1* is related to changes in the pattern of histone methylation, whose maintenance provides a memory of cold exposure in winter barley plants (Oliver *et al.*, 2009). This general mechanism is well established; however, important questions remain open. For instance, what are the precise environmental cues that govern the dynamics of this process? A second open question is which additional genes may play important roles in the vernalization pathway. In this respect, Bouché *et al*. (2017) remarked that much remains to be learned about this process, including identifying additional components, beyond the *VRN1*/*VRN2* system. Indeed, there are phenotypic differences in vernalization effect among winter cultivars sharing *HvVRN1*/*HvVRN2* haplotypes that are still unexplained (Rizza *et al.*, 2016). For instance, it has been suggested that additional genes may be acting as regulators of *VRN2* when exposed to cold (Chen and Dubcovsky, 2012; Sharma *et al.*, 2017). Some genes are good candidates to play a

role in the vernalization pathway, like *ODDSOC2* (in barley, *HvOS2*), the monocot ortholog of *Arabidopsis thaliana FLOWERING LOCUS C* (*FLC*). This gene is a flowering repressor also downregulated by vernalization in barley (Greenup *et al.*, 2010) and *Brachypodium distachyon* (Ruelens *et al.*, 2013), probably caused by binding of VRN1 to its promoter region (Deng *et al.*, 2015).

HvFT3, a FT-like member of the PEBP family, and candidate gene for *PPD-H2* (Faure *et al.*, 2007; Kikuchi *et al.*, 2009), it was described as a promoter of flowering under short days (SD) in winter cultivars (Laurie *et al.*, 1995; Casao *et al.*, 2011*a*), particularly under Mediterranean conditions (Cuesta-Marcos *et al.*, 2008; Casao *et al.*, 2011*b*; Borràs-Gelonch *et al.*, 2012). Its role has been recently clarified specifically controlling spikelet initiation, but not floral development (Mulki *et al.*, 2018).

The photoperiod response regulator gene *PPD-H1*, also known as *HvPRR37* (Campoli *et al.*, 2012) determines the sensitivity to LD (Turner *et al.*, 2005), and accelerates flowering mediating the induction of *HvFT1*, in winter cultivars after vernalization is fulfilled. There is also evidence of the involvement of several members of the family of *CONSTANS*-like genes in the vernalization and photoperiod pathways. *CO1* and *CO2* are LD-flowering promoters modulated by circadian clock and day-length (Griffiths *et al.*, 2003; Nemoto *et al.*, 2003). In wheat, CO2 competes with VRN2 to bind the NF-Y proteins, in a mechanism to integrate environmental cues through regulation of *HvFT1* (Li *et al.*, 2011). Another member of this family, *HvCO9* (or *HvCMF11* in Cockram et al., 2012) is a paralog of *HvVRN2* (Higgins *et al.*, 2010), and has been identified as a negative regulator of flowering, whose expression has been reported under non-inductive SD conditions (Kikuchi *et al.*, 2012).

This study focuses on the identification of factors (genes and environmental conditions) responsible for repression of flowering in winter barley. Previous

studies have demonstrated that *HvVRN2* expression needs induction by long days (Trevaskis *et al.*, 2006), but the exact day-length that triggers this gene is unknown, as most studies have been performed in growth chambers, under fixed photoperiods. This question is relevant from the agronomic point of view. Song *et al*. (2018) highlighted the importance of optimizing controlled conditions to reflect closely the natural environments. Thus, our approach was addressed trying to mimic the photoperiod conditions in natural Mediterranean environments. We hypothesize that there is a vernalization window for satisfying the cold requirement, in order to make the plant competent to flower at the right time and achieve a good yield. In the experiments presented here, the first objective was to determine the day-length threshold leading to induction of the repressor *HvVRN2*. A second objective was to characterize further the role of other possible inducers and repressors of flowering under incomplete or null vernalization. We investigate the effects of photoperiod on the transcript levels of selected genes in winter barley, by examining photoperiod responses in the medium-long term (21 – 90 days) in two winter cultivars, 'Hispanic' and 'Barberousse', that present different adaptation patterns (Igartua *et al*., 1999; Mansour *et al*., 2018). Our final aim was to provide new information on the complex mechanism of flowering in suboptimal conditions, to facilitate breeding for present and future climate conditions.

2.2. Methods

2.2.1. Plant materials

Two winter cultivars, representative of barleys grown in Spain, with adaptation patterns likely related to differences in vernalization requirement (Igartua *et al*., 1999; Mansour *et al*., 2018), were studied. 'Barberousse' (six-rowed, ('Hauter' × ('Hatif de Grignon' × 'Ares')) × 'Ager') is an old French cultivar developed by Ringot and registered in 1977, well adapted to the coldest areas of Spain. 'Hispanic'

(two-rowed, 'Mosar' × ('Flika' × 'Lada')) is a French commercial cultivar developed by Florimond Desprez and registered in 1993, showing broad adaptation in Spain, and even acceptable agronomics in the Nile delta (Mansour *et al.*, 2018). Both cultivars were multiplied in isolation at the EEAD-CSIC farm, collected from bagged spikes, from original seed provided by the companies. They have the same allelic combination in *HvVRN1* (winter allele), *HvVRN2*, and *PPD-H1*, but differ in *HvFT1* and *HvFT3* (*PPD-H2*, present in 'Hispanic', defective allele in 'Barberousse') (Mansour *et al.*, 2018).

2.2.2. Plant growth, phenotyping and sampling

2.2.2.1. Experiment 1 – Sowings under increasing natural photoperiod

For each variety, we used two 1L-pots at each sowing time (standard substrate made of peat, fine sand and perlite, from a mix with 46 kg, 150 kg and 1L, respectively). Pots were sown with 7 seeds once a week, sequentially, from Feb 11th until April 8th 2015, in a glasshouse in Zaragoza (41°43'N, 00°49'W) under natural photoperiod (Figure 2.1) and controlled temperature (22±1°C day / 18±1°C night). Unless specified, plants were not vernalized (NV). Spatial homogeneity in irradiance was obtained rotating the plants each week. As vernalized control, three pots of each variety were sown on Feb 11th. They were grown during 7 days (until germination) under glasshouse conditions, and then were vernalized (VER) under short photoperiod (8 h light) and 6 ± 2°C for 49 days. After the cold treatment, plants were transferred to the same glasshouse on April 8th, when natural photoperiod was 13 h. Duration of daylight at sowing and sampling dates was gathered from http://www.timeanddate.com/sun, taking sunrise and sunset as the times when the upper edge of the Sun's disc touches the horizon.
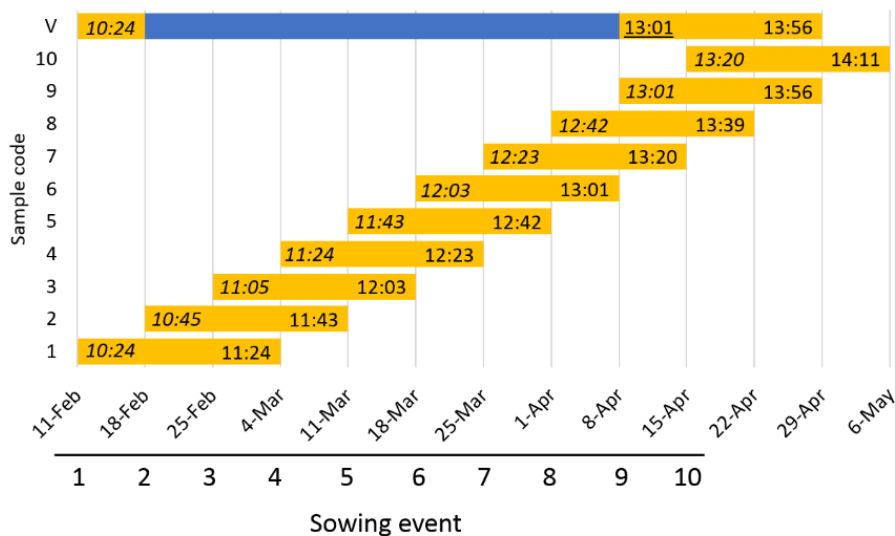
Figure 2.1. Experiment planning. Each sowing and its sampling are represented. Yellow bars show the time that plants were kept under non-vernalized conditions. Blue bar shows the time spent in the vernalization chamber. X-axis represent dates of start of experiment and sampling date (three weeks after sowing). The second numbers inside the yellow bars are the day-length at sampling date (HH:MM). The first numbers in italics represent day-length at sowing day, and underlined numbers are day-length in the shift day (vernalized plants were transferred to glasshouse). Sunrise and sunset are the times when the upper edge of the Sun's disc touches the horizon.

For gene expression, the last expanded leaf of three 21-day-old plants (3-leaf stage) was sampled 8 h after dawn, frozen in liquid nitrogen, homogenized (Mixer Mill model MM301, Retsch) and conserved at -80°C until RNA isolation.

On a fixed date (19th May, day-length 15 h, 97 days after the first sowing), we took a cross-sectional sample across sowing events. The last expanded leaf of each weekly-sown plant was sampled 12 h after dawn for RNA isolation. Then, dissection of the plants (all stems of each plant) was made in order to determine the development of the apex (with naked eye, reproductive apex was equivalent to more than 3 mm).

2.2.2.2. Experiment 2 – Growth chamber, 12 h light

Seventy-two seeds of each variety were sown in 12-well trays (650 cc) and allowed to germinate during 7 days in a growth chamber at 12 h light, 20°C/12 h dark, 16°C, 65% HR and light intensity of 300 µmol m^{-2}s^{-1} PAR. Then, the trays were divided in three groups that received the following treatments: (A) NV, (B) 14-days VER and (C) 28-days VER. Group A stayed at the growth chamber while B and C were transferred to a vernalization chamber, 8 h light/16 h night and constant temperature (6 ± 2°C). Groups B and C were returned to the growth chamber after 14 and 28 days of cold treatment, respectively. After forty days at the growth chamber, three plants of each variety and treatment were transferred to a 1L pots to let them grow until flowering. Development according to the Zadoks scale (first node, DEV31, and awns appearance DEV49) (Zadoks *et al.*, 1974) was recorded along the experiment every 3-5 days. In addition, apex dissections were carried out at selected time points to establish the Waddington developmental stage (Waddington *et al.*, 1983). The experiment ended 136 days after sowing.

For gene expression, the last expanded leaf of four plants was sampled 14, 28, 35 or 49 days after germination (A) or after the end of the VER treatment (B and C), 10 hours into the light period (2 hours before the end of the day, as in Mulki and von Korff, 2016; Mulki *et al.*, 2018).

Even though a single point may not be reflective of expression at other times during the day, in all the experiments, sampling times were chosen to capture high expression of the genes involved, taking into account the period and amplitude of their circadian rhythms. *HvVRN2* expression was tested in leaf samples, taken at different times along the light period in 'Barberousse' plants (28 days old, and 16 h light) (Figure S 2.5), with high and comparable expression levels throughout the day.

2.2.2.3.   Vernalization response of 'Hispanic' and 'Barberousse'

In the course of earlier experiments, carried out in the Phytotron of Martonvásár (Hungary), both varieties were exposed to different VER treatments (0, 15, 30 or 45 days, $5\pm2°C$, 8 h light), and then transferred to a growth chamber with 16 h day-length, $18°C$ and light intensity of $340\ \mu mol\ m^{-2}\ s^{-1}$. Flowering date was recorded at each treatment (Figure S 2.1).

2.2.3.   Gene expression analysis

RNA extraction was carried out using NucleoSpin RNA Plant Kit (Macherey-Nagel) following manufacturer instructions. Total RNA ($1\mu g$) was employed for cDNA synthesis using SuperScript III Reverse Transcriptase (Invitrogen) and oligo $(dT)_{20}$ primer (Invitrogen). Real-time PCR quantification (ABI 7500, Applied Biosystems) was performed for samples from each time point from NV plants and for VER plants as control treatment. Three biological replicates and two technical replicates were performed per sample and pair of primers (*HvVRN1*, *HvVRN2*, *PPD-H1*, *HvCO2*, *HvCO9*, *HvOS2, HvFT1*, and *HvFT3*). Primer sequences and conditions are specified in Table S 2.5. Expression levels were normalized to *Actin* expression, taking into account primer efficiencies.

2.2.4.   Gene sequencing

Polymorphisms in *HvCO2*, *HvCO9* and *HvOS2* were identified by sequencing genomic DNA PCR-amplified overlapping fragments. Primers were designed to amplify each gene (Table S 2.5). The resulting sequences have been deposited at the European Nucleotide Archive as part of project PRJEB27962. BLASTN sequence comparisons (Altschul *et al.*, 1990) were carried out against the barley 'Morex' reference genome (Mascher *et al.*, 2017), and 'Morex', 'Barke' and 'Bowman' whole genome barley sequences (Mayer *et al.*, 2012) at the IPK

(http://webblast.ipk-gatersleben.de/barley_ibsc/) web server. Sequence comparisons against NCBI nucleotide database, cv. 'Haruna Nijo' (Sato *et al.*, 2016) and cv. 'Zangqing320' genomic sequences (Dai *et al.*, 2018) were also performed. Sequence alignments were carried out in MEGA-X v.10.0.4 (Kumar *et al.*, 2018). Predicted protein alignments were carried out in ClustalW (Larkin *et al.*, 2007). Protein domains were annotated according to Cockram *et al*. (2012), Greenup *et al*. (2010) and Prosite v20.79 (http://prosite.expasy.org/). The online tool SIFT (http://sift.bii.a-star.edu.sg) was used to predict the likely impact of amino acid substitutions on protein function, using as reference 'Morex' (Mascher *et al.*, 2017). Scores below 0.05 are predicted to affect protein function. Putative VRN1 regulatory elements were predicted by scanning a motif compiled from ChIP-seq peaks reported in Deng *et al*. (2015) and annotated in http://floresta.eead.csic.es/footprintdb/index.php?motif=VRN1&db=EEADannot (Sebastian and Contreras-Moreira, 2014). Briefly, upstream sequences of target barley genes were retrieved from the RSAT plant mirror (http://plants.rsat.eu, Nguyen *et al*., 2018) and *matrix-scan-quick* used to scan the motif using a genomic Markov model of order 2 (upstream-noorf_Hordeum_vulgare.IBSCv2.37). Only sites with weight >= 3.7 were considered.

2.2.5. Statistical analysis

Statistical analyses were carried out with R software (R Core Team, 2017). For gene expression results, the mean of two technical replications of ΔCt (Ct actin − Ct target) was used as unit. Analyses of variance for phenotypes or gene expression data were performed considering all factors (genotype, sampling time, vernalization treatment) as fixed. Multiple comparisons were obtained by Fisher's protected Least Significant Differences (LSD) with the R package 'agricolae' (de Mendiburu, 2016). Pearson correlations were carried out with 'cor' function.

2.3.   Results

Both 'Hispanic' and 'Barberousse' responded to vernalization, with a marked acceleration of development as the cold period applied increased from 0 to 45 days with day-length of 16 h (Figure S 2.1). There were also overall differences in earliness.

2.3.1.   Gene expression under increasing natural photoperiod

In order to determine the day-length threshold that induces the expression of *HvVRN2*, experiment 1 involved sequential sowings in a greenhouse, one week apart. Natural day-length at sampling (for 21-day-old plants) increased from ~11 h 30 min at the first sowing to ~14 h at the 9th sowing event, and also for the VER control (Figure 2.1).

Surprisingly, expression of *HvVRN2* was detected at all time points, in plants both 14 and 21 days old. It was low in the first sowings, which were grown under shorter photoperiods (Figure 2.2). Between 12 and 13 h photoperiods, corresponding to the end of March in our latitude, the levels of *HvVRN2* increased in both genotypes. At 21 days, there were significant differences in *HvVRN2* expression between genotypes and sowings, without interaction between them (Table S 2.1), indicating similar pattern of responses across genotypes. A contrast between the four earliest sowings (1-4) *vs* the five latest (5-9) explained as much as 78% of the variation between sowings, rendering the remaining variance (genotypes by sampling point, within day-lengths groups), non-significant (Table S 2.2A). Therefore, the surge in expression between sowings 4 and 5 is the main factor affecting *HvVRN2* expression for both genotypes. This same trend was also detected in 14-day-old plants, with slightly lower expression values overall (Figure S 2.2).

Expression of *HvCO2* increased in both genotypes up to sowing 4. Then, it decreased to very low levels, not rising again until sowing 8 and 9. The main change

in expression patterns occurred again between sowings 4 and 5, for both genotypes (Table S 2.2B).

HvVRN1 expression was detected only in VER plants (Figure 2.2), and *HvFT1* was not detected in any sample at this stage (data not shown). Without vernalization, neither genotype showed expression of *HvFT3* (Figure 2.2). This was expected for 'Barberousse', as it has the null allele, but we did not anticipate this result for 'Hispanic'. In this genotype, the expression levels were below the detection limit, except for VER plants.

In general, 'Barberousse' presented higher *HvOS2* expression levels than 'Hispanic' (Table S 2.1), except for the last samplings, when *HvOS2* expression was barely detectable in both genotypes (Figure 2.2). Expression of *HvCO9* was low and variable, with no observable trends for any genotype. *PPD-H1* expression showed fluctuations in expression apparently independent from genotypes.

At the end of the experiment (May 19th, with 15 h of light), the number of apices at reproductive stage per plant was recorded (Figure S 2.3). 'Hispanic' plants were more developed than 'Barberousse's. Among NV plants, only the second sowing event of 'Hispanic' reached the stage Z49 (first awns visible) at the end of the experiment (83 days after sowing). No data were available for the first sowing at that moment, as plants were dissected earlier, again with only 'Hispanic' showing reproductive apices after 72 days. At termination, VER 'Hispanic' and 'Barberousse' plants also showed apices at reproductive stage, 'Barberousse' more delayed than 'Hispanic'.
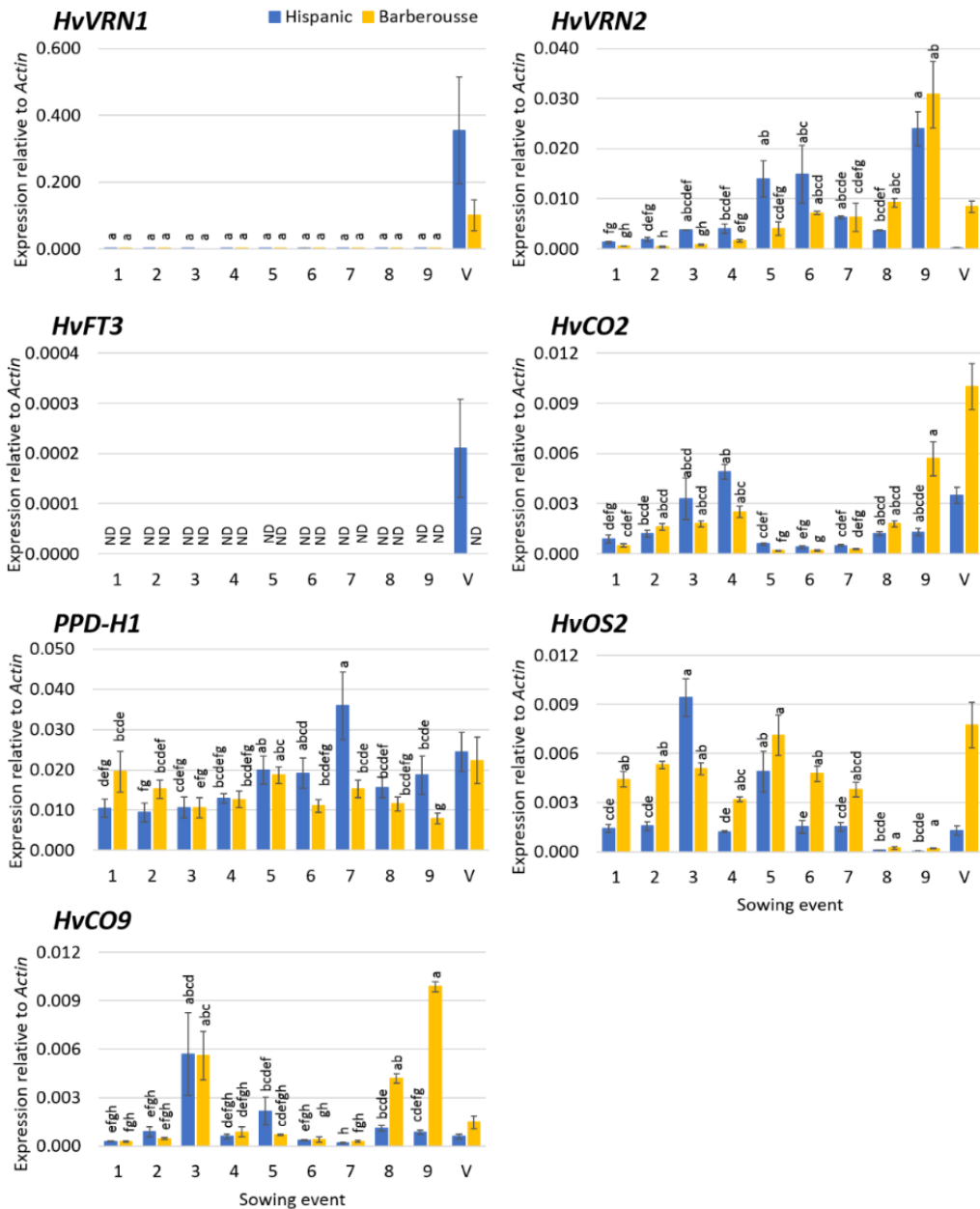
Figure 2.2. Gene expression three weeks after sowing, in the natural photoperiod experiment.

X-axis represent the successive sowings, from 11th February until 8th April. Unvernalized plants (sowings 1 to 9) and vernalized control (V) of 'Hispanic' (blue) and 'Barberousse' (yellow) are *(Continue)* plotted. Mean of 3 biological replicates. Error bars are SEM. ND, Not detected. *HvFT1* expression is not reported as it was null for all non-vernalized

samples. For each NV time-point, bars with the same letter are not significantly different at P<0.05 according to ANOVA that included genotypes and all sampling times.

Expression levels on this same date were analysed (Figure 2.3, Table S 2.3), across all sowings. For all NV plants, flowering promoters (*HvVRN1*, *HvFT1* and *HvFT3*) were induced only in 'Hispanic' oldest plants, at the first point available (sowing event 2), and were not expressed in 'Barberousse', in full accordance with apex development. Concurrently, in plants from sowing 2, repressors *HvVRN2* and *HvOS2* were down-regulated in 'Hispanic', and induced in 'Barberousse'.

2.3.2. Gene expression affected by plant age and length of vernalization treatment

Experiment 1 made evident that gene expression was dependent on the plant's developmental stage (Figure 2.3). Therefore, for some genes, induction was dependent on plant age. A second experiment was conceived, to assess the relevance of other factors on gene expression, namely day-length, plant age and degree of vernalization. Thus, we set the day-length at 12h, representative of day-length around the start of stem elongation in natural conditions in our region, and short enough not to elicit LD responses. This was combined with increasing yet insufficient vernalization.
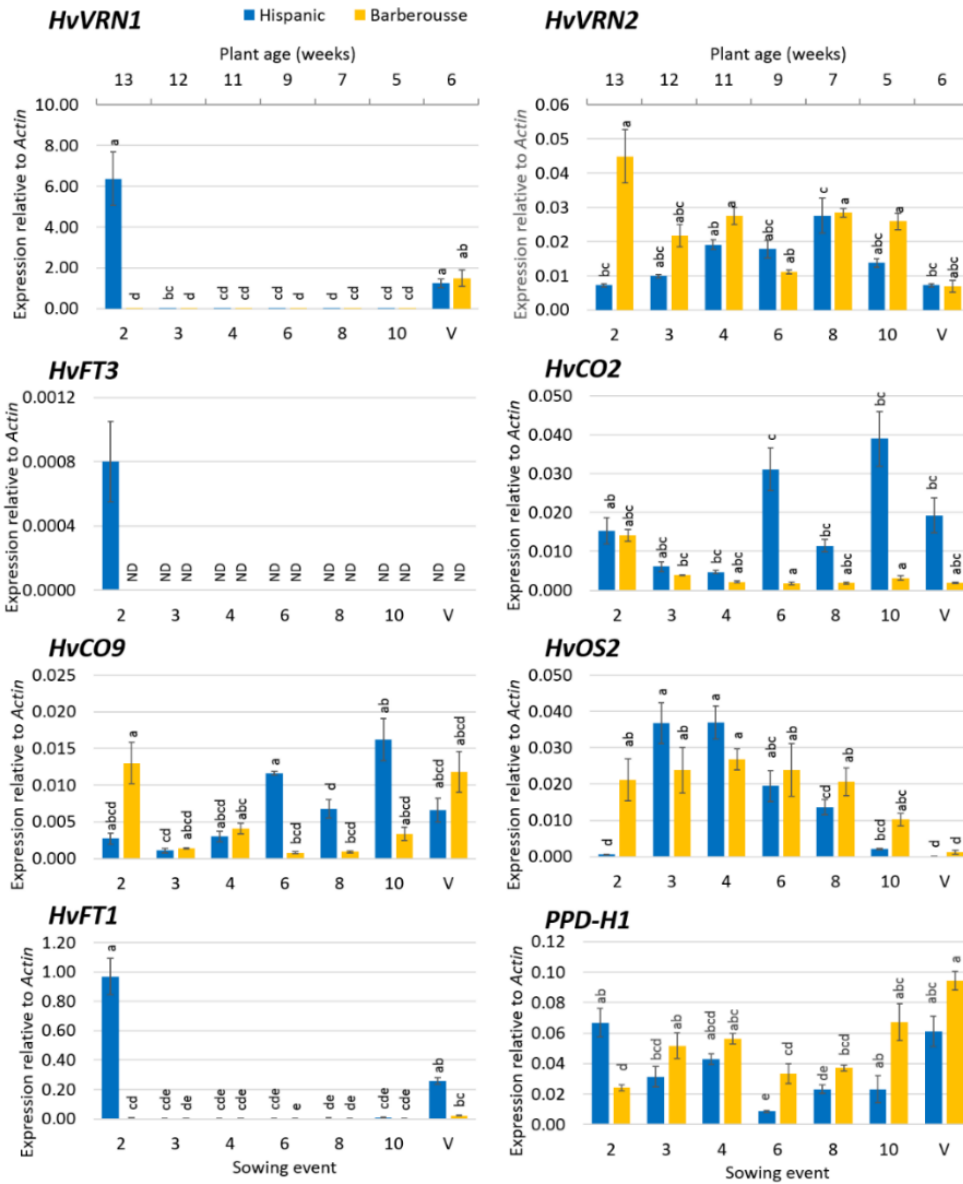
Figure 2.3. Cross-sectional gene expression under 15 h of natural daylight of the sequential sowings under natural photoperiod experiment.

X- upper axis represent the weeks after sowing of unvernalized plants.

Control plants (V) were maintained under natural photoperiod for 6 weeks after 49 days of vernalization. Mean of 3 biological replicates. Error bars are SEM. For each sampling time-point and genotype, bars with the same letter are not significantly different at $P < 0.05$ according to ANOVA that included all factors.

● ● ●

Time to awn tipping was shortened in an inversely proportional manner to the duration of the VER treatment (Figure 2.4). NV 'Hispanic' plants reached awn tipping (DEV49) after 126 days, whereas 'Barberousse' did not reach that stage during the entire duration of the experiment (136 days). Plants from both VER treatments reached DEV49 before the NV plants did. Most of this shortening occurred in the period until first node appearance (DEV31), although some additional acceleration was observed between DEV31 and DEV49.

Expression analysis showed higher *HvVRN1* induction the longer the VER duration in both varieties (Figure 2.5, Table S 2.4). Concurrently to the larger expression of *HvVRN1, HvVRN2* was repressed, as expected. Expression of *HvCO9* and *HvOS2* was also reduced with increasing VER. These three repressors showed higher levels in 'Barberousse' than in 'Hispanic' (Figure 2.5), which is in accordance with the delayed flowering of 'Barberousse' (Figures 2.4 and 2.6). A similar pattern of expression of *HvCO2* and *HvFT1* was observed (r = 0.61). Expression of *HvCO2* was markedly higher at 49 days, with an overall trend of increase with plant age (Figure 2.5).
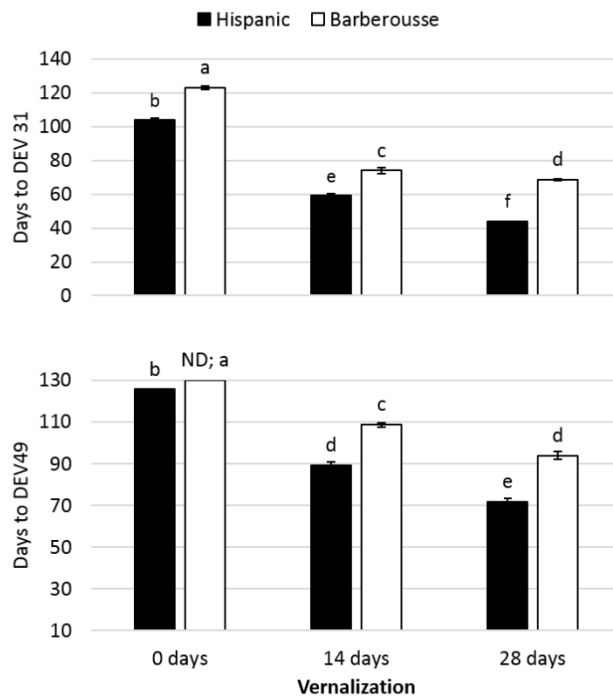
Figure 2.4. Days to appearance of first node (DEV31) and awn-tipping (DEV49) in plants grown under 12 h light, in response to different vernalization treatments.
Error bars are SD. For each genotype and treatment, bars with the same letter are not significantly different at P<0.05.
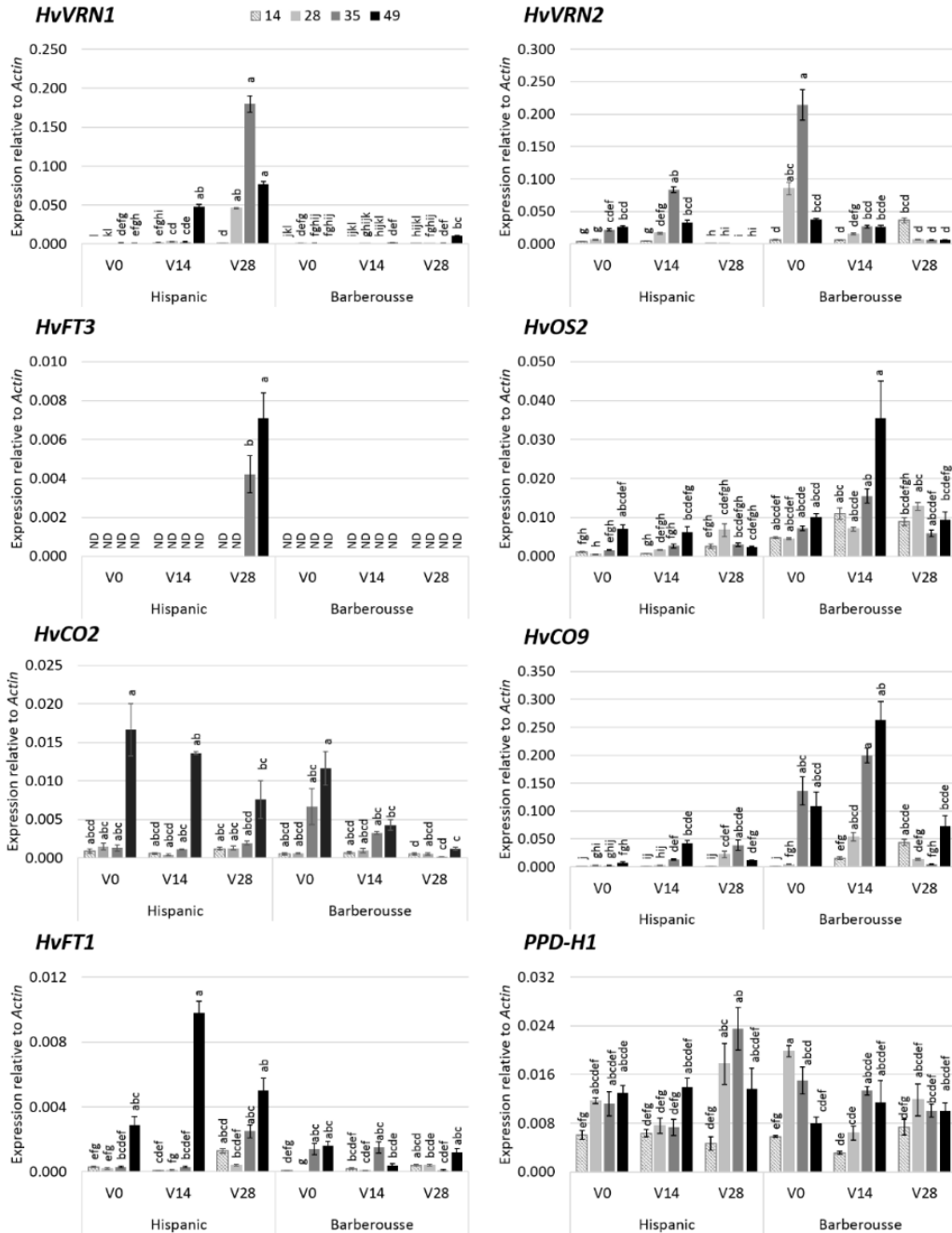
Figure 2.5. Gene expression under 12 h daylight in growth chamber.
X-axis represent days of vernalization chamber. Increasing grey scale is the days after the end of the vernalization treatment when leaves were sampled (14, 28, 35 or 49 days). *(Continue)*

Mean of 3 biological replicates. Error bars are SEM. For each genotype, treatment and sampling time-point, bars with the same letter are not significantly different at $P < 0.05$ according to ANOVA that included all factors.

HvFT3 transcript levels were present in 'Hispanic', only after plants where 28-days VER, and concurrent with a total absence of *HvVRN2*.

The increased expression levels of the flowering promoter genes and the decreased levels of the flowering repressors (Figure 2.5) across treatments and genotypes agree with the patterns of development observed (Figure 2.6). Four weeks after vernalization, apex transition from vegetative to reproductive stage (from W2 to W3; Figure 2.6A), occurred only in 'Hispanic' VER 28 days plants. 'Barberousse' apices at all treatments, and 'Hispanic', VER 0 or 14 days, only reached this stage much later in time (Figure 2.6B).
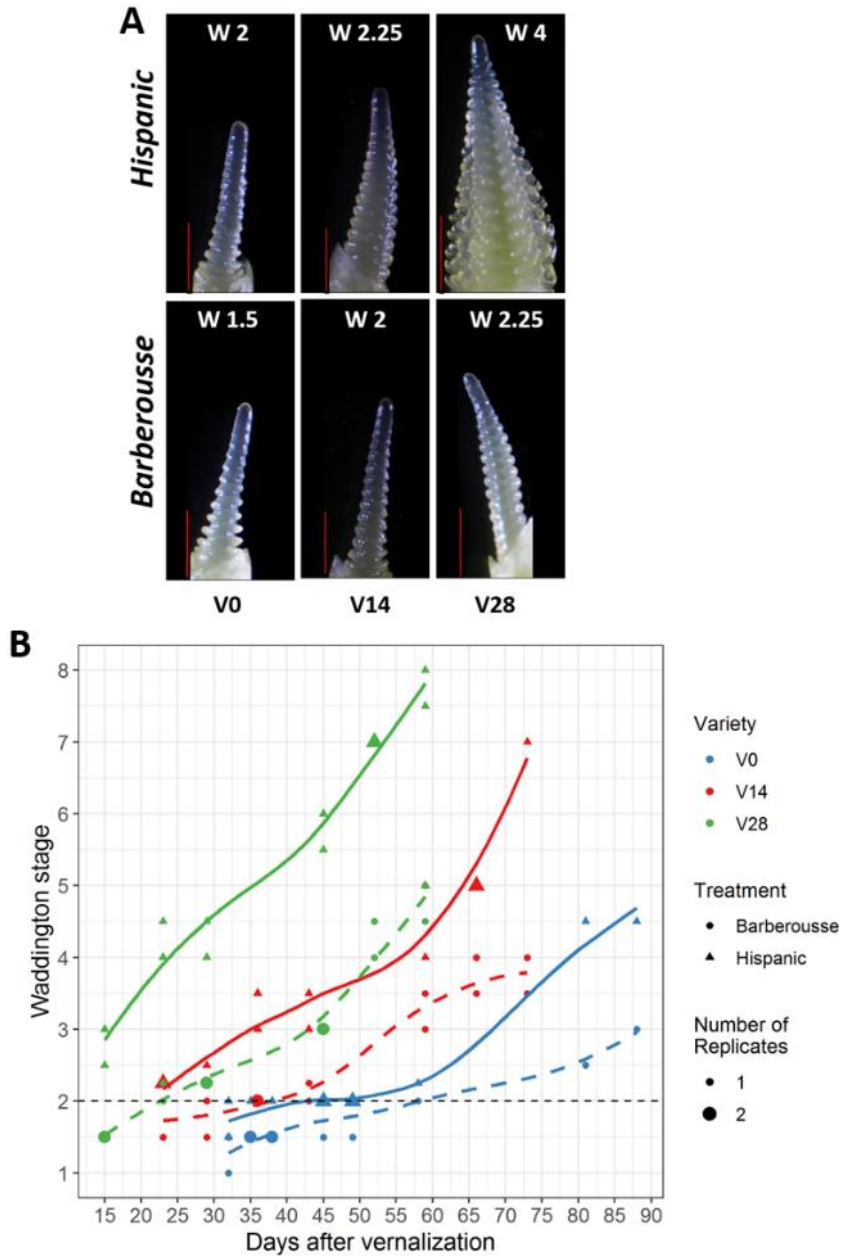
Figure 2.6. Apex dissection of plants grown under 12h light.

A) 4 weeks after each vernalization treatment. Red bar is 500 µm. B) Apex development over time after different vernalization durations. Solid lines correspond to 'Hispanic' and dashed lines to 'Barberousse'. The size of each dot represents the number of apices (biological replicates) at that Waddington stage. Black dashed horizontal line marks WD2: the double ridge stage, considered as transition from vegetative to reproductive phase.

2.3.3.   Sequence polymorphisms of *HvCO2*, *HvCO9* and *HvOS2* between 'Barberousse' and 'Hispanic'

We analyzed the complete nucleotide sequences of 'Barberousse' and 'Hispanic' for the genes *HvCO2*, *HvCO9*, and partial sequences for *HvOS2*, searching for polymorphisms that may affect protein function or regulation of expression. There were coding sequence polymorphisms between the two cultivars in all three genes (Tables S 2.6-S 2.8, weblinks in page 66). The SNPs found in *HvCO2* were synonymous (Figure 2.7A) and, therefore, unlikely to be related to functional differences. Alignment of our sequences against 'Morex' (AF490470) and 'Igri' (AF490469) *HvCO2* alleles in public databases revealed two non-synonymous SNPs (T74A, A239T), but were unlikely to alter protein function (SIFT scores of 1.00 and 0.47, respectively, Figure S 2.4A).
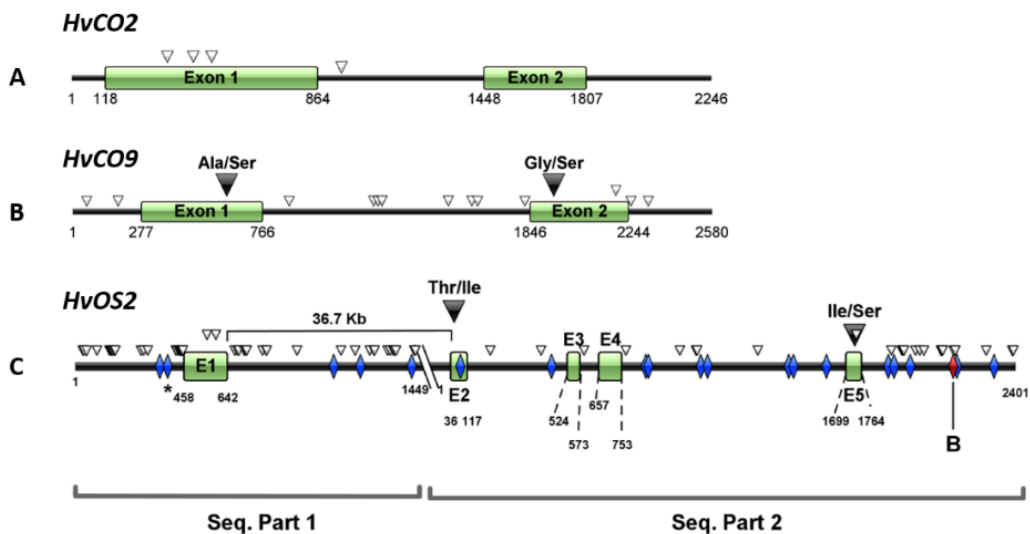
Figure 2.7. Gene sequences of A) *HvCO2*, B) *HvCO9* and C) *HvOS2*, and polymorphisms between 'Barberousse' and 'Hispanic'.
White triangles: synonymous change of aminoacid or intron variant. Black triangles: non-synonymous polymorphism. Diamonds: predicted VRN1-target sites (Deng *et al.*, 2015). Blue diamonds: sites are conserved. Red diamonds, sites appear only in 'Barberousse' (B) or 'Hispanic' (H).

Three SNPs were found in the coding sequence of *HvCO9* between 'Barberousse' and 'Hispanic', two of them non-synonymous (Figure 2.7B). Both substitutions (S116A, S196G) could affect protein function (SIFT scores of 0.00 and 0.02, respectively). The peptide sequence of domain CCT was invariable in these two lines, also when compared to 'Morex' (AB592332) and 'Steptoe' (AB592331) (Figure S 2.4B). According to the SNPs found, 'Barberousse' was like 'Steptoe' and 'Hispanic' as 'Morex' (Table S 2.7).

The sequence of *HvOS2* was split in two parts. The first one comprises part of the upstream region, exon 1 and the beginning of intron 1 (~ 800 bp out of 36.7 kb). The second part contains 35 bp at the end of intron 1, and coding and non-coding regions from remaining exons 2 to 5 (Figure 2.7C). Five SNPs were found within the coding sequence, with two causing amino acid substitutions (T66I and I150S). The second one, found in 'Hispanic' and 'Igri', another winter cultivar (Figure S 2.4C), could affect protein function (SIFT scores of 1.00 and 0.00, respectively). The MADS-box domain was invariable. A high number of predicted VRN1 regulatory sites where identified throughout the gene sequence. The upstream region and intron 1 showed several polymorphisms, which could affect regulation of *HvOS2*, apart from VRN1 regulatory sites (Figure 2.7C, Table S 2.8).

2.4.   Discussion

The main purpose of our study was to shed light on the genes affecting development of winter barley before they receive full vernalization. This is an understudied area in barley and other cereals, and its knowledge may open new opportunities for fine-tuning the development of new cultivars to the expected winter temperatures. Vernalization and photoperiod pathways in winter cereals and *Brachypodium* are remarkably similar (Higgins *et al.*, 2010; Trevaskis, 2010; Campoli and von Korff, 2014; Bouché *et al.*, 2017; Sharma *et al.*, 2017). This proximity has allowed a direct

translation of knowledge regarding genes and mechanisms between species (Song *et al.*, 2015; Bouché *et al.*, 2017; Woods *et al.*, 2019). Therefore, any progress made in barley will be easily transferred to other crop species, like wheat. The experiments were performed under controlled conditions, carefully chosen to respond to questions that arise when barley is grown under natural conditions. The complexity found is challenging, leading to new questions but, on the other hand, brings attention to the richness of responses within winter barleys that result from the interplay of several genes.

2.4.1. Expression of *HvVRN2* is upregulated beyond 12 h 30 min natural daylight in absence of vernalization

Under typical autumn sowings, winter barley is capable of responding to long photoperiods only after fulfilling a variety-specific low temperature requirement. Current accepted hypotheses indicate that *HvVRN1* is gradually induced under SD and low temperature conditions, and then represses *HvVRN2* to promote flowering. In addition, that *HvVRN2* expression is triggered by LD (16 h light) and downregulated in SD (8 h light), to almost complete repression (Trevaskis *et al.*, 2006).

Surprisingly, we found expression of *HvVRN2,* even if at low levels, in NV plants under natural SD (sowings 1-4 in experiment 1). This finding opens the possibility that *HvVRN2* may have an effect in autumn sowings, prior to its downregulation by *HvVRN1*. Although it was not expected, some recently published experiments agree with this result. Research in *Brachypodium* found low expression of the *HvVRN2* orthologue in short days, with level of expression dependent on day-length (Woods *et al.*, 2019). In barley, expression of *HvVRN2* under SD, caused by overexpression of *HvCO2*, has also been reported (Mulki and von Korff, 2016). Sampling time was not optimum for *HvCO2* in our experiments, since this gene is expressed mainly

during the night (Turner *et al.*, 2005; Campoli *et al.*, 2012). Accordingly, the levels of *HvCO2* expression detected in our study were low. This notwithstanding, we observed shifts in its expression, concurrent with changes in *HvVRN2* expression, which confirm their connection as hypothesized by Mulki and von Korff (2016). *HvVRN2* gene expression remained low until a surge around sowing event 5 (Figure 2.2), coincident with an increase of natural daylight between 12 - 13 h (end of March), and a concurrent change of pattern of expression of *HvCO2*, responding to photoperiod cues, in unvernalized conditions. We propose that these events indicate an important shift in gene expression patterns in winter barleys, which could have an effect in plant development. In this sense, Karsai *et al.* (2006) also found a heading date QTL, co-locating with *HvVRN2*, but only when day-length exceeded 12 hours, although it is possible that the vernalization period of 42 days provided in that experiment was not enough to fulfil the needs of all those plants. This is more evidence that the role of an active *HvVRN2* allele has observable phenotypic consequences at around 12 h of day-length.

The control of these two genes has been linked to *PPD-H1*. Mulki and von Korff (2016) presented evidence of a feedback loop, between *HvVRN2* and *PPD-H1*, whereas the induction of *HvCO2* by *PPD-H1*, proposed in the past (Campoli and von Korff, 2014), is currently questioned (Chen *et al.*, 2014; Song *et al.*, 2015). A competition between VRN2 and CO2 proteins for binding to NF-Y proteins has been reported (Li *et al.*, 2011), which is consistent with the feedback loop described by Mulki and von Korff (2016) for non-vernalized plants. *PPD-H1* shows a broad expression peak around 12 h of light in LD (Turner *et al.*, 2005; Campoli *et al.*, 2012). Consequently, to reach maximum expression levels, days of 12 h or longer are required. The gradual increase of expression of *HvCO2* and *HvVRN2* with longer days observed in our study is consistent with their position downstream of *PPD-H1*. The tipping point at 12 h 30 min actually agrees with the date when natural day-length surpasses the maximum expression threshold for *PPD-H1*.

● ● ●

2.4.2.   Earliness differences between two unvernalized winter genotypes are not due to *HvVRN2* levels

The comparison of the two unvernalized winter cultivars showed a faster early development of 'Hispanic', as revealed by differences in pace of apex development. In both experiments 'Hispanic' developed or flowered always earlier than 'Barberousse'. Differences in *HvVRN2* expression cannot be the only cause of earliness differences. This indicates the presence of additional factors affecting differentially apex development in 'Hispanic' and 'Barberousse', in the absence of vernalization.

The two cultivars differ in an unknown, but surely large, number of genes. We cannot be sure which genes are causing the differences in earliness between them. However, these differences are manifested in plants without full vernalization, and seem related to vernalization responsiveness. Therefore, it is justified to look into other genes that may act in the vernalization pathway. Currently, there is enough evidence substantiating that expression of *OS2* genes in winter cereals is suppressed by cold and could have a role in the process of vernalization. It has been proposed that *Brachypodium BdODDSOC2* "plays a role in setting the length of the vernalization requirement in a rheostatic manner, i.e. higher *ODDSOC2* transcript levels before cold result in a longer cold period needed to saturate the vernalization requirement" (Sharma *et al.*, 2017), although its specific role in the vernalization response is not clear. Across our experiments, expression of *HvOS2* was concurrent with the absence of *HvVRN1*, being lowest in plants that flowered. This coincidence was already observed in barley, wheat and *Brachypodium* (Greenup *et al.*, 2010; Sharma *et al.*, 2017). In addition, in the two experiments (all samplings, except one point in experiment 1), 'Barberousse' consistently showed higher levels of *HvOS2* transcripts than 'Hispanic', what agrees with the delayed development and later *HvVRN1* appearance observed in 'Barberousse'. The predicted amino acid

sequences from *HvOS2* showed polymorphisms in the coding sequence between both varieties, entailing potential change in protein function, and many other polymorphisms in non-coding regions, which could explain the expression differences. This is the first report describing sequence variation in *HvOS2*.

Recently, it was shown that the protein VRN1 binds to the promoters of *VERNALIZATION2* and *ODDSOC2* in barley (Deng *et al.*, 2015). Therefore, we explored the possibility that the genotypes differed in VRN1 binding sites. We identified putative VRN1-regulatory sites in *HvOS2*, and found that most of them were identical in both genotypes, leading us to exclude them as cause of dissimilar gene expression among genotypes. However, the variations in intron 1 and some VRN1-regulatory sites in 3'UTR might indicate regulatory differences among the cultivars, as found in *Arabidopsis*. Considerable natural variation in noncoding regions, affecting regulation of *FLC* (homolog of *HvOS2*) has been reported in *Arabidopsis* (Gazzani *et al.*, 2003; Michaels *et al.*, 2003; Li *et al.*, 2014; Whittaker and Dean, 2017). Future research will be needed to ascertain the involvement of *HvOS2* in the vernalization mechanism and the effect of the polymorphisms found in coding and non-coding sequences

2.4.3. *HvFT3* expression is not constitutive in winter cultivars, it needs induction by cold and plant development

We found differences in responsiveness to SD between the genotypes. 'Hispanic' developed faster than 'Barberousse' and flowered without vernalization. It also flowered earlier in the natural photoperiod experiment, when day-lengths increased from SD to LD (72 days in the first sowing event, without vernalization), than under SD conditions only (126 days at 12 h, Figure 2.4). The two varieties differ (among others) in the presence/absence of *HvFT3*. We hypothesized that this could be a key factor differentiating their response to insufficient vernalization. This gene bears

particular agronomic relevance for Mediterranean environments, as it stands at the peak of flowering time QTL and grain yield QTL x Environment peaks in several populations (Cuesta-Marcos *et al.*, 2008, 2009; Karsai *et al.*, 2008; Francia *et al.*, 2011; Tondelli *et al.*, 2014). A supporting role for promotion to flowering in winter cultivars, receiving less than full vernalization under field conditions, was proposed for *HvFT3* (Casao *et al.*, 2011*b*). Its expression is usually reported in SD, although it is also found in LD conditions (Kikuchi *et al.*, 2009; Casao *et al.*, 2011*a*). In our experiments, *HvFT3* transcripts were only detected: (a) after full or partial vernalization, in early-medium development (Figures 2.2 and 2.5), and (b) in absence of vernalization, in rather late developmental stages, and only in plants sown under shortest day-lengths (Figure 2.3). We expected expression of *HvFT3*, the "short photoperiod" gene, at least in the earliest sowings in the experiment with natural photoperiods. Instead, it was effectively repressed, either by the low but always present *HvVRN2*, or by other repressors. Under constant photoperiod of 12h, *HvFT3* was detected in 'Hispanic' only after four weeks VER (2 weeks were insufficient) and 5 weeks in growth chamber (Figure 2.5). Thus, *HvFT3* was expressed in a winter cultivar only after some cold exposure, and increasingly with plant age. It is particularly remarkable that the expression of *HvFT3* was correlated with earlier flowering, although it was detected only after the transition from vegetative to reproductive apex had occurred (Figure 2.6). This late effect on development is consistent with findings in spring wheat varieties (Halliwell *et al.*, 2016), and in barley (Mulki *et al.*, 2018). This last study evidenced that genotypes with *HvFT3* accelerated the initiation of spikelet primordia and the early reproductive development but required LD to flower.

The induction of *HvFT3* in sowing event 2 (Figure 2.3), together with the progressive increase of the transcripts after 28-days VER, when *HvVRN2* is not detected, are consistent with the antagonistic role between *HvVRN2* and *HvFT3* revealed by Casao *et al.* (2011a). *HvVRN2* absence allows induction of *HvFT3,*

although it would not ensure *HvFT3* expression, hinting at the possible involvement of other repressors. In this respect, a possible relationship of *HvOS2* with *HvFT3* was suggested in the literature, (Cuesta-Marcos *et al.*, 2015). Future research on this possible role would shed light on the control of *HvFT3*.

HvFT3 expression occurred in samplings coincident with that of *HvVRN1* and *HvFT1*. Parallel expression of *FT* genes has been found in grasses. Lv *et al.* (2014) reported that developmental changes regulated by *FT1* were related to transcript levels of other *FT*-like genes, such as *FT3*, in *Brachypodium* and wheat. Under LD, these authors only found upregulation of *FT3* when *FT1* was upregulated, as in our findings with 12 h day-length. Their concurrent expression could be related to the interactions between FT1 and other FT-like proteins, including FT3, with proteins FD-like and 14-3-3, all components of the florigen activation complex (FAC), in wheat and barley (Li *et al.*, 2015).

2.5. Conclusion

The results reported do not provide a full description of the dynamics of gene expression, and the conclusions derived are limited to conditions tested. Nevertheless, they open a series of questions that are worthy of further research.

The use of different sowing events, under natural increasing photoperiod corroborate that *HvVRN2* transcript levels are always present in absence of a cold-effective induction, and that the level of expression of *HvVRN2* is highly dependent on day-length. We provide evidence that the plants exhibit a shift in the pattern of expression of genes from the vernalization and photoperiod pathways, when day-length reaches around 12 h 30 min. To isolate these effects from genetic background, additional research with isogenic lines will be needed. In particular, future experiments combining sequential sowings in natural photoperiod with gradual vernalization treatments would shed light on possible effects on plant

development and potential agronomic consequences of the expression shift observed, when vernalization is not complete. Further research to ascertain these possible agronomic effects with segregating populations and isogenic lines for *HvVRN2* is underway.

Other repressors appear to be acting in the process of vernalization. *HvOS2* is a suitable candidate, given the evidence accumulating in other grasses, and the genotypic differences found in our study. This hypothesis should be tested with plant materials sharing genetic background, to avoid confounding effects of other segregating genes.

HvFT3, a central gene for winter barley performance in Southern Europe, is not induced just by short days. In winter cultivars, it must receive additional induction through LD, and/or a cold period, to be effective in reducing time to flowering.

The photoperiod conditions of the experiments here described correspond to a wide range of late spring sowings for winter barley in the Mediterranean area. The genetic mechanisms and the environmental controls investigated in this study will be useful to define both varieties and agronomics of winter cereals best suited for current and future climate conditions.

2.6.   References

Altschul SF, Gish W, Miller W, Myers EW, Lipman DJ. 1990. Basic local alignment search tool. Journal of Molecular Biology **215**, 403–410.

Borràs-Gelonch G, Denti M, Thomas WTB, Romagosa I. 2012. Genetic control of pre-heading phases in the Steptoe x Morex barley population under different conditions of photoperiod and temperature. Euphytica **183**, 303–321.

Bouché F, Woods D, Amasino RM. 2017. Winter Memory throughout the Plant Kingdom: Different Paths to Flowering. Plant Physiology **173**, 27–35.

Campoli C, von Korff M. 2014. Genetic control of reproductive development in temperate cereals. In: Fornara F, ed. Advances in botanical research: Vol. 72. The molecular genetics of floral transition and flower development. New York: Academic Press, 131–158.

Campoli C, Shtaya M, Davis SJ, von Korff M. 2012. Expression conservation within the circadian clock of a monocot: natural variation at barley *Ppd-H1* affects circadian expression of flowering time genes, but not clock orthologs. BMC Plant Biology **12**, 97.

Casao MC, Igartua E, Karsai I, Lasa JM, Gracia MP, Casas AM. 2011*a*. Expression analysis of vernalization and day-length response genes in barley (*Hordeum vulgare* L.) indicates that *VRNH2* is a repressor of *PPDH2* (*HvFT3*) under long days. Journal of Experimental Botany **62**, 1939–1949.

Casao MC, Karsai I, Igartua E, Gracia MP, Veisz O, Casas AM. 2011*b*. Adaptation of barley to mild winters: A role for *PPDH2*. BMC Plant Biology **11**, 164.

Chen A, Dubcovsky J. 2012. Wheat TILLING Mutants Show That the Vernalization Gene *VRN1* Down-Regulates the Flowering Repressor *VRN2* in Leaves but Is Not Essential for Flowering. PLoS Genetics **8**, e1003134.

Chen A, Li C, Hu W, Lau MY, Lin H, Rockwell NC, Martin SS, Jernstedt JA, Lagarias JC, Dubcovsky J. 2014. PHYTOCHROME C plays a major role in the acceleration of wheat flowering under long-day photoperiod. Proceedings of the National Academy of Sciences of the United States of America **111**, 10037–10044.

Cockram J, Thiel T, Steuernagel B, Stein N, Taudien S, Bailey PC, O'Sullivan DM. 2012. Genome Dynamics Explain the Evolution of Flowering Time CCT Domain Gene Families in the Poaceae. PLoS ONE **7**, e45307.

Cuesta-Marcos A, Igartua E, Ciudad FJ, *et al.* 2008. Heading date QTL in a spring × winter barley cross evaluated in Mediterranean environments. Molecular Breeding **21**, 455–471.

Cuesta-Marcos A, Casas AM, Hayes PM, Gracia MP, Lasa JM, Ciudad F, Codesal P, Molina-Cano JL, Igartua E. 2009. Yield QTL affected by heading date in Mediterranean grown barley. Plant Breeding **128**, 46–53.

Cuesta-Marcos A, Muñoz-Amatrián M, Filichkin T, Karsai I, Trevaskis B, Yasuda S, Hayes P, Sato K. 2015. The Relationships between Development and Low Temperature

Tolerance in Barley Near Isogenic Lines Differing for Flowering Behavior. Plant and Cell Physiology **56**, 2312–2324.

Dai F, Wang X, Zhang XQ, Chen Z, Nevo E, Jin G, Wu D, Li C, Zhang G. 2018. Assembly and analysis of a *qingke* reference genome demonstrate its close genetic relation to modern cultivated barley. Plant Biotechnology Journal **16**, 760–770.

Danyluk J, Kane NA, Breton G, Limin AE, Fowler DB, Sarhan F. 2003. TaVRT-1, a Putative Transcription Factor Associated with Vegetative to Reproductive Transition in Cereals. Plant Physiology **132**, 1849–1860.

Deng W, Casao MC, Wang P, Sato K, Hayes PM, Finnegan EJ, Trevaskis B. 2015. Direct links between the vernalization response and other key traits of cereal crops. Nature Communications **6**, 5882.

Digel B, Pankin A, von Korff M. 2015. Global transcriptome profiling of developing leaf and shoot apices reveals distinct genetic and environmental control of floral transition and inflorescence development in barley. The Plant Cell **27**, 2318–2334.

Distelfeld A, Li C, Dubcovsky J. 2009. Regulation of flowering in temperate cereals. Current Opinion in Plant Biology **12**, 178–184.

Faure S, Higgins J, Turner A, Laurie DA. 2007. The *FLOWERING LOCUS T*-like gene family in barley (*Hordeum vulgare*). Genetics **176**, 599–609.

Francia E, Tondelli A, Rizza F, *et al.* 2011. Determinants of barley grain yield in a wide range of Mediterranean environments. Field Crops Research **120**, 169–178.

Gazzani S, Gendall AR, Lister C, Dean C. 2003. Analysis of the Molecular Basis of Flowering Time Variation in Arabidopsis Accessions. Plant Physiology **132**, 1107–1114.

Greenup AG, Sasani S, Oliver SN, Talbot MJ, Dennis ES, Hemming MN, Trevaskis B. 2010. *ODDSOC2* is a MADS Box Floral Repressor that Is Down-Regulated by Vernalization in Temperate Cereals. Plant Physiology **153**, 1062–1073.

Griffiths S, Dunford RP, Coupland G, Laurie DA. 2003. The Evolution of *CONSTANS*-Like Gene Families in Barley, Rice, and Arabidopsis. Plant Physiology **131**, 1855–1867.

Halliwell J, Borril P, Gordon A, Kowalczyk R, Pagano ML. 2016. Systematic investigation of *FLOWERING LOCUS T*-like Poaceae gene families identifies the short-day expressed flowering pathway gene, *TaFT3* in wheat (*Triticum aestivum* L.). Frontiers in Plant Science **7**, 857.

Hemming MN, Fieg S, James Peacock W, Dennis ES, Trevaskis B. 2009. Regions associated with repression of the barley (*Hordeum vulgare*) *VERNALIZATION1* gene are not required for cold induction. Molecular Genetics and Genomics **282**, 107–117.

Higgins JA, Bailey PC, Laurie DA. 2010. Comparative genomics of flowering time pathways using *Brachypodium distachyon* as a model for the temperate grasses. PLoS ONE **5**, e10065.

Igartua E, Casas AM, Ciudad F, Montoya JL, Romagosa I. 1999. RFLP markers associated with major genes controlling heading date evaluated in a barley germ plasm

pool. Heredity **83**, 551-559.

Karsai I, Meszaros K, Szucs P, Hayes PM, Lang L, Bedo Z. 2006. The influence of photoperiod on the *Vrn-H2* locus (4H) which is a major determinant of plant development and reproductive fitness traits in a facultative x winter barley (*Hordeum vulgare* L.) mapping population. Plant Breeding **125**, 468–472.

Karsai I, Szucs P, Koszegi B, Hayes PM, Casas AM, Bedo Z, Veisz O. 2008. Effects of photo and thermo cycles on flowering time in barley: A genetical phenomics approach. Journal of Experimental Botany **59**, 2707–2715.

Karsai I, Szucs P, Mészáros K, Filichkina T, Hayes PM, Skinner JS, Láng L, Bedo Z. 2005. The *Vrn-H2* locus is a major determinant of flowering time in a facultative x winter growth habit barley (*Hordeum vulgare* L.) mapping population. Theoretical and Applied Genetics **110**, 1458–1466.

Kikuchi R, Kawahigashi H, Ando T, Tonooka T, Handa H. 2009. Molecular and Functional Characterization of PEBP Genes in Barley Reveal the Diversification of Their Roles in Flowering. Plant Physiology **149**, 1341–1353.

Kikuchi R, Kawahigashi H, Oshima M, Ando T, Handa H. 2012. The differential expression of *HvCO9*, a member of the *CONSTANS*-like gene family, contributes to the control of flowering under short-day conditions in barley. Journal of Experimental Botany **63**, 773–784.

Kumar S, Stecher G, Li M, Knyaz C, Tamura K. 2018. MEGA X: Molecular Evolutionary Genetics Analysis across Computing Platforms. Molecular Biology and Evolution **35**, 1547–1549.

Larkin MA, Blackshields G, Brown NP, *et al.* 2007. Clustal W and Clustal X version 2.0. Bioinformatics (Oxford, England) **23**, 2947–2948.

Laurie DA, Pratchett N, Snape JW, Bezant JH. 1995. RFLP mapping of five major genes and eight quantitative trait loci controlling flowering time in a winter × spring barley (*Hordeum vulgare* L.) cross. Genome **38**, 575–585.

Li C, Distelfeld A, Comis A, Dubcovsky J. 2011. Wheat flowering repressor VRN2 and promoter CO2 compete for interactions with NUCLEAR FACTOR-Y complexes. Plant Journal **67**, 763–773.

Li P, Filiault D, Box MS, *et al.* 2014. Multiple *FLC* haplotypes defined by independent *cis*-regulatory variation underpin life history diversity in *Arabidopsis thaliana*. Genes & Development **28**, 1635–1640.

Li C, Lin H, Dubcovsky J. 2015. Factorial combinations of protein interactions generate a multiplicity of florigen activation complexes in wheat and barley. Plant Journal **84**, 70–82.

Lv B, Nitcher R, Han X, Wang S, Ni F, Li K, Pearce S, Wu J, Dubcovsky J, Fu D. 2014. Characterization of *Flowering Locus T1* (*FT1*) gene in *Brachypodium* and wheat. PLoS ONE **9**, e94171.

Mansour E, Moustafa ESA, Qabil N, Abdelsalam A, Wafa HA, El Kenawy A, Casas

AM, Igartua E. 2018. Assessing different barley growth habits under Egyptian conditions for enhancing resilience to climate change. Field Crops Res. **224**, 67-75

Mascher M, Gundlach H, Himmelbach A, *et al.* 2017. A chromosome conformation capture ordered sequence of the barley genome. Nature **544**, 427–433.

Mayer KFX, Waugh R, Langridge P, *et al.* 2012. A physical, genetic and functional sequence assembly of the barley genome. Nature **491**, 711–717.

de Mendiburu F. 2016. agricolae: Statistical Procedures for Agricultural Research. https://cran.r-project.org/package=agricolae.

Michaels SD, He Y, Scortecci KC, Amasino R. 2003. Attenuation of FLOWERING LOCUS C activity as a mechanism for the evolution of summer-annual flowering behavior in *Arabidopsis*. Proceedings of the National Academy of Sciences of the United States of America **100**, 10102–10107.

Mulki MA, Bi X, von Korff M. 2018. FLOWERING LOCUS T3 Controls Spikelet Initiation But Not Floral Development. Plant Physiology **178**, 1170–1186.

Mulki MA, von Korff M. 2016. *CONSTANS* Controls Floral Repression by Up-Regulating *VERNALIZATION2* (*VRN-H2*) in Barley. Plant Physiology **170**, 325–337.

Nemoto Y, Kisaka M, Fuse T, Yano M, Ogihara Y. 2003. Characterization and functional analysis of three wheat genes with homology to the *CONSTANS* flowering time gene in transgenic rice. Plant Journal **36**, 82–93.

Nguyen NTT, Contreras-Moreira B, Castro-Mondragon, J.A. Santana-Garcia W, *et al.* 2018. RSAT 2018: regulatory sequence analysis tools 20th anniversary. Nucleic Acids Research **46**, W209–W214.

Oliver SN, Finnegan EJ, Dennis ES, Peacock WJ, Trevaskis B. 2009. Vernalization-induced flowering in cereals is associated with changes in histone methylation at the *VERNALIZATION1* gene. Proceedings of the National Academy of Sciences of the United States of America **106**, 8386–8391.

R Core Team. 2017. R: A langauge and environment for statistical computing. https://www.r-project.org/.

Rizza F, Karsai I, Morcia C, Badeck F-W, Terzi V, Pagani D, Kiss T, Stanca AM. 2016. Association between the allele compositions of major plant developmental genes and frost tolerance in barley (*Hordeum vulgare* L.) germplasm of different origin. Molecular Breeding **36**, 156.

Ruelens P, de Maagd RA, Proost S, Theißen G, Geuten K, Kaufmann K. 2013. FLOWERING LOCUS C in monocots and the tandem origin of angiosperm-specific MADS-box genes. Nature Communications **4**, 2280.

Sasani S, Hemming MN, Oliver SN, *et al.* 2009. The influence of vernalization and day-length on expression of flowering-time genes in the shoot apex and leaves of barley (*Hordeum vulgare*). Journal of Experimental Botany **60**, 2169–2178.

Sato K, Tanaka T, Shigenobu S, Motoi Y, Wu J, Itoh T. 2016. Improvement of barley

genome annotations by deciphering the Haruna Nijo genome. DNA Research **23**, 21–28.

Sebastian A, Contreras-Moreira B. 2014. footprintDB: a database of transcription factors with annotated cis elements and binding interfaces. Bioinformatics **30**, 258–265.

Sharma N, Ruelens P, Dhauw M, Maggen T, Dochy N, Torfs S, Kaufmann K, Rohde A, Geuten K. 2017. A Flowering Locus C Homolog Is a Vernalization-Regulated Repressor in *Brachypodium* and Is Cold-Regulated in Wheat. Plant Physiology **173**, 1301–1315.

Song YH, Kubota A, Kwon MS, *et al.* 2018. Molecular basis of flowering under natural long-day conditions in *Arabidopsis*. Nature Plants. **4**, 824–835.

Song YH, Shim JS, Kinmonth-Schultz HA, Imaizumi T. 2015. Photoperiodic Flowering: Time Measurement Mechanisms in Leaves. Annual Review of Plant Biology **66**, 441–464.

Tao F, Rötter RP, Palosuo T, *et al.* 2017. Designing future barley ideotypes using a crop model ensemble. European Journal of Agronomy **82**, 144–162.

Tondelli A, Francia E, Visioni A, *et al.* 2014. QTLs for barley yield adaptation to Mediterranean environments in the 'Nure' × 'Tremois' biparental population. Euphytica **197**, 73–86.

Trevaskis B. 2010. The central role of the *VERNALIZATION1* gene in the vernalization response of cereals. Functional Plant Biology **37**, 479–487.

Trevaskis B, Bagnall DJ, Ellis MH, Peacock WJ, Dennis ES. 2003. MADS box genes control vernalization-induced flowering in cereals. Proceedings of the National Academy of Sciences of the United States of America **100**, 13099–13104.

Trevaskis B, Hemming MN, Peacock WJ, Dennis ES. 2006. *HvVRN2* responds to day-length, whereas *HvVRN1* is regulated by vernalization and developmental status. Plant Physiology **140**, 1397–1405.

Turner A, Beales J, Faure S, Dunford RP, Laurie DA. 2005. The Pseudo-Response Regulator *Ppd-H1* Provides Adaptation to Photoperiod in Barley. Science **310**, 1031–1034.

Waddington SR, Cartwright PM, Wall PC. 1983. A quantitative Scale of Spike Initial and Pistil Development in Barley and Wheat. Annals of Botany **51**, 119–130.

Whittaker C, Dean C. 2017. The *FLC* Locus: A Platform for Discoveries in Epigenetics and Adaptation. Annual Review of Cell and Developmental Biology **33**, 555–575.

Woods D, Dong Y, Bouche F, Bednarek R, Rowe M, Ream T, Amasino R. 2019. A florigen paralog is required for short-day vernalization in a pooid grass. eLife **8**, 1–16.

Yan L, Loukoianov A, Blechl A, Tranquilli G, Ramakrishna W, SanMiguel P, Bennetzen JL, Echenique V, Dubcovsky J. 2004. The wheat *VRN2* gene is a flowering repressor down-regulated by vernalization. Science **303**, 1640–1644.

Yan L, Loukoianov A, Tranquilli G, Helguera M, Fahima T, Dubcovsky J. 2003. Positional cloning of the wheat vernalization gene *VRN1*. Proceedings of the National Academy of Sciences of the United States of America **100**, 6263–6268.

Zadoks JC, Chang TT, Konzak CF. 1974. A Decimal Code for the Growth Stages of Cereals. Weed Research **14**, 415–421.

von Zitzewitz J, Szucs P, Dubcovsky J, Yan L, Francia E, Pecchioni N, Casas A, Chen THH, Hayes PM, Skinner JS. 2005. Molecular and structural characterization of barley vernalization genes. Plant Molecular Biology **59**, 449–467.

2.7.   Supplementary material

Table S 2.1. Analysis of variance for the ΔCt corresponding to the expression of genes of 'Hispanic' and 'Barberousse' in 3-week-old plants under natural photoperiods without vernalization. Between 3 and 4 biological replicates per gene were used.

Source of variation	HvVRN1		HvVRN2		HvCO2	
	df	ms	df	ms	df	ms
Var.	1	1.68 ns	1	25.18 **	1	0.62 ns
Sow.Ev.	8	15.15 ns	8	15.92 ***	8	16.21 ***
Var. * Sow.Ev.	8	8.75 ns	8	3.05 ns	8	2.77 ns
Residuals	34	9.30	34	2.05	35	2.20

Source of variation	PPD-H1		HvOS2		HvCO9	
	df	ms	df	ms	df	ms
Var.	1	0.78 ns	1	30.94 ***	1	5.85 ns
Sow.Ev.	8	1.18 *	8	2.24 *	8	149.06 ***
Var. * Sow.Ev.	8	1.15 *	8	1.38 ns	8	31.37 ns
Residuals	51	0.43	35	0.81	35	90.20

Var., Variety; Sow. Ev., Sowing event; df, degrees of freedom; ms, mean squares; ns, not significant; *, **, *** significant effects at P<0.05, < 0.01, < 0.001.

Table S 2.2. ANOVA of A) *HvVRN2* and B) *HvCO2* expression in 21 days-old plants of two varieties grown in absence of vernalization under natural photoperiods.

A) *HvVRN2* Source of variation	Df	SS	MS	F value	**Pr(>F)**	
Variety (Var)	1	25.18	25.18	12.28	0.0013	**
Sowing event (Sowing)	8	127.36	15.92	7.77	7.17E-06	***
Group	1	99.36	99.36	48.47	5.00E-08	***
Within group	7	28.00	4.00	1.95	0.0916	
Var * Sowing	8	24.43	3.05	1.49	0.1976	
Var * Group	1	4.93	4.93	2.40	0.1303	
Var * within group	7	19.50	2.79	1.36	0.2542	
Residuals	34	69.70	2.05			
B) *HvCO2* Source of variation	Df	SS	MS	F value	**Pr(>F)**	
Variety (Var)	1	0.62	0.62	0.28	0.599	
Sowing event (Sowing)	8	129.64	16.21	7.35	1.07E-05	***
Group	1	17.74	17.74	8.05	0.00752	**
Within group	7	111.90	15.99	7.25	2.23e-05	***
Var * Sowing	8	22.19	2.77	1.26	0.296	
Var * Group	1	0.25	0.25	0.12	0.736	
Var * within group	7	21.93	3.13	1.42	0.228	
Residuals	35	77.14	2.20			

Plants were sown sequentially from Feb 11th to Apr 8th (sowing events 1-9). For this analysis, the nine sowing events were grouped as 1-4 (shorter photoperiod) and 5-9 (longer photoperiod), with the threshold at 12h 30m as the splitting point. This subfactor was named "Group". We subdivided the differences between sowing events and the interaction between sowing events and variety in two components: the variance due to the differences between the two groups and the variance due to differences between sowing events within groups. Df, degrees of freedom; SS, sum of squares; MS, mean squares; *, **, *** significant effects at $P < 0.05$, < 0.01, < 0.001.

Table S 2.3. Analysis of variance for the ΔCt corresponding to the expression of genes of 'Hispanic' and 'Barberousse' plants grown under natural photoperiods without vernalization, and sampled on a set date, with 15 h light. Between 3 and 4 biological replicates per gene were used.

Source of variation	*HvVRN1* df	ms	*HvVRN2* df	ms	*HvCO2* df	ms	*PPD-H1* df	ms	*HvOS2* df	ms	*HvCO9* df	ms	*HvFT1* df	ms
Var.	1	179.0 *	1	33.92 **	1	23.03 *	1	1.99 ns	1	103.11 ***	1	3.73 ns	1	176.9 ***
Sow. Ev.	6	213.5 ***	6	2.87 ns	6	2.34 ns	6	3.82 ***	6	36.94 ***	6	10.51 ns	6	93.3 ***
Var. * Sow. Ev	6	119.7 **	6	2.55 ns	6	8.44 ns	6	1.54 *	6	10.2 ns	6	13.88 ns	6	13.3 ns
Residuals	40	28.1	40	2.92	26	4.31	26	0.54	29	5.93	33	7.04	30	10.9

Var., Variety; Sow. Ev., Sowing event; df, degrees of freedom; ms, mean squares; ns, not significant; *, **, *** significant effects at $P < 0.05, < 0.01, < 0.001$.

Table S 2.4. Analysis of variance for the ΔCt corresponding to the expression of genes of 'Hispanic' and 'Barberousse' in plants grown under 12 h light, with different vernalization treatments (0, 14 and 28 days).

Source of variation	HvVRN1 df	ms	HvVRN2 df	ms	HvCO2 df	ms	PPD-H1 df	ms	HvOS2 df	ms	HvCO9 df	ms	HvFT1 df	ms
Var.	1	222.2 ***	1	116.5 ***	1	4.8 ns	1	0.44 ns	1	102.8 ***	1	139.4 ***	1	6.2 ns
Vern.	2	181.5 ***	2	134.3 ***	2	52.6 **	2	1.72 **	2	2.1 ns	2	26.3 ***	2	53.4 **
Age	3	61.3 ***	3	7.9 **	3	40.0 *	3	4.55 ***	3	5.4 ns	3	71.6 ***	3	140.2 ***
Var. * Vern.	2	88.6 ***	2	64.6 ***	2	9.6 ns	2	0.69 ns	2	7.2 ns	2	17.9 **	2	7.8 ns
Var. * Age	3	3.4 ns	3	1.0 ns	3	10.1 ns	3	0.21 ns	3	1.0 ns	3	1.7 ns	3	10.3 ns
Vern. * Age	6	5.9 ns	6	12.4 ***	6	6.5 ns	6	0.88 ns	6	3.2 ns	6	9.7 **	6	18.6 ns
Var. * Vern. * Age	6	11.1 **	6	2.4 ns	6	10.8 ns	6	1.05 ns	6	1.7 ns	6	18.5 ***	6	16.7 ns
Residuals	48	2.6	48	1.4	47	14.1	48	0.53	48	2.8	48	2.9	49	10.4

Var., Variety; Vern., Vernalization; df, degress of freedom; ms, mean squares; ns, not significant; *, **, *** significant effects at $P <$ 0.05, < 0.01, < 0.001. Between 3 and 4 biological replicates per gene were used.

Table S 2.5. Primer sequences for gene expression assay and sequencing. F, Forward; R, Reverse.

Gene expression

Gene	Primer sequence (5'-3')	Reference
HvCO2[b]	F: CATCACTTGTGACCCAAGACC R: CTATAGTTCCATAATTGCTCC	Griffiths *et al.* (2003)
HvCO9[a]	F: AAGCTGATGCGGTACAAAGAGA R: GAACCACCCGAGGTCGAG	Kikuchi *et al.* (2012)
HvFT1[a]	F: ATCTCCACTGGTTGGTGACAGA R: TTGTAGAGCTCGGCAAAGTCC	Yan *et al.* (2006)
HvFT3[b]	F: GGTTGTGGCTCATGTTATGC R: CTACTCCCCTTGAGAACTTTC	F: Kikuchi *et al.* (2009); R: Faure *et al.* (2007)
HvOS2[a]	F: CAATGCTGATGACTCAGATGCT R: CGCTATTTCGTTGCGCCAAT	Greenup *et al.* (2010)
Ppd-H1[b]	F: CAAATCAAAGAGCGGCGATC R: TCTGACTTGGGATGGTTCACA	Hemming *et al.* (2008)
HvVRN1[a]	F: TATGAGCGCTACTCTTATGC R: TGAAGCTCAGAAATGGATTCG	Trevaskis *et al.* (2006)
HvVRN2[a]	F: GAGCCACCATCGTGCCATTC R: GCCGCTTCTTCCTCTTCTC	Trevaskis *et al.* (2006)
Actin	F: GCCGTGCTTTCCCTCTATG R: GCTTCTCCTTGATGTCCCTTA	Trevaskis *et al.* (2006)

Sequencing

Gene	Primer sequence (5'-3')	Length (bp)	Region
HvCO2	**Morex_contig_6805**		
CO2.1F	TTTTCGCTCACTGGATTCCAC	983	5' UTR, exon 1
CO2.2R	GCCTTGAAGTGGTACGAACTC		
CO2.7F	GCAAGGGAGCAATTATGGAA	988	Exon1, intron, exon 2
CO2.8R	GTGGTGACAGCATGTGGTTC		
CO2.5F	TAGTACCGGACAACACCAGAC	782	Exon 2, 3' UTR

CO2.6R	TCCCCAAGAAGTGTGTATCCA		
HvCO9	**Morex_contig_67944**		
CO9.1F	ACGTAAGGAACCCTCCCATC	996	5'UTR, exon 1
CO9.2R	TAACAATTTGCACCACACGC		
CO9.3F	AGTTCCAGTTCTTCGGGCAG	783	Exon 1, intron
CO9.4R	ATTACTAGTGTGGGCCGAGG		
CO9.5F	CAAATATTTCTGCGTGTGGTGC	949	Intron
CO9.6R	CGTTTCTCTCCCGCAATAAGG		
CO9.7F	TTCGAAATGCCATGCTCTTCC	910	Exon 2, 3'UTR
CO9.8R	CCGCCCCACCTCAATTTATTT		
HvOS2	**HORVU3Hr1G095240**		
OS2.1F	TTTTTCACAGCGTGGATAAGG	936	5'UTR, exon 1, intron
OS2.2R	TTGGCCGTGACAATAATAAGC		
OS2.3F	CCGGTAAATCAAGGCTGCTC	829	Intron 1, partial
OS2.4R	GCACAACAAACTCTCGGTGA		
OS2.5F	ATTTCCAGCAGAGCCTAAAGC	918	Exon2-exon 4
OS2.6R	TGAAAATGGCCAAAAACAGAGC		
OS2.7F	ACTTCCTGGTAGCCCTTGAG	854	Exon 4, intron 4
OS2.8R	ACAACAGAGCCAACTTGTCG		
OS2.9F	CTTAGTTGCTGCAGTCTCACTC	877	Intron 4, exon 5
OS2.10R	TACCAAATGCATGCACATCACA		
OS2.11F	AGAGCCTGGCATGAGAGTTC	855	Exon 5, 3'UTR
OS2.12R	CCCAGGGAAGACACTTGCTA		

[a] For these genes, each reaction contained 10 µl of SYBR Green Master Mix (Applied Biosystems), 0.2 µM of each primer and 250 ng of cDNA in a volume of 20 µl. Reactions were run with the following conditions: 10 min at 95℃, 44 cycles of 15 s at 95℃ and 1 min at 60℃, followed by a melting curve program (60-95℃) implying temperature increases of 1℃ each minute.

[b] For these genes, each reaction contained 5 µl of PowerUp SYBR Green Master Mix (Applied Biosystems), 0.2 µM of each primer and 250 ng of cDNA in a volume of 10 µl. Reactions were run with the following conditions: 2 min at 50℃, 2 min at 95℃, 44 cycles of 15 s at 95℃, 15 s at 60℃ and 45 s at 75℃, and a melting curve program (60-95℃) of 1℃ of temperature increment for each minute.

Tables S 2.6 (a-d); S 2.7 (a-d); S 2.8 (a-h) can be found in the following links:

Table S 2.6. *HvCO2* polymorphisms. A) Information of the sequences obtained for the gene *HvCO2* var. 'Barberousse' and var. 'Hispanic'. B) Polymorphisms found for HvCO2 sequences. C) Alignments of *HvCO2* gene sequences. D) Alignments of HvCO2 predicted protein sequences.

https://www.ncbi.nlm.nih.gov/pmc/articles/PMC6434887/bin/12870_2019_1727_MOES M2_ESM.xlsx

Table S 2.7. *HvCO9* polymorphisms. A) Information of the sequences obtained for the gene HvCO9 var. 'Barberousse' and var. 'Hispanic'. B) Polymorphisms found for *HvCO9* sequences. C) Alignments of *HvCO9* gene sequences. D) Alignments of HvCO9 predicted protein sequences.

https://www.ncbi.nlm.nih.gov/pmc/articles/PMC6434887/bin/12870_2019_1727_MOES M3_ESM.xlsx

Table S 2.8. *HvOS2* polymorphisms. A) Information of the sequences obtained for the gene *HvOS2* var. 'Barberousse' and var. 'Hispanic'. B) Polymorphisms found for HvOS2 CDS sequences. C-F) Alignments of *HvOS2* sequences - exon 1 (C), exons 2–5 (D), CDS (E), predicted protein (F). G-H) Predicted VRN1 regulatory sites in *HvOS2* exon 1 (G) and exons 2–5 (H), in var. 'Barberousse' and var. 'Hispanic'.

https://www.ncbi.nlm.nih.gov/pmc/articles/PMC6434887/bin/12870_2019_1727_MOES M4_ESM.xlsx
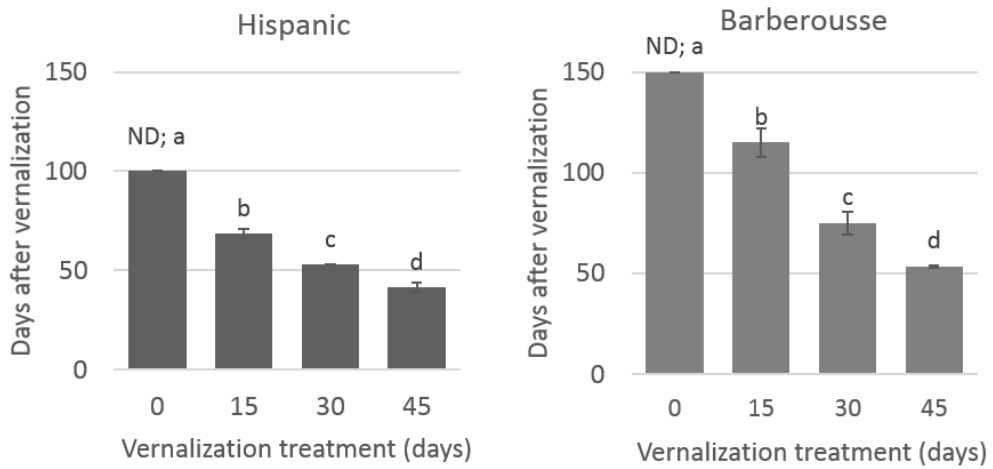
Figure S 2.1. Flowering date under different vernalization treatments.

Both varieties, 'Hispanic' and 'Barberousse', were studied independently. Hispanic's experiment ended after 100 days, whereas Barberousse's experiment ended 150 days after starting. ND: not determined. For each vernalization treatment, bars with different letter are significantly different at P<0.05 (LSD test).
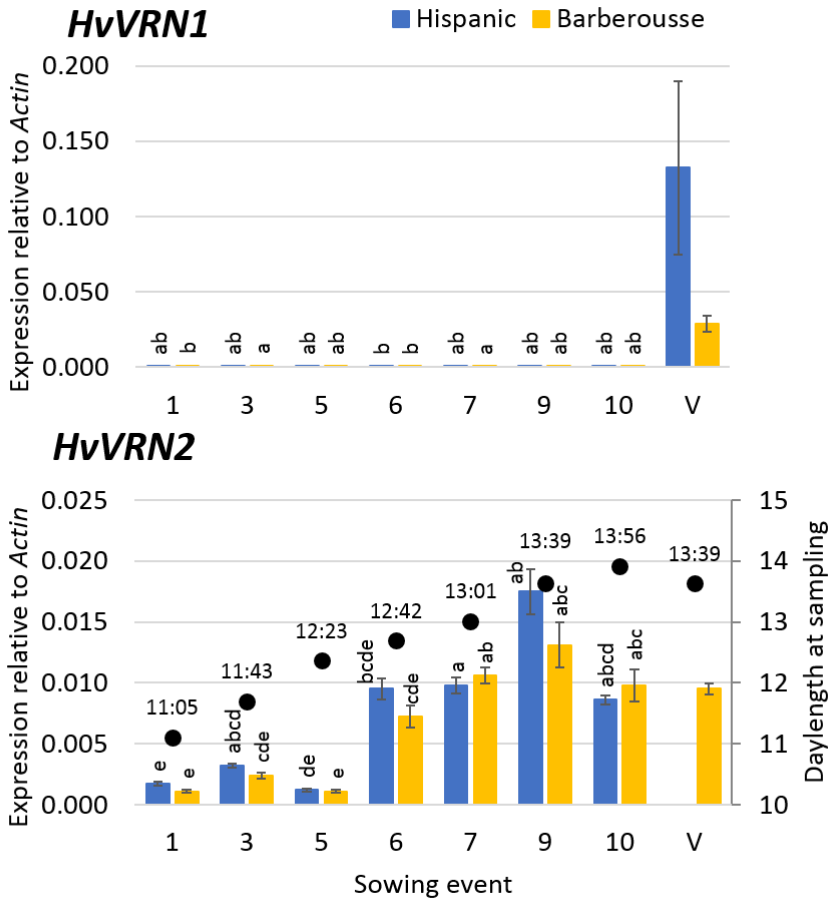
Figure S 2.2. Gene expression in 2-week-old plants sown under natural and increasing photoperiod (without vernalization and control).

X-axis represents the successive sowings, from 11th February until April 15th. Unvernalized plants (sowings 1 to 10) and vernalized control (V) of 'Hispanic' (blue) and 'Barberousse' (yellow). Black dots denote day-length at sampling date (labels in HH:MM). Mean of 3 biological replicates. Error bars are SEM. For each NV time-point, bars with the same letter are not significantly different at $P<0.05$ according to ANOVA that included genotypes and all sampling times.
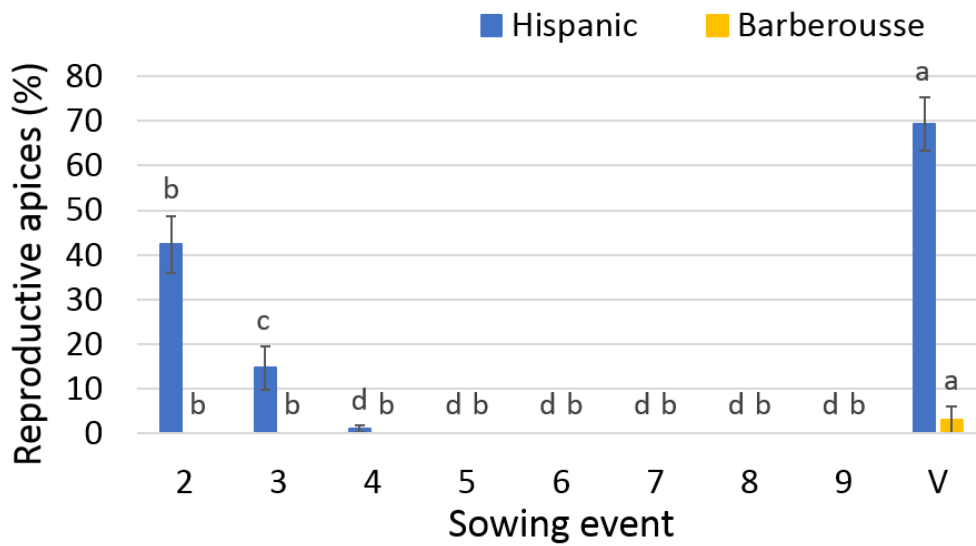
Figure S 2.3. Percentage of reproductive apices with respect to the total (vegetative and reproductive) after 100 days of the experiment.

Mean of 10-12 plants. Error bars are SD. For each variety, bars with the same letter are not significantly different at P<0.05 (LSD test).
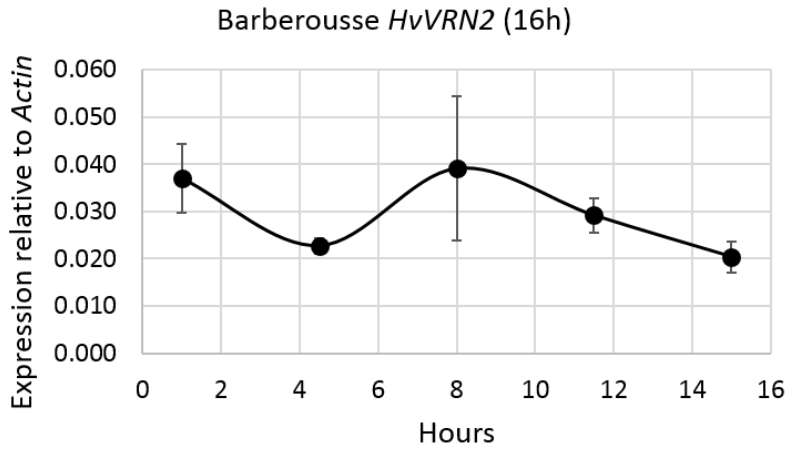
Figure S 2.4. *HvVRN2* diurnal expression in 'Barberousse' unvernalized plants grown under LD (16 h light).

Samples were taken at 1, 4.5, 8, 11.5 and 15 h since the start of the light period. Error bars represent standard error of mean of three biological replicates.

A) HvCO2

```
Morex_AF490470      MNCNFNSDLLEKEAGRTSFPWARPCDGCHAAPSAVYCCADAAYLCSSCDTQVHSANRVAS
Igri_AF490469       MNCNFNSDLLEKEAGRTSFPWARPCDGCHAAPSAVYCCADAAYLCSSCDTQVHSANRVAS
Barberousse_HvCO2   MNCNFNSDLLEKEAGRTSFPWARPCDGCHAAPSAVYCCADAAYLCSSCDTQVHSANRVAS
Hispanic_HvCO2      MNCNFNSDLLEKEAGRTSFPWARPCDGCHAAPSAVYCCADAAYLCSSCDTQVHSANRVAS
                    ***************************************************************
                                                    B-box domain (1)

Morex_AF490470      RHERVRVCETCESTPAVLACHADAAALCTACDAQVHSANPIAQRHQRVPVLPLPAVAIPA
Igri_AF490469       RHERVRVCETCESTPAVLACHADAAALCTACDAQVHSANPIAQRHQRVPVLPLPAVAIPA
Barberousse_HvCO2   RHERVRVCETCESAPAVLACHADAAALCTACDAQVHSANPIAQRHQRVPVLPLPAVAIPA
Hispanic_HvCO2      RHERVRVCETCESAPAVLACHADAAALCTACDAQVHSANPIAQRHQRVPVLPLPAVAIPA
                    ***********:*********************************************
                    (1)                     B-box domain (2)

Morex_AF490470      ASGFAEAEASVTAHGDKEGGEEVDSWLLRRNSDDNNCANKIDRYFNLVGYNMYYDNITCD
Igri_AF490469       ASGFAEAEASVTAHGDKEGGEEVDSWLLRRNSDDNNCANKIDRYFNLVGYNMYYDNITCD
Barberousse_HvCO2   ASGFAEAEASVTAHGDKEGGEEVDSWLLRRNSDDNNCANKIDRYFNLVGYNMYYDNITCD
Hispanic_HvCO2      ASGFAEAEASVTAHGDKEGGEEVDSWLLRRNSDDNNCANKIDRYFNLVGYNMYYDNITCD
                    ***********************************************************

Morex_AF490470      PRPQEQYRMQEQQHVQNRYREKEGCECVVPPQVVMASEQQGSNYGTIGAGQAASVTAMAS
Igri_AF490469       PRPQEQYRMQEQQHVQNRYREKEGCECVVPPQVVMASEQQGSNYGTIGAGQAASVTAMAS
Barberousse_HvCO2   PRPQEQYRMQEQQHVQNRYREKEGCECVVPPQVVMASEQQGSNYGTIGAGQAASVTAMTS
Hispanic_HvCO2      PRPQEQYRMQEQQHVQNRYREKEGCECVVPPQVVMASEQQGSNYGTIGAGQAASVTAMTS
                    ***********************************************************:*

Morex_AF490470      TYTASISNDISFSSMEVGIVPDNTRPNISNRNILTSSEAIELSGHSLQMPVHFSSMDREA
Igri_AF490469       TYTASISNDISFSSMEVGIVPDNTRPNISNRNILTSSEAIELSGHSLQMPVHFSSMDREA
Barberousse_HvCO2   TYTASISNDISFSSMEVGIVPDNTRPNISNRNILTSSEAIELSGHSLQMPVHFSSMDREA
Hispanic_HvCO2      TYTASISNDISFSSMEVGIVPDNTRPNISNRNILTSSEAIELSGHSLQMPVHFSSMDREA
                    *******************************************************  __

Morex_AF490470      RVLRYKEKKQARKFQKTIRYATRKAYAEARPRIKGRFAKRSDIEHEENHMLSPPALPDTS
Igri_AF490469       RVLRYKEKKQARKFQKTIRYATRKAYAEARPRIKGRFAKRSDIEHEENHMLSPPALPDTS
Barberousse_HvCO2   RVLRYKEKKQARKFQKTIRYATRKAYAEARPRIKGRFAKRSDIEHEENHMLSPPALPDTS
Hispanic_HvCO2      RVLRYKEKKQARKFQKTIRYATRKAYAEARPRIKGRFAKRSDIEHEENHMLSPPALPDTS
                    *****************************************************
                                        CCT domain

Morex_AF490470      SYNTVPWF
Igri_AF490469       SYNTVPWF
Barberousse_HvCO2   SYNTVPWF
Hispanic_HvCO2      SYNTVPWF
                    ********
```

B) HvCO9

```
Barberousse_HvCO9    MSAASGAACRVCGGGSEDCSCLLQRGRGVAAARCGVADLNRGFPGMFGQAAEEPAAVDVV
Steptoe_AB592331     MSAASGAACRVCGGGSEDCSCLLQRGRGVAAARCGVADLNRGFPGMFGQAAEEPAAVDVV
Hispanic_HvCO9       MSAASGAACRVCGGGSEDCSCLLQRGRGVAAARCGVADLNRGFPGMFGQAAEEPAAVDVV
Morex_AB592332       MSAASGAACRVCGGGSEDCSCLLQRGRGVAAARCGVADLNRGFPGMFGQAAEEPAAVDVV
                     ************************************************************

Barberousse_HvCO9    SGGGGAAAVGLQEFQFFGQEDHESVAWLFNDHAPIGGEDRLQHRSAVTEQLQRRQAFDAY
Steptoe_AB592331     SGGGGAAAVGLQEFQFFGQEDHESVAWLFNDHAPIGGEDRLQHRSAVTEQLQRRQAFDAY
Hispanic_HvCO9       SGGGGAAAVGLQEFQFFGQEDHESVAWLFNDHAPIGGEDRLQHRSAVTEQLQRRQSFDAY
Morex_AB592332       SGGGGAAAVGLQEFQFFGQEDHESVAWLFNDHAPIGGEDRLQHRSAVTEQLQRRQSFDAY
                     *******************************************************:****

Barberousse_HvCO9    AEYQPGHGLTFDVPVPVPLSRDVVDTAILGLGGGNPVTSAATIMPYCGRETLTFTEAAAS
Steptoe_AB592331     AEYQPGHGLTFDVPVPVPLSRDVVDTAILGLGGGNPVTSAATIMPYCGRETLTFTEAAAS
Hispanic_HvCO9       AEYQPGHGLTFDVPVPVPLSRDVVDTAILGLGGGNPVTSAATIMPYCGRETLTFTEAAAS
Morex_AB592332       AEYQPGHGLTFDVPVPVPLSRDVVDTAILGLGGGNPVTSAATIMPYCGRETLTFTEAAAS
                     ************************************************************

Barberousse_HvCO9    SVVDPNDDTAAGLANGGAYSAGPSGGGGVVGDVPAPTELREAKLMRYKEKRKRRRYEKQI
Steptoe_AB592331     SVVDPNDDTAAGLANGGAYSAGPSGGGGVVGDVPAPTELREAKLMRYKEKRKRRRYEKQI
Hispanic_HvCO9       SVVDPNDDTAAGLANSGAYSAGPSGGGGVVGDVPAPTELREAKLMRYKEKRKRRRYEKQI
Morex_AB592332       SVVDPNDDTAAGLANSGAYSAGPSGGGGVVGDVPAPTELREAKLMRYKEKRKRRRYEKQI
                     ***************.********************************************
                                                            CCT domain (continued)
Barberousse_HvCO9    RYASRKAYAEMRPRVKGRFAKVPDGGEGAAPSPPQQPTQAAGYEPSRLDLGWFRS
Steptoe_AB592331     RYASRKAYAEMRPRVKGRFAKVPDGGEGAAPSPPQQPTQAAGYEPSRLDLGWFRS
Hispanic_HvCO9       RYASRKAYAEMRPRVKGRFAKVPDGGEGAAPSPPQQPTQAAGYEPSRLDLGWFRS
Morex_AB592332       RYASRKAYAEMRPRVKGRFAKVPDGGEGAAPSPPQQPTQAAGYEPSRLDLGWFRS
                     ******************************************************
                            CCT domain
```

C) HvOS2

```
Morex_HORVU3Hr1G095240.6    MARRGRVELRRIEDRTSRQVRFSKRRSGLFKKAFELSVLCDAEVALLVFSPAGRLYEYAS
Hispanic_HvOS2             MARRGRVELRRIEDRTSRQVRFSKRRSGLFKKAFELSVLCDAEVALLVFSPAGRLYEYAS
Barberousse_HvOS2          MARRGRVELRRIEDRTSRQVRFSKRRSGLFKKAFELSVLCDAEVALLVFSPAGRLYEYAS
Zangqing320               MARRGRVELRRIEDRTSRQVRFSKRRSGLFKKAFELSVLCDAEVALLVFSPAGRLYEYAS
Igri_HM130526             MARRGRVELRRIEDRTSRQVRFSKRRSGLFKKAFELSVLCDAEVALLVFSPAGRLYEYAS
                          ************************************************************
                                          MADS-box domain (continued)
Morex_HORVU3Hr1G095240.6    SSIEGTYDRYQAFAGAGKDVSEGGASNNNVNDPSNIQSRLKDITSWSLQNNADDSDANEL
Hispanic_HvOS2             SSIEGIYDRYQAFAGAGKDVSEGGASNNNDGDPSNIQSRLKDITSWSLQNNADDSDANEL
Barberousse_HvOS2          SSIEGTYDRYQAFAGAGKDVSEGGASNNNDGDPSNIQSRLKDITSWSLQNNADDSDANEL
Zangqing320               SSIEGTYDRYQAFAGAGKDVSEGGASNNNDGDPSNIQSRLKDITSWSLQNNADDSDANEL
Igri_HM130526             SSIEGTYDRYQAFAGAGKDVSEGGASNNNDGDPSNIQSRLKDITSWSLQNNADDSDANEL
                          ***** ********************** .*****************************
                                MADS-box domain
Morex_HORVU3Hr1G095240.6    VKLEKLLTDALKKTKSKKILAQRNSGAGTIASGENSRRF
Hispanic_HvOS2             VKLEKLLTDALKKTKSKKILAQRNSGAGTSASGENSRRF
Barberousse_HvOS2          VKLEKLLTDALKKTKSKKILAQRNSGAGTIASGENSRRF
Zangqing320               VKLEKLLTDALKKTKSKKILAQRNSGAGTIASGENSRRF
Igri_HM130526             VKLEKLLTDALKKTKSKKILAQRNSGAGTSASGENSRRF
                          **************************** *********
```

Figure S 2.5. Alignments of (A) HvCO2, (B) HvCO9, and (C) HvOS2 predicted proteins. Protein domains for HvCO2 (Cockram *et al*., 2012); HvCO9 [Prosite v20.79 (http://prosite.expasy.org/)], and HvOS2 (Greenup *et al*., 2010) are indicated.

2.7.1. References

Cockram J, Thiel T, Steuernagel B, Stein N, Taudien S, Bailey PC, et al. 2012. Genome Dynamics Explain the Evolution of Flowering Time CCT Domain Gene Families in the Poaceae. PLoS One. **7**, e45307.

Faure S, Higgins J, Turner A, Laurie DA. 2007. The *FLOWERING LOCUS T-*like gene family in barley (*Hordeum vulgare*). Genetics. **176**, 599–609.

Greenup AG, Sasani S, Oliver SN, Talbot MJ, Dennis ES, Hemming MN, et al. 2010. *ODDSOC2* is a MADS box floral repressor that is down-regulated by vernalization in temperate cereals. Plant Physiol. **153**, 1062–1073.

Griffiths S, Dunford RP, Coupland G, Laurie DA. 2003. The Evolution of *CONSTANS*-Like Gene Families in Barley, Rice, and Arabidopsis. Plant Physiol. **131**,1855–1867.

Hemming MN, Peacock WJ, Dennis ES, Trevaskis B. 2008. Low-temperature and day-length cues are integrated to regulate FLOWERING LOCUS T in barley. Plant Physiol. **147**, 355–366.

Kikuchi R, Kawahigashi H, Ando T, Tonooka T, Handa H. 2009. Molecular and functional characterization of PEBP genes in barley reveal the diversification of their roles in flowering. Plant Physiol. **149**, 1341–1353.

Kikuchi R, Kawahigashi H, Oshima M, Ando T, Handa H. 2012. The differential expression of *HvCO9*, a member of the *CONSTANS*-like gene family, contributes to the control of flowering under short-day conditions in barley. J Exp Bot. **63**, 773–784.

Trevaskis B, Hemming MN, Peacock WJ, Dennis ES. 2006. *HvVRN2* responds to day-length, whereas *HvVRN1* is regulated by vernalization and developmental status. Plant Physiol. **140**, 1397–1405.

Waddington SR, Cartwright PM. 1983. A quantitative Scale of Spike Initial and Pistil Development in Barley and Wheat. Ann Bot. **51**, 119–130.

Yan L, Fu D, Li C, Blechl a, Tranquilli G, Bonafede M, et al. 2006. The wheat and barley vernalization gene VRN3 is an orthologue of FT. Proc Natl Acad Sci. **103**, 19581–19586

Chapter

3

PPD-H1 DEPENDENT CONNECTIONS BETWEEN CLOCK AND FLOWERING TIME GENES IN BARLEY DURING CHANGING PHOTOPERIODS

Chapter 3

Chapter 3. *PPD-H1*-dependent connections between clock and flowering time genes in barley during changing photoperiods

3.1. Introduction

Plants respond to external cues to coordinate and optimize their development with their surroundings. This is critical to coordinate flowering and seed production with optimal seasonal conditions. Photoperiod (day-length) is a major seasonal cue that coordinates flowering with the changing seasons. Perception of photoperiod is mediated by a "circadian clock", a gene network that establishes endogenous biological rhythms that allow plants to measure day-length. The genetic components of the circadian clock have been studied intensively in *Arabidopsis thaliana*, and are now increasingly the focus for research in crops (Millar, 2016; Gil and Park, 2018).

The circadian clock of *Arabidopsis* is comprised of self-regulatory feedback loops that establish rhythmic waves of gene expression that repeat each day-night cycle. The central loop of the circadian clock in *Arabidopsis* is composed of transcription factors belonging to the MYB family, as *CCA1* (*CIRCADIAN CLOCK ASSOCIATED 1*) and *LHY* (*LATE ELONGATED HYPOCOTYL*), and transcription factors belonging to the PSEUDO RESPONSE REGULATORS (PRR) family, as *TIMING OF CAB EXPRESSION1* (*TOC1*) (Gendron *et al.*, 2012; Huang *et al.*, 2012; Fung-Uceda *et al.*, 2018). In the established model in *Arabidopsis*, *CCA1* has a maximum expression peak before dawn, and its protein represses *TOC1*. In the evening, TOC1 suppresses the expression of *CCA1* and *LHY*. In addition, CCA1 and LHY form another feedback loop promoting *PRR7* and *PRR9*, whose proteins in turn repress also *CCA1* and *LHY* sequentially during the day. A third loop acts in the evening, when the Evening complex (EC), composed by *EARLY FLOWERING 3* (*ELF3*), *EARLY FLOWERING 4* (*ELF4*) and *LUX ARHYTHMO* (*LUX*, also

known as *PHYTOCLOCK1*, *PCL1*), is active and represses the *PRR* genes early at night (reviewed by Johansson and Staiger, 2015). Also, in the evening, *GIGANTEA* (*GI*) is induced to repress *TOC1* and *EC*, whose inhibition is maintained at night by CCA1/LHY.

Rhythmic clock-gene expression triggers biological responses through regulation of output genes. In Arabidopsis, clock-regulated expression of *CONSTANS (CO)* plays a central role in accelerating flowering when plants experience long days (e.g. 16 hours daylight). CO is expressed with a daily rhythm that peaks in the late afternoon (Kobayashi *et al.*, 1999; Suárez-López *et al.*, 2001; Valverde *et al.*, 2004). In long days the peak in CO expression coincides with daylight, and this activates expression of *FLOWERING LOCUS T (FT)* (Valverde *et al.*, 2004). *FT* encodes a mobile protein signal that travels from leaves to the shoot apex to trigger floral development (Abe *et al.*, 2005; Wigge *et al.*, 2005; Corbesier *et al.*, 2007; Tamaki *et al.*, 2007).

Barley (*Hordeum vulgare* L.) is an important cereal crop that is used for food and fodder, and as an ingredient in beer and whiskey production. Barley is also a useful diploid model for other temperate cereals that have more complex genetics, such as wheat (*Triticum aestivum*), oats (*Avena sativa*) and rye (*Secale cereale*). Like *Arabidopsis*, long days accelerate flowering of barley through inducing expression of *FT* (*HvFT1)* expression (Turner *et al.*, 2005). Orthologues for several *Arabidopsis* circadian clock genes have been identified in barley and mutations in these genes influence *HvFT1* expression and alter flowering behaviour. These include an orthologue of *ELF3* (*HvELF3*) (Faure *et al.*, 2012; Zakhrabekova *et al.*, 2012), a barley homologue of *LUX* (Mizuno *et al.*, 2012; Campoli *et al.*, 2013; Gawroński *et al.*, 2014) and *PHOTOPERIOD1* (*PPD-H1*), a *PRR* gene related to *AtPRR7* (Turner *et al.*, 2005). This suggests that the model for clock-dependent photoperiod responses developed in *Arabidopsis* might also apply to cereals.

There are reasons to suggest that the basis for photoperiodic flowering responses in cereals might not correspond to the model developed in *Arabidopsis*. Firstly, while some clock genes, such as *TOC1*, are conserved between *Arabidopsis* and cereals, others have diverged independently, including the *PRR* family (Campoli *et al.*, 2012*b*; Calixto *et al.*, 2015). So, there cannot be direct gene-for-gene functional equivalence between the circadian oscillator of barley and *Arabidopsis*. A second more profound difference is in the sensitivity of the barley circadian oscillator to external cues. Unlike *Arabidopsis*, initiation of circadian oscillations in barley requires a day-night cycle, with dawn and dusk cues (Deng *et al.*, 2015*b*). More importantly with respect to the potential role of the circadian clock in regulating photoperiod responses, the circadian oscillator of barley exhibits different waveforms of clock gene expression in short-versus-long photoperiods and shows profound and rapid responses to changes in day-length, in clear contrast to the behaviour of the circadian clock of *Arabidopsis* (Deng *et al.*, 2015*b*). This strong day-length dependency of clock gene expression in barley seems incompatible with the suggestion that the circadian oscillator provides a passive internal reference to measure day-length. An alternative view is that the day-length sensitivity of the barley circadian oscillator plays an active role in triggering photoperiod responses.

In this study, we examine the relationships between the day-length, circadian rhythms and florigen induction in barley. In particular, we focus on the short-term responses of the circadian oscillator and photoperiod-response pathways following shifts of plants from short-to-long days or *vice versa*. We show that changes in clock gene expression patterns occur concomitantly with *PPD-H1*-dependent changes in florigen expression.

3.2.   Materials and methods

3.2.1.   Plant material

Two near-isogenic lines (NILs), named B5 and B6, with different PPD-H1 genotype, were used in this study. Both NILs were generated by five rounds of backcrossing a barley line that shows a strong flowering response to long days (Waite Institute 4441) (Oliver *et al.*, 2013). These isolines are spring type, with no vernalization requirement due to the presence of the *HvVRN1-7* allele, which activates flowering without need for overwintering. Both lines carry *HvVRN2*, a long-day expressed repressor of flowering that normally blocks flowering before overwintering. The lines differ for the *PPD-H1* allele: B5 contains the LD-sensitive allele (*PPD-H1* wildtype) and B6 the LD-insensitive one (*ppd-H1*). *PPD-H1* alleles in both NILs differ by a non-synonymous mutation in the CCT domain of the protein, affecting its function (Turner *et al.*, 2005).

3.2.2.   Growth conditions

For each line, 3 seeds/pot (60 pots in total) were grown in two growth chambers (CONVIRON G1000) at constant temperature (20ºC), and different light regimes: SD, short day conditions, with 8h day/16 h night; and LD, long day conditions, 16h day/8h night. In addition, we studied the response of shifting plants between light regimes (SD-LD; LD-SD). Plants were transferred in a 2-3 leaf stage (12 days after sowing), 8h after turning on the lights. Thus, four treatments were applied, SD, LD, SD-LD and LD-SD, as described in figure 3.1.
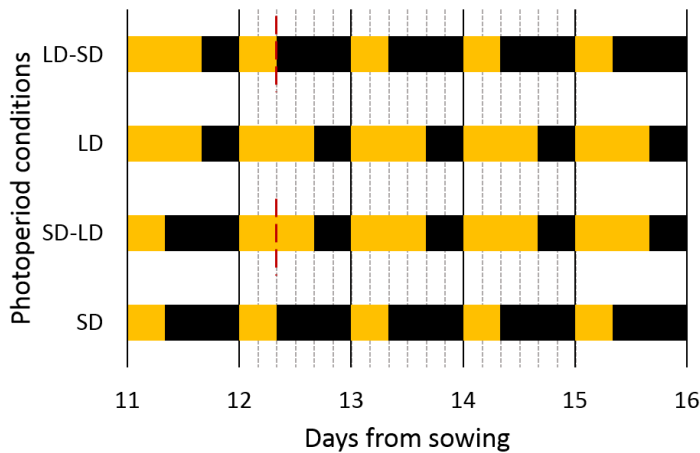
Figure 3.1. Scheme of the experiment.

Yellow bars represent duration of light period in each day (8 h in SD and 16 h in LD); black bars denote duration of dark period in each day. Red dotted line indicates the moment of the day when plants were transferred to new photoperiod conditions. Grey dotted lines represent each one of the leaf sampling for gene expression studies. From the start of the experiment, conditions were the same as in the 11th day after sowings. The daylight conditions experienced until the end of the experiment were the same as in the 16th day after sowing.

3.2.3. Plant phenotyping

Plants were then harvested at specific time points for shoot apex dissection to monitor developmental progressions. For apex dissection, five plants per line and treatment were collected and dissected under a Leica M80 stereomicroscope with integrated camera (Leica). Sampling occurred at two timepoints; 19 and 26 days after sowing, which correspond to 7 and 14 days after day-length shift treatments. Waddington stage (Waddington *et al.*, 1983) was used to describe developmental progression of the main shoot apex (MSA). Apex length was measured in 26-day-old plants, through image analysis using ImageJ software (Schneider *et al.*, 2012). Additionally, for each treatment days to awns appearance was determined for a subset of 5-12 plants (DEV49, Zadoks *et al.*, 1974).

3.2.4. Gene expression studies

For gene expression studies (qRT-PCR), last expanded leaves were sampled, immediately frozen in liquid nitrogen and stored at −80°C until processing. Leaves of 4 different plants in each treatment were collected every 4 hours for 3 days, starting the day of the transfer at the transition to lights on in the morning (Figure 3.1). Total RNA was extracted using Maxwell® RSC Plant RNA kit (Promega) in a Maxwell® RSC Instrument (Promega) in accordance with the manufacturer's instructions. The first-strand cDNA was synthesized from 2 µg of total RNA, using SuperScript III Reverse Transcriptase (Invitrogen). Quantitative Real Time PCR (qRT-PCR) was carried out in a CFX384 BioRad instrument with SYBR Green and Platinum Taq DNA Polymerase (Invitrogen). Genes studied were: *HvCCA1*, *HvTOC1*, *HvGI*, *HvFT1*, *PPD-H1* (*HvPRR37*), *HvCO1*, *HvCO2*, *HvVRN1*, *HvVRN2*, *HvFT3*, *HvOS2*, *HvLUX*, and *Actin* as housekeeping gene. Relative transcript levels were calculated by the ΔΔCt method (Livak and Schmittgen, 2001), taking into account the primers' amplification efficiencies (Table 3.1).

Table 3.1. Primer list.

ID	PRIMER SEQUENCE (5'-3')	Reference
HvCO2	F: AGTGGACTCTTGGCTCCTCA R: CATGCTGCTGTTCTTGCATT	Campoli *et al.* (2012*b*)
HvCO1	F: CGTGCTTCGGCATACGCCTTCC R: CTGCTGGGGCTAGTGCTTAC	Deng *et al.* (2015*b*)
HvFT1	F: ATGAGGACCTTCTACACGCT R: GGCTCTCGTACCACATCACC	Hemming *et al.* (2012)
HvFT3	F: GGTTGTGGCTCATGTTATGC R: CTACTCCCCTTGAGAACTTTC	Forward: Kikuchi *et al.* (2009); Reverse: Faure *et al.* (2007)
HvOS2	F: CAATGCTGATGACTCAGATGCT R: CGCTATTTCGTTGCGCCAAT	Greenup et al. (2010)
PPD-H1	F: CAAATCAAAGAGCGGCGATC R: TCTGACTTGGGATGGTTCACA	Hemming et al. (2008)
HvVRN1	F: GGAAACTGAAGGCGAAGGTTGA R: TGGTTCTTCCTGGCTCTGATATGTT	Greenup *et al.* (2010)
HvVRN2	F: GAGCCACCATCGTGCCATTC R: GCCGCTTCTTCCTCTTCTC	Trevaskis *et al.* (2006)

HvCCA1	F: CGACAAGACACAGCAAGCAT R: CTTCATCTTGCTCCCCTCTG	Deng *et al.* (2015*b*)
HvTOC1	F: TCCAGGGACGTTGAGTTGGTT R: TTTTGAGCGGTTGGGGGTTG	Deng *et al.* (2015*b*)
HvGI	F: AGGCGAAATGGTAATGTTGC R: CAGACATCTGCGTTTCAGGA	Deng *et al.* (2015*b*)
HvLUX	F: AATTCAGTCCACGGATGCTC R: CTTCACTTCAGCTCCCCTTG	Campoli *et al.* (2013)
Actin	F: GCCGTGCTTTCCCTCTATG R: GCTTCTCCTTGATGTCCCTTA	Trevaskis *et al.* (2006)

F, primer forward; R, primer reverse.

3.2.5.   Statistical analysis

All calculations were carried out in R (R Core Team, 2017). All data presented are mean values ± the standard error of the mean (SEM). The ΔCt (Ct target – Ct actin) was used to describe gene expression results. For all experiments, where day-length treatments were compared, differences between mean values at every time point were tested by a Student's t test assuming a two-tailed distribution and equal variance. Pearson correlations were calculated using the package 'corrplot' (Wei and Simko, 2017) and the function *Cor.test* to obtain the significance of correlations. Boxplots of the ΔCt were performed in the package 'ggplot2' (Wickham, 2016), considering all the three days data. Analyses of variance for expression of each gene were performed considering all factors (two varieties, 4 treatments, 3 days and 6 time-points) as fixed, taken into account 3-8 replicates.

3.3.   Results

3.3.1.   Developmental responses to day-length shifts

Developmental responses to different photoperiods were examined in backcross 5 near-isogenic lines that differed for natural variants of the photoperiod sensitivity gene, *PPD-H1*. Plants were grown under short days (SD, 8 h light) or long days

(LD, 16 h light), in a 24 h-cycle (Figure 3.1). Both lines, the *PPD-H1* sensitive (B5) and the *ppd-H1* insensitive (B6), flowered earlier in LD than in SD (Figure 3.2a). In LD, B6 was slower than the sensitive (B5 flowered 13 days earlier than B6). This was also evident at early phases, as observed in main shoot apex (MSA) comparisons (Figure 3.2b). In two-week-old seedlings, the stamen primordium was already present for B5 plants (W 4.0 – 5.0, appearance of pistil – extending of carpel), whereas B6 plants had just passed the double ridge (W 2.0).

Plants transferred from SD to LD conditions at the two-leaf stage (SD-LD) flowered rapidly compared to plants maintained in SD. Plants shifted to LD at the two-leaf stage showed only a slight delay of flowering relative to plants that experienced only LD (6 days for B5, 3 days for B6). Two weeks after the shift to LD there was a significant acceleration of MSA development for B5 plants, which was at W 4.0 – 5.0 (appearance of pistil – extending of carpel), compared to plants maintained in SD which had not yet developed double ridges (W 2.0). LD also accelerated development of B6, though to a lesser extent than B5, reaching the W 2.5 – 3.5 (glume primordium – stamen primordium) two weeks after the shift to LD. When plants were shifted from LD to SD conditions (LD-SD), development slowed, and heading was delayed (Figure 3.2a). Seven days after the shift, there were differences at MSA level between both lines in LD-SD conditions (Figure 3.2b). In summary, we observed rapid developmental responses to day-length shifts and the B6 line that carries the insensitive allele of *PPD-H1* was less responsive to a SD-LD shift than the near-isogenic B5 line, which carries the wildtype *PPD-H1* gene.

a) Heading date
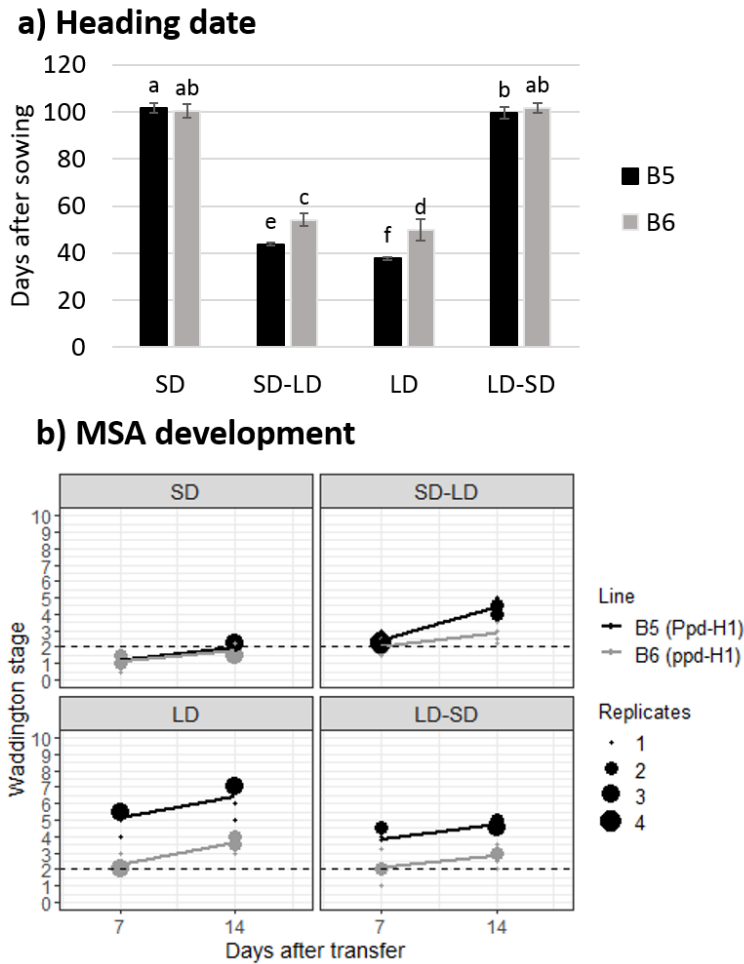
b) MSA development

Figure 3.2. Photoperiod effect in the development.
B5 (black) and B6 (grey) lines carrying different combinations of *PPD-H1* (wildtype and insensitive respectively), grown under SD (8 h light/16 h darkness) and LD (16 h light/8 h darkness), and the shift between both when plants were 12 days old. a) Heading date (days from sowing to awn emergence on the main stem). Error bars are standard deviations for 5–12 plants for each genotype. Genotypes and treatments with different letters are significantly different (P< 0.05). b) Main shoot apices (MSA) development, depending on the *PPD-H1* allele variant. Differences at development stage (Waddington scale) between 7 and 14 days after the transfer (corresponding to 19 and 26 days after sowing), in control and shift treatments. The size of the dots denotes the number of replicates (maximum 5 replicates) with the same stage at a given time point. Dotted line denotes the transition from vegetative to reproductive stage (W 2.0).

3.3.2. Expression of flowering time genes

We next examined the transcriptional activity of genes known to regulate the timing of flowering in cereals. Plants were sampled over 72 hours for each treatment, starting 12 days after sowing, when plants were at the 2-leaf stage. The flowering promoters *HvVRN1* and *HvFT1* were expressed at higher levels in SD versus LD, whereas *HvOS2* was expressed at higher levels in SD (Figure 3.3). In both lines, *HvFT1* expression was below the detection limit under SD conditions. Conversely, under LD conditions *HvFT1* was induced, showing a bimodal expression pattern. A similar bimodal pattern was detected in *HvVRN1* peaking at 4 and 12 h in LD, only in B5 (*PPD-H1* wildtype). We observed clear differences comparing the gene expression levels between the near-isogenic lines. *HvFT1* expression was significantly higher in B5. Similarly, this line showed higher *HvVRN1* expression levels than B6. *HvOS2* was expressed at higher levels in B6, under SD conditions, consistent with a reciprocal relationship with *HvVRN1* transcript levels. Also, in B6, *HvVRN2* showed higher expression levels in LD, consistent with LD-specific expression and potential repression by *HvVRN1* (Trevaskis *et al.*, 2006; Deng *et al.*, 2015*a*). Interestingly, *HvFT3* was expressed at higher levels in B6 than in B5, irrespective of day-length.
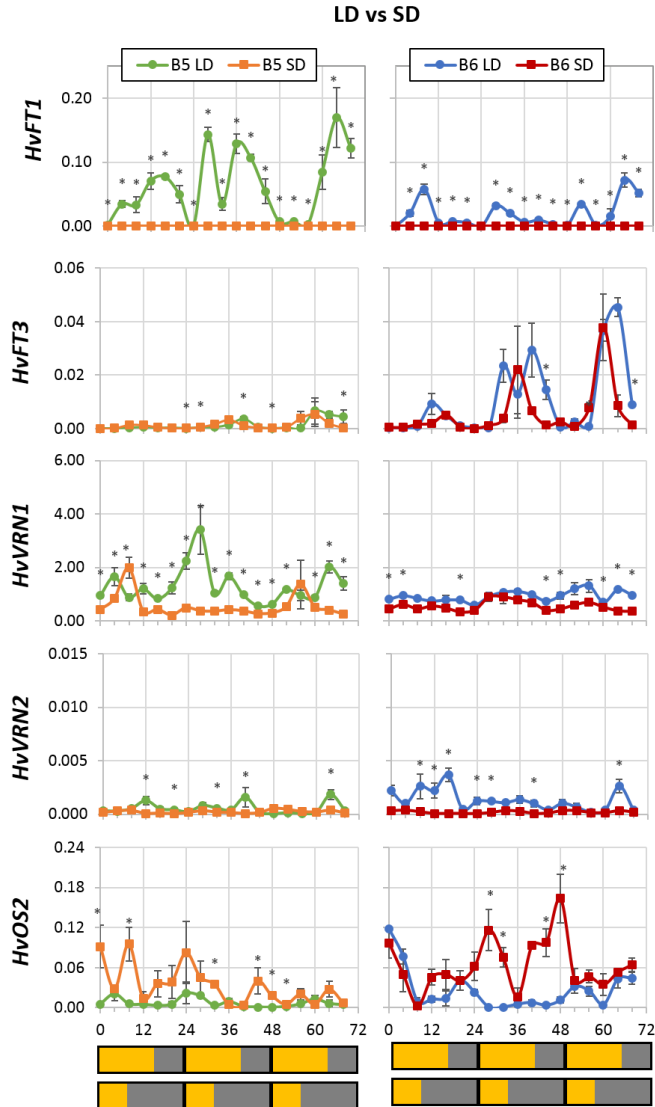
Figure 3.3. Gene expression of the flowering time genes (*HvFT1*, *HvFT3*, *HvVRN1*, *HvVRN2* and *HvOS2*) in *PPD-H1* wildtype (B5) and insensitive (B6) lines under SD (8h light) and LD (16 h light).

Expression levels relative to *Actin*. From left to right, SD (solid orange line) is compared to LD (solid green line) in B5; SD (solid red line) is compared to LD (solid blue line) in B6. Bars at the bottom of the figure represent the photoperiod conditions: day in yellow and night in grey. Error bars are standard error of the mean. * means significantly different expression levels at a certain timepoint (T-student test, * P< 0.05).

When plants were shifted from SD to LD conditions, *HvFT1* was induced (Figure 3.4.). This was first evident after 8 hours in LD and increased through subsequent days. Similarly, *HvFT3* was induced after the first day-night cycle following the shift, and expression was maintained in subsequent cycles. *HvVRN2* levels, though low, were also induced slightly by LD.

Conversely, *HvOS2* transcript levels were reduced within the first 4 hours levels in SD-LD shifted plants, though this difference was not maintained in subsequent days. There was no clear change in expression of *HvVRN1* in plants shifted to LD. The overall gene-expression responses of the near-isogenic lines to day-length shifts were similar between the near isogenic lines, notwithstanding that B6 showed higher levels of *HvFT3*, *HvVRN2* and *HvOS2*, whereas B5 had higher levels of *VRN1* and *HvFT1* expression.

When plants were shifted from LD to SD, *HvFT1* was rapidly and strongly supressed within 4 hours of the shift (Figure 3.4). This decrease was maintained throughout the subsequent timepoints assayed and was clearest in B5, which had higher expression levels of this gene in LD during the time course assayed. *HvFT3* expression was maintained in plants shifted to SD, contrasting with a trend towards increasing expression in plants maintained in LD. This was most evident in B6, which had higher *HvFT3* expression over the time course assayed. In B6, *HvVRN2* and *HvOS2* expression increased when plants were shifted to SD. In B5 *HvVRN1* expression decreased in plants shifted to SD.

(Next page)
Figure 3.4. Gene expression of the flowering time genes (*HvFT1*, *HvFT3*, *HvVRN1*, *HvVRN2* and *HvOS2*) in *PPD-H1* wildtype (B5) and insensitive (B6) lines in SD (8h light), LD (16 h light) and the shifts (SD-LD and LD-SD).
(Continued)

SD vs SD-LD

LD vs LD-SD

Expression levels relative to *Actin*. From left to right, SD (solid orange line) is compared to shift from SD to LD treatment (dotted green line) in B5; SD (solid red line) is compared to shift from SD to LD treatment (dotted blue line) in B6; LD (solid green line) is compared to shift from LD to SD treatment (dotted orange line) in B5; LD (solid blue line) is compared to shift from LD to SD treatment (dotted red line) in B6. Bars at the bottom of the figure represent the photoperiod conditions: day in yellow, night in grey and shift in dotted line. Error bars are standard error of the mean. * means significantly different expression levels at a certain timepoint (T-student test, * P< 0.05).

3.3.3.   Impact of day-length on expression of clock genes

Expression of the circadian clock genes *HvCCA1*, *HvTOC1*, *HvGI*, and *HvLUX* were assayed in the same samples as those in the experiments outlined above. As expected, *HvCCA1*, *HvGI*, *HvLUX* and *HvTOC1* all showed rhythmic expression and each gene peaked at different times during the day (Figure 3.5). Consistent with a previous study (Deng *et al*., 2015*b*) there were marked differences in the waveforms of gene expression in SD versus LD (Figure 3.5). *HvCCA1* had higher expression in SD than LD, with an overall trend towards earlier daily expression peaks in SD. *HvGI* and *HvLUX* were induced in the evening (8-12h after lights were turned on), peaking earlier in SD than LD. Similarly, expression of *HvTOC1* peaked earlier in SD. Expression patterns for *HvCCA1*, *HvGI* and *HvLUX* were similar in both lines. Compared to B6, B5 showed more distinct differences in SD-versus-LD waveform of *HvTOC1*, with broader waves of transcripts in LD (Figure 3.5).
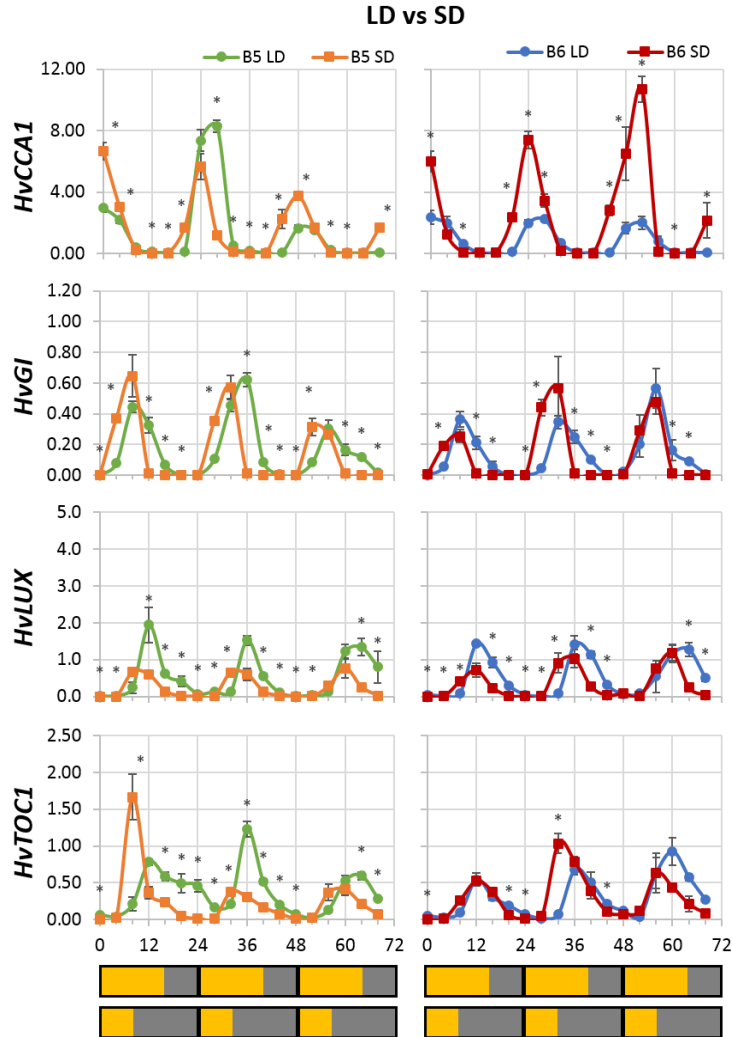
Figure 3.5. Gene expression of the circadian clock genes (*HvCCA1*, *HvGI*, *HvLUX* and *HvTOC1*) in *PPD-H1* wildtype (B5) and insensitive (B6) lines under SD (8h light) and LD (16 h light).

Expression levels relative to *Actin*. From left to right, SD (solid orange line) is compared to LD (solid green line) in B5; SD (solid red line) is compared to LD (solid blue line) in B6. Bars at the bottom of the figure represents the photoperiod conditions: day in yellow and night in grey. Error bars are standard error of the mean. * means significantly different expression levels at a certain timepoint (T-student test, * P< 0.05).

The impacts of day-length shifts on clock gene expression patterns were then examined. Changing day-length triggered rapid changes expression patterns of the clock genes, with waveforms shifting towards those observed in the SD or LD control treatments (Figure 3.6). In general, this can be described as a shift towards earlier daily peaks of clock gene expression in plants shifted to SD, and a shift to later peak expression in LD (Figure 3.6). Statistical differences between control and shift treatments were detected within hours of the shift to new light regimes (Figure 3.6). Generally, the response to day-length shifts was similar in the two near-isogenic lines. The most notable difference between line responses was for *HvTOC1*. A shift from LD to SD triggered larger changes in the waveform of *HvTOC1* expression in B5 (*PPD-H1* wildtype) line than in B6 (*PPD-H1* insensitive allele) (Figure 3.6).

(Next page)

Figure 3.6. Gene expression of the clock genes (*HvCCA1*, *HvGI*, *HvLUX* and *HvTOC1*) in *PPD-H1* wildtype (B5) and insensitive (B6) lines, in SD (8h light), LD (16 h light) and the shifts (SD-LD and LD-SD).
Expression levels relative to *Actin*. From left to right, SD (solid orange line) is compared to shift from SD to LD treatment (dotted green line) in B5; SD (solid red line) is compared to shift from SD to LD treatment (dotted blue line) in B6; LD (solid green line) is compared to shift from LD to SD treatment (dotted orange line) in B5; LD (solid blue line) is compared to shift from LD to SD treatment (dotted red line) in B6. Bars at the bottom of the figure represent the photoperiod conditions: day in yellow, night in grey and shift in dotted line. Error bars are standard error of the mean. * means significantly different expression levels at a certain timepoint (T-student test, * P< 0.05).

●●●

3.3.4. Expression of *PPD-H1* and clock output genes

HvCO1, HvCO2 and *PPD-H1* potentially link the clock to biological outputs such as flowering. The expression of these genes was assayed in the experiments described above. Differences in the timing of expression were found for *HvCO1* and *PPD-H1* between SD and LD conditions (Figure 3.7). Expression of *PPD-H1* was induced after dawn (lights-on) and decreased with darkness in both conditions. Under SD a single and narrow expression peak was detected, with maximum expression at 4 h; whereas a wide peak was observed in LD conditions. The peak of *HvCO1* expression under SD was at 16 h, whereas under LD this peak was delayed to 20 h (Figure 3.7). *HvCO2* transcript levels showed lower and less rhythmic oscillations than *HvCO1* and there was no clear pattern of response to day-length shifts (Figure 3.7). Overall, the gene expression patterns observed in SD and LD were similar in the near-isogenic lines.

When plants were shifted from SD to LD, the expression peaks of *PPD-H1* and *HvCO1* broadened (Figure 3.8). *PPD-H1* expression changed 4 hours after the shift, inducing a second peak at 16 h in both B5 and B6, which was maintained in the subsequent day-night cycles. *HvCO1* oscillations changed, peaking later after the shift. In SD-LD both lines showed similar patterns of expression, except for the higher expression levels of *HvCO1* in B5. When plants were transferred from LD to SD, *PPD-H1* and *HvCO1* peak expression shortened, with lower expression 4h after the shift to SD. *PPD-H1* maintained the this "compressed" expression peak during the subsequent day-night cycles. *HvCO1* showed an earlier peak after the shift. *HvCO2* showed low levels with no clear rhythm. In these conditions, expression was similar in both lines.
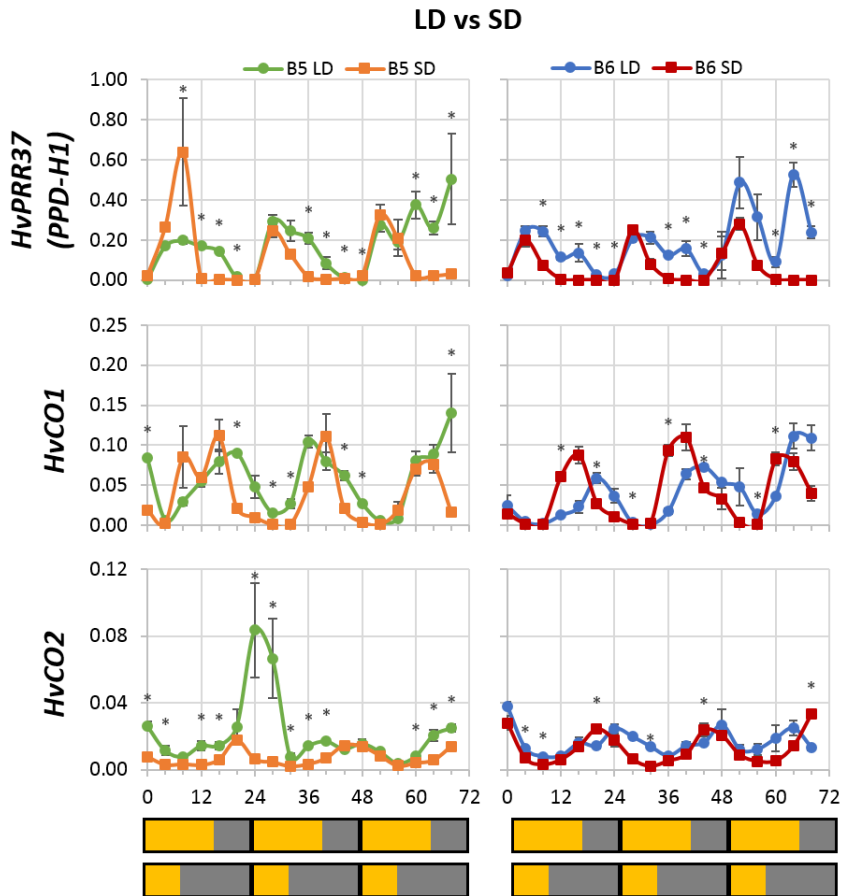
Figure 3.7. Gene expression of *PPD-H1* and the clock output genes (*HvCO1* and *HvCO2*) in *PPD-H1* wildtype (B5) and insensitive (B6) lines under SD (8h light) and LD (16 h light).

Expression levels relative to *Actin*. From left to right, SD (solid orange line) is compared to LD (solid green line) in B5; SD (solid red line) is compared to LD (solid blue line) in B6. Bars at the bottom of the figure represent the photoperiod conditions: day in yellow and night in grey. Error bars are standard error of the mean. * means significantly different expression levels at a certain timepoint (T-student test, * P< 0.05).
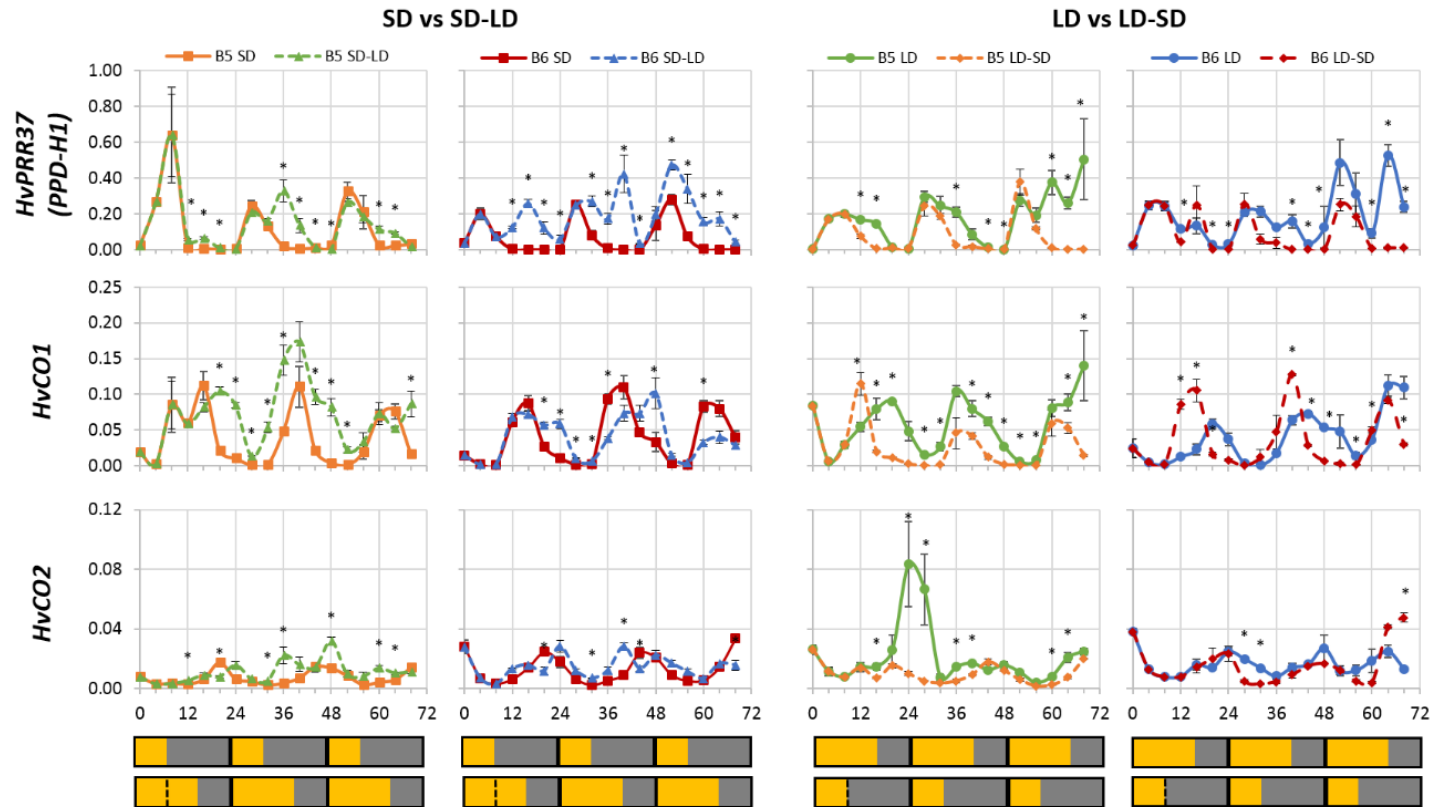
Figure 3.8. Gene expression of *PPD-H1* and the clock output genes (*HvCO1* and *HvCO2*) in *PPD-H1* wildtype (B5) and insensitive (B6) lines, in SD (8h light), LD (16 h light) and the shifts (SD-LD and LD-SD).
(Continued)

Expression levels relative to *Actin*. From left to right, SD (solid orange line) is compared to shift from SD to LD treatment (dotted green line) in B5; SD (solid red line) is compared to shift from SD to LD treatment (dotted blue line) in B6; LD (solid green line) is compared to shift from LD to SD treatment (dotted orange line) in B5; LD (solid blue line) is compared to shift from LD to SD treatment (dotted red line) in B6. Bars at the bottom of the figure represent the photoperiod conditions: day in yellow, night in grey and shift in dotted line. Error bars are standard error of the mean. * means significantly different expression levels at a certain timepoint (T-student test, * P< 0.05).

3.3.5. Relation between expression of circadian clock, clock outputs and flowering time genes

Statistical analyses of variance in transcript levels was carried out for each gene (Table 3.2). There were no differences between B5 (*PPD-H1* wildtype) and B6 (*PPD-H1* insensitive) when comparisons were made between genes expression levels averaged over the three-day experimental time course. However, a significant interaction between variety and treatment was detected for *HvCCA1* and, particularly, for *HvTOC1*, the two genes of the central loop of the clock. *HvCCA1* expression was stable across treatments in the B5 whereas the B6 showed slightly lower expression in LD conditions (Figure 3.9). The opposite was observed for *HvTOC1*, whose expression showed no differences for B6 across treatments, but was lower in SD than LD in B5 (Figure 3.9). This opposite behaviour could explain the negative correlation found between *HvCCA1* and *HvTOC1* expression (Figure 3.10). Some of the correlations between transcript levels of pairs of genes showed that both genes either increased or decreased together, revealing a correspondence, probably through a shared pathway. Other consistent correlations for clock genes across the four treatments were *HvCCA1* and *HvLUX*, and *HvCCA1* and *HvFT3*, both inverse correlations.

All the clock output genes and the flowering time genes, except *HvCO2* showed significant differences between both genotypes, and all showed significant

interaction between variety and treatment (Table 3.2). All responded to day-length cues, as the effect of treatment was significant in all of them (Table 3.2). The positive correlations among these genes in LD for both lines suggest common pathways or underlying gene regulatory mechanisms. In SD, some of these correlations turned negative, indicating a change in the relationships among them. Although low correlations were found between *PPD-H1* and *HvVRN1* (r = 0.39 – 0.59, Figure 3.10), the relationships between variety, treatment and transcript levels of *HvVRN1*, *HvVRN2* and *HvOS2*, in which B5 had higher *HvVRN1* and lower *HvVRN2* and *HvOS2* expression than B6 (Table 3.2, Figure 3.9), indicates a regulation by *PPD-H1*, possibly at the transcriptional level, though this might be indirect (other genes acting as intermediates, for example).

Table 3.2. Analysis of variance for the ΔCt corresponding to the expression of genes of NILS B5 sensitive (*PPD-H1)* and B6 insensitive (*ppd-H1*) in 2-week-old plants sampling every 4 hours covering 3 days of expression data, in plants growing under 4 different photoperiod treatments (SD, SD-LD, LD, LD-SD).

Source of variation	HvCCA1			HvGI			HvLUX		
	df	ms		df	ms		df	ms	
Variety (V)	1	0.50	ns	1	10.60	ns	1	0.50	ns
Treatment (T)	3	6.90	*	3	113.40	***	3	107.30	***
Day	2	22.50	***	2	1.90	ns	2	12.00	*
Time	5	780.40	***	5	1167.50	***	5	861.20	***
V : T	3	9.10	*	3	4.70	ns	3	3.20	ns
Residuals	437	2.40		428	3.60		445	3.70	
Missingness	15			24			7		

Source of variation	HvTOC1			PPD-H1			HvCO1		
	df	ms		df	ms		df	ms	
Variety	1	1.62	ns	1	27.00	*	1	16.49	**
Treatment	3	24.46	***	3	361.20	***	3	63.07	***
Day	2	3.79	ns	2	14.80	ns	2	0.82	ns
Time	5	262.54	***	5	480.90	***	5	279.32	***
V : T	3	16.47	***	3	102.60	***	3	18.90	***
Residuals	432	1.52		425	5.60		427	2.40	
Missingness	20			27			25		

Source of variation	HvCO2			HvFT1			HvFT3		
	df	ms		df	ms		df	ms	
Variety	1	1.87	ns	1	593.00	***	1	892.70	***
Treatment	3	20.19	***	3	6721.00	***	3	51.70	***
Day	2	1.60	ns	2	19.00	ns	2	142.90	***
Time	5	47.86	***	5	327.00	***	5	522.50	***
V : T	3	6.98	***	3	106.00	*	3	29.50	**
Residuals	445	0.79		423	35.00		423	7.20	
Missingness	7			29			29		

Source of variation	HvVRN1			HvVRN2			HvOS2		
	df	ms		df	ms		df	ms	
Variety	1	4.66	***	1	62.00	***	1	210.58	***
Treatment	3	40.87	***	3	93.88	***	3	125.08	***
Day	2	1.15	ns	2	9.31	ns	2	7.26	ns
Time	5	6.30	***	5	21.23	***	5	11.22	*
V : T	3	2.10	**	3	27.93	***	3	73.61	***
Residuals	448	0.40		439	3.77		429	4.60	
Missingness	4			13			23		

*, **, *** significant effects; ns, non-significant at P < 0.05, < 0.01, < 0.001. df; degree of freedom; ms; mean square. N = 3 – 8 replicates.
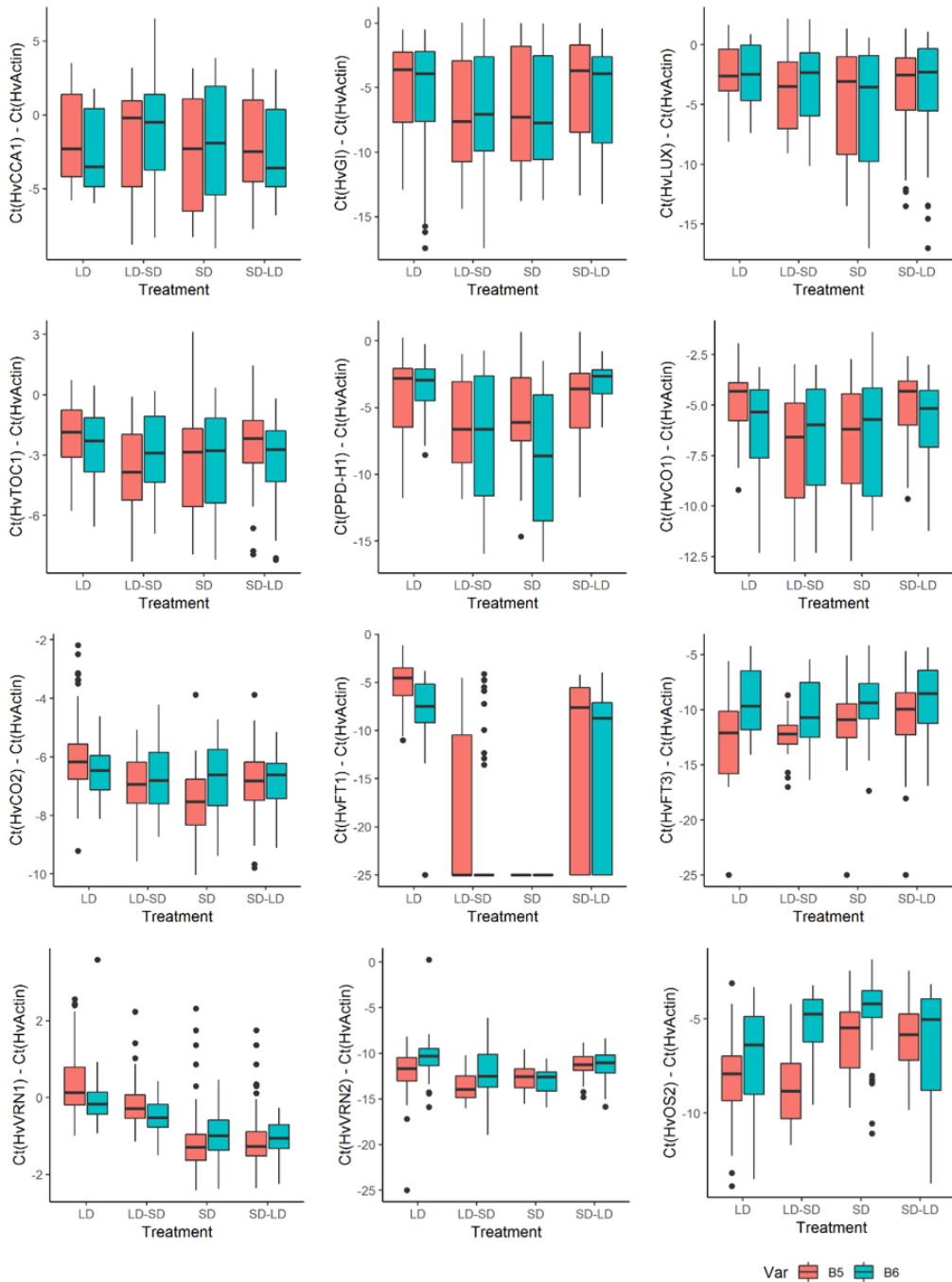
Figure 3.9. General pattern of expression, as ΔCt values, averaged over three days. ΔCt values are the difference Ct target gene – Ct *Actin*. Six points per day, and three days are represented. In general, the higher the ΔCt values, the higher the gene expression (relative to *Actin*).
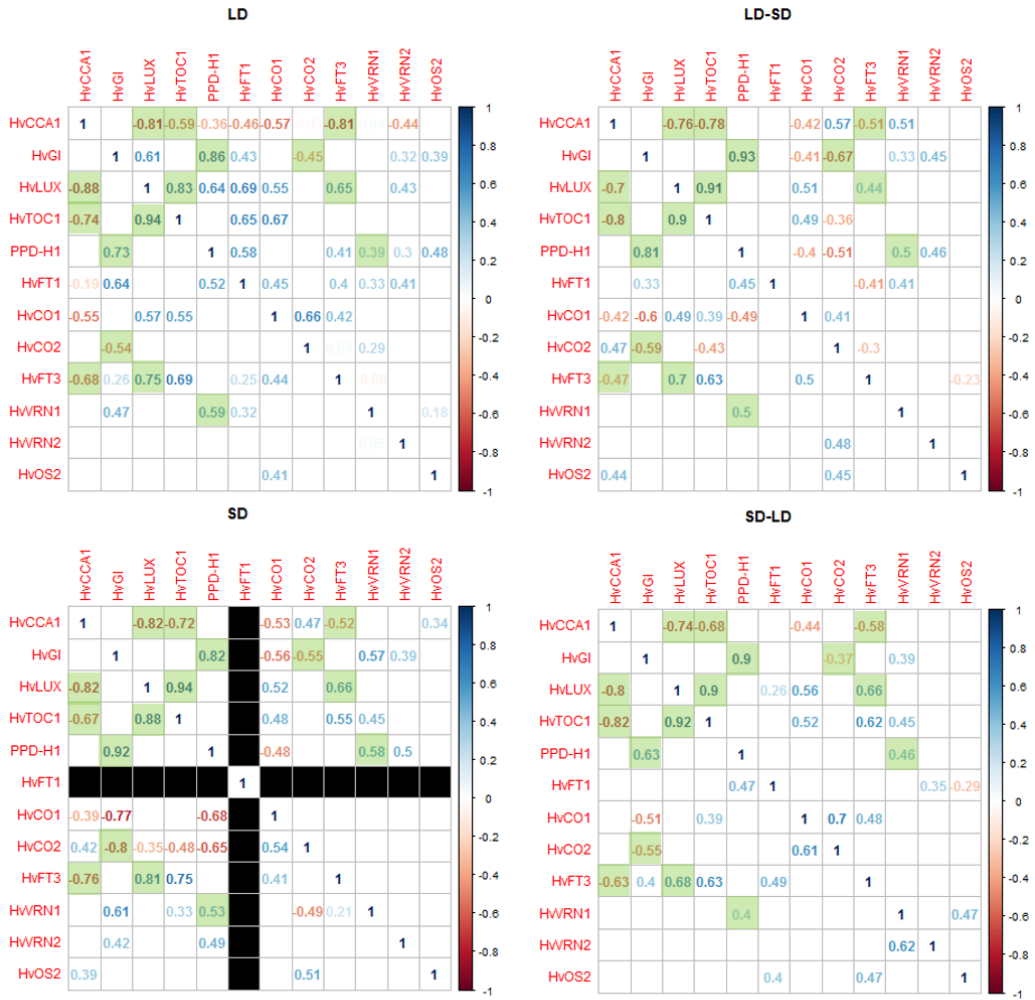
Figure 3.10. Correlations between expression of genes studied.

Only significant correlations are shown (P<0.05). Upper triangle corresponds to correlations in the sensitive genotype (B5), and lower triangle to the insensitive genotype (B6). Black squares indicate that no expression was detected under those conditions. Black cells indicate absence of data. Green squares correspond to stable correlations, independent on genotype and day-length.

3.4.   Discussion

3.4.1.   *HvFT1* induction within the first day in the shift conditions is independent of the *PPD-H1* allele.

The near-isogenic lines studied differ in the functionality of the *PPD-H1* gene, resulting in different day-length responsiveness, with earlier flowering of B5 under LD (control and shift treatments). Observations of the main shoot apex confirmed that this developmental response started in early phases during the plant lifecycle (Figure 3.2b). Transcript levels of *PPD-H1* were similar in the near-isogenic lines. However, the two isolines showed different regulation of flowering time genes. As described by Turner *et al.* (2005), early flowering of barley plants with the wildtype *PPD-H1* allele is associated with increased levels of *HvFT1* in LD.

Aiming to observe molecular responses to changing photoperiods, we tested the effect of the natural mutation at *PPD-H1* on the expression of flowering time genes over a three-day period. The expression pattern of *HvFT1* was bimodal, as observed in *Arabidopsis* (Song *et al.*, 2018). *HvFT1* expression change rapidly when plants were shifted SD-LD, within first day in both lines. *HvFT1* expression increased each subsequent day in B5 but did not reach levels seen in LD grown plants. Initial LD-induction of *HvFT1* expression was weaker in B6, and there was no increase in peak transcript levels in subsequent days. On the basis of these observations we conclude that the initial induction of *HvFT1* occurs irrespective of the *PPD-H1* allelic variation contrasted in this study. The different *PPD-H1* alleles do, however, seem to influence the level to which *HvFT1* is induced by LD.

There was no clear relationship between expression of clock output genes and the differential LD expression of *HvFT1* in the contrasting *PPD-H1* genotypes. Although the wildtype B5 line showed high levels of *HvCO1* in SD-LD, these were not associated with contrasting levels or accelerated induction of *HvFT1*. Campoli

et al. (2012*a*) over-expressed *HvCO1* in barley and this accelerated flowering, but that *PPD-H1* genotype influenced *HvFT1* expression independently of *HvCO1* transcript levels. Contrastingly, acceleration of MSA development in SD-LD (Figure 3.2b) was associated with the presence of the sensitive *PPD-H1* allele and the high expression levels of *HvCO1* in B5 after the shift SD-LD (Figure 8), hinting at a relationship between them. Interestingly, Hayama *et al.* (2017) reported that the *PPD-H1* homologue in *Arabidopsis* stabilizes the transcription of *CO*, regulating the abundance of its product under LD, which might explain partially the results of our study under SD-LD conditions. Thus, *HvCO1* might be effective integrating the photoperiod signals in the flowering pathway.

The mechanism is complex, and the flowering repressors might also be playing a role at these early stages. The low *HvFT1* expression levels of the B6 insensitive line were concurrent with relatively higher expression levels of flowering repressors (*HvVRN2* and *HvOS2*), delayed development of the MSA, and later flowering. Thus, both repressors were expressed rapidly after the shift (*HvVRN2* induced in LD; *HvOS2* induced in SD), particularly in the B6 insensitive line, which is coherent with the slower development observed in B6. Expression of these flowering repressors associated with the vernalization response in spring lines was not expected. Both are expected to be fully repressed by expression of *HvVRN1*, but this was not the case. Photoperiod insensitivity has been associated with spring cultivars cultivated in Northern latitudes (Turner *et al.*, 2005), which are sown after winter and do not accelerate flowering in LD. An active expression of these repressors in spring lines could delay development beyond an agronomic optimum, and thus could suffer purifying selection in spring germplasm. In fact, this hypothesis is consistent with the fact that spring barleys usually carry the non-functional allele of *HvVRN2*. Less is known about the diversity of *HvOS2* (Monteagudo *et al.*, 2019), homologue of the major repressor of flowering in *Arabidopsis* FLC (Greenup *et al.*, 2010).

● ● ●

3.4.2. *PPD-H1* affects the rhythmicity of flowering time genes

As the transcript levels of *PPD-H1* did not vary much between the two lines, we hypothesize that its effect depends on the functionality of the *PPD-H1* protein.

Theory states that *HvFT3* is the gene that promotes flowering particularly under SD conditions, but it is also active in LD conditions when the levels of *HvVRN2* are reduced (Casao *et al.*, 2011). Here, we found *HvFT3* expression mainly under LD conditions, and in presence of *HvVRN2*. The insensitive line showed higher levels of this flowering promoter than the sensitive line (Figures 3.3 and 3.4), being the most important difference in expression between the two genotypes of all the genes studied (Table 3.2). As was discussed by Mulki *et al.* (2018), *HvFT3* effect is stage-dependent, affecting spikelet initiation and early reproductive development, although they also found that *HvFT3* expression levels were influenced by natural variation at *PPD-H1* which affected *HvFT1* expression levels. Accordingly, the lower expression levels of *HvFT3* in B5 in our experiment, could be explained either by a stage-dependency (being B5 plants more developed than B6), or by a regulation of *HvFT3* expression by *HvFT1*.

The isolines studied carry an *HvVRN1* allele (*HvVRN1-7*) that does not induce a vernalization requirement (Hemming *et al.*, 2009). Therefore, in principle, we did not expect differences in its expression. However, we found some differences between the lines, hinting at an effect of the *PPD-H1* alleles. Kitagawa *et al.* (2012) suggested that *VRN1* expression is not directly regulated by the photoperiod pathway mediated by *PPD-1* in wheat, and that any difference should be due to *VRN2* expression. However, we detected high *HvVRN1* levels under LD in both lines, coinciding with *HvVRN2* expression, with the only difference in *HvVRN1* rhythmicity in the sensitive line.

Diurnal expression of spring *VRN1* was demonstrated in wheat, whose upregulation followed the accumulation of *FT* in LD, with independence on the *PPD* allele

(Shimada *et al.*, 2009). Here, we found that rhythmicity of *HvVRN1* was exclusive of the sensitive line and only in LD. Thus, the expression of a spring *VRN1* allele (as *HvVRN1-7*) seems affected by photoperiod in the presence of a sensitive *PPD-H1* allele, as in Campoli *et al.* (2012*a*).

As the promoter of *HvFT1* is a direct target of the *HvVRN1* protein (Deng *et al.*, 2015*a*), rhythmicity in *HvVRN1* might explain the fluctuating levels of *HvFT1* in the sensitive line. However, the *HvFT1* induction in the SD-LD occurred in both lines, with low and arrhythmic levels of *HvVRN1*, indicates that, although not so efficiently, the induction of *HvFT1* by LD is controlled by different pathways.

Other direct targets of the VRN1 protein, *HvVRN2* and *HvOS2*, were detected in higher levels in the insensitive line, which showed induced but arrhythmic expression of *HvVRN1*. This is consistent with the reported relationship between *PPD-H1* variants and *HvVRN2* (Kitagawa *et al.*, 2012; Mulki and von Korff, 2016). The novelty in our study is that we use lines that do not need vernalization and, hence, no role of these repressors was expected a priori. However, there were clear differences between the two lines, which seem to be related to the different induction of *HvVRN1* by *PPD-H1*, rather than a direct effect of *PPD-H1* on *HvVRN2*.

3.4.3. Changing photoperiods modify the oscillations of clock genes

Circadian oscillations were activated after twelve days in SD and LD. There were differences in the length of the expression wave of the clock genes with different day-lengths, and in the clock downstream genes *PPD-H1* and *HvCO1*. Day-length had an effect on the oscillation patterns of the clock genes, marked by dawn and dusk cues. Those cues regulate the initiation of circadian oscillations (Deng *et al.*, 2015*b*) and their modification after photoperiod shifts. In our study, duration of

light prior to transition to other photoperiods influenced oscillation of most of the genes, especially in clock genes, as in Deng *et al.* (2015*b*). In these genes, peak expression occurred earlier in SD and later in LD (Figure 3.5). After both shifts, timing of peaks rapidly adjusted towards the new conditions (Figure 3.2).

During the three-day span covered by this study, *PPD-H1* affected diurnal oscillations of clock outputs, photoperiod and vernalization genes, and did not affect to most of the clock genes (Table 3.2), as was already observed by previous reports of single-day experiments (Turner *et al.*, 2005; Campoli *et al.*, 2012*b*; Ejaz and von Korff, 2017). However, the clock gene *HvTOC1* showed a differential response to the day-length transitions depending on the allelic variant at *PPD-H1*. *HvTOC1* responded to the shift conditions faster in the sensitive line (Figure 3.6). We suggest that a sensitive *PPD-H1* allele would be necessary to generate a rapid response to dusk cues through *HvTOC1* (Figure 3.2), which might be reflected in downstream flowering time genes (discussed previously). *PPD-1* and *TOC1* belong to the PRR family, which are highly conserved genes between monocot and dicot species, but *PPD-H1* have evolved independently (Calixto *et al.*, 2015). *PPD-H1* (*HvPRR37*) is the ortholog of *AtPRR7*. An effect of AtPRR7 on the circadian clock was found when comparing the effects of the wild-type allele with mutant prr7-11 (reviewed by Webb *et al.,* 2019). As *PPD-H1* is the long photoperiod response gene, the presence of the functional gene might mark the day-length (being more sensitive to dusk cues), allowing the adjustment of the oscillator to the increasing photoperiods. In this case, the different sensitivity to dusk cues could confer an advantage, allowing a robust response to environmental perturbations.

The oscillations of clock output genes were also modified by the shift. The patterns of expression of these genes changed within the first day-night cycle, revealing a rapid adaptation to the new photoperiods either by changing the waveform (*HvCO1*) or the number of peaks per day cycle (*PPD-H1* and *HvFT1*). We did not

observe a rapid response for *HvCO2,* possibly because *HvCO2* plays its role at more advanced development phases (Kitagawa *et al.*, 2012; Digel *et al.*, 2015).

3.5.   Conclusion

We have observed that clock genes respond after the photoperiod shift modifying their expression patterns. In the transition between photoperiods, the rapid adjustment of the circadian rhythms allows a quick response to environmental cues, which can be related to a robust adaptation to perturbations in the environment. We have found consequences of the action of genes responsible of photoperiod response in the circadian clock (*HvTOC1* responded rapidly to the shift in the sensitive NIL), in clock outputs and flowering time genes, in good agreement with the differential development observed for the two lines. Here, we provide molecular details about the flexibility of the circadian regulation and its contribution to photoperiod responses and flowering time in barley. Extending the knowledge of the molecular regulation of the circadian clock would lead to a better understanding of crop adaptation mechanisms in the field, which will be useful for developing varieties fine-tuned to the environment.

3.6.   References

Abe M, Kobayashi Y, Yamamoto S, Daimon Y, Yamaguchi A, Ikeda Y, Ichinoki H, Notaguchi M, Goto K, Araki T. 2005. FD, a bZIP protein mediating signals from the floral pathway integrator FT at the shoot apex. Science. **309**, 1052–1056.

Calixto CPG, Waugh R, Brown JWS. 2015. Evolutionary Relationships Among Barley and *Arabidopsis* Core Circadian Clock and Clock-Associated Genes. Journal of Molecular Evolution **80**, 108–119.

Campoli C, Drosse B, Searle I, Coupland G, Von Korff M. 2012*a*. Functional characterisation of *HvCO1*, the barley (*Hordeum vulgare*) flowering time ortholog of *CONSTANS*. Plant Journal **69**, 868–880.

Campoli C, Shtaya M, Davis SJ, von Korff M. 2012*b*. Expression conservation within the circadian clock of a monocot: natural variation at barley *Ppd-H1* affects circadian expression of flowering time genes, but not clock orthologs. BMC Plant Biology **12**, 97.

Campoli C, Pankin A, Drosse B, Casao CM, Davis SJ, Von Korff M. 2013. *HvLUX1* is a candidate gene underlying the *early maturity 10* locus in barley: Phylogeny, diversity, and interactions with the circadian clock and photoperiodic pathways. New Phytologist **199**, 1045–1059.

Casao MC, Igartua E, Karsai I, Lasa JM, Gracia MP, Casas AM. 2011. Expression analysis of vernalization and day-length response genes in barley (*Hordeum vulgare* L.) indicates that *VRNH2* is a repressor of *PPDH2* (*HvFT3*) under long days. Journal of Experimental Botany **62**, 1939–1949.

Corbesier L, Vincent C, Jang S, *et al.* 2007. FT Protein Movement Contributes to Long-Distance Signaling in Floral Induction of Arabidopsis. Science **316**, 1030–1033.

Deng W, Casao MC, Wang P, Sato K, Hayes PM, Finnegan EJ, Trevaskis B. 2015*a*. Direct links between the vernalization response and other key traits of cereal crops. Nature Communications **6**, 5882.

Deng W, Clausen J, Boden S, Oliver SN, Casao MC, Ford B, Anderssen RS, Trevaskis B. 2015*b*. Dawn and Dusk Set States of the Circadian Oscillator in Sprouting Barley (*Hordeum vulgare*) Seedlings. PloS one **10**, e0129781.

Digel B, Pankin A, von Korff M. 2015. Global transcriptome profiling of developing leaf and shoot apices reveals distinct genetic and environmental control of floral transition and inflorescence development in barley. The Plant Cell **27**, 2318–2334.

Ejaz M, von Korff M. 2017. The genetic control of reproductive development under high ambient temperature. Plant Physiology **173**, 294–306.

Faure S, Higgins J, Turner A, Laurie DA. 2007. The *FLOWERING LOCUS T*-like gene family in barley (*Hordeum vulgare*). Genetics **176**, 599–609.

Faure S, Turner AS, Gruszka D, Christodoulou V, Davis SJ, von Korff M, Laurie DA. 2012. Mutation at the circadian clock gene *EARLY MATURITY 8* adapts domesticated

barley (*Hordeum vulgare*) to short growing seasons. Proceedings of the National Academy of Sciences of the United States of America **109**, 8328–8333.

Fung-Uceda J, Lee K, Seo PJ, Polyn S, De Veylder L, Mas P. 2018. The Circadian Clock Sets the Time of DNA Replication Licensing to Regulate Growth in *Arabidopsis*. Developmental Cell **45**, 101-113.

Gawroński P, Ariyadasa R, Himmelbach A, *et al.* 2014. A Distorted Circadian Clock Causes Early Flowering and Temperature-Dependent Variation in Spike Development in the *Eps-3A^{m}* Mutant of Einkorn Wheat. Genetics **196, 1253–1261.

Gendron JM, Pruneda-Paz JL, Doherty CJ, Gross AM, Kang SE, Kay SA. 2012. *Arabidopsis* circadian clock protein, TOC1, is a DNA-binding transcription factor. Proceedings of the National Academy of Sciences of the United States of America **109**, 3167–3172.

Gil KE, Park CM. 2018. Thermal adaptation and plasticity of the plant circadian clock. New Phytologist **221**, 1215–1229.

Greenup AG, Sasani S, Oliver SN, Talbot MJ, Dennis ES, Hemming MN, Trevaskis B. 2010. *ODDSOC2* Is a MADS Box Floral Repressor That Is Down-Regulated by Vernalization in Temperate Cereals. Plant Physiology **153**, 1062–1073.

Hayama R, Sarid-Krebs L, Richter R, Fernández V, Jang S, Coupland G. 2017. PSEUDO RESPONSE REGULATORs stabilize CONSTANS protein to promote flowering in response to day length. The EMBO Journal **36**, 904–918.

Hemming MN, Fieg S, James Peacock W, Dennis ES, Trevaskis B. 2009. Regions associated with repression of the barley (*Hordeum vulgare*) *VERNALIZATION1* gene are not required for cold induction. Molecular Genetics and Genomics **282**, 107–117.

Hemming MN, Walford SA, Fieg S, Dennis ES, Trevaskis B. 2012. Identification of High-Temperature-Responsive Genes in Cereals. Plant Physiology **158**, 1439–1450.

Huang W, Pérez-García P, Pokhilko A, Millar AJ, Antoshechkin I, Riechmann JL., Mas P. 2012. Mapping the Core of *Arabidopsis* Circadian Clack defines the network structure of the oscillator. Science **338**, 75–79.

Johansson M, Staiger D. 2015. Time to flower: Interplay between photoperiod and the circadian clock. Journal of Experimental Botany **66**, 719–730.

Kikuchi R, Kawahigashi H, Ando T, Tonooka T, Handa H. 2009. Molecular and functional characterization of PEBP genes in barley reveal the diversification of their roles in flowering. Plant Physiology **149**, 1341–1353.

Kitagawa S, Shimada S, Murai K. 2012. Effect of *Ppd-1* on the expression of flowering-time genes in vegetative and reproductive growth stages of wheat. Genes & Genetic Systems **87**, 161–168.

Kobayashi Y, Kaya H, Goto K, Iwabuchi M, Araki T. 1999. A Pair of Related Genes with Antagonistic Roles in Mediating Flowering Signals. Science **286**, 1960–1962.

Livak KJ, Schmittgen TD. 2001. Analysis of relative gene expression data using real-

time quantitative PCR and the 2(-Delta Delta C(T)) Method. Methods **25**, 402–408.

Mizuno N, Kinoshita M, Kinoshita S, Nishida H, Fujita M, Kato K, Murai K, Nasuda S. 2016. Loss-of-function mutations in three homoeologous *PHYTOCLOCK 1* genes in common wheat are associated with the extra-early flowering phenotype. PLoS ONE **11**, e0165618.

Millar AJ. 2016. The Intracellular Dynamics of Circadian Clocks Reach for the Light of Ecology and Evolution. Annual Review of Plant Biology **67**, 595–618.

Monteagudo A, Igartua E, Contreras-moreira B, Gracia MP, Ramos J, Karsai I, Casas AM. 2019. Fine-tuning of the flowering time control in winter barley : the importance of *HvOS2* and *HvVRN2* in non-inductive conditions. BMC Plant Biology **19**, 113.

Mulki MA, Bi X, von Korff M. 2018. FLOWERING LOCUS T3 Controls Spikelet Initiation But Not Floral Development. Plant Physiology **178**, 1170–1186.

Mulki MA, von Korff M. 2016. *CONSTANS* Controls Floral Repression by Up-Regulating *VERNALIZATION2* (*VRN-H2*) in Barley. Plant Physiology **170**, 325–337.

Oliver SN, Deng W, Casao MC, Trevaskis B. 2013. Low temperatures induce rapid changes in chromatin state and transcript levels of the cereal *VERNALIZATION1* gene. Journal of Experimental Botany **64**, 2413–2422.

R Core Team. 2017. R: A langauge and environment for statistical computing. https://www.r-project.org.

Schneider CA, Rasband WS, Eliceiri KW. 2012. NIH Image to ImageJ: 25 years of image analysis. Nature Methods **9**, 671–675.

Shimada S, Ogawa T, Kitagawa S, *et al.* 2009. A genetic network of flowering-time genes in wheat leaves, in which an *APETALA1/FRUITFULL*-like gene, *VRN1*, is upstream of *FLOWERING LOCUS T*. Plant Journal **58**, 668–681.

Song YH, Kubota A, Kwon MS, *et al.* 2018. Molecular basis of flowering under natural long-day conditions in *Arabidopsis*. Nature Plants.

Suárez-López P, Wheatley K, Robson F, Onouchi H, Valverde F, Coupland G. 2001. *CONSTANS* mediates between the circadian clock and the control of flowering in *Arabidopsis*. Nature **410**, 1116–1120.

Tamaki S, Matsuo S, Wong HL, Yokoi S, Shimamoto K. 2007. Hd3a protein is a mobile flowering signal in rice. Science. **316**, 1033–1036.

Trevaskis B, Hemming MN, Peacock WJ, Dennis ES. 2006. *HvVRN2* responds to day-length, whereas *HvVRN1* is regulated by vernalization and developmental status. Plant Physiology **140**, 1397–1405.

Turner A, Beales J, Faure S, Dunford RP, Laurie DA. 2005. The Pseudo-Response Regulator *Ppd-H1* Provides Adaptation to Photoperiod in Barley. Science **310**, 1031–1034.

Valverde F, Mouradov A, Soppe W, Ravenscroft D, Samach A, Coupland G. 2004. Photoreceptor Regulation of CONSTANS Protein in Photoperiodic Flowering. Science

303, 1003–1006.

Waddington SR, Cartwright PM, Wall PC. 1983. A quantitative Scale of Spike Initial and Pistil Development in Barley and Wheat. Annals of Botany **51**, 119–130.

Webb AAR, Seki M, Satake A, Caldana C. 2019. Continuous dynamic adjustment of the plant circadian oscillator. Nature Communications **10**, 4–9.

Wei T, Simko V. 2017. R package 'corrplot': Visualization of a Correlation Matrix. Version 0.84. https://github.com/taiyum/corrplot.

Wickham H. 2016. ggplot2: Elegant Graphisc for Data Analysis. Springer-Verlag, New York.

Wigge PA, Kim MC, Jaeger KE, Busch W, Schmid M, Lohmann JU, Weigel D. 2005. Integration of spatial and temporal information during floral induction in *Arabidopsis*. Science. **309**, 1056–1059.

Zadoks JC, Chang TT, Konzak CF. 1974. A Decimal Code for the Growth Stages of Cereals. Weed Research **14**, 415–421.

Zakhrabekova S, Gough SP, Braumann I, *et al.* 2012. Induced mutations in circadian clock regulator *Mat-a* facilitated short-season adaptation and range extension in cultivated barley. Proceedings of the National Academy of Sciences of the United States of America **109**, 4326–4331.

Chapter 4

DIVERSITY IN DEVELOPMENTAL RESPONSES TO LIGTH SPECTRAL QUALITY IN BARLEY

Chapter 4. Diversity in developmental responses to light spectral quality in barley

4.1.   Introduction

Plants depend on ambient light conditions to regulate their development and to be able of adapting to changing environments. As plants are sessile organisms, they measure quantity (intensity), quality (spectral composition), direction and duration (photoperiod) of light to regulate their development and to acclimatise to the surrounding environment (Franklin, 2009; Ugarte *et al.*, 2010; Monostori *et al.*, 2018). The integration of several cues is essential for the plant to decipher what is happening around it and respond accordingly. In an example exposed by Casal and Qüesta (2018): "the same photoperiod can take place in late summer and spring", thus an unique signal does not provide enough information, and more signals are needed to solve that ambiguity, similarly to what occurs in winter crops, in which the memory of winter temperatures complements photoperiodic information to define the season. Spectral composition is a parameter of light sensed by plants that vary with altitude, latitude, seasons, and climatic and atmospheric factors (Holmes and Smith, 1977*a*). During the day, spectral energy distribution of solar light changes between day, dawn and dusk, thus light quality contributes to determine the precise timing of photoperiod signals. Also, the relative levels of blue, red and far-red wavelengths change in many circumstances, for instance in presence of clouds. Thus, natural light spectra vary in a continuous state of flux, being accompanied by other environmental changes (Morgan and Smith, 1981). Finally, the radiation that reaches a plant is affected by these factors and by the canopy of neighbours in the vicinity (Holmes and Smith, 1977*b*). All these circumstances cause spectral differences that lead to complex interactions, affecting plant growth (Kami *et al.*, 2010).

Flowering is a complex process that involves signals from several pathways recording information from the plant and the environment, and promoting transition to the reproductive stage under favourable conditions. Barley (*Hordeum vulgare* L.) and wheat (*Triticum* spp.) are long-day (LD) plants, flowering earlier under increasing day-lengths. Flowering promotion is controlled through the interplay of the major flowering time genes, *VERNALIZATION 1* (*HvVRN1*), *VERNALIZATION 2* (*HvVRN2*) and the homologous of *FLOWERING LOCUS T* (*FT*), *HvFT1*. Vernalization and photoperiod signals must be integrated to allow timely flowering; thus, the aforementioned genes interplay with the long and short photoperiod response genes, *PHOTOPERIOD RESPONSE1* (*PPD-H1*, whose candidate is *HvPRR37* (Turner *et al.*, 2005), and *PHOTOPERIOD RESPONSE2* (*PPD-H2*, whose candidate is *HvFT3*, Faure *et al.,* 2007), respectively.

In the previous chapter of this thesis, we observed that regulation of these genes was closely related to circadian clock (Chapter 3). Gierczik *et al.* (2017) reported that light quality altered the circadian clock expression in barley. In *Arabidopsis thaliana*, modification of the red to far-red ratio (R:FR) and temperature affected the long day pattern of expression of *FT* (Song *et al.*, 2018), being essential to mimic the natural conditions in growth chambers.

The effect of light quality in plant growth has been widely studied, especially in horticultural and ornamental species. Nowadays, new protocols for growing crops as fast as possible in indoor facilities are at the cutting edge of plant breeding research (Watson *et al.*, 2018). Optimizing the spectral composition of the growth chambers must be considered when planning an experiment, to favour fast development or facilitating replication of the results. Monostori *et al.* (2018) demonstrated that light quality and quantity affected wheat growth and development, metabolic processes, grain yield and flour quality, opening the possibility to optimize growth conditions and to obtain desired traits and products.

● ● ●

The R:FR ratio has been extensively studied due to its relation with vegetation shade and its consequent involvement in shade avoidance syndrome, including comparisons of different light sources (Wit *et al.*, 2016; Demarsy *et al.*, 2017; Fiorucci and Fankhauser, 2017). Lately, much attention has been given to other waveband ratios to which plant responsiveness is also highly dependent on the species and cultivar of interest (Gómez and Izzo, 2018). In wheat, for instance, light quality was determinant in stem elongation, which was influenced by blue, green and far-red light antagonistically (Monostori *et al.*, 2018).

Our work has focused on the effect on plant development of two conventional artificial lighting regimens that provide different spectral quality. Specifically, we investigated the effect of two broad-spectrum light sources, both emitting continuous visible light spectra. One is fluorescent light with high proportions of photons in the green-yellow (GY) and red (R) regions. The other one is metal halide light bulbs, which produce several wavelength peaks distributed evenly across the entire spectrum, which becomes more balanced than the fluorescent one. Our aims are 1) characterizing the effect of different lighting regimes and examining the consequences of transferring plants between both conditions, and 2) examining the molecular effect on vernalization and photoperiod pathways at early developmental phases. We have compared the responses on morphology and development, including apex examination, and gene expression studies of major flowering time genes in barley.

4.2. Materials and Methods

4.2.1. Plant material

We chose 11 barley varieties with different allelic constitution for major flowering time genes, related to vernalization and photoperiod pathways (*HvVRN1*, *HvVRN2*, *HvFT1*, *PPD-H1*, *HvFT3*), as described in Table 4.1. Plants were fully vernalized

(5±2°C for 52 days under 8 h light/16 h night) prior to the start of the experiment. Then, plants were moved to independent growth chambers with different light bulbs, fluorescent or metal halide. All of them were established under long day photoperiod conditions (16 h light/8h night), constant temperature of 18 ± 1°C during day and night, and the same light intensity (~250 µmol m^{-2} s^{-1}).

4.2.2. Light spectral conditions

The experiments were carried out in the Phytotron facilities of the Agricultural Research Institute of the Hungarian Academy of Sciences, at Martonvásár (Hungary) using Conviron PGR-15 growth chambers (Conviron Ltd., Canada).

Two lamp types were used: fluorescent (F) and metal halide (M) light bulbs. Both are broad spectrum light sources, with major differences within the photosynthetically active region (PAR, 400-700 nm). Absolute photon irradiance was obtained with a USB400-UV-VIS Spectrometer (Ocean Optics, USA), measuring PAR at the top of the plant canopy. Spectral data were based on 0.21 nm intervals from 350 to 873 nm, calculated as spectral photon distribution and the summation over the interval as photon flux (Sager *et al.*, 1988). Spectral energy distribution of light, in both light sources, was studied in the 350-850 nm wavelength region (Figure 4.1A). The ratios between the photon flux densities at different wavelengths are given in figure 4.1B (following Mortensen and Stromme, 1987). Blue region (B) in the range 400-500 nm; green-yellow (GY), 500-600 nm; red (R), 600-700 nm; far-red (FR), 700-800 nm. Major differences within the PAR region are due to green-yellow-red ratio (GY:R) and red-far-red ratio (R:FR) (Figure 4.1). Fluorescent light has greater GY:R and R:FR ratios than those produced by metal halide. Slight differences were found also in the blue-green-yellow ratio (B:GY), with lower levels under fluorescent conditions than under

metal halide. In general, fluorescent light was rich in the green-yellow and red regions, whereas metal halide spectrum was more balanced across the PAR region.

		Fluorescent (F)	Metal Halide (M)
B/R		0.93	0.94
B/GY		0.42	0.74
GY/R		2.21	1.28
R/FR		7.41	2.13
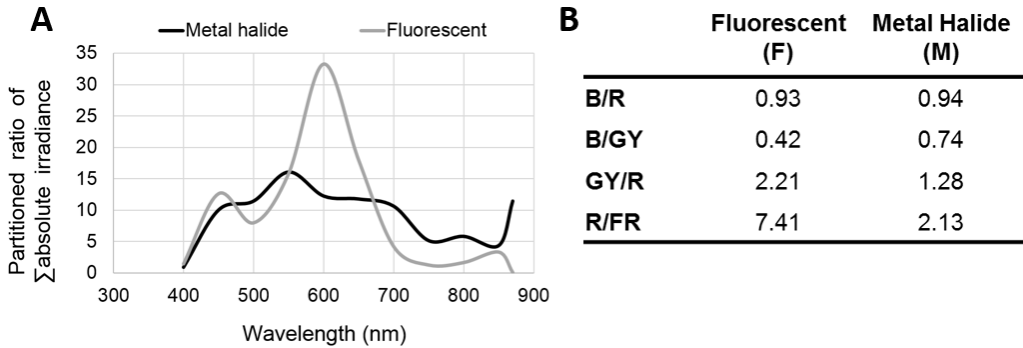
Figure 4.1. Spectral composition of fluorescent (F) and metal halide (M) light bulbs. A) Proportion of irradiance (%) measured in the growth chambers. B) Ratios between different wavebands. Ratio measured as photon flux density. B, blue (400-500 nm); GY, green-yellow (500-600 nm); R, red (600-700 nm); FR, far-red (700-800 nm).

4.2.3.   Comparison between light quality treatments

The study consisted in two control treatments and two shift treatments; all carried out in separate growth chambers. For the control treatments, the plants were kept at the same growth chamber (M or F) for the full duration of the experiment. The shift treatments involved another two growth chambers. Plants were moved to one of them after vernalization and, 10 days later, they were interchanged (M plants moved to F chamber and *vice versa*). These treatments will be coded as MF and FM. For phenotypic measurements, sixteen plants per genotype were sown in individual pots, and four were placed at each growth chamber, making four replicates per genotype and treatment. Additionally, 20 seeds per genotype and treatment were sown in groups of 5 plants/pot, which were used for destructive samplings to record apex development stage and for gene expression studies.

4.2.1.   Phenotypic measurements

Plant development was monitored twice a week by counting leaf and tiller number, measuring plant height, and checking for first node appearance (plant developmental stage 31, or DEV31) and appearance of the awns just visible above the last leaf sheath (DEV49). All these data were used to dissect the development in phenophases, defined based on stages of the Zadoks' scale (Zadoks *et al.*, 1974), following the description of Tottman *et al.* (1979).

Plant height was measured as the attachment height, in cm, of the last leaf sheath on the main stem. Dynamics of plant height, which follows a sigmoid curve, with three phases (slow initial growth, intensive stem elongation, and final slow growth), was characterised with linear regressions. Their intersections led to determining the onset of intensive stem elongation (DEV30), and the end of the stem elongation (ZDSE). The interval elapsed between both points is considered the period of stem elongation, and will be referred to as "length of stem elongation period", or LSE. The rate of growth during the stem elongation phase was described as stemochron (cm^{-1}).

Dynamics of leaves were characterized with linear regressions over time. The parameters of the equation $y = ax + b$ were used to determine the date of appearance of the flag leaf (DEV37), as follows:

$$DEV37\ (days) = \frac{(final\ leaf\ number - 0.9) - a}{b}$$

The date of full expansion of the flag leaf (DEV39) was calculated as follows:

$$DEV39\ (days) = \frac{final\ leaf\ number - a}{b}$$

Phyllocron was evaluated as the rate of leafing out.

Table 4.1. List of the barley genotypes examined and allelic variants for the major flowering time genes.

Variety	Origin	Rows	Growth [a]	HvVRN1 [b]	HvVRN2 [c]	HvFT1 [d]	PPD-H1 [e]	HvFT3 [f]
Kold	USA	6	W	vrn1	VRN2	AG	PPD1	ppd2
Price	USA	6	W	vrn1	VRN2	TC	PPD1	PPD2
WA1614-95	USA	6	F	vrn1	vrn2	AG	PPD1	ppd2
Haruna Nijo	Japan	2	F	vrn1	vrn2	TC	PPD1	PPD2
Eight-Twelve	USA	6	W	vrn1	VRN2	AG	PPD1	PPD2
Scio	USA	6	F	vrn1	vrn2	AG	PPD1	PPD2
Dicktoo	USA	6	F	vrn1	vrn2	TC	PPD1	ppd2
Ragusa	Croatia	6	F	VRN1-6	vrn2	AG	PPD1	ppd2
Esterel	France	6	W	vrn1	VRN2	TC	PPD1	ppd2
SBCC016	Spain	6	W	VRN1-6	VRN2	AG	PPD1	PPD2
SBCC046	Spain	6	W	VRN1-6	VRN2	AG	PPD1	ppd2

a Growth habit deduced from the alleles at loci *HvVRN1* and *HvVRN2*. W, winter; F, facultative.

b Alleles based on the size of intron 1 (Hemming *et al.*, 2009)

c Presence/absence of *HvZCCT* (Karsai *et al.*, 2005)

d Alleles based on two SNPs in intron 1 (Yan *et al.*, 2006).

e Alleles based on SNP22 (Turner *et al.*, 2005)

f Presence/absence of *PPD-H2* (Faure *et al.*, 2007)

In control conditions, apex dissection was carried out 8, 23, 31, 37 and 45 days after the end of the vernalization period. In the shift conditions, apex dissection was carried out 20, 30 and 41 days after the vernalization period. At each sampling point, 3 plants per variety and treatment were dissected. Phenotyping consisted on recording apex length (mm) and apex stage following the Waddington's scale

(Waddington *et al.*, 1983). For gene expression analysis, the last fully expanded leaf was collected in the middle of the light cycle at each particular treatment, 20 days after the end of the vernalization period, in three plants per genotype and sampling.

The plants were grown to full maturity and the following yield components were evaluated: number of nodes in the main stem, length of the last internode in the main stem (cm), spike length in the main stem (cm), number of spikelets in the main stem's spike, number of fertile tillers (reproductive tillers), number of seeds in the main stem, individual seed weight in the main stem (g), total number of seeds per plant and individual seed weight in the whole plant (g).

4.2.2. Gene expression

Total RNA was isolated from leaf tissue with TRIzol Reagent (Thermo Fisher Scientific, Ltd) followed by the Qiagen RNeasy Plant Mini kit, in accordance with the manufacturer instructions (Qiagen, Ltd.). Then, the material was extracted in the QIAcube equipment (Qiagen Ltd). One microgram of total RNA was used for cDNA synthesis using the Revert Aid First Strand cDNA synthesis kit (Thermo Fisher Scientific, Ltd) with the standard protocol provided by the company. The quantitative real time PCR was carried out in three biological and two technical replicates in a Rotor-Gene Q equipment (Qiagen Ltd) with SYBR-Green Master Mix. Genes evaluated are described in table S 4.1. Expression was normalized to *Actin* using the Rotor-Gene software, also accounting for the amplification efficiency.

4.2.3. Statistical analysis

Data from 11 varieties growing in four different treatments (MF, FM, M, F) were used in the analyses, taking into account the average of 3-4 biological replicates.

ANOVA was carried out in Genstat v18 (VSN International, 2017). Other analyses were carried out in R (R Core Team, 2017). Multiple comparisons were obtained by Fisher's protected Least Significant Differences (LSD) with the R package 'agricolae' (de Mendiburu, 2016). Pearson correlations were obtained using the package 'corrplot' (Wei and Simko, 2017). Principal component analysis (PCA) was performed with the R function 'prcomp' using the singular value decomposition, and based on the correlation matrix. Biplot was carried out with the package 'ggplot2' (Wickham, 2016). To assess the phenotypic diversity through a cluster analysis, all variables in common in all the treatments were taken into account, and highly related variables were discarded. Finally, 17 phenotypic traits were used to carry out the cluster analysis (Table S 4.2). Cluster analysis (UPGMA) was done with the package "factoextra" (Kassambara and Mundt, 2017). The best grouping result was chosen as the one with the highest cophenetic correlation and the lowest Gower distance.

4.3.   Results

4.3.1.   Developmental responses to light quality

In general, barley plants grown under fluorescent (F) lighting flowered later than in metal halide (M) conditions (Figure 4.2, M and F). Among the phenological phases encompassing the flowering process (phenophases), time to first node appearance (DEV31) and from there until the onset of stem elongation phase (DEV30) were the most affected by the lighting conditions (much longer in F).
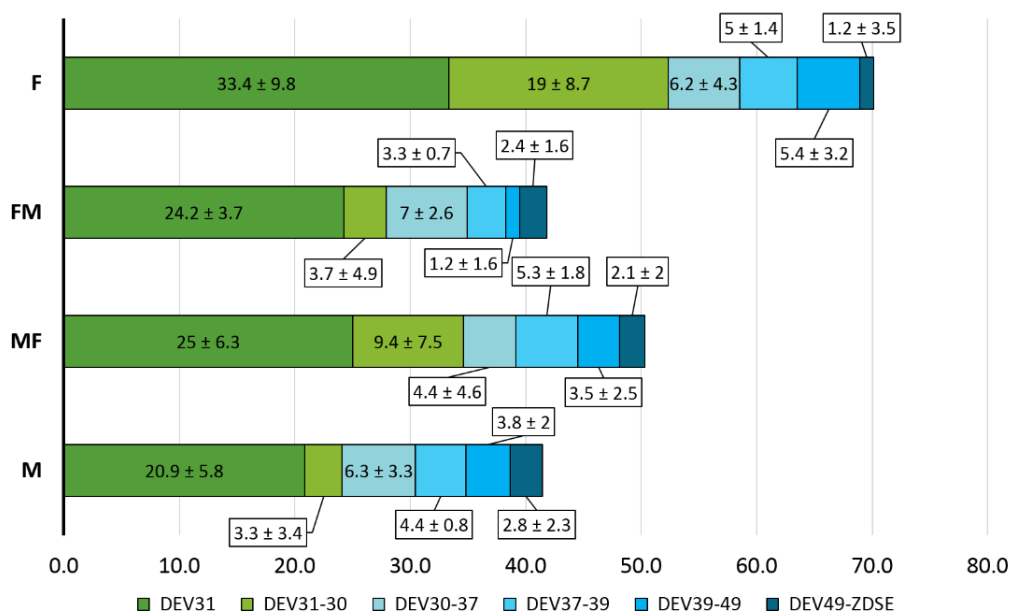
Figure 4.2. Duration of the different developmental phases under different lighting treatments.
Metal halide (M), 10 days in fluorescent and then shift to metal halide (FM); fluorescent (F) and 10 days in metal halide and then shift to fluorescent (MF) bulbs. Mean of 11 varieties and standard deviation are represented as numbers in each phase.

Regarding the shift treatments, in general, plants in MF took longer to reach the end of the stem elongation (ZDSE) than plants in FM, but developed earlier than those in F conditions (Figure 4.2). In both shifts, plants showed similar average duration of DEV31 phase, which took around 25 days. However, from that moment on, FM conditions shortened the duration of the different phenophases, becoming more similar to development in M conditions. Overall, the differences in phase duration among treatments were more concentrated in two stages, before and after onset of stem elongation (DEV30). The total duration of the phases were 24.2, 27.9, 34.4 and 52.4 days (at M, FM, MF, F, respectively) before DEV30, whereas after DEV30, the sum showed little variation among treatments, 13.9, 15.3, 17.3 and 17.8

days, at FM, MF, M and F, respectively. The analyses of variance revealed significant differences between treatments, varieties and the interaction treatment × variety for all the developmental phases (Table 4.2).
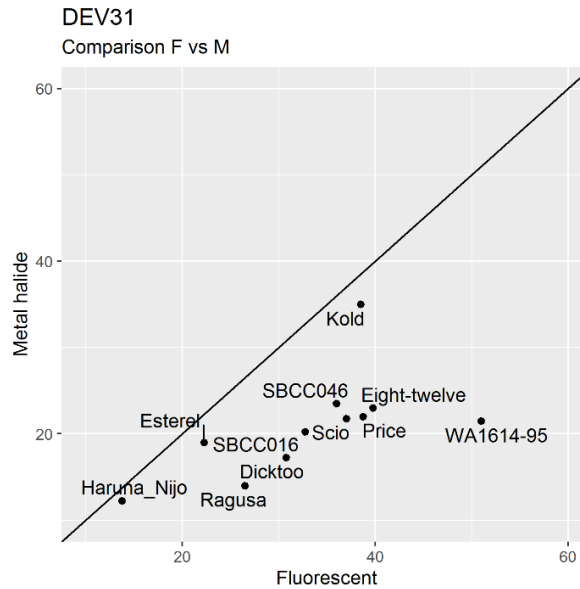
Figure 4.3. Scatter plot representing the comparison of days to first node appearance (DEV31) in fluorescent versus metal halide conditions.
Each dot represents the average of 4 biological replicates per variety.

Treatments M and FM showed rather similar duration of the phenophases (Figure 4.2). Ten days in fluorescent conditions caused slight delay in occurrence of DEV31 and DEV30 (later FM), but this delay was almost completely offset by the hastening of the three last phases. Larger differences were found when comparing F and MF: most of the phenophases were shorter after a period of 10 days under M conditions (Figure 4.2), with the largest differences in the first two phases (DEV31 and DEV31-30). A brief exposition of 10 days under metal halide lighting (MF) supposed an acceleration of node appearance (DEV31) up to 17.5 days, and an acceleration of awns appearance (DEV49) up to 31 days (Figure S1).

The varieties showed different patterns of development in the control conditions (Figure 4.3, Figure S 4.1). Some varieties reached the first node stage (DEV31) at the same time despite the lighting system used, whereas fluorescent light delayed the transition in other cases, as can be noticed by the distance from the dots to the 1:1 line (Figure 4.3). A diversity of responses was observed, with Haruna Nijo and Kold as the most stable across light treatments.

Table 4.2. Analyses of variance for DEV31 and DEV49 dates and for the entire growth duration divided in two phases, before and after DEV30.

Source of variation	d.f.	Sums of squares	Mean squares	Variance ratio	F probability
DEV31					
Replicates	3	31.6	10.5	4.0	
Treatment	3	3724.9	1241.6	467.3	<.001
Variety	10	5409.6	541.0	203.6	<.001
Treatment.Variety	30	2044.7	68.2	25.7	<.001
Residual	128	340.1	2.7		
DEV49					
Replicates	3	18.4	6.1	2.1	
Treatment	3	26233.6	8744.5	3025.2	<.001
Variety	10	16317.5	1631.7	564.5	<.001
Treatment.Variety	30	4515.4	150.5	52.1	<.001
Residual	128	370.0	2.9		
End of vernalization - DEV30					
Replicates	3	8.7	2.9	0.6	
Treatment	3	20622.8	6874.3	1471.3	<.001
Variety	10	13380.6	1338.1	286.4	<.001
Treatment.Variety	30	4432.4	147.7	31.6	<.001
Residual	128	598.1	4.7		
Duration of stem elongation (LSE)					
Replicates	3	11.2	3.7	0.5	
Treatment	3	408.7	136.2	18.6	<.001
Variety	10	495.2	49.5	6.8	<.001
Treatment.Variety	30	580.0	19.3	2.6	<.001
Residual	128	938.7	7.3		

Df, degrees of freedom

4.3.1. Dynamics of apices

Dissection of plants was carried out at different time points of the experiment to study the development of the apices. Waddington stage and apex length were recorded. Apex development was delayed in plants growing under fluorescent conditions (Figure 4.4). For apices dissected 10 days after the shift, two contrasting patterns were detected: shifted plants in FM showed the same delayed pattern as the plants from the initial F chamber but plants in MF progressed as readily as plants in M. Thus, the initial period under metal halide light produced a developmental boost that accelerated development even after the shift to fluorescent lighting conditions. From 10 days after the shift to the last apex dissection, we observed different patterns of responses: (A) plants that adapted to the new conditions, showing the expected pattern of growth according to the new conditions (Scio and Price), and (B) plants which showed small or no differences between treatments (Kold, Haruna Nijo, Ragusa).

Comparing shift treatments, varieties showed differences at apex stage after 20 days from the transfer to the new lighting conditions (mean in FM = 6.36; mean in MF = 5.04; t-test p-value = 0.006), whereas apex length was less variable at that stage (mean in FM = 14.95 mm; mean MF = 9.33 mm ; t-test p-value = 0.126), and became very distinct between treatments at the last sampling (Figure 4.5). These results revealed that light quality had a rapid effect on the development of the floral organs.
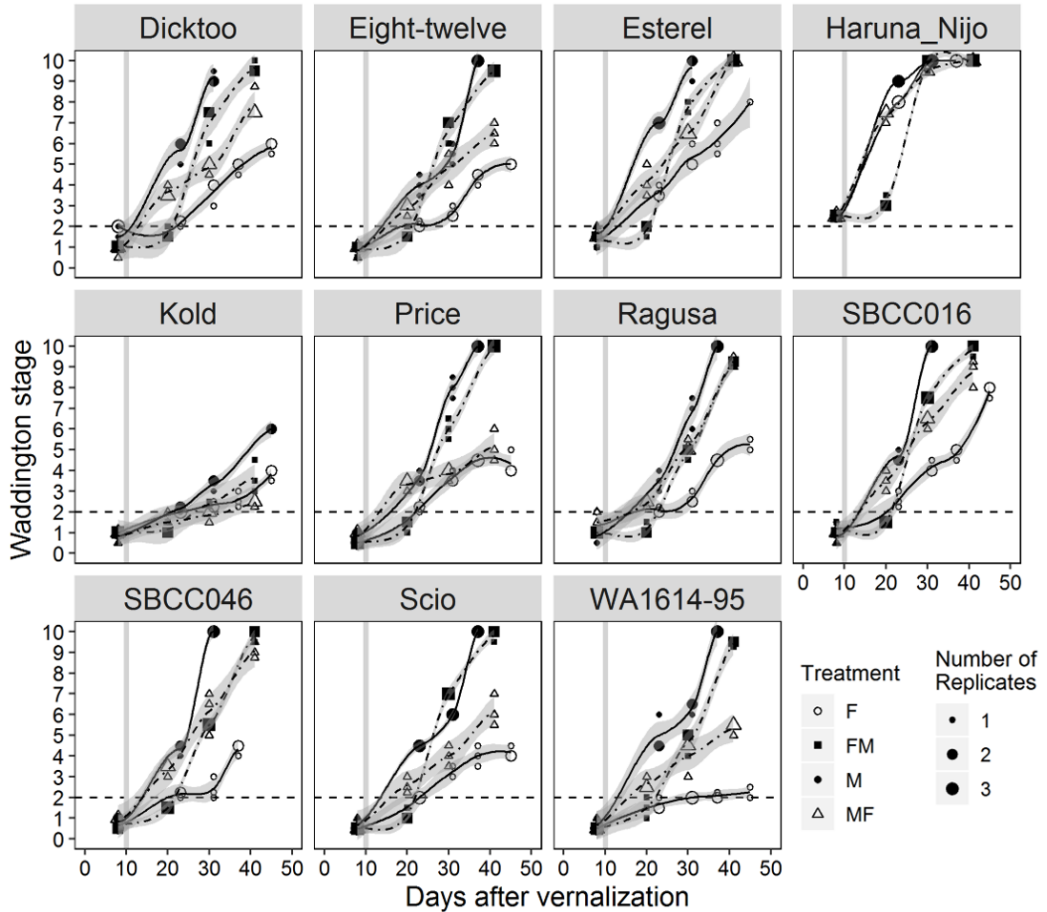
Figure 4.4. Dynamics of apex development under different light quality conditions. Each block represents a variety. Solid lines denote control treatments (white point is fluorescent, black point is metal halide), and dashed lines denote shift treatments (FM in squares, MF in triangles). The size of each dot represents the number of apices (biological replicates) at that Waddington stage. Dashed horizontal lines mark W 2.0, the double ridge stage, considered as transition from vegetative to reproductive phase. Vertical solid grey line denotes the shift day: the day when light quality treatments were changed. The shaded area indicates the 95% confidence interval (loess smooth line) calculated using a polynomial regression model.
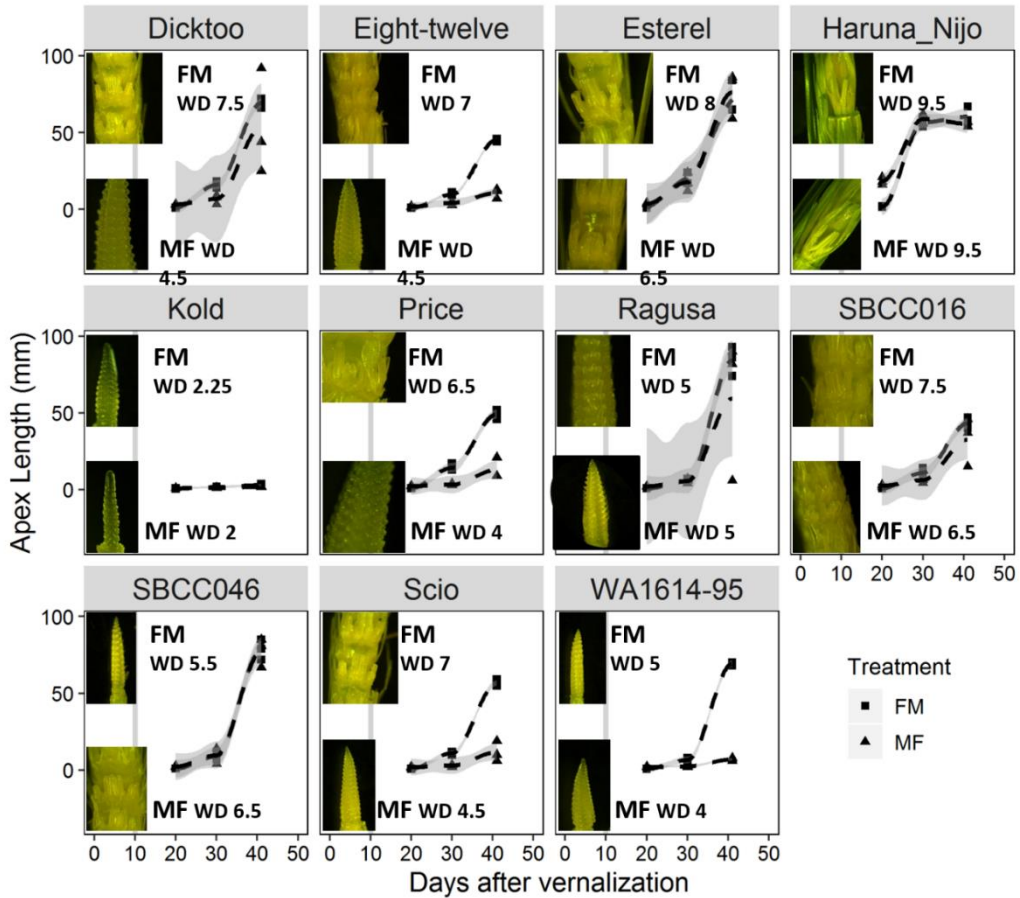
Figure 4.5. Dynamics of apex length and morphology in the shift treatments. Triangles represent MF and rectangles, FM. The vertical solid grey line denotes the shift day (the day when plants were switched between growth chambers with different light quality treatments). The shaded area indicates the 95% confidence interval (loess smooth line) calculated using a polynomial regression model. Apex photos were taken 30 days after the end of the vernalization.

4.3.2. Dynamics of plant height

We appreciated diversity in the responsiveness to light quality in the dynamics of plant height (Figure 4.6). Final plant height was independent of the treatment, but the pattern of growth was different. Some varieties showed a common behaviour in M, FM and MF, and different in F (Haruna Nijo, Ragusa, Esterel, SBCC016 and

SBCC046); other varieties showed different development under the four treatments, with plants reaching the onset of stem elongation first under M, then in FM and MF, and finally in F conditions (Kold, Price, WA1614-95, Eight-Twelve, Scio and Dicktoo). Both groups differed in their geographic origin and combination of flowering time alleles (Table 4.1). The first group comes from Japan and Europe; the second one comes from USA.
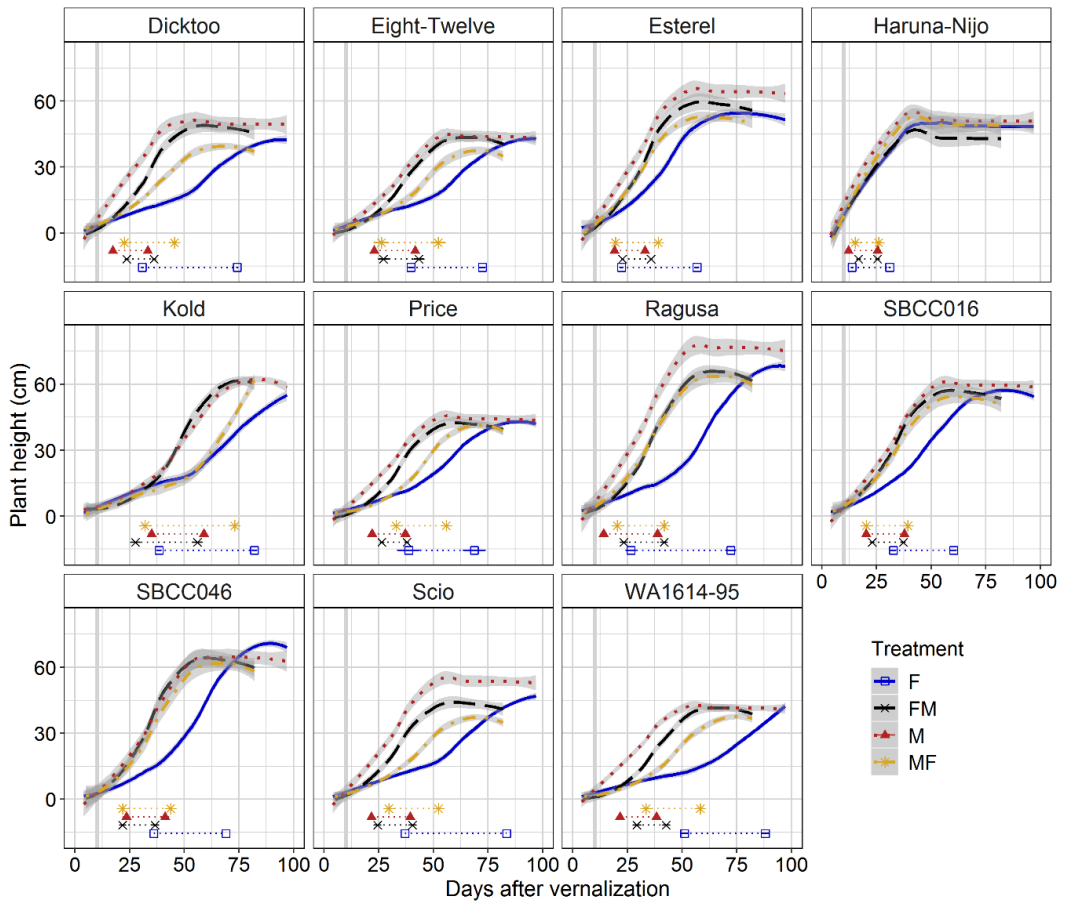
Figure 4.6. Dynamics of plant heght under different light quality conditions.
Each block represents a variety. Solid line, fluorescent (F); dashed line, FM; dotted line, metallic (M); dot-dashed line, MF. Each line represents the average of 4 biological replicates. The shaded area indicates the 95% confidence interval (loess smooth line) calculated using a polynomial regression model. Under the curves, horizontal lines represent the time from first node appearance (DEV31, first dot) to awns appearance

(DEV49) in the main stem. Vertical solid grey lines denote the shift day (the day when plants were switched between growth chambers with different light quality treatment).

4.3.3. Reproductive fitness traits

The different duration of the developmental phases affected the traits measured at harvest. Plants grown under fluorescent conditions showed more nodes, shorter last internode, more spikelets per spike, less and lighter seeds (Figure 4.7) and more final leaves (Figure S 4.2) than the rest of treatments. Results showed differences between treatments for all the traits, except the number of seeds in the main ear (ANOVA p-value = 0.182). Plants grown in metal halide conditions showed an accelerated phyllochron and had heavier seeds than plants grown under fluorescent conditions. Plants grown in FM showed more reproductive tillers and number of seeds than those in M. Despite fluorescent light resulted in maximum number of tillers in many varieties (Figure S 4.3), it showed a reduced number of reproductive tillers (Figure 4.7).
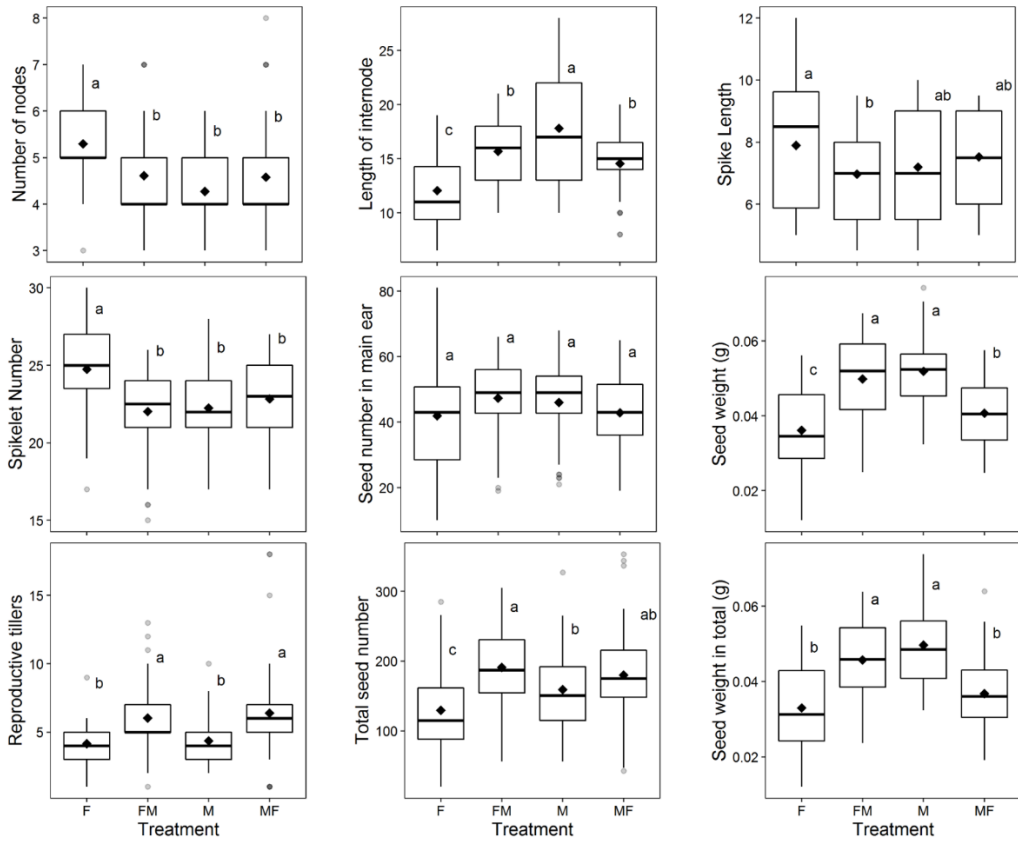
Figure 4.7. Boxplot of traits measured at harvest in the different light quality treatments. Results from 4 plants per variety in 11 varieties. Four different light quality treatments are included: F, fluorescent; FM, ten days in fluorescent and then shift to metal halide; M, metal halide; MF, ten days in metal halide and then shift to fluorescent conditions. Data average is represented as black diamond inside of the boxplot. From left to right: number of nodes in the main stem; length of last internode in cm; length of the main spike in cm; number of spikelets per main spike; individual seed weight (mg) in the main ear; number of reproductive tillers; total seed number and individual seed weight in the whole plant. Different letters represent significant differences between treatments in a post-hoc LSD-test, with a P-value <0.05

4.3.4. Gene expression

Expression of the major flowering time genes was analysed in leaves of plants after 20 days of the end of the vernalization treatment in all the conditions (10 days after the shift in FM and MF, Figure 4.8).

HvFT1 was expressed in Haruna Nijo, the earliest variety in this study. The latest variety Kold expressed *HvVRN2* under all treatments. Expression was much lower in other genotypes. *HvFT3*, when the functional variant was present, was upregulated under fluorescent condition in most cases (Scio was the exception). Both genes were expressed in that condition. Thus, the antagonism between *HvVRN2* and *HvFT3* was not perfect.
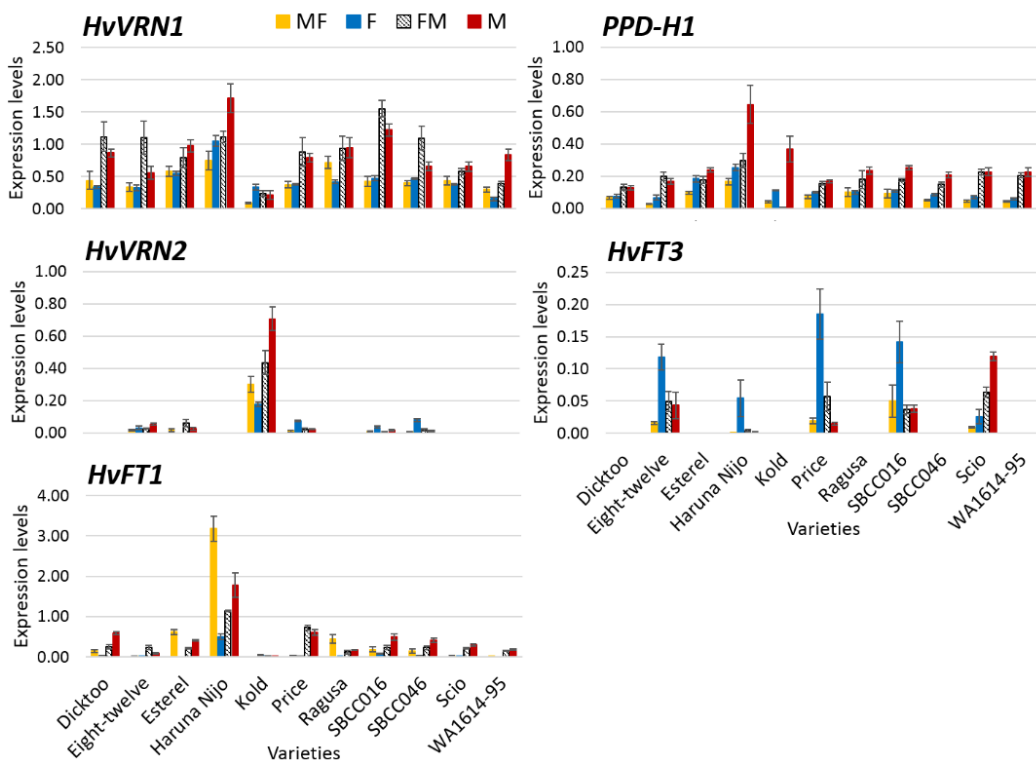
Figure 4.8. Gene expression under the different treatments.
Samples were taken 20 days after the end of the vernalization treatment. Gene expression relative to Actin. Mean of 3 biological replicates. Bars represent SEM.

An effect of light quality on *HvVRN1* and *PPD-H1* was observed, showing higher expression under M and FM conditions. The responses of those genes showed a rapid adaptation to new conditions, as *HvVRN1* and *PPD-H1* expression levels were more similar between MF and F conditions, and between FM and M conditions (Figure 4.8). Expression of *PPD-H1* and *HvVRN1* showed a moderately high Pearson correlation (R=0.59).

The duration of the different phenophases and the expression of the major flowering time genes were compared to determine their relations, as overall means (Figure S 4.4), and specifically in each treatment (Figure S 4.5 and Tables S 4.3 and S 4.4). High expression levels of the promoters (*HvVRN1*, *HvFT1* and *PPD-H1*) were related to rapid appearance of the first node and transition to an erect growth (DEV31 and DEV31-30). Gene expression was measured 20 days after the end of the vernalization treatment. For all varieties, except Haruna Nijo, sampling time occurred either before DEV31, or between DEV31 and DEV30 (Figure S 4.1). *HvFT3* expression was not related with duration of phenological phases (Figures S 4.4 and S 4.5).

As indicated before, most of the variation in duration of development in response to light conditions occurred before DEV30. We did a principal component analysis including the duration of just the two stages before and after DEV30 for each genotype at each treatment, together with gene expression (Figure 4.9, excluding *HvVRN2* and *HvFT3*, which are absent in about half of the genotypes). The first and the second components explained 41.11% and 16.03% of variance, respectively (Figure 4.9). The first component clearly separates the varieties according to treatments, by overall earliness, with M and FM on the right-hand side and F on the left, with MF intermediate. This component also separates between early and late varieties overall, particularly Scio and WA1614-95, the slowest under fluorescent conditions, from Haruna Nijo, the fastest variety in all conditions. Regarding gene

expression, *Ppd-H1*, *HvVRN1* and *HvFT1* have large loadings on the first component, indicating their negative correlation with the duration of the DEV30 phase. The second component presented the largest loadings for stem elongation phase, LSE. Also, when including all the phenophases and gene expression data in the analysis (Figure S 4.4), DEV31 and DEV31-30 are the variables with largest, and negative, loads on the first component, meaning that they attain higher values at the F treatment, and lower at M and FM. DEV37-30, in particular, had the largest loading. *HvVRN2* contributed positively in this axis, where Kold and Haruna Nijo have maximum and minimum values, respectively.
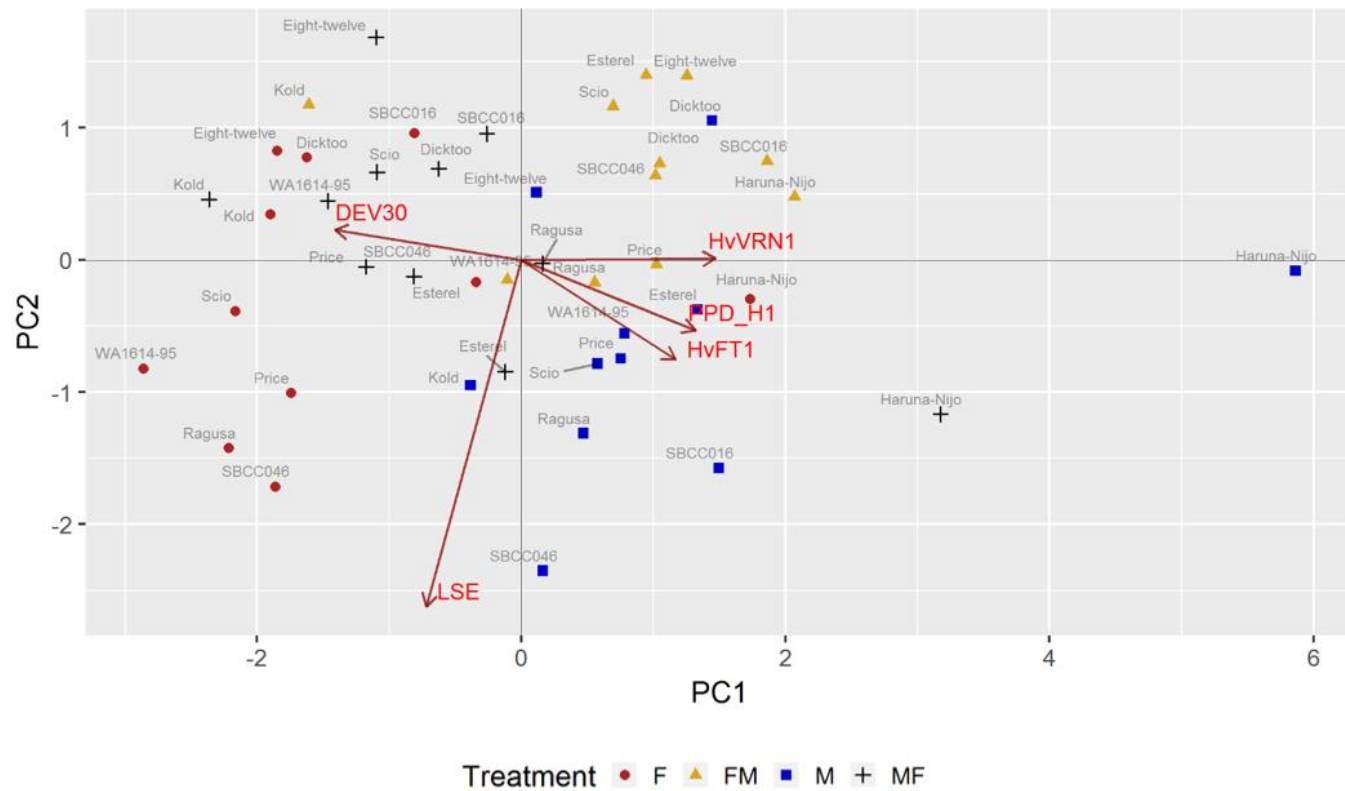
Figure 4.9. Principal component analysis of gene expression of *HvVRN1*, *HvFT1* and *PPD-H1*, and two phases of development: days from the end of vernalization to the onset of the stem elongation (DEV30), and length of the stem elongation phase (LSE).

In each treatment, the contribution of the two main components was similar to the general PCA. The most explained component was earliness and the second one was duration of the elongation, except under fluorescent conditions, in which duration of stem elongation showed the highest contribution (Table S 4.3 and S 4.4). In general, correlations and PCA suggested that high expression of the promoter genes of flowering favoured the acceleration of the first node appearance and the transition to the erect stage among other phenological phases, whereas the expression of *HvVRN2* was associated with lengthening of the stem elongation phase (Figure S 4.4).

4.3.5. Diversity in the response to different light sources

As observed previously, the responses to the different light quality conditions were complex, because responsiveness was dependent on varieties and traits (Table S 4.5).

The 11 varieties used in this study were grouped based on their phenological and morphological parameters (Figure 4.10). Additionally, we carried out an exploratory analysis to classify the varieties considering their response to the four treatments, using 17 traits, which included phenological and morphological responses (Table S 4.2). As a result, varieties were divided in 2 groups, with Haruna Nijo and Kold as extremes (Figure 4.10), despite being the most insensitive varieties: Haruna Nijo was the earliest and Kold the latest across treatments. The groups were not associated with the allelic variants for the major flowering time genes, although varieties were mainly divided by geographical origin. Thus, varieties from USA (Price, Eight-twelve, WA1614-95 and Scio) clustered together, with the exception of Dicktoo, which was located in the European group (Ragusa, Esterel, SBCC016 and SBCC046), close to Ragusa. These results were coincident with the qualitative classifications summarized in Table S 4.5. In general, European

varieties were less influenced by light quality treatments, whereas most of the American varieties responded showing an accelerated pattern of development under metal and shift conditions.
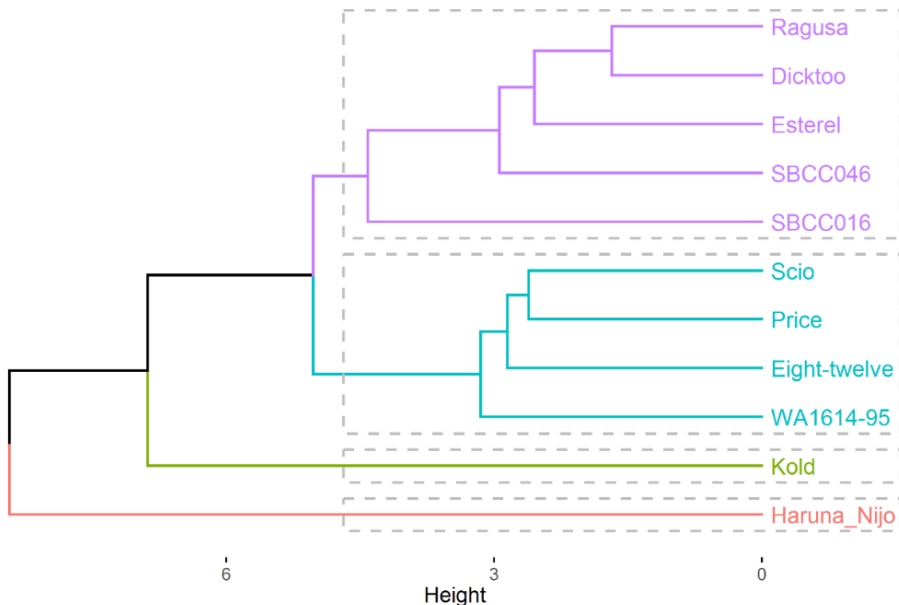
Figure 4.10. Dendrogram for the 11 barley cultivars, based on phenology traits measured under 4 conditions (F, FM, MF, M).

4.4. Discussion

4.4.1. Balanced spectra accelerated plant development

Under the same light intensities, temperature and photoperiod, we observed striking differences in development that were due to the light sources' spectra. Fluorescent lights were rich in the green-yellow and red regions, whereas a more balanced spectra across the PAR region was produced by metal halide bulbs. Our results showed that metal halide conditions were more efficient promoting development than fluorescent light bulbs.

In this work, we have observed that light quality affects to the duration of specific phenological phases, chiefly before the onset of stem elongation. The first node appearance (DEV31) and the transition between prostrate to erect state of the plant (DEV31-30) took longer to occur under fluorescent conditions (Figure 4.2). This was consistent with the dynamics of apex development (Figure 4.4) and phyllochron (Figure S 4.2), which were accelerated in metal conditions. Tillering was more profuse in fluorescent conditions (Figure S 4.3) although at the end of the experiment, plant growth under F showed fewer reproductive tillers than plants grown in M (Figure 4.7). In addition, plants grown in F showed less and lighter seeds (Figure 4.7). Therefore, the longer early phases under F conditions led to a longer phase of tiller production, but these plants were unable to grow all those tillers until the end and, even in that case, were less efficient in grain filling. Contrasting with our observations, Tibbitts *et al.* (1983) found that ear emergence and spikelet number in wheat were not affected by lamp treatments (M, M-Incandescent, and other light bulbs types). These authors also reported that chlorophyll concentration was greater in plants growing under M lamps, which might explain the differences in seed weight found due to a more efficient photosynthesis. Monostori *et al.* (2018) associated the balanced B:R ratios to increased grain number, and also reported that light quality affected the composition and quality of wheat flour. In our study, light spectra of metal halide bulbs accelerated development reducing time to elongation phase, producing plants with less biomass and higher number of productive tillers, with heavier seeds than fluorescent conditions.

It is well known that light quality, specifically the relative proportions of red and far-red light (R:FR ratio) provides a powerful signal that regulates both vegetative development and the transition to flowering in plants (Halliday *et al.*, 2003). Plants detect the presence of neighbouring vegetation through monitoring the ratio of R to FR wavelengths. In response to low R:FR light ratio, many plants display a rapid

and pronounced phytochrome-mediated architectural adaptation known as the shade avoidance syndrome (Franklin and Whitelam, 2005; Franklin, 2009; Casal, 2013; Ballaré and Pierik, 2017). In shade intolerant plants, such as *Arabidopsis*, this syndrome is characterized by an increase in the elongation growth rate of stems and petioles, reduced chlorophyll content, increased apical dominance and early flowering (Smith and Whitelam, 1997; Ballaré and Pierik, 2017). The different responses observed in this study could be related to the differences in intensity in some parts of the spectra, in particular the R:FR ratios of the systems. Fluorescent lights produced very high R:FR ratios (Figure 4.1). Metal halide bulbs also showed high ratios of R:FR compared to natural conditions (~1.1), but 3 times lower than fluorescent. Considering this, one could expect that plant responses under metal halide conditions could resemble those inducing shade avoidance responses. Plants grown with metal halide light showed more rapid stem elongation, flowered earlier, but had reduced number of tillers (Figure S 4.3), all responses associated with shade avoidance. Yet, plant height at the end of the experiment was similar among treatments (Figure 4.6), whereas delayed apex development, extensive tillering (Figure S 4.3) and late flowering (Figure 4.2) were observed in plants grown under fluorescent conditions. In this regard, Ugarte *et al.* (2010) analysed the growth of 10 wheat cultivars under low red/far-red ratios and concluded that although plant height was unaffected, low R:FR ratios significantly reduced grain yield per plant (through grain number and, secondarily, through grain weight per plant). In our study, the comparison between M and F indicated that, on average, plants had heavier seeds with metal halide lights (Figure 4.7). All these observations suggest that even though metal halide may elicit a "shade-avoidance" response, the R:FR ratio is not low enough as to encompass a yield penalty. Other authors have already examined the effect of specific wavelengths in wheat growth and development. Monostori *et al.* (2018) have found that different light wavebands (blue, green and far red) act antagonistically over wheat development, specifically at lower

intensities. These authors revealed that a balanced ratio between blue and red lights accelerated flowering time in wheat. At first sight, this might agree with our results. However, the ratio B:R under metal halide and fluorescent conditions in our experiment is very similar and close to 1. Also, green light affects plant processes though cryptochrome dependent and independent mechanisms, and its effect is opposed to those driven by red and blue wavebands (Folta and Maruhnich, 2007). As fluorescent spectrum was saturated on green and red wavelengths, it could explain the delay observed in barley plants developed under this lighting regime.

4.4.2.   Genes and gene expression underlying light responses

The characterization of *Arabidopsis* null-mutants led to the confirmation that the shade-avoidance syndrome is regulated by phytochromes, acting in a functionally redundant manner (Franklin and Whitelam, 2005). Hanumappa *et al.* (1999) identified an early flowering mutant phenotype of barley, insensitive to photoperiod, which was deficient in phytochrome B. Traditionally, breeding efforts have been focused on optimizing grain yield, and not biomass. In fact, intense selection by plant breeders has acted to attenuate some but not all shade avoidance responses within modern crop varieties (Kebrom and Brutnell, 2007). Recently, Kegge *et al.* (2015) reported that changes in the red: far-red light conditions influenced the emission of volatile organic compounds in barley leading to affect carbon allocation in neighbouring plants.

As red and blue light activate phytochromes and cryptochromes, it is sensible to expect that a balanced spectrum in these regions might lead to rapid reproductive responses. Some reports also highlighted the importance of green light on processes, through cryptochrome dependent mechanisms, and possibly other pathways. Its effect is generally opposed to those driven by red and blue wavebands (Folta and Maruhnich, 2007). In *Arabidopsis*, it has been reported that green

wavebands have an inhibitory effect on *FT* expression, caused by direct inactivation of Cry2 protein (Banerjee *et al.*, 2007), although this effect occurs mainly under low light conditions. It is worth noting that responses to green light vary among plant families, and wheat has been reported to respond to green-yellow light band (500-600 nm) by promoting earlier flowering (Kasajima *et al.*, 2007). In our experiment, fluorescent spectrum was richer on the green and red wavelengths than metal halide, which could explain the delay observed in barley plants developed under this lighting regime.

The distinct spectra of fluorescent and metal halide bulbs caused differences in the expression levels of the major flowering times genes, even after full vernalization and day length of 16 h provided equally inductive conditions for all genotypes in both chambers. Positive regulators of flowering (*HvVRN1*, *PPD-H1* and *HvFT1*) showed higher transcript levels in metal halide conditions than in fluorescent conditions for most of the varieties under study (Kold was the exception, although its expression levels were probably too low to be very precise). This effect was clear and is one of the main findings of this study. This was in accordance with the delay of early developmental phases observed under fluorescent conditions, and with the inhibitory effect of green wavebands on *FT* in *Arabidopsis*, mentioned before (Banerjee *et al.*, 2007). Other studies have found a dependence of *FT* levels on light-quality, in this case related to the effect of different R:FR ratios on *Arabidopsis* mutants, and suggested a regulation by phyA and ELF3 (Song *et al.,* 2018). As broad-spectrum light sources were used in this work, we cannot discard the involvement of other wavebands in the downregulation of flowering promoters under fluorescent conditions or the upregulation under the balanced spectra of metal halide bulbs. In fact, the upregulation of the flowering promoters was in accordance with the low levels of the repressor of flowering, *HvVRN2* in metal halide conditions.

Differences in *HvVRN1* gene expression within varieties could be due to the light quality-dependent regulation of the autonomous pathway. There have been reports of an effect of far-red conditions on flowering time across *Arabidopsis* accessions that carry mutations in the autonomous pathway (Kim *et al.*, 2008). These authors suggested that responsiveness of those mutants to far-red light was mainly due to an increased photoperiod pathway under far-red light conditions, and its consequent promotion of flowering. In barley, *HvVRN2* expression is under photoperiod control, being upregulated by long days. Here, we found increased *HvVRN2* mRNA level in plants growing under fluorescent conditions, which was related to the reduced levels of *HvVRN1* and the lengthening of the early phases. Despite the antagonistic relationship of *HvVRN2* and the short-day flowering promoter, *HvFT3*, both were concurrently induced, being upregulated under fluorescent conditions, compared to other treatments. *HvFT3* has been given a promotor role specifically under early phases of development (Mulki *et al.*, 2018). We suggest that the flowering induction effect of *HvFT3* fades away under fluorescent light.

In the previous chapter of this thesis, we could observe that core oscillator genes modified their expression levels in response to a shift between photoperiods that produced a rapid response in the flowering time genes. In this work, we highlight the high correlation between *HvVRN1* and *PPD-H1* gene expression, explained by the similar levels found between F conditions and MF, and between M and FM conditions. Only 10 days after the shift between conditions, expression of both genes was adapted to the new lighting treatment. *PPD-H1* gene plays a key role in the sensitivity to long day conditions in barley, and also works as output of the circadian clock, as was explained in the previous chapter of this thesis (introduction of Chapter 3). Recently, it has been reported the alteration of the circadian clock with light quality in barley (Gierczik *et al.*, 2017). We hypothesize that *PPD-H1* and *HvVRN1* are downstream factors of clock components that have been affected by the different light spectra conditions experienced. According with this, Pearce *et*

●●●

al. (2016) identified a strong downregulation of the *PPD-1* gene and different expression of circadian clock components in wheat mutants lacking *PHYB* or *PHYC*. That finding could support our hypothesis, although more study is needed.

4.4.3.   Mixture of spectra during different phases benefits plant growth

In general, plants subjected to shift conditions behaved closer to the metal halide control, even though MF plants passed most of the time under fluorescent conditions. We compared control and shift to determine whether 10 days in other lighting regime had effect on development. We observed that the pattern of development in FM was very similar to M conditions. Thus, plants that started their development under fluorescent conditions were delayed, but recovered very fast. The delayed development caused by fluorescent lighting in early phases was overcome rapidly in metal halide conditions (Figure 4.5). On the contrary, when plants were maintained 10 days in metal halide conditions, plants did not behave as plants in control fluorescent conditions. Plant development in MF was more rapid than under fluorescent conditions. Thus, 10 days in M was enough to remarkably accelerate the development, which was not as severely impaired by the fluorescent spectrum as for plants grown continuously in that condition.

This combination of chambers could be of interest in the acceleration or deceleration of development depending on needs in multiplication of seeds in growth chamber. For instance, fluorescent light could be used in the early stages, which ensures longer spikes, with more spikelets, and then switch to metal halide, which is best in terms of seed set and seed size. Shift conditions resulted in higher number of reproductive tillers than in the controls (Figure 4.7), which could be implemented to increase yield in plants growing under artificial conditions. However, not all the varieties responded equally, and those more delayed under

fluorescent conditions produced more tillers but not all of them were productive. Thus, mix of different light regimes could be advantageous, but probably, different varieties would need different protocols based on their responsiveness to light quality conditions.

4.4.4. Different sensitivity to light quality and biological sense for the diversity found

There were diverse responses to lighting treatments among the varieties under study. All plants were vernalized previously to eliminate possible influences of other factors than light on development inductive conditions. In all the treatments, the spring barley Haruna Nijo was the earliest variety, being insensitive to light quality. This genotype carries a mutation in the *Phytochrome C* gene, conferring an extremely early phenotype, both under SD and LD conditions (Nishida *et al.*, 2013; Pankin *et al.*, 2014). We observed a gradation of responses to light quality in the other ten genotypes studied. Further research will be needed to unravel the genetic factors underlying these different responses.

This different sensitivity to light quality conditions might have its biological significance in the plant strategies that confer different ecological behaviour to cope with competitors and environment (Smith, 1982). So far, research efforts on diversity of responses to light quality has been mainly focused on different responses to low R:FR, for instance, to develop plants insensitive plants to the canopy of neighbours (Merotto Jr. *et al.*, 2009). Maloof *et al.* (2001) found that certain Arabidopsis tall lines were less affected by low R:FR than short lines, and genotypes from lower latitudes were taller than genotypes from higher latitudes. Similarly, the varieties here studied showed a different plant height dynamic associated with the different location. European varieties (Ragusa, Esterel, SBCC016 and SBCC046) and the Japanese one (Haruna Nijo) tended to be taller

and showed lower responsiveness to light quality conditions than those from USA (Kold, Price, WA1614-95, Eight-Twelve, Scio and Dicktoo), which were also shorter overall. This difference in plant height probably reveals different breeding histories. Three of the European varieties were selected straight out of landraces (Ragusa, both SBCC lines), whereas all American ones come from modern breeding programs. For this reason, it is likely that American varieties carry some semi-dwarf allele. A possible link between plant height and light sensitivity should be taken into account in further studies in this area.

4.5.   Conclusion

Modulation of light has proven to be an appropriate testing ground to evaluate plant developmental responses, and the relationships between some of the pathways affecting plant growth. There appears to be considerable variability among crop genotypes regarding light quality sensitivity, which could be used in the selection and development of crop cultivars with greater competition ability. The natural variation found in the responsiveness to light quality reinforces the need of future research in genetic control of responses to different light parameters. Based on our results, we suggest that light spectra regulate the vernalization and photoperiod genes probably through the regulation of upstream elements of signalling pathways. Whether phytochromes or cryptochromes are behind the differences found between the balanced spectra of metal halide conditions and the green and red saturated spectrum of fluorescent light bulbs, deserves further research. Here, the characterization of light quality effects has highlighted the important effect of the spectrum on early developmental stages, affecting the moment of onset of stem elongation, and downstream effects on the morphology of the plant and yield components. We have found that it is possible to optimize the indoor growth conditions to manipulate crops and optimize breeding strategies.

4.6.   References

Ballaré CL, Pierik R. 2017. The shade-avoidance syndrome: Multiple signals and ecological consequences. Plant, Cell & Environment **40**, 2530–2543.

Banerjee R, Schleicher E, Meier S, Viana RM, Pokorny R, Ahmad M, Bittl R, Batschauer A. 2007. The Signaling State of *Arabidopsis* Cryptochrome 2 Contains Flavin Semiquinone. Journal of Biological Chemistry **282**, 14916–14922.

Casal JJ. 2013. Photoreceptor signaling networks in plant responses to shade. Annual Review of Plant Biology **64**, 403–427.

Casal JJ, Qüesta JI. 2018. Light and temperature cues : multitasking receptors and transcriptional integrators. New Phytologist **217**, 1029–1034.

Demarsy E, Goldschmidt-clermont M, Ulm R. 2017. Coping with 'Dark Sides of the Sun' through Photoreceptor Signaling. Trends in Plant Science **23**, 260–271.

Faure S, Higgins J, Turner A, Laurie DA. 2007. The *FLOWERING LOCUS T*-like gene family in barley (*Hordeum vulgare*). Genetics **176**, 599–609.

Fiorucci A, Fankhauser C. 2017. Review Plant Strategies for Enhancing Access to Sunlight. Current Biology **27**, R931–R940.

Folta KM, Maruhnich SA. 2007. Green light: A signal to slow down or stop. Journal of Experimental Botany **58**, 3099–3111.

Franklin KA. 2009. Light and temperature signal crosstalk in plant development. Current Opinion in Plant Biology **12**, 63–68.

Franklin KA, Whitelam GC. 2005. Phytochromes and shade-avoidance responses in plants. Annals of Botany **96**, 169–175.

Gierczik K, Novák A, Ahres M, *et al.* 2017. Circadian and light regulated expression of CBFs and their upstream signalling genes in barley. International Journal of Molecular Sciences **18**, 1828.

Gómez C, Izzo LG. 2018. Increasing efficiency of crop production with LEDs. AIMS Agriculture and Food **3**, 135–153.

Halliday KJ, Salter MG, Thingnaes E, Whitelam GC. 2003. Phytochrome control of flowering is temperature sensitive and correlates with expression of the floral integrator *FT*. The Plant Journal **33**, 875–885.

Hanumappa M, Pratt LH, Cordonnier-Pratt M-M, Deitzer GF. 1999. A Photoperiod-Insensitive Barley Line Contains a Light-Labile Phytochrome B. Plant Physiology **119**, 1033–1040.

Hemming MN, Fieg S, James Peacock W, Dennis ES, Trevaskis B. 2009. Regions associated with repression of the barley (*Hordeum vulgare*) *VERNALIZATION1* gene are not required for cold induction. Molecular Genetics and Genomics **282**, 107–117.

Holmes MG, Smith H. 1977*a*. The function of phytochrome in the natural environment - I. Characterization of daylight for studies in photomorphogenesis and photoperiodism. Photochemistry and Photobiology **25**, 533–538.

Holmes MG, Smith H. 1977*b*. The function of phytochrome in the natural environment - II. The influence of vegetation canopies on the spectral energy distribution of natural daylight. Photochemistry and Photobiology **25**, 539–545.

Kami C, Lorrain S, Hornitschek P, Fankhauser C. 2010. Light-regulated plant growth and development. Current Topics in Developmental Biology **91**, 29–66.

Karsai I, Szucs P, Mészáros K, Filichkina T, Hayes PM, Skinner JS, Láng L, Bedo Z. 2005. The *Vrn-H2* locus is a major determinant of flowering time in a facultative x winter growth habit barley (*Hordeum vulgare* L.) mapping population. Theoretical and Applied Genetics **110**, 1458–1466.

Kasajima S, Inoue N, Mahmud R, Fujita K, Kato M. 2007. Effect of light quality on developmental rate of wheat under continuous light at a constant temperature. Plant Production Science **10**, 286–291.

Kassambara A, Mundt F. 2017. factoextra: Extract and Visualize the Results of Multivariate Data Analyses. R package, version 1.0.5. http://cran.r-project.org/package=factoextra.

Kebrom TH, Brutnell TP. 2007. The molecular analysis of the shade avoidance syndrome in the grasses has begun. Journal of Experimental Botany **58**, 3079–3089.

Kegge W, Ninkovic V, Glinwood R, Welschen RAM, Voesenek LACJ, Pierik R. 2015. Red: far-red light conditions affect the emission of volatile organic compounds from barley (*Hordeum vulgare*), leading to altered biomass allocation in neighbouring plants. Annals of botany **115**, 961–970.

Kim SY, Yu X, Michaels SD. 2008. Regulation of *CONSTANS* and *FLOWERING LOCUS T* Expression in Response to Changing Light Quality. Plant Physiology **148**, 269–279.

Maloof JN, Borevitz JO, Dabi T, *et al.* 2001. Natural variation in light sensitivity of *Arabidopsis*. Nature **29**, 441–446.

de Mendiburu F. 2016. agricolae: Statistical Procedures for Agricultural Research. R Package, version 1.2-4. https://cran.r-project.org/web/packages/agricolae/agricolae.pdf.

Merotto Jr. A, Fischer A, Vidal R. 2009. Perspectives for using light quality as an advanced ecophysiological weed management tool. Planta Daninha **27**, 407–419.

Monostori I, Heilmann M, Kocsy G, *et al.* 2018. LED Lighting – Modification of Growth, Metabolism, Yield and Flour Composition in Wheat by Spectral Quality and Intensity. Frontiers in Plant Science **9**, 605.

Morgan DC, Smith H. 1981. Non-photosynthetic Responses to Light Quality. In: Lange, OL; Nobel, PS; Osmond, CB; Ziegler H, ed. Physiological Plant Ecology I. Responses to the Physical Environment. Springer, Berlin, Heidelberg, 109–134.

Mortensen LM, Stromme E. 1987. Effect of light quality on some greenhouse crops.

Scientia Horticulturae **33**, 27–36.

Mulki MA, Bi X, von Korff M. 2018. FLOWERING LOCUS T3 Controls Spikelet Initiation But Not Floral Development. Plant Physiology **178**, 1170–1186.

Nishida H, Ishihara D, Ishii M, *et al.* 2013. *Phytochrome C* is a key factor controlling long-day flowering in barley. Plant Physiology **163**, 804–14.

Pankin A, Campoli C, Dong X, *et al.* 2014. Mapping-by-sequencing identifies *HvPHYTOCHROME C* as a candidate gene for the *early maturity 5* locus modulating the circadian clock and photoperiodic flowering in barley. Genetics **198**, 383–396.

Pearce S, Kippes N, Chen A, Debernardi JM, Dubcovsky J. 2016. RNA-seq studies using wheat *PHYTOCHROME B* and *PHYTOCHROME C* mutants reveal shared and specific functions in the regulation of flowering and shade-avoidance pathways. BMC Plant Biology **16**, 141.

R Core Team. 2017. R: A langauge and environment for statistical computing. https://www.r-project.org.

Sager JC, Smith WO, Edwards JL, Cyr KL. 1988. Photosynthetic Efficiency and Phytochrome Photoequilibria Determination Using Spectral Data. Transactions of the ASAE **31**, 1882–1889.

Smith H. 1982. Light quality, photoperiod, and plant strategy. Annual Review of Plant Physiology **33**, 481–518.

Smith H, Whitelam GC. 1997. The shade avoidance syndrome: Multiple responses mediated by multiple phytochromes. Plant, Cell and Environment **20**, 840–844.

Song YH, Kubota A, Kwon MS, *et al.* 2018. Molecular basis of flowering under natural long-day conditions in *Arabidopsis*. Nature Plants **4**, 824–835.

Tibbitts T, Morgan D, Warrington IJ. 1983. Growth of lettuce , spinach , mustard , and wheat plants under four combinations of high-pressure sodium , metal halide , and tungsten halogen lamps at equal PPFD. Journal of America Society for Horticultural Science **108**, 622–630.

Tottman DR, Makepeace RJ, Broad H. 1979. An explanation of the decimal code for the growth stages of cereals, with illustrations. Annals of Applied Biology **93**, 221–234.

Turner A, Beales J, Faure S, Dunford RP, Laurie DA. 2005. The Pseudo-Response Regulator *Ppd-H1* Provides Adaptation to Photoperiod in Barley. Science **310**, 1031–1034.

Ugarte CC, Trupkin SA, Ghiglione H, Slafer G, Casal JJ. 2010. Low red/far-red ratios delay spike and stem growth in wheat. Journal of experimental botany **61**, 3151–3162.

VSN International. 2017. Genstat for Windows 19th Edition. VSN International, Hemel Hempstead, UK. https://genstat.co.uk.

Waddington SR, Cartwright PM, Wall PC. 1983. A quantitative Scale of Spike Initial and Pistil Development in Barley and Wheat. Annals of Botany **51**, 119–130.

Watson A, Ghosh S, Williams MJ, *et al.* 2018. Speed breeding is a powerful tool to

accelerate crop research and breeding. Nature Plants **4**, 23–29.

Wei T, Simko V. 2017. R package 'corrplot': Visualization of a Correlation Matrix. Version 0.84. https://github.com/taiyum/corrplot.

Wickham H. 2016. ggplot2: Elegant Graphisc for Data Analysis. Springer-Verlag, New York.

Wit M De, Keuskamp DH, Bongers FJ, *et al.* 2016. Integration of Phytochrome and Cryptochrome Signals Determines Plant Growth during Competition for Light. Current Biology, 3320–3326.

Yan L, Fu D, Li C, Blechl A, Tranquilli G, Bonafede M, Sanchez A, Valarik M, Yasuda S, Dubcovsky J. 2006. The wheat and barley vernalization gene *VRN3* is an orthologue of FT. Proceedings of the National Academy of Sciences of the United States of America **103**, 19581–19586.

Zadoks JC, Chang TT, Konzak CF. 1974. A Decimal Code for the Growth Stages of Cereals. Weed Research **14**, 415–421.

4.7.　　Supplementary material

Table S 4.1. Primer sequences for gene expression assay.

ID	PRIMER SEQUENCE (5'-3')	Reference
HvVRN1	F: TATGAGCGCTACTCTTATGC R: TGAAGCTCAGAAATGGATTCG	Trevaskis *et al.* (2006)
HvVRN2	F: GAGCCACCATCGTGCCATTC R: GCCGCTTCTTCCTCTTCTC	Trevaskis *et al.* (2006)
HvFT1	F: ATCTCCACTGGTTGGTGACAGA R: TTGTAGAGCTCGGCAAAGTCC	Yan *et al.* (2006)
PPD-H1	F: CAAATCAAAGAGCGGCGATC R: TCTGACTTGGGATGGTTCACA	Hemming *et al.* (2008)
HvFT3	F: GGTTGTGGCTCATGTTATGC R: CTACTCCCCTTGAGAACTTTC	Forward: Kikuchi *et al.* (2009); Reverse: Faure *et al.* (2007)
Actin	F: GCCGTGCTTTCCCTCTATG R: GCTTCTCCTTGATGTCCCTTA	Trevaskis *et al.* (2006)

F, primer forward; R, primer reverse.

Faure S, Higgins J, Turner A, Laurie DA. 2007. The *FLOWERING LOCUS T*-like gene family in barley (*Hordeum vulgare*). Genetics **176**, 599–609.

Hemming MN, Peacock WJ, Dennis ES, Trevaskis B. 2008. Low-Temperature And Day-Length Cues Are Integrated to Regulate FLOWERING LOCUS T in Barley. Plant Physiology **147**, 355–366.

Kikuchi R, Kawahigashi H, Ando T, Tonooka T, Handa H. 2009. Molecular and functional characterization of PEBP genes in barley reveal the diversification of their roles in flowering. Plant Physiology **149**, 1341–1353.

Trevaskis B, Hemming MN, Peacock WJ, Dennis ES. 2006. *HvVRN2* responds to day-length, whereas *HvVRN1* is regulated by vernalization and developmental status. Plant Physiology **140**, 1397–1405.

Yan L, Fu D, Li C, Blechl A, Tranquilli G, Bonafede M, Sanchez A, Valarik M, Yasuda S, Dubcovsky J. 2006. The wheat and barley vernalization gene VRN3 is an orthologue of FT. Proceedings of the National Academy of Sciences of the United States of America **103**, 19581–19586.

Table S 4.2. Description of traits used for cluster analyses.

	Variable	Description
1	DEV31	Days* to the first node appearance
2	DEV49	Days* to awns appearance
3	FLN	Final leaves number
4	LFdev31	Leaves number at DEV31
5	PhyllDays	Phyllochron (leaves days^{-1})
6	PhFinal	Final plant height
7	LSE	Length (days) of stem elongation phase
8	PH49	Plant height at DEV49
9	PH31	Plant height at DEV31
10	SGdays	Stem growth ratio (cm days^{-1})
11	DEV30	Days* to onset of stem elongation
12	DEV37	Days* to initiation of flag leaf
13	DEV39	Days* to complete flag leaf formation
14	ZDSE	Days* to end of stem elongation
15	Spike_length	Spike length in the main stem at harvest
16	Spikelet_number	Number of spikelets (triplets) in the main stem's spikeat harvest
17	Rep_Till	Number of fertile side tillers in addition to the main spikeat harvest

*Days from the end of vernalization.

Table S 4.3. Principal components and values of each phase in each treatment.

	Fluorescent		MF		Metal halide		FM	
	PC1 (37.52%)	PC2 (21.85%)	PC1 (39.53%)	PC2 (26.71%)	PC1 (34.05%)	PC2 (27.16%)	PC1 (42.44%)	PC2 (26.82%)
DEV31	**0.347**	0.187	**0.393**	**2.000**	**-0.400**	-0.173	0.086	**0.352**
DEV31-30	**0.330**	-0.215	**0.314**	0.277	0.068	-0.204	**0.282**	**0.377**
DEV30-37	-0.030	0.538	-0.105	0.489	-0.268	**-0.374**	**0.390**	-0.114
DEV37-39	**0.418**	-0.154	0.225	**-0.390**	-0.234	**0.405**	**-0.365**	0.221
DEV39-49	0.058	**-0.478**	0.204	**-0.406**	-0.156	**0.475**	**-0.387**	0.191
DEV49-ZDSE	-0.053	0.340	-0.336	0.092	0.114	-0.313	0.199	**-0.458**
LSE	0.132	0.479	-0.085	0.291	-0.310	-0.194	0.229	-0.281
HvVRN1	**-0.434**	-0.066	**-0.410**	-0.176	**0.460**	0.073	-0.192	-0.286
HvVRN2	-0.031	0.037	0.161	0.459	-0.220	**-0.334**	**0.324**	**0.306**
HvFT1	**-0.448**	-0.004	**-0.376**	-0.007	**0.442**	-0.067	-0.179	**-0.332**
PPD-H1	**-0.415**	-0.121	**-0.434**	0.002	**0.316**	-0.118	**-0.374**	-0.153
HvFT3	-0.093	0.106	0.011	-0.139	-0.143	**0.358**	**-0.268**	0.195

Values of variable eigenvectors. Percentage of variances explained by each principal component is represented for each treatment. Extreme values are highlighted in bold

Table S 4.4. Principal components and values of each variety in each treatment.

	Fluorescent		MF		Metal halide		FM	
	PC1 (37.52%)	PC2 (21.85%)	PC1 (39.53%)	PC2 (26.71%)	PC1 (34.05%)	PC2 (27.16%)	PC1 (42.44%)	PC2 (26.82%)
Dicktoo	1.036	1.063	0.853	**-2.169**	0.600	-1.414	0.253	-0.821
Eight-twelve	0.798	-0.480	**2.268**	**-2.203**	-1.090	**2.327**	**-3.317**	2.575
Esterel	-0.473	**-1.598**	-1.771	0.692	1.056	-1.256	-0.920	0.817
Haruna_Nijo	**-5.850**	-0.104	**-4.710**	-0.109	**5.111**	-0.303	-1.142	-2.699
Kold	0.044	-0.950	**2.227**	**4.460**	**-2.597**	**-3.330**	**5.191**	**2.761**
Price	-0.147	**2.120**	1.391	-0.311	-0.067	-0.549	-0.361	-1.158
Ragusa	1.392	**-1.999**	-2.126	0.686	0.562	1.546	1.647	-1.189
SBCC016	-0.534	-0.695	-0.732	-0.683	0.118	0.267	-0.445	-0.736
SBCC046	0.120	**2.785**	-0.197	0.529	-1.482	-1.052	1.113	-1.354
Scio	1.608	**-1.597**	0.986	-0.897	-1.529	**2.738**	**-2.503**	**2.032**
WA1614-95	**2.006**	1.454	**1.811**	0.004	-0.681	1.026	0.484	-0.227

Values are the coordinates of the individuals on the principal components. Extreme values are highlighted in bold.

Table S 4.5. Overview of the responsiveness of the different varieties to the light quality conditions assayed.

	Allelic Variants				DEV31	DEV49	Plant height dynamic	Apex dynamic	Apex length
	HvVRN1	*HvVRN2*	*HvFT1*	*HvFT3*	S/I	S/I	S/I	S/I	S/I
Dicktoo	vrn1	vrn2	TC	ft3	S	S	S	S	S
Eight-twelve	vrn1	VRN2	AG	FT3	S	S?	S	S	S
Esterel	vrn1	VRN2	TC	ft3	I	S?	I?	I?	I
Haruna Nijo	vrn1	vrn2	TC	FT3	I	I	I	I?	I
Kold	vrn1	VRN2	AG	ft3	I	I?	I?	I	I
Price	vrn1	VRN2	TC	FT3	S	S?	S	S	S
Ragusa	VRN1-6	vrn2	AG	ft3	S	S	I?	I?	S?
SBCC016	VRN1-6	VRN2	AG	FT3	S	S	I?	I?	S
SBCC046	VRN1-6	VRN2	AG	ft3	S	S?	I?	S	S
Scio	vrn1	vrn2	AG	FT3	S	S	S	S	S
WA1614-95	vrn1	vrn2	AG	ft3	S	S	S	S	S

S, variety that shows sensitivity to light quality; F, variety that shows insensitivity to light quality. Question mark indicates that the responsiveness is dependent on the treatment, e.g. when dynamic of plant height is similar in metal halide and both shifts (FM and MF), but different in fluorescent conditions.
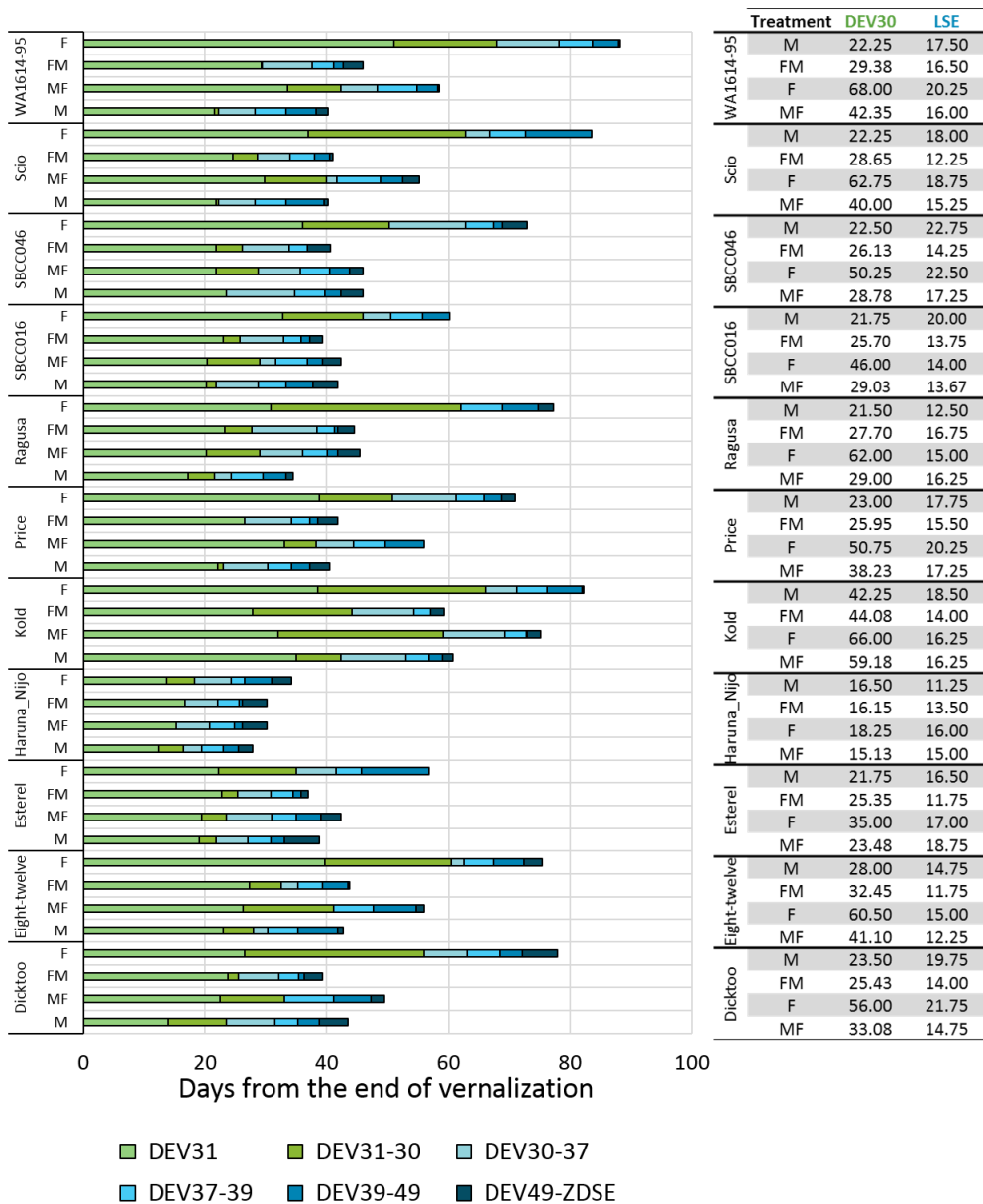
Figure S 4.1. Duration of phenophases in each variety and treatment.

The table represents the days from the end of vernalization to the onset of stem elongation (DEV30), which comprises DEV31 and DEV30, and the length of the stem elongation phase (LSE), as days from DEV30 to the end of stem elongation (ZDSE). Mean of 3-4 biological replicates is represented.

● ● ●
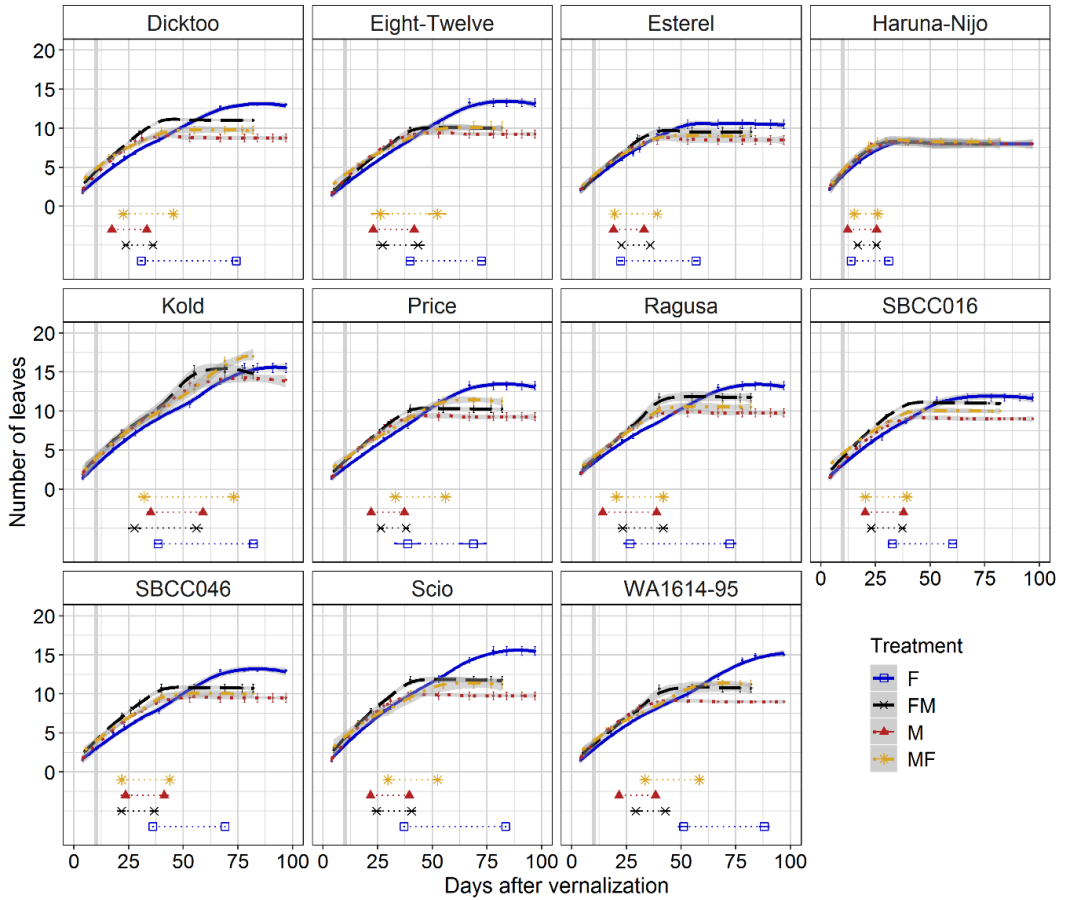
Figure S 4.2. Dynamic of the number of leaves under different light quality conditions. Each block represents a variety. Solid line, fluorescent; dashed line, FM; dotted line, M; dot-dashed line, MF. Each line represents the average of 4 biological replicates. The shaded area indicates the 95% confidence interval (Loess smooth line) calculated using a polynomial regression model. Under the curves, horizontal lines represent the time from first node appearance (DEV31, first dot) to awns appearance (DEV49) in the main stem. Vertical solid grey line denotes the shift day: the day when light quality treatments were changed.
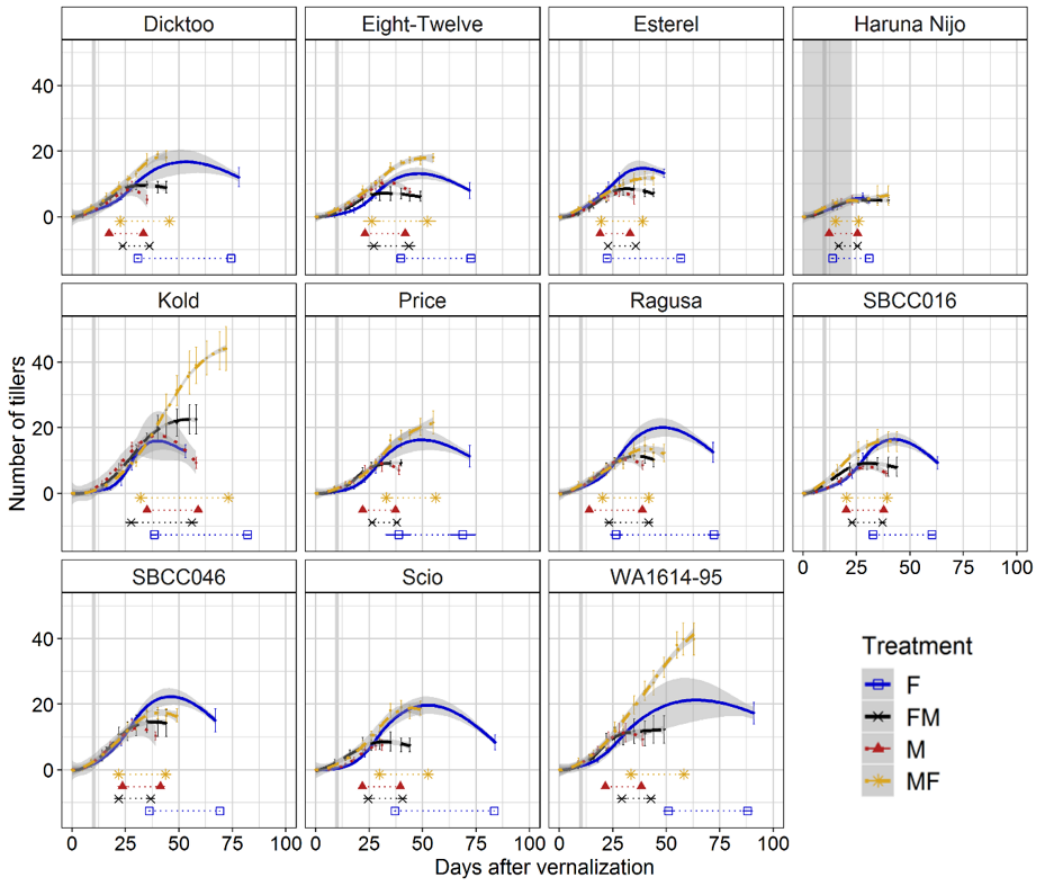
Figure S 4.3. Dynamics of the number of tillers under different light quality conditions. Each block represents a variety. Solid line, fluorescent; dashed line, FM; dotted line, M; dot-dashed line, MF. Each line represents the average of 4 biological replicates. The shaded area indicates the 95% confidence interval (Loess smooth line) calculated using a polynomial regression model. Under the curves, horizontal lines represent the time from first node appearance (DEV31, first dot) to awns appearance (DEV49) in the main stem. Vertical solid grey line denotes the shift day: the day when light quality treatments were changed.
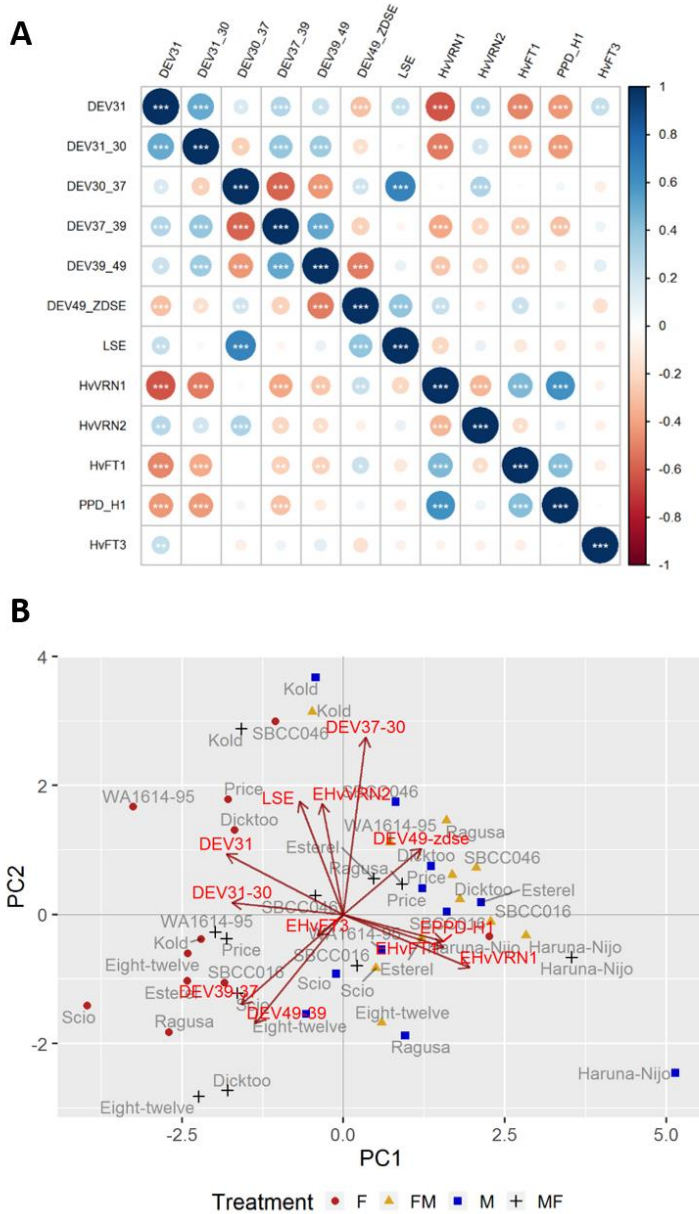
Figure S 4.4. Relations between phenophases and expression of flowering time genes (Pearson correlations and PCA biplot).

A) Pearson correlations, taking into account the averages of 11 varieties in 4 light quality treatments (for phenophases, n=4; for gene expression, n=3). B) Biplot for the principal component analysis based on the correlation matrix for all four treatments combined. PC1 and PC2 explain 32.64% and 19.43% of the variance, respectively.
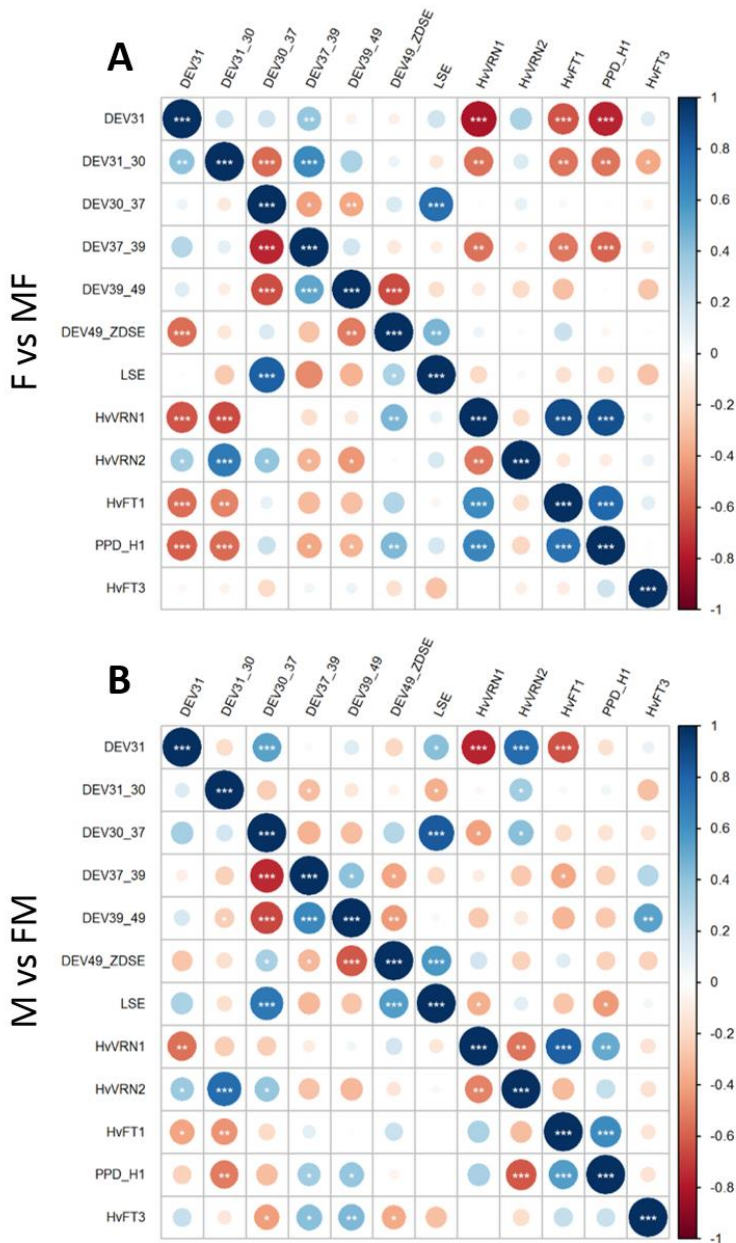
Figure S 4.5. Pearson correlations between phenophases and gene expression data per light quality treatment.

The data set consisted on averages of 11 varieties per light quality treatments (for phenophases, n=4; for gene expression, n=3). A) Upper triangle represents Pearson

correlations found in the fluorescent conditions; lower triangle denotes Pearson correlations found in the MF conditions (plants were subjected to 10 days in metal halide conditions and then were transferred to fluorescent conditions to the end of the experiment). B) Upper triangle represents Pearson correlations found in the metal halide conditions; lower triangle denotes Pearson correlations found in the FM conditions (plants were subjected to 10 days in fluorescent conditions and then were transferred to metal halide conditions to the end of the experiment).

Chapter

5

DIFFERENTIAL GENE EXPRESSION IN RESPONSE TO LIGHT QUALITY IN BARLEY

Chapter 5. Differential gene expression in response to light quality in barley

5.1. Introduction

As sessile organisms, plants have evolved adapting and surviving in a wide variety of environments. One of their main developmental triggers is light. They depend on ambient light conditions to regulate their development and to adapt to changing environments. Light is a signal for regulating growth and development, through its duration, quantity and quality (Franklin, 2009; Ugarte *et al.*, 2010). Light and temperature signals are receiving increasing attention, and more efforts are being dedicated to unravel the catalogue of cross-talk and nodes at which both signals converge (Franklin *et al.*, 2014).

Light quality and intensity are not constant in nature, as revealed by the different profiles of spectral distribution of photons that occur in different moments of the day, seasons, climates, and atmospheric conditions (Holmes and Smith, 1977; Smith, 1982). The responses of crops and plants to light features have been thoroughly studied (Franklin, 2009; Ugarte *et al.*, 2010; Monostori *et al.*, 2018). There is a gap, however, for the study of possible natural genetic variation in crop plants and its effect on crop development and adaptation.

Plants have a sophisticated system of photosensory receptors, such as phytochromes and cryptochromes, among others (review in Casal, 2013). The light quality effects have been widely studied in *Arabidopsis* (Adams *et al.*, 2009), but less is known in cereals (Ugarte *et al.*, 2010). Differential regulation of compounds whose levels are affected by light quality signals may reflect different susceptibilities to competition in different species or crop varieties. The concentration and efficiency of these compounds (phytochromes, cryptochromes, …) that can control the dynamics of

●●●

R/FR signalling is probably highly variable in different species and crop varieties. (Merotto Jr. *et al.*, 2009).

As was reported in the previous chapter (Chapter 4), genetic variability was found in the response to light quality environments. Cluster analysis showed two different groups of barley plants based on their different development when growing under fluorescent and/or metal halide conditions. One group was represented by the varieties most sensitive to light quality changes, and the second group the less responsive ones. Among the eleven varieties used, we chose three to further investigate the genes behind the different responses to light quality conditions. The earliest, Haruna Nijo, and the latest, Kold, were discarded due to their extreme behaviour. Thus, to explore the pathways activated or repressed in the different light quality conditions, one insensitive line (less responsive to light quality), Esterel, and two sensitive lines (showing major differences between light quality conditions, explained in Chapter 4), Price and WA1614-95 were chosen. We also observed an effect of light quality on the expression of flowering time genes. This observation opened new questions about the regulation of photoperiod and vernalization pathways. Actually, the relation between signalling pathways in barley (*Hordeum vulgare* L.) is not well-known (Nishida *et al.*, 2013).

De novo and reference guided assemblies of transcriptomes of the three genotypes, subjected to the two light conditions, were obtained. Gene expression changes in leaves were evaluated and compared among treatments. Finding genes that are involved in plant development may help to identify light-response pathways that, eventually, could be targeted for breeding purposes.

5.2.   Materials and Methods

5.2.1.   Plant material and phenotyping

We selected Esterel, Price and WA1614-95 (Table S 5.1) from the 11 barley varieties described in the previous chapter (Chapter 4, Table 4.1). These 11 varieties carried different allelic variants for major flowering time genes, related to vernalization and photoperiod pathways (*HvVRN1*, *HvVRN2*, *HvFT1*, *HvFT3*, described in Chapter 4, table 4.1). Data were collected from plants subjected to different light quality treatments, after following a full-vernalization treatment ($5\pm2°C$ for 52 days under 8 h light/16 h night) to synchronize the development of the three genotypes. The light treatments were established in two independent growth chambers, with long days (16 h light/8 h night), and 18 $\pm1°C$ constant temperature, and the same light intensity (250 µmol m^{-2} s^{-1}). Temperature was continuously monitored through an air sampling channel, located at the centre of the cabinet at canopy level. Two lamp types were used: Sylvania cool white fluorescent with fluorescent (F) and Tungsram HGL-400 metal halide (M) light bulbs. The height of the lamps in the F chamber was adjusted once per week to 1.4 m above the canopy, to match the light intensity of the M chamber, in which the lights were set at a fixed height. The experiment was carried out in the Phytotron facilities of the Agricultural Research Institute of the Hungarian Academy of Sciences, Martonvásár (Hungary), using Conviron PGR-15 growth chambers (Conviron Ltd., Canada).

For phenotypic measurements, sixteen plants per genotype were sown in individual pots, and four were placed at each growth chamber, making four replicates per genotype and treatment. These results are mostly reported in the previous chapter. Additionally, 20 seeds per genotype and treatment, sown in groups of 5 plants/pot, were used for destructive samplings to record apex development stage, and for gene

expression studies. Plant development was monitored twice a week, checking for first node appearance (plant developmental stage 31, or DEV31) and appearance of the awns just visible above the last leaf sheath (DEV49). All these data were defined based on stages of the Zadoks' scale (Zadoks *et al.*, 1974), following the description of Tottman *et al.* (1979). Apex dissection was carried out 23 days after the end of the vernalization period in 3 plants per variety and treatment. Phenotyping consisted on recording apex stage following the Waddington's scale (Waddington *et al.*, 1983). The plants were grown to full maturity.

5.2.2.   RNA extraction and transcriptome sequencing

The three genotypes, Esterel, Price and WA1614-95 were used for transcriptome analysis. Three biological replicates per genotype and treatment were tested. Each biological replicate pooled of the last expanded leaves of two plants. Sampling was carried out in the middle of the light cycle in each particular treatment, 20 days after the end of the vernalization period, and frozen in N_2 liquid.

Total RNA was isolated with TRIzol (Thermo Fisher Scientific, Ltd.) followed by the Qiagen RNeasy plant mini kit, in accordance with the manufacturer instructions (Qiagen, Ltd.). Then, the material was extracted in the QIAcube equipment (Qiagen, Ltd.). RNA quality was assessed with a NanoDrop 2000 spectrophotometer (Thermo Fisher Scientific, Ltd.), agarose gel electrophoresis and Bioanalyzer 2100 (Agilent, USA; RIN $\geq$ 6.3). These last two steps were carried out by Novogene (HK) Co. Ltd. (China), who performed the sequencing, made *de novo* and reference guided transcript assemblies, gene expression analysis and an initial differential expression analysis. Library construction was developed from enriched RNA, using oligo(dT) beads. Then, mRNA was randomly fragmented in fragmentation buffer, followed by cDNA synthesis using random hexamers and reverse transcriptase. After first-strand synthesis, a custom second-strand synthesis

buffer (Illumina, USA) is added, with dNTPs, RNase H and *Escherichia coli* polymerase F to generate the second strand by nick-translation and AMPure XP beads are used to purify the cDNA. The final cDNA library is ready after a round of purification, terminal repair, A-tailing, ligation of sequencing adapters, size selection and PCR enrichment. Library concentration was first quantified using a Qubit 2.0 fluorometer (Life Technologies), and then diluted to 1 ng/μl before checking insert size on an Agilent 2100 and quantifying to greater accuracy by quantitative PCR (library activity > 2 nM). Eighteen barcoded libraries were multiplexed and sequenced, yielding 50 Million reads per sample on average, 2x150 bp paired-end reads at Novogene (China) in an Illumina HiSeq^{TM} 2500 sequencer. The whole dataset consisted of 18 samples, i.e. 3 biological replicates, from 3 varieties and 2 light conditions.

5.2.3. RNAseq data processing: de novo and reference-guided assemblies

Raw reads were processed with Illumina CASAVA v1.8. Low-quality reads (reads with more than 50% low quality base ($Q \leq 20$)) were removed. Reads were assembled following two different procedures, *de novo* and reference-guided, with the software Trinity (Haas *et al.*, 2013) (Figure 5.1). The first assembly was done *de novo* using only sequenced transcript reads (median length 366 bp); the second used the genomic sequence of barley cultivar Morex as reference (Mascher *et al.*, 2017) (median length 618 bp). In both cases, raw transcripts of all three genotypes combined were subsequently clustered in order to produce unigenes. In these approaches, the longest transcript from each gene was selected. The *de novo* analysis included a step of hierarchical clustering to remove the redundancy and keep the longest transcripts, which were chosen as unigenes. This step was carried out by Corset v1.05 (-m 10 to remove redundancy). Both assemblies, raw transcripts and unigenes, were used as references in the subsequent steps (Figure 5.1).

5.2.4. Quantification and analysis of gene expression

Two different approaches were developed to map the filtered reads and quantify the transcript abundances: a) RSEM/DESeq, carried out by Novogene and b) Kallisto/Sleuth (Figure 5.1), made in-house. In the DE analysis, three comparisons were carried out to describe within line variation (same lines in two light conditions), and 6 comparisons to describe variation across lines (pairs of different lines in the same lighting conditions).

The first approach consisted on mapping the clean reads to Corset filtered transcriptomes (unigenes from *de novo* and reference-guided assemblies). Next, they were quantified in RSEM v1.2.26 (bowtie2 mismatch 0). Then, two differential expression (DE) analysis (one for each assembly) were performed with DESeq 1.10.1 (Anders and Huber, 2010), taking into account a padj < 0.05.

The second approach consisted on mapping the clean reads against different barley reference sequences using Kallisto (Bray *et al.*, 2016) to identify and map the transcripts, and produce Transcripts Per Million (TPM), followed by Sleuth (Pimentel *et al.*, 2017) to perform the DE analysis. The data sets used as reference were Morex coding sequences (**Morex CDS sequences**) and **Morex transcripts** (Mascher *et al.*, 2017), **Haruna Nijo transcripts** (Sato *et al.*, 2016) and Zangqing320 a resource made with longer PacBio sequences, from here on noted as **Tibetan transcripts**, (Dai *et al.*, 2018). In addition, the four assemblies generated in this work by Novogene were used as references (***de novo* assembly**, **unigenes from the *de novo* assembly**, **reference-guided assembly**, **unigenes from the reference-guided assembly**).

DE isoforms were detected using a false discovery rate adjusted p values (named hereby "q-value") threshold of 0.05. As plants responded better to metal halide light, such condition was considered as control, thus DE genes are expressed in terms of being up or down-regulated under fluorescent light. To reduce the number

of DE genes to a workable number, we focused on DE genes with q-value < 0.01 to draw Venn diagrams, and identify the genes most likely affected by light quality.

We used R software (R Core Team, 2017) to carry out the following procedures. For quality control, we calculated the Pearson correlation coefficient between transcript abundances (as count estimates) of reference guided assembly with Morex CDSs sequence (Mascher *et al.*, 2017) [gene expression] across biological samples with the package "corrplot" (Wei and Simko, 2017). Clusters of different replicates (except LS9_F_2, deleted due to apparent contamination) were assessed using the different references for read quantification. We used the 'heatmap' function in R to generate gene expression heatmaps, and hierarchical clusters were developed with the 'hclust' function in R.
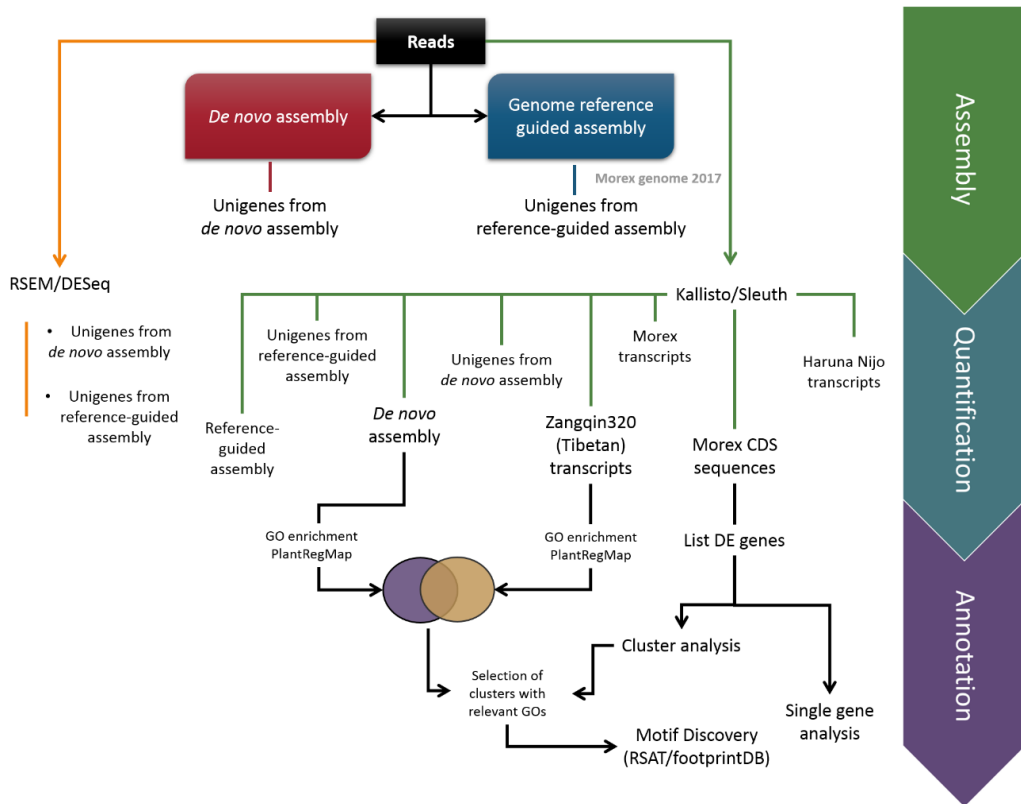
Figure 5.1. Pipeline of the RNA-seq analysis.

5.2.5.   GO enrichment analysis

GO term enrichment analysis was performed independently on the DE isoforms, calculated for within genotype comparisons, and derived from the mappings against the Tibetan and *de novo* transcripts references with PlantRegMap (Jin *et al.*, 2017). It uses reciprocal best BLAST hits to map gene IDs in the input to the IDs of the genes loaded in the database. GO enrichment is calculated by Fisher's Exact Test. GOs with a P-value < 0.05 were considered as enriched, and those in the intersection of both references highly reliable.

For all within genotype comparisons, DE genes obtained from Morex CDS 2017 were clustered based on their TPM values estimated with Kallisto in both light treatments. Clustering was done using the 'eclust' function from the 'factoextra' R package (Kassambara and Mundt, 2017). The optimal number of clusters was calculated by determining the value from which the total within-cluster sum of squares was stabilized.

5.2.6.   Motif discovery

We assigned to each cluster the GO annotation of the DE (q<0.05) genes it contained. We manually selected a few clusters containing relevant GO terms (e.g. response to stress, response to light, etc.). In order to retrieve promoter sequences of the corresponding clustered DE genes, we extracted upstream sequences (−1,000, +200 nucleotides around annotated Transcription Start Site, TSS) for each gene, from the server plants.rsat.eu (last visited June 07th, 2019) and performed the motif discovery protocol described in (Contreras-Moreira *et al.*, 2016). For each cluster analysed, 50 clusters of the same size made by random picking upstream barley sequences were used as negative controls for assessing the significance of motifs found   (parameters   MAXSIGGO=60   MAXSIG=10   MINCOR=0.7 MINNCOR=0.5). Resulting motifs were compared to motifs annotated in database

footprintDB (Sebastian and Contreras-Moreira, 2014). The complete motif discovery results are available at http://rsat.eead.csic.es/plants/data/light_report.

5.3. Results

5.3.1. Diversity in the response to different light sources

Under M conditions, development was accelerated, compared to F, as revealed by the less developed apices, in plants dissected after 23 days (Figure 5.2A). In the end, all three varieties flowered earlier in M than in F. However, Esterel showed the least differences between treatments in days to appearance of first node (DEV31, Figure 5.2B) and days to awns appearance (DEV49, Figure 5.2C and D), WA1614-95 presented the largest differences, and Price was in an intermediate position. Considering these results, Esterel was selected as less responsive or insensitive genotype, whereas Price and WA1614-95 were chosen as sensitive and highly sensitive genotypes, respectively. These three genotypes appeared in two different branches of the dendrogram presented in Chapter 4 (Figure 4.10), separating the most sensitive from the most insensitive genotypes.

A **23 d after vernalization**
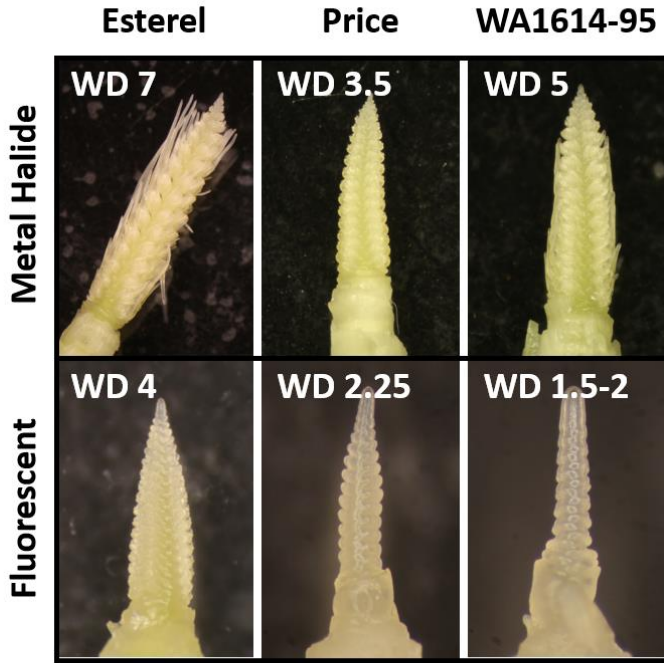
B DEV31
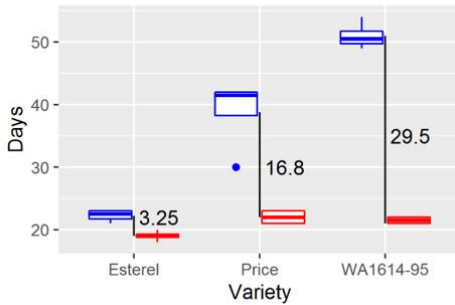
C DEV49
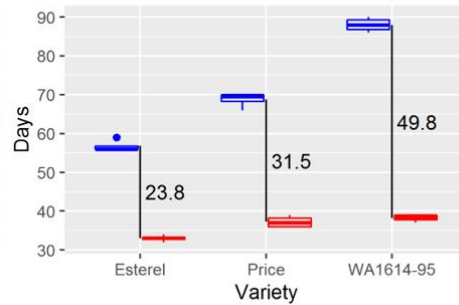
Condition ☐ Fluorescent ☐ Metal halide

D Esterel   Price   WA1614-95
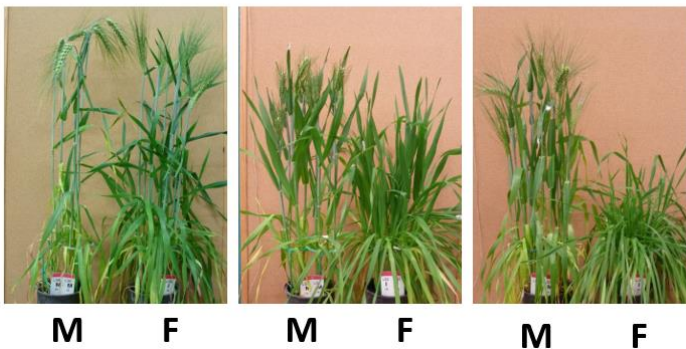
(Previous figure)

Figure 5.2. Phenotypic differences between varieties.

A) Apex development in plants dissected 23 days after the end of the vernalization treatment. WD, Waddington stage. B and C) Boxplot of the days to first node appearance (DEV31) and awns appearance (DEV49), in days from the end of the vernalization treatment, measured in 4 biological replicates. Vertical black lines represent the days of difference between fluorescent and metal halide conditions. D) Plants photographed 58 days after the end of the vernalization treatment.

5.3.2. RNA-seq performance

Sequencing cDNA of leaf samples in 18 samples produced a total amount of 1.92 billion of pair-end reads. The joint *de novo* assembly for the three genotypes, contained 375,488 isoforms, from which 181,337 unigenes were obtained, whereas the guided-reference assembly (with Morex genome, Mascher *et al*., 2017, as reference) consisted of fewer number of targets, and longer contigs (Figure 5.3A).

Clean reads were mapped back to their respective *de novo* and reference-guided assemblies, to estimate the abundance of each transcript. As the genome of Morex is the widely used reference, and the most informative in terms of annotation, reads were also mapped to transcripts and CDS. The references based on Morex are not complete, as it is based on just one genotype, and it has some gaps (as found by Dai *et al.*, 2018). We used a total of eight references and ten different analyses to declare DE genes (Figure 5.1, Figure 5.3A).

The number of DE genes varied between experiments (Figure 5.3B), as the reference has an influence in the number of genes localized. However, the proportion of DE genes was similar, regardless the method or reference used. Pair-wise comparisons of gene expression levels within genotypes identified less DE genes in Price (1087-2870, depending on the reference and procedure) than in WA1614-95 (1162-4219) and Esterel (1322-3434). The number of DE genes reported by RSEM/DESeq and Kallisto/Sleuth were different even when the same

reference was used (Figure 5.3B, references 2 vs 9 and 4 vs 10). The trend in the number of upregulated or downregulated genes varied with the reference used (Figure 5.3C).

A

Reference	Source	Unigenes	Number seq.	Median length (bp)	Quantification method	
					K/S	R/D
Reference-guided assembly	This work	No	211732	618	1	
Unigenes from reference-guided assembly	This work	Yes	160223	988	2	9
De novo assembly	This work	No	375488	366	3	
Unigenes from *de novo* assembly	This work	Yes	182337	779	4	10
Zangqing320 (Tibetan) transcripts	Dai et al. 2018	Yes	56043	3239	5	
Morex transcripts	Mascher et al. 2017	No	334126	3040	6	
Morex CDS sequences	Mascher et al. 2017	Yes	81279	408	7	
Haruna Nijo transcripts	Sato et al. 2016	Yes	51249	1426	8	

Figure 5.3. List of analyses done to identify DE genes, using different references.

A) Details of the reference transcriptomes used. B) Number of differentially expressed genes (DE) in each of the comparisons tested (q-value <0.05), number-coded as indicated in A. Each histogram represents a complete DE experiment, where each bar is the number of genes for each comparison. C) Number of upregulated (upF) or downregulated (downF) in each variety, in the quantification, mapping against different references; four are provided as examples. The metal halide conditions have been used as control.

Nine comparisons (M vs F for each one of three genotypes, and comparisons between pairs of genotypes for each light quality condition) were carried out in 10 different references (Figure 5.4). Clustering the biological replicates was used as an indirect measure of the goodness of the references. Biological replicates were better grouped using some mapping references than others (Figure 5.4). Among them, *de novo* assembly, the reference guided assembly and the Tibetan transcripts were the mapping references that grouped the replicates more correctly, indicating their higher reliability.

Reference	Number of correct clusterings
Reference-guided assembly	7
Unigenes from reference-guided assembly	8
De novo assembly	8
Unigenes from *de novo* assembly	4
Zangqin320 (Tibetan) transcripts	8
Morex transcripts	6
Morex CDS sequences	7
Haruna Nijo transcripts	6
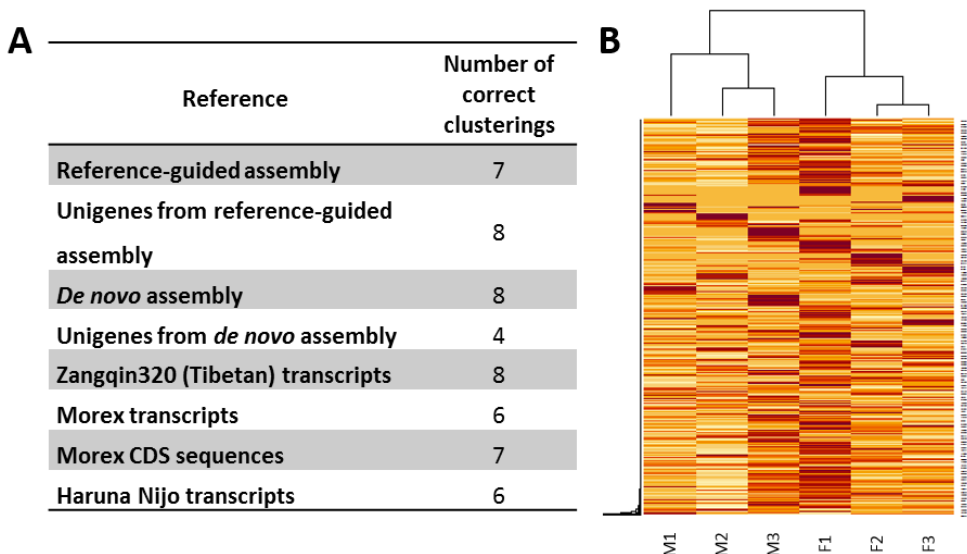
Figure 5.4. Number of correct clustering of biological samples in the heatmap generated for the nine comparisons (3 comparisons within varieties and 6 comparisons between varieties). A) Table of correct clusterings in the different references. B) Example of a correct cluster (1000 random transcripts in Price, using the reference of Morex CDS sequences).

The analysis included three biological replicates per genotype and condition. Correlation coefficients between gene expressions (estimated counts) for the replicates was used as quality control. In all cases, but one, correlations between biological replicates within genotypes were high. There was one exception. The relatively high correlation of one of the Esterel replicates (Esterel_F2) with Price replicates indicates possible contamination. Consequently, this Esterel replicate was discarded from downstream analyses. Additionally, it is remarkable that Price and WA1614-95 replicates were highly correlated in M conditions (Figure 5.5A), whereas transcript abundances of both genotypes were more different in F conditions (Figure 5.5B). Esterel had low correlations with the other genotypes in both conditions.
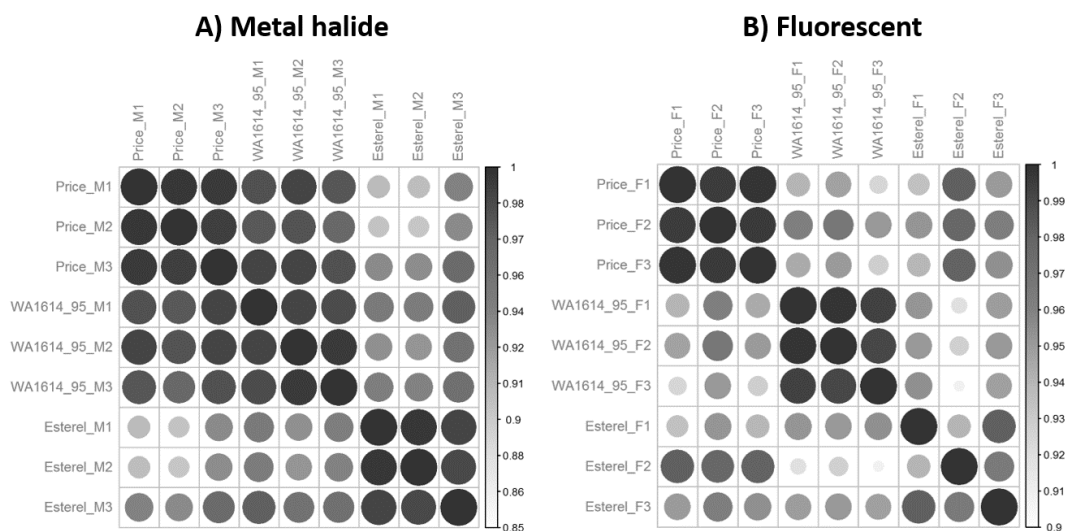
Figure 5.5. Correlation across biological replicates.
The values used were transcript abundances (as counts estimates) of the different replicates mapped against Morex CDS sequences. A) Correlation of gene expression under metal halide bulbs. B) Correlation of gene expression under fluorescent light.

5.3.3.　　Gene expression analysis

As the aim of this experiment is to unravel differential genotypic responses to light quality, we focused the analysis of DE genes in the within genotype comparisons. Morex CDS sequences was the reference with the highest number of targets (Figure 5.3B), and was chosen for this purpose. Using that reference, genotypes Price, WA1614-95 and Esterel contained 2869, 4218 and 3433 DE genes, respectively, for a q-value < 0.05. We used the relatively high number of transcripts detected with this threshold for cluster analysis of expression patterns. To focus on single genes most likely affected by light conditions, we focused in DE genes with q < 0.01, and denoted them as "key genes". Key DE genes in Esterel were predominantly downregulated (in F compared to M), whereas Price showed more upregulated than downregulated genes (Figure 5.6), whereas WA1614-95 showed similar number of up- and down-regulated DE genes.
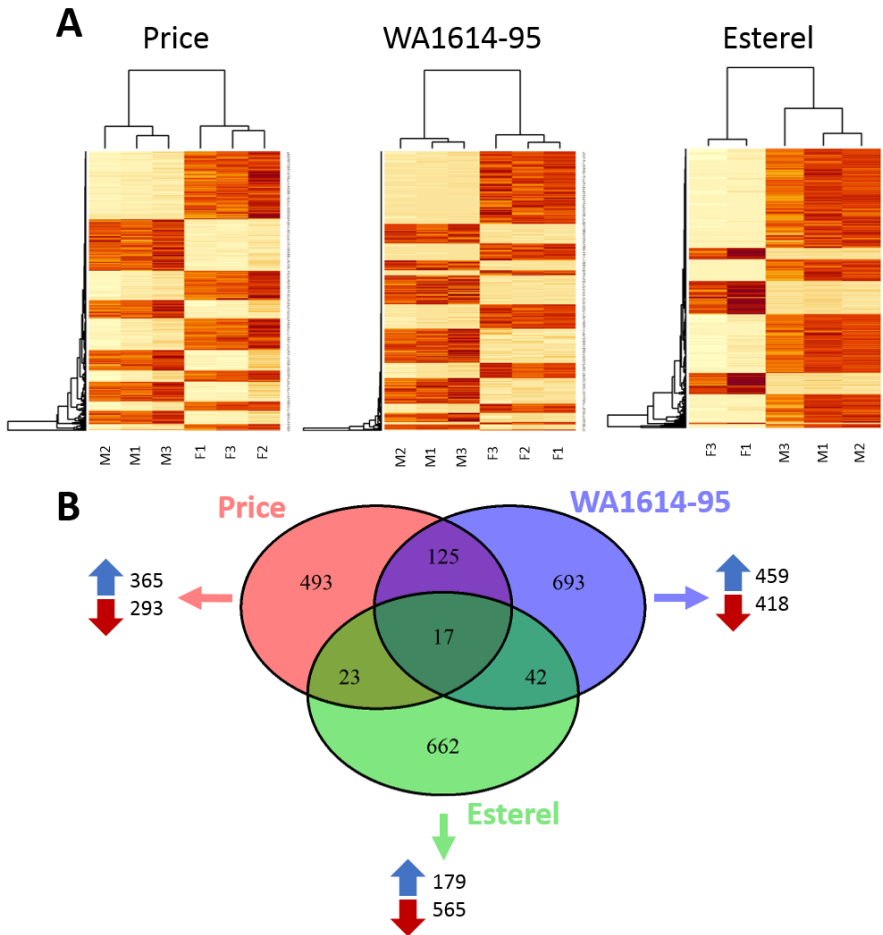
Figure 5.6. Key DE genes in the three genotypes. Only DE genes with q-value < 0.01 are represented.

A) Cluster of differential expressed (DE) genes with q-value < 0.01. Color: red, upregulated; yellow, downregulated. Morex CDS sequences used as reference. Three biological replicates per variety and condition are represented, except for Esterel in fluorescent light, which has two replicates. F, fluorescent; M, metal halide. B) Venn diagram showing the intersection between pairs and between all genotypes. Blue and red arrows indicate the number of key DE genes upregulated or down regulated in fluorescent conditions in each genotype.

The intersection of key genes for the three genotypes detected 17 genes. A transcript annotated as *HvFT1* appeared twice, on chromosomes 3H and 7H, with the same expression levels. It is clear from the literature that *HvFT1* is placed exclusively on

7H (Yan *et al.*, 2006). Therefore, the hit on 3H comes from a duplication of this gene in the Morex genome, which contains a very large number of fragmented genes (Beier *et al.*, 2017; Prade *et al.*, 2018), which could be a result of artefacts generated in the assembly process. Among the 16 key DE genes standing, only one gene was found differentially expressed among genotypes (upregulated in F in the sensitive genotypes and downregulated in the insensitive Esterel), although no information about its function was available. The rest showed the same direction of differential expression for the three genotypes. Among them, *HvBM3* (Barley MADS-box 3), *HvBM8*, *PPD-H1* (*PSEUDO RESPONSE REGULATOR 7*, *HvPRR37*, Turner *et al.*, 2005), *HvFT1* (*FLOWERING LOCUS T*-like, Yan *et al.*, 2006) were downregulated under fluorescent conditions, whereas *HvVRT-2* (*VEGETATIVE TO REPRODUCTIVE TRANSITION-2*) and *RVE7*-like (*EARLY PHYTOCHROME RESPONSIVE 1/REVEILLE7*) were upregulated in fluorescent light in the three genotypes (Table 5.1). Also, *RVE7*-like and *HvVRT-2* were expressed at higher levels in WA1614-95, whereas *HvBM3*, *HvBM8*, *PPD-H1* and *HvFT1* showed higher expression levels in the insensitive line, Esterel (Figure 5.7).

Table 5.1. Table 1. List of DE genes in the intersection between the three varieties. Upregulated (u) and downregulated (d) genes in fluorescent conditions are showed for each genotype.

Target ID	Description	Gene	Citation	Price	WA1614-95	Esterel
Price ∩ WA1614-95 ∩ Esterel						
HORVU0Hr1G003020.3	MADS-box transcription factor 18	HvBM3	1, 2	d	d	d
HORVU2Hr1G063800.7	MADS-box transcription factor 15	HvBM8	1, 2	d	d	d
HORVU7Hr1G036130.1	MADS-box transcription factor 55	HvVRT-2	3, 4	u	u	u
HORVU7Hr1G083670.3	Cytochrome P450 superfamily protein			u	u	u
HORVU2Hr1G013400.32	pseudo-response regulator 7	HvPRR37 (PPD-H1)	5	d	d	d
HORVU4Hr1G090860.12	metacaspase 1	cell death		u	u	u
HORVU5Hr1G071940.2	UDP-Glycosyltransferase superfamily protein			u	u	u
HORVU2Hr1G024120.10	terpenoid synthase 13			d	d	d
HORVU0Hr1G038850.2	Protein kinase superfamily protein			u	u	u
HORVU3Hr1G111550.2	undescribed protein			u	u	d
HORVU3Hr1G021880.1	undescribed protein	Glycosyltransferase		d	d	d
HORVU3Hr1G087100.1	FLOWERING LOCUS T 1			d	d	d
HORVU7Hr1G024610.1	FLOWERING LOCUS T 1	HvFT1 (VRN-H3)	6, 7	d	d	d
HORVU5Hr1G029260.1	calcium-dependent protein kinase 24			d	d	d
HORVU2Hr1G063810.1	undescribed protein			d	d	d
HORVU2Hr1G104580.2	At5g37260-like protein	RVE7-like		u	u	u
HORVU1Hr1G076460.3	Non-symbiotic hemoglobin 1			u	u	u

Legend	u	Upregulated in fluorescent with q.value<0.01
	d	Downregulated in fluorescent with q.val <0.01

1, Schmitz *et al*., 2000; 2, Ejaz and von Korff 2017; 3, Kane *et al*., 2005; 4, Szucs *et al*., 2006; 5, Turner *et al*., 2005; 6, Yan *et al*., 2006; 7, Casas *et al*., 2011.

When we looked into DE genes shared by two varieties (Table S 5.2), Price and WA1614-95 (both considered sensitive lines to light quality) had the largest number (125, 66 upregulated and 59 downregulated in F). In the set of DE genes shared by Esterel and Price, 20 genes showed differential expression with the same sign (14 up and 6 down), and 3 genes were different (up-regulated in Price and down-regulated in Esterel). In the DE gene set shared by Esterel and WA1614-95, there were 13 genes with similar, and 29 with opposite trends. WA1614-95 had more up- (35) than downregulated (7) genes, whereas Esterel had more down- (32) than upregulated (10).
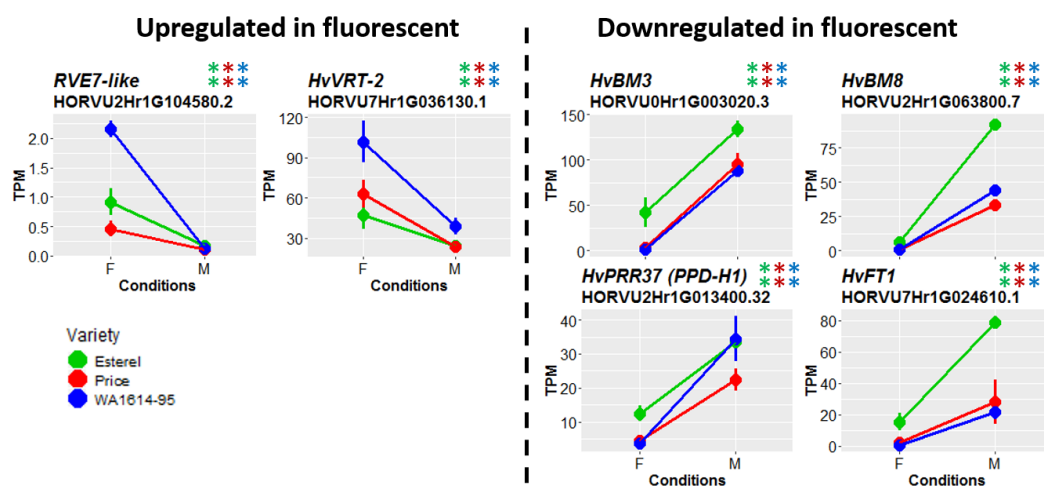
Figure 5.7. Examples of key genes with similar expression patterns in the three genotypes. Two asterisks of the same colour indicate that differences are significant at q<0.01. Genes are separated in two groups: upregulated (left) and downregulated (right) under fluorescent conditions. The three genotypes are Esterel (green), Price (red) and WA1614-95 (blue), in fluorescent (F) or metal halide conditions (M).

5.3.4. Clusters of DE genes and GO enrichment analysis

To determine genes with common regulation patterns, the DE genes (q-value < 0.05), according to the Morex CDS sequences reference, were grouped based on

their expression patterns in each of the within genotype comparisons. The optimal number of clusters was 39 for Price, 30 for Esterel, and 17 for WA1614-95.

We carried out a GO enrichment analysis to find functional commonalities among the genes present in each cluster through shared GO terms.

This was first attempted using the Morex CDS sequences reference. However, due to the incomplete annotation of the Morex 2017 genome (for instance, several GO terms involved in light stress were missing), we took a second approach, which consisted on running a GO enrichment analysis on our own data (*de novo* assembly DE genes) and the Tibetan transcripts, using PlantRegMap (Jin et al., 2017). The *de novo* transcriptome offered a good start to fill the gaps found in Morex. In addition, the long reads and contigs generated by PacBio sequencing of Tibetan transcriptome provide a better coverage to amend those regions without information in Morex. This, together with the best clustering of replicates in the *de novo* assembly and Tibetan transcripts (Figure 5.4) are signals of good performance and would provide a more reliable annotation.

These two data sets (DE genes, p-value < 0.05) were independently subjected to GO enrichment analysis. The intersection of the resultant sets of terms was declared as the final dataset of enriched GOs, for robustness. Terms involved in responses relevant for the study are summarized in Table 5.2. The GO annotation highlighted terms involved in cellular responses to light stimulus that were upregulated in F in the insensitive genotype, and downregulated in the sensitive genotypes, together with other categories, as carbohydrate catabolic process, cellular response to oxidative stress, cellular response to radiation and response to abiotic stimulus. Also, enriched GO list contained genes involved in the response to red/far-red light solely in Price, and to light intensity and UV-A exclusively in WA1614-95. The genes under those terms were downregulated in fluorescent conditions.

Table 5.2. Enriched GO terms relevant for the plant response to different light quality conditions.

GO term		Esterel	Price	WA1614-95
Cellular response to light stimulus	GO:0071482	blue	red	red
Carbohydrate catabolic process	GO:0016052		red	red
Cellular response to oxidative stress	GO:0034599		red	red
Cellular response to radiation	GO:0071478		red	red
Chlorophyll metabolic process	GO:0015994		red	red
Photosynthesis, light harvesting	GO:0009765		red	red
Response to abiotic stimulus	GO:0009628		red	red
Cellular response to abiotic stimulus	GO:0071214	blue	green	red
Response to UV	GO:0009411	blue		
Response to starvation	GO:0042594	red		
Cellular response to external stimulus	GO:0071496	red	blue	
Coenzyme binding	GO:0050662	blue	red	
Cell wall	GO:0005618	red		blue
Vacuolar membrane	GO:0005774	red		blue
Metabolic process	GO:0008152	red		blue
Cellular response to high light intensity	GO:0071486			red
Cellular response to light intensity	GO:0071484			red
Response to high light intensity	GO:0009644			red
Response to UV-A	GO:0070141			red
Reproductive structure development	GO:0048608		red	
Reproductive system development	GO:0061458		red	
Response to heat	GO:0009408		red	
Cellular response to red or far red light	GO:0071489		blue	
Response to red or far red light	GO:0009639		blue	

Blue, upregulated in fluorescent conditions; red, downregulated in fluorescent conditions; green, terms appear as up and downregulated genes.

The information of the enriched GOs fed back into the clusters generated with DE genes from Morex CDS mapping. Then, we manually selected clusters with presence of relevant GO terms. Motif discovery was done for a selection of clusters with relevant GOs (http://rsat.eead.csic.es/plants/htmllink.cgi?title=RSAT-Data&file=data/).

The clusters revealed different patterns of expression (Figure S 5.2). Upstream sequences of genes within these clusters showed enriched MYB-like DNA conserved motifs (Figure 5.8). These clusters also contained MYB transcription factors, suggesting that these proteins could be coordinating the expression of genes within the clusters. Specifically, cluster 10 was enriched in GO terms involved in the plant response to light stimulus, showing upregulated genes in fluorescent conditions in all the genotypes, although differences were more apparent in sensitive genotypes Price and WA1614-95 (Figure 5.8). Common motifs were discovered in upstream regions of those genes, with a highly significant motif pattern (1.44), which is comparable to the negative controls (grey bars in the histogram). The consensus sequence was similar to that of *Arabidopsis thaliana MYB52*, annotated in footprintDB.
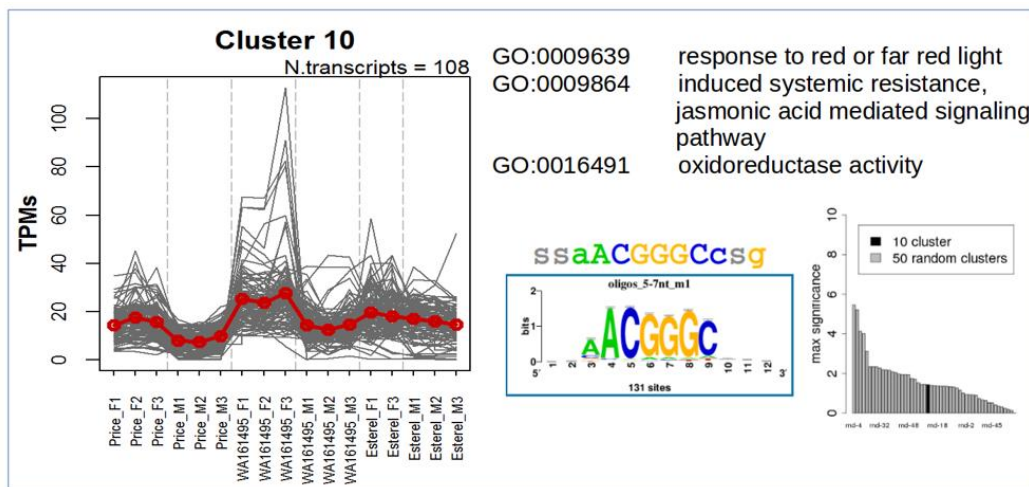
Figure 5.8. Representation of the DE genes that compose cluster 10, and results from motif discovery.

The number of genes that shared this pattern is 108. At left, from up to the bottom, relevant GO terms enriched in this cluster are described, and results from the motif discovery are represented. The consensus sequence was discovered in an upstream region covering [-1000, 200] bp. The significance of the motif is given by the height of the letters, as bits in a total of 131 sites. Histogram on the right represents the maximum significance obtained

when running the analysis against negative controls (grey bars). The consensus sequence found is similar to that of A. thaliana MYB52, annotated in footprintDB.

5.3.5.   Single gene analysis

A large number of DE genes were found. We focused in detail on DE genes involved in light perception (phytochromes, cryptochromes), circadian clock, flowering initiation and development (Figure 8).

Among these genes, we found that *HvPhyC* was DE in the three genotypes, whereas *HvPhyB* and *HvCry2* were only differentially expressed in Price, and no differences were found for *HvPhyA* and *HvCry1a* (Figure S 5.3). *HvPhyC* was upregulated in fluorescent conditions, whereas *HvPhyB* and *HvCry2* were downregulated in the same conditions (or upregulated in M).

The three genotypes showed reduced transcript levels of *PPD-H1*, *HvFT1* (Figure 5.7) and *HvVRN1* in F (Figure 5.9), consistent with the delayed plant development in fluorescent conditions. Esterel showed higher expression levels than the sensitive genotypes for *HvFT1* and *HvVRN1*, in accordance with its accelerated development in both conditions. In addition, the three genotypes showed increased transcript levels, under fluorescent light, of the flowering repressors *HvOS2*, *HvVRT2* and an orthologue of *RVE7*-like in wheat. WA1614-95, which was the latest flowering genotype in fluorescent, showed the highest transcript levels of these repressor genes.

We also identified some differentially expressed genes which encode components of the circadian clock: *HvCCA1*, *HvLUX* upregulated in F; *HvGI*, *HvPRR95*, *HvPRR73* downregulated in F; and clock output genes, as *HvCO1*, upregulated in F.
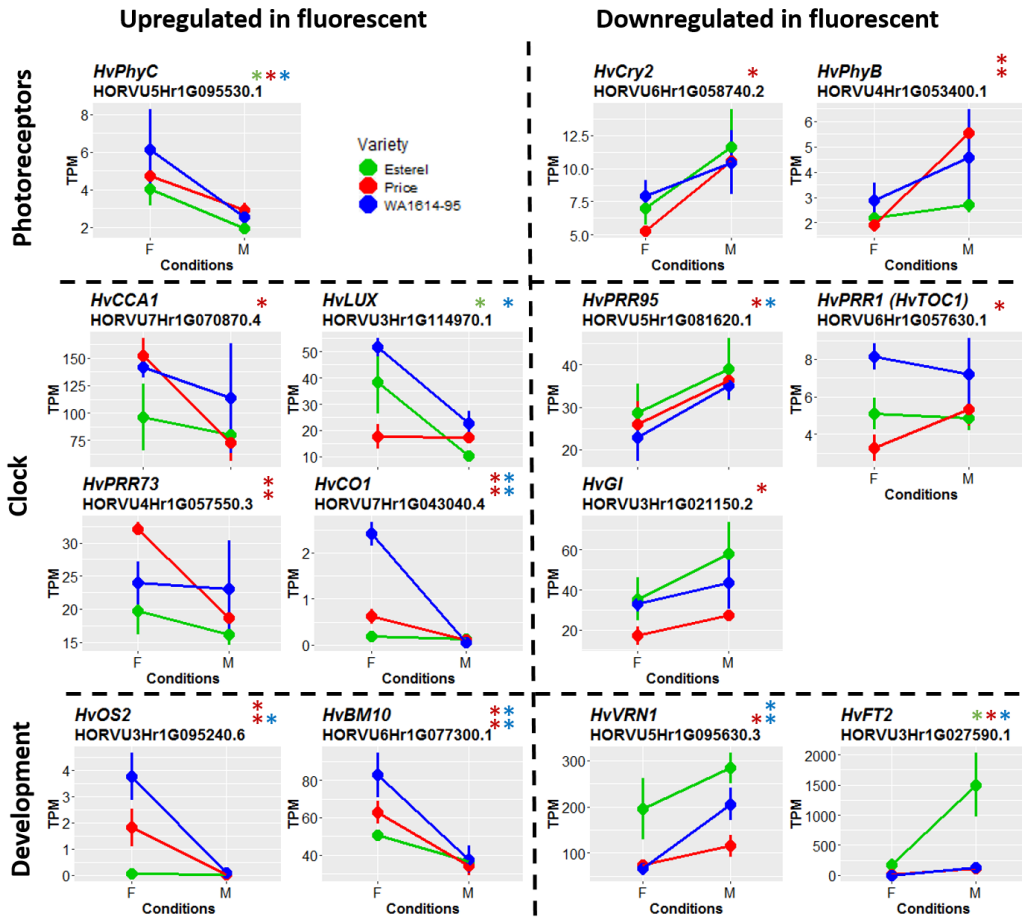
Figure 5.9. Selection of flowering related DE genes related to photoreceptors, circadian clock and development (q-value < 0.05).

Genes are separated in two groups: upregulated (left) and downregulated (right) under fluorescent conditions. F, fluorescent conditions; M, metal halide conditions. *, differences between treatments are significant at q value < 0.05: two asterisks, significant at q<0.01).

Two members of the *C-REPEAT/DREB BINDING FACTOR* (CBF) family (*HvCBF14*, HORVU5Hr1G080350.1; *HvCBF4a*, HORVU5Hr1G80300.1), one member of the *COLD-RESPONSIVE* (COR) family (*WCOR15A*, HORVU4Hr1G090860.12) and one from the *INDUCER of CBF EXPRESSION* (*ICE*), ortholog of rice (*ICE-like* annotated as *metacaspase I*, HORVU2Hr1G099820.2), all of which are relevant in the acquisition of freezing tolerance, were upregulated in fluorescent light (Figure 5.10).
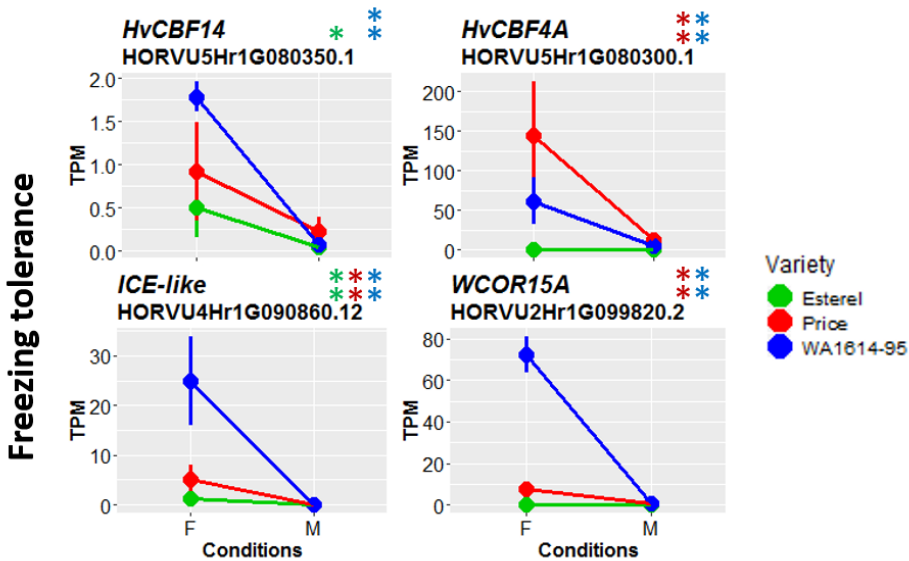
Figure 5.10. Selection of freezing tolerance DE genes (q-value < 0.05).
Genes are separated in two groups: upregulated (left) and downregulated (right) under fluorescent conditions. F, fluorescent conditions; M, metal halide conditions. *, differences between treatments are significant at q value < 0.05: two asterisks, significant at q<0.01).

5.4.   Discussion

Different light sources had a great influence on growth and development as evidenced in the previous chapter. Although all genotypes had been vernalized prior to the start of the experiment, plants grown under fluorescent light showed delayed development, as compared to those under metal halide light. Briefly, the two light sources used in this study present large differences across their broad spectra. Fluorescent light presented particularly high peaks at the 550-650 nm regions, corresponding to green and red wavebands. Metal halide bulbs had a more balanced spectrum. There were no differences in light intensity between the chambers and, therefore, plant development and differences in flowering regulation must be a consequence of the spectral distribution of the lighting sources.

The three varieties differed in growth habit. *HvVrn2* is present in Esterel and Price and absent in WA1614-95 (Table S 5.1). Therefore, Esterel and Price are winter varieties, whereas WA1614-95 is a spring variety. The vernalization treatment placed them at a similar developmental stage (between Z11 and Z12) at the beginning of the light treatments. They showed small developmental differences in M, but very large differences in F, already visible at DEV31 (Figure 5.2). As noted in Chapter 4, we observed that differences in development between treatments were a consequence of variations at the early growth phases, mainly the time to first node appearance (DEV31) and from there to the onset of stem elongation phase (DEV30). Sampling for RNA-seq took place three days before examination of the apices presented in Figure 5.2, so all of them had started the reproductive phase, or at least were very close to it. Growth differences were paralleled by dramatic changes in leaf gene expression starting at the light sensing apparatus, and affecting several key developmental pathways.

5.4.1. Signalling pathways affected by light quality

Higher plants possess two types of signal-transducing photoreceptors, phytochromes (PhyA, PhyB, PhyC in cereals) absorbing principally in the 600-800 nm waveband, and the blue-absorbing cryptochromes (Cry1, Cry2), absorbing only in the 300-500 nm band (Smith, 1982). Phytochrome proteins are characterized by a red/far-red photochromicity, changing their spectral absorbance properties upon light absorption. They have two interchangeable isomeric forms. They are synthesized in the biologically inactive, R light-absorbing Pr form, turn into the biologically active, FR light-absorbing Pfr form upon absorption of R light (Rockwell *et al.*, 2006). Upon absorption of FR light, phytochromes in the Pfr state revert to the inactive Pr state (Rockwell *et al.*, 2006). Phytochromes are dimeric proteins. The role of homo and heterodimers is still an open area of research but it has been proven than both *PhyB* and *PhyC* genes are required for the induction of

wheat flowering under LD (Pearce *et al.*, 2016). Phytochrome dimers, and also cryptochromes interact with transcription factors known as PHYTOCHROME INTERACTING FACTORS (PIFs) (Leivar and Monte, 2014; Pedmale *et al.*, 2016). In *Arabidopsis*, PIFs regulate downstream targets including clock genes (Oakenfull and Davis, 2017) and flowering time genes (Leivar and Monte, 2014). Therefore, photoreceptors are at the top of fundamental processes controlling many aspects of plant growth and development in response to light.

The different spectra provided by the light sources in this experiment could affect the function of light receptors and, as a consequence, plant growth. We examined the expression of phytochromes and cryptochromes, and found significantly higher expression of *HvPhyC* under fluorescent light in all three genotypes, and an opposite trend for *HvPhyB* and *HvCry2*, although significant only in Price (consistent with their antagonist role, reported by Más *et al.*, 2000). On the other hand, acceleration of flowering in M was associated with high levels of *HvPhyB* and *HvCry2*, whereas *HvPhyC* levels were lower. In our results, apparently, F light caused a strong imbalance of the expression of these three signaling genes, which could lead to a disruption of the balances of phytochromes, between active and inactive forms, patterns of occurrence of homo- and heterodimers, and ratios of phytochromes and cryptochromes. These imbalances could be at the top of the changes in expression found in downstream pathways that will be commented later.

Mutants of *HvPhyC* in barley have shown altered flowering through the modulation of the expression of *PPD-H1* and *HvFT1* (Nishida *et al.*, 2013; Pankin *et al.*, 2014) confirming the importance of *HvPhyC* on downstream components of flowering pathways. We observed very similar *HvPhyC* responses in our three varieties, which is consistent with the fact that all three present a common *HvPhyC* allele. This allele is different from the extra-early mutant reported in those two studies. Our results are in line with the findings of Chen *et al.* (2014) in wheat, who reported

a strong effect of light signaling on expression of flowering time genes and on development, in wheat mutants carrying two silent PHYC homeologs. Our experiment did not modify the genes but, rather, the environmental cues affecting their expression. It seems that the overexpression of *HvPhyC* in F light in our study had an effect resembling the situation resulting from not having a functional gene in wheat. Actually, both *PhyC* and *PhyB* are required for the photoperiodic induction of flowering in wheat (Pearce *et al.*, 2016). Null mutants of either of these two genes in wheat produced late-flowering plants, sterile and with altered vegetative development (Pearce *et al.*, 2016). The altered expressions of the two phytochromes in our study may have shifted the proportions of their proteins off-balance from the optimum proportion for unrestricted progression towards flowering.

5.4.2.   Different gene expression in flowering pathways

One role proposed for PhyC is to activate *PPD-1* in LD (Nishida *et al.*, 2013; Chen *et al.*, 2014; Woods *et al.*, 2014) The link between PhyC and flowering promotion under LD is supported by several evidences in wheat and barley. For instance, Alqudah *et al.* (2014) found significant associations for duration of awn primordium-tipping phases at the locus *HvVRN1-HvPhyC* only in *PPD-H1* sensitive lines. In line with this idea, Kiseleva *et al.* (2017) correlated expression levels of *PPD-1* and *PhyC* in wheat, suggesting that, *PPD-1* expression at night could positively regulate *PhyC* expression.

However, the opposite signs of DE between *HvPhyC* and *PPD-H1* (as well as with flowering promoter *HvFT1*), and the common sign with flowering repressors (*RVE7-like*, *VRT2*, and *HvVRN2*, as was observed in Chapter 4) raises some questions. Under F light, we observed high expression of *HvPhyC* concurrent with reduced expression of *PPD-H1*. One possible explanation is that the high *HvPhyC*

expression does not result in an increased presence of the active forms of the protein, but rather the opposite.

The delayed development observed in F was paralleled by dramatic changes in leaf gene expression of several genes acting in pathways linked to development, which were overrepresented among the 16 genes differentially expressed in the three cultivars assayed: two members of the barley MADS-box transcription factor family, *HvBM3* and *HvBM8* (Schmitz *et al.*, 2000), and the flowering time genes *PPD-H1* and *HvFT1* were upregulated in metal halide. On the contrary, another MADS box gene, *VRT-2* (Kane *et al.*, 2005), a member of the MYB family of transcription factors, homolog of *RVE-7*, and an *ICE*-like protease showed higher expression under fluorescent light.

PPD-H1 activity could be the common cause of the patterns observed for *HvFT1*, *HvBM3* and *HvBM8* expression. *PPD-H1* mediates long-day induction of *HvFT1* (Turner *et al.*, 2005), and *HvBM3* and *HvBM8* also are known targets of *PPD-H1* under LD (Digel *et al.*, 2015, 2016; Ejaz and von Korff, 2017), all of them with a flowering inducing effect. *HvVRT-2*, on the other hand, represses floral development during winter, possibly to counteract induction of flowering by vernalization (Trevaskis *et al.*, 2007). *EPR1/RVE-7* is related to the circadian clock and contributes to the refinement of clock output pathways, ultimately mediating the correct oscillatory behavior of target genes (Kuno *et al.*, 2003).

Another gene differentially expressed between fluorescent and metal halide light in the three varieties corresponds to a non-symbiotic hemoglobin, upregulated under fluorescent light. Recently, Rubio *et al.* (2019) have reported the presence of non-symbiotic hemoglobins in the nuclei, chloroplasts and amyloplasts of *Arabidopsis thaliana* and *Lotus japonica*, and in the cytoplasm of Arabidopsis cells. This is the first report of hemoglobin expression in barley leaves in response to light quality and should be explored further.

5.4.3.   Differentially   expressed   genes   differing   between sensitive and insensitive varieties

In general, Esterel and WA1614-95 had more DE genes than Price and, in particular Esterel, had the highest number of down-regulated genes in F. This was unexpected, as it seems that the least responsive variety from the phenotype point of view, Esterel, undergoes more changes than the sensitive lines at transcript level. However, the results of GO enrichment analysis showed that terms relevant for light responses were more abundant and upregulated in F in Esterel than in the other two genotypes (Table 5.2). Contrastingly, WA1614-95 responses were associated with reduced expression of genes relative to oxidative stress, UV-A light, light intensity and photosynthesis. The commonalities of DE genes among genotypes roughly matched the phenotypic differences. There was a striking similarity between WA1614-95 and Price, with all 125 genes affected in the same direction, indicating that some pathways were affected in the same way in both varieties. The smaller number of commonly DE genes between Esterel and WA1614-95 which, on the other hand, presented mostly opposite patterns, indicated important differences between these varieties in the affected pathways.

There were flowering time genes related to the vernalization pathway, *HvVRN1*, *HvOS2* and *HvBM10* that were differentially expressed in the sensitive varieties but not in the insensitive one. *HvVRN1* is the central gene responsible for modulation of the vernalization response. It should have been fully induced after vernalization in all three varieties (even more so in WA1614-95 which does not need vernalization), but it was much less induced in F light in Price and WA1614-95, mimicking an incipient de-vernalization. *ODDSOC2* is the cereal homolog of Arabidopsis *FLC* (Greenup *et al.*, 2010), and was identified as a target for *VRN1* in barley (Deng *et al.*, 2015). Therefore, it is not surprise that its expression is a negative of *HvVRN1*'s.

●●●

To uncover other key genes that may be involved in the differential genotypic sensitivities, we examined the DE genes in the intersection of each pair of varieties, and in the triple intersection (Table S 5.2). In the triple intersection, there was a single gene which showed opposite variation between Esterel and the other two varieties. Hypothetically, this gene is a good candidate to be placed at a high hierarchy level to explain the phenotypic differences between sensitive and insensitive varieties. Unfortunately, this gene lacks annotation, but could be a good target for further research. As mentioned, a majority of genes in the intersection WA1614-95 ∩ Esterel had opposite trends of expression. Among those genes, WRKY family transcription factors and genes codifying protein kinases were over-represented, being upregulated in fluorescent in the sensitive genotype WA1614-95 and downregulated in the insensitive Esterel. WRKYs transcription factors trigger cell wall modifications in order to block the entrance of UV light into the cell, a mechanism never described in barley, but observed in grapevines (Lesniewska *et al.*, 2004). If this mechanism was acting in opposite directions in Esterel and WA1614-95, it could justify partially the delayed development in WA1614-95.

DE genes were also overrepresented in GOs involved in cellular responses to light stimulus, which appeared active in fluorescent conditions in the insensitive genotype, Esterel, whereas the sensitive lines showed less activity in these genes. The sensitive lines also showed reduced activity in genes related to carbohydrate catabolic process, response to oxidative stress, radiation and abiotic stimulus respect to metal halide conditions.

In *Arabidopsis*, Franklin and Whitelam (2007) observed that the phytochrome signalling was mediated by circadian clock. Thus, the complex relation between photoreceptors and clock might provide a reason for the differences in downstream development genes, and in the phenotype. It is remarkable that *HvPhyB*, *HvCry2*

and most of the clock genes represented, were differentially expressed only in Price. Also, Price is the only genotype of the three studied that carries a functional allele of *HvFT3*. Thus, despite being a sensitive genotype to the light quality conditions, the presence of *HvFT3* could provide an additional developmental boost that would make it earlier under fluorescent conditions with respect the other sensitive genotype, WA1614-95, but not with respect to the earliest of the three, Esterel.

5.4.4. Collateral effects of light quality: freezing tolerance genes

The family of C-repeated/DRE binding factors (CBF) is known by their role providing frost tolerance. Among the subgroups that compose this family, we have found that two members of the CBF4-clade (*HvCBF14* and *HvCBF4a*, Skinner *et al.*, 2005) were upregulated in fluorescent conditions. It has been suggested that the CBF regulon in Arabidopsis is upregulated by phytochromes in low R:FR light, and under higher temperatures than those that confer cold acclimation, but not optimum for development (Franklin and Whitelam, 2007). Similarly, freezing tolerance genes were affected in phyB-null mutants in wheat (Pearce *et al.*, 2016) and Arabidopsis (Franklin and Whitelam, 2007), and in the downregulation of one member of the *INDUCER of CBF EXPRESSION* (*ICE*) gene family (Badawi *et al.*, 2008). All these evidences suggest a role for PhyB in light-mediated activation of cold acclimation pathway.

In our work, although barley apices in both treatments reached the double ridge stage (W1.5-W2.0), meaning they had turn into reproductive shoot apical meristems, plants under fluorescent light were relatively delayed. This observation is also reflected by the upregulation of several members of the CBF family. *HvCBF14* is induced in barley plants grown under fluorescent light supplemented with far red light, increasing their freezing tolerance (Novák *et al.*, 2016).

Stockinger *et al.* (2007) reported that in vrn-H1 genotypes requiring vernalization, such as Esterel and Price, CBF expression levels were dampened after plants were vernalized, and dampened CBF expression was accompanied by robust expression of Vrn-1. In our experiment, even though the plants had been vernalized, *HvVRN1* expression was lower under fluorescent light, which agrees with that observation.

5.5.   Conclusion

Controlled conditions do not mimic the natural conditions, but are valuable tools in research. Here, we studied the interaction between light sources and development in barley varieties showing natural differential growth patterns under broad spectrum light sources. There appears to be considerable variability among barley genotypes regarding light quality sensitivity, which could be used in the selection and development of crop cultivars. We have seen that, especially in sensitive genotypes, fluorescent lights, with over-represented regions at green and red wave bands, delay flowering, downregulating genes related to responses to oxidative stress, radiation, abiotic stimulus, intensity, UV-A and red/far red light. Expression patterns of *HvPhyC*, *HvCry2* and *HvPhyB,* placed at the top of the signalling cascades, could partially explain the differences between treatments and varieties. Differences in light quality affected expression of circadian clock genes, flowering time genes and freezing tolerance, among others, resembling plant responses to temperature. Hence, several of the differences found might be attributed to the relation between *PPD-H1*, *HvVRN1* and *HvFT1*. The natural variation found is large, and it serves to advance in deciphering the biology behind the different responses to light quality. Possible agronomic consequences of these natural responses should be considered, taking into account variability in light spectra that occur in agricultural settings.

5.6. References

Adams S, Allen T, Whitelam GC. 2009. Interaction between the light quality and flowering time pathways in *Arabidopsis*. The Plant Journal **60**, 257–267.

Alqudah AM, Sharma R, Pasam RK, Graner A, Kilian B, Schnurbusch T. 2014. Genetic dissection of photoperiod response based on GWAS of pre-anthesis phase duration in spring barley. PLoS ONE **9**, e113120.

Anders S, Huber W. 2010. Differential expression analysis for sequence count data. Genome biology **11**, R106.

Badawi M, Reddy YV, Agharbaoui Z, Tominaga Y, Danyluk J, Sarhan F, Houde M. 2008. Structure and functional analysis of wheat *ICE* (inducer of CBF expression) genes. Plant & Cell Physiology **49**, 1237–1249.

Beier S, Himmelbach A, Colmsee C, *et al.* 2017. Construction of a map-based reference genome sequence for barley , *Hordeum vulgare* L. Scientific Data **4**, 170044.

Bray NL, Pimentel H, Melsted P, Pachter L. 2016. Near-optimal probabilistic RNA-seq quantification. Nature Biotechnology **34**, 525–527.

Casal JJ. 2013. Photoreceptor signaling networks in plant responses to shade. Annual review of plant biology **64**, 403–427.

Casas AM, Djemel A, Ciudad FJ, Yahiaoui S, Ponce LJ, Contreras-Moreira B, Gracia MP, Lasa JM, Igartua E. 2011. *HvFT1* (*VrnH3*) drives latitudinal adaptation in Spanish barleys. Theoretical and Applied Genetics **122**, 1293–1304.

Chen A, Li C, Hu W, Lau MY, Lin H, Rockwell NC, Martin SS, Jernstedt JA, Lagarias JC, Dubcovsky J. 2014. PHYTOCHROME C plays a major role in the acceleration of wheat flowering under long-day photoperiod. Proceedings of the National Academy of Sciences of the United States of America **111**, 10037–10044.

Contreras-Moreira B, Castro-Mondragon JA, Rioualen C, Cantalapiedra CP, van Helden J. 2016. RSAT::Plants: Motif Discovery Within Clusters of Upstream Sequences in Plant Genomes. In: Hehl R, ed. Plant Synthetic Promoters: Methods and Protocols. New York, NY: Springer New York, 279–295.

Dai F, Wang X, Zhang XQ, Chen Z, Nevo E, Jin G, Wu D, Li C, Zhang G. 2018. Assembly and analysis of a *qingke* reference genome demonstrate its close genetic relation to modern cultivated barley. Plant Biotechnology Journal **16**, 760–770.

Deng W, Casao MC, Wang P, Sato K, Hayes PM, Finnegan EJ, Trevaskis B. 2015. Direct links between the vernalization response and other key traits of cereal crops. Nature Communications **6**, 5882.

Digel B, Pankin A, von Korff M. 2015. Global transcriptome profiling of developing leaf and shoot apices reveals distinct genetic and environmental control of floral transition and inflorescence development in barley. The Plant Cell **27**, 2318–2334.

Digel B, Tavakol E, Verderio G, Tondelli A, Xu X, Cattivelli L, Rossini L, von Korff M. 2016. Photoperiod-H1 (Ppd-H1) Controls Leaf Size. Plant Physiology **172**, 405–415.

Ejaz M, von Korff M. 2017. The Genetic Control of Reproductive Development Under High Ambient Temperature. Plant Physiology **173**, 294–306.

Franklin KA. 2009. Light and temperature signal crosstalk in plant development. Current Opinion in Plant Biology **12**, 63–68.

Franklin KA, Toledo-Ortiz G, Pyott DE, Halliday KJ. 2014. Interaction of light and temperature signalling. Journal of Experimental Botany **65**, 2859–2871.

Franklin KA, Whitelam GC. 2007. Light-quality regulation of freezing tolerance in *Arabidopsis thaliana*. Nature Genetics **39**, 1410.

Greenup AG, Sasani S, Oliver SN, Talbot MJ, Dennis ES, Hemming MN, Trevaskis B. 2010. *ODDSOC2* is a MADS Box Floral Repressor that Is Down-Regulated by Vernalization in Temperate Cereals. Plant Physiology **153**, 1062–1073.

Haas BJ, Papanicolaou A, Yassour M, *et al.* 2013. *De novo* transcript sequence reconstruction from RNA-Seq: reference generation and analysis with Trinity. Nature protocols **8**, 1494–1512.

Holmes MG, Smith H. 1977. The function of phytochrome in the natural environment - II. The influence of vegetation canopies on the spectral energy distribution of natural daylight. Photochemistry and Photobiology **25**, 539–545.

Jin J, Tian F, Yang DC, Meng YQ, Kong L, Luo J, Gao G. 2017. PlantTFDB 4.0: Toward a central hub for transcription factors and regulatory interactions in plants. Nucleic Acids Research **45**, D1040–D1045.

Kane NA, Danyluk J, Tardif G, Ouellet F, Laliberté J-F, Limin AE, Fowler DB, Sarhan F. 2005. *TaVRT-2*, a Member Of The *StMADS-11* Clade of Flowering Repressors, Is Regulated by Vernalization and Photoperiod in Wheat. Plant Physiology **138**, 2354–2363.

Kassambara A, Mundt F. 2017. factoextra: Extract and Visualize the Results of Multivariate Data Analyses. R package, version 1.0.5. http://cran.r-project.org/package=factoextra.

Kiseleva AA, Potokina EK, Salina EA. 2017. Features of *Ppd-B1* expression regulation and their impact on the flowering time of wheat near-isogenic lines. BMC Plant Biology **17**, 172.

Kuno N, Moller SG, Shinomura T, Xu X, Chua N-H, Furuya M. 2003. The novel MYB protein EARLY-PHYTOCHROME-RESPONSIVE1 is a component of a slave circadian oscillator in Arabidopsis. The Plant Cell **15**, 2476–2488.

Leivar P, Monte E. 2014. PIFs: Systems Integrators in Plant Development. The Plant Cell **26**, 56–78.

Lesniewska E, Adrian M, Klinguer A, Pugin A. 2004. Cell wall modification in grapevine cells in response to UV stress investigated by atomic force microscopy.

Ultramicroscopy **100**, 171–178.

Más P, Devlin PF, Panda S, Kay SA. 2000. Functional interaction of phytochrome B and cryptochrome 2. Nature **408**, 207–211.

Mascher M, Gundlach H, Himmelbach A, *et al.* 2017. A chromosome conformation capture ordered sequence of the barley genome. Nature **544**, 427–433.

Merotto Jr. A, Fischer A, Vidal R. 2009. Perspectives for using light quality as an advanced ecophysiological weed management tool. Planta Daninha **27**, 407–419.

Monostori I, Heilmann M, Kocsy G, *et al.* 2018. LED Lighting – Modification of Growth, Metabolism, Yield and Flour Composition in Wheat by Spectral Quality and Intensity. Frontiers in Plant Science **9**, 605.

Nishida H, Ishihara D, Ishii M, *et al.* 2013. *Phytochrome C* is a key factor controlling long-day flowering in barley. Plant physiology **163**, 804–814.

Novák A, Boldizsár Á, Ádám É, Kozma-Bognár L, Majláth I, Båga M, Tóth B, Chibbar R, Galiba G. 2016. Light-quality and temperature-dependent *CBF14* gene expression modulates freezing tolerance in cereals. Journal of Experimental Botany **67**, 1285–1295.

Oakenfull RJ, Davis SJ. 2017. Shining a light on the *Arabidopsis* circadian clock. Plant, Cell & Environment **40**, 2571–2585.

Pankin A, Campoli C, Dong X, *et al.* 2014. Mapping-by-sequencing identifies *HvPHYTOCHROME C* as a candidate gene for the *early maturity 5* locus modulating the circadian clock and photoperiodic flowering in barley. Genetics **198**, 383–396.

Pearce S, Kippes N, Chen A, Debernardi JM, Dubcovsky J. 2016. RNA-seq studies using wheat *PHYTOCHROME B* and *PHYTOCHROME C* mutants reveal shared and specific functions in the regulation of flowering and shade-avoidance pathways. BMC Plant Biology **16**, 141.

Pedmale UV, Huang SC, Zander M, *et al.* 2016. Cryptochromes interact directly with PIFs to control plant growth in limiting blue light. Cell **164**, 233–245.

Pimentel H, Bray NL, Puente S, Melsted P, Pachter L. 2017. Differential analysis of RNA-seq incorporating quantification uncertainty. Nature Methods **14**, 687.

Prade VM, Gundlach H, Twardziok S, *et al.* 2018. The pseudogenes of barley. The Plant Journal **93**, 502–514.

R Core Team. 2017. R: A langauge and environment for statistical computing. https://www.r-project.org.

Rockwell NC, Su Y-S, Lagarias JC. 2006. Phytochrome structure and signaling mechanisms. Annual Review of Plant Biology **57**, 837–858.

Rubio MC, Calvo-Begueria L, Diaz-Mendoza M, *et al.* 2019. Phytoglobins in the nuclei, cytoplasm and chloroplasts modulate nitric oxide signaling and interact with abscisic acid. The Plant journal. Doi: 10.1111/tpj.14422.

Sato K, Tanaka T, Shigenobu S, Motoi Y, Wu J, Itoh T. 2016. Improvement of barley genome annotations by deciphering the Haruna Nijo genome. DNA Research **23**, 21–28.

Schmitz J, Franzen R, Ngyuen TH, Garcia-Maroto F, Pozzi C, Salamini F, Rohde W. 2000. Cloning, mapping and expression analysis of barley MADS-box genes. Plant Molecular Biology **42**, 899–913.

Sebastian A, Contreras-Moreira B. 2014. footprintDB: a database of transcription factors with annotated cis elements and binding interfaces. Bioinformatics **30**, 258–265.

Skinner JS, von Zitzewitz J, Szucs P, Marquez-Cedillo L, Filichkin T, Amundsen K, Stockinger EJ, Thomashow MF, Chen THH, Hayes PM. 2005. Structural, functional, and phylogenetic characterization of a large CBF gene family in barley. Plant molecular biology **59**, 533–551.

Smith H. 1982. Light quality, photoperiod, and plant strategy. Annual Review of Plant Physiology **33**, 481–518.

Stockinger EJ, Skinner JS, Gardner KG, Francia E, Pecchioni N. 2007. Expression levels of barley Cbf genes at the Frost resistance-H2 locus are dependent upon alleles at Fr-H1 and Fr-H2. The Plant journal **51**, 308–321.

Szucs P, Skinner JS, Karsai I, Cuesta-Marcos A, Haggard KG, Corey AE, Chen THH, Hayes PM. 2007. Validation of the *VRN-H2/VRN-H1* epistatic model in barley reveals that intron length variation in *VRN-H1* may account for a continuum of vernalization sensitivity. Molecular Genetics and Genomics **277**, 249–261.

Tottman DR, Makepeace RJ, Broad H. 1979. An explanation of the decimal code for the growth stages of cereals, with illustrations. Annals of Applied Biology **93**, 221–234.

Trevaskis B, Hemming MN, Dennis ES, Peacock WJ. 2007. The molecular basis of vernalization-induced flowering in cereals. Trends in Plant Science **12**, 352–357.

Turner A, Beales J, Faure S, Dunford RP, Laurie DA. 2005. The Pseudo-Response Regulator *Ppd-H1* Provides Adaptation to Photoperiod in Barley. Science **310**, 1031–1034.

Ugarte CC, Trupkin SA, Ghiglione H, Slafer G, Casal JJ. 2010. Low red/far-red ratios delay spike and stem growth in wheat. Journal of experimental botany **61**, 3151–3162.

Waddington SR, Cartwright PM, Wall PC. 1983. A quantitative Scale of Spike Initial and Pistil Development in Barley and Wheat. Annals of Botany **51**, 119–130.

Wei T, Simko V. 2017. R package 'corrplot': Visualization of a Correlation Matrix. Version 0.84. https://github.com/taiyum/corrplot.

Woods DP, Ream TS, Minevich G, Hobert O, Amasino RM. 2014. PHYTOCHROME C is an essential light receptor for photoperiodic flowering in the temperate grass, *Brachypodium distachyon*. Genetics **198**, 397–408.

Yan L, Fu D, Li C, Blechl A, Tranquilli G, Bonafede M, Sanchez A, Valarik M, Yasuda S, Dubcovsky J. 2006. The wheat and barley vernalization gene *VRN3* is an orthologue of *FT*. Proceedings of the National Academy of Sciences of the United States of America **103**, 19581–19586.

Zadoks JC, Chang TT, Konzak CF. 1974. A Decimal Code for the Growth Stages of Cereals. Weed Research **14**, 415–421.

5.7. Supplementary material

Table S 5.1. List of the barley genotypes examined and allelic variants for the major genes of flowering time.

Variety name	Origin	Rows	Growth habit	HvVRN1[a]	HvVRN2[b]	HvFT1[c]	PPD-H1[d]	HvFT3[e]
Price	USA	6	Winter	vrn1	VRN2	TC	PPD1	PPD2
WA1614-95	USA	6	Facultative	vrn1	vrn2	AG	PPD1	ppd2
Esterel	France	6	Winter	vrn1	VRN2	TC	PPD1	ppd2

[a] Alleles based on the size of intron 1 (Szucs *et al.*, 2007; Hemming *et al.*, 2009)

[b] Presence/absence of HvZCCT (Yan *et al.*, 2004)

[c] Alleles based on two SNPs in intron 1, as reported previously (Yan *et al.*, 2006).

[d] Alleles based on SNP22 (Turner *et al.*, 2005)

[e] Presence/absence of PPD-H2 (Faure *et al.*, 2007)

References

Faure S, Higgins J, Turner A, Laurie DA. 2007. The *FLOWERING LOCUS T*-like gene family in barley (*Hordeum vulgare*). Genetics **176**, 599–609.

Hemming MN, Fieg S, James Peacock W, Dennis ES, Trevaskis B. 2009. Regions associated with repression of the barley (*Hordeum vulgare*) *VERNALIZATION1* gene are not required for cold induction. Molecular Genetics and Genomics **282**, 107–117.

Szucs P, Skinner JS, Karsai I, Cuesta-Marcos A, Haggard KG, Corey AE, Chen THH, Hayes PM. 2007. Validation of the *VRN-H2/VRN-H1* epistatic model in barley reveals that intron length variation in *VRN-H1* may account for a continuum of vernalization sensitivity. Molecular Genetics and Genomics **277**, 249–261.

Turner A, Beales J, Faure S, Dunford RP, Laurie DA. 2005. The Pseudo-Response Regulator *Ppd-H1* Provides Adaptation to Photoperiod in Barley. Science **310**, 1031–1034.

Yan L, Loukoianov A, Blechl A, Tranquilli G, Ramakrishna W, SanMiguel P, Bennetzen JL, Echenique V, Dubcovsky J. 2004. The wheat *VRN2* gene is a flowering repressor down-regulated by vernalization. Science **303**, 1640–1644.

Yan L, Fu D, Li C, Blechl A, Tranquilli G, Bonafede M, Sanchez A, Valarik M, Yasuda S, Dubcovsky J. 2006. The wheat and barley vernalization gene *VRN3* is an orthologue of *FT*. Proceedings of the National Academy of Sciences of the United States of America **103**, 19581–19586.

Table S 5.2. List of DE genes in the intersection between pairs of varieties, besides those included in the triple intersection.

Target ID	Description	Gene	Citation	Price	WA1614-95	Esterel
Price ∩ Esterel						
HORVU5Hr1G077790.4	beta glucosidase 11			u	u	u
HORVU1Hr1G039820.1	Fatty acid hydroxylase superfamily			u	u	u
HORVU4Hr1G001420.14	GDSL esterase/lipase			u	-	u
HORVU2Hr1G005220.3	Chalcone synthase 2			u	u	u
HORVU3Hr1G108670.1	Transcription factor ORG2			d	-	d
HORVU6Hr1G001630.1	undescribed protein			d	-	d
HORVU4Hr1G078470.1	alcohol dehydrogenase 1			d	-	d
HORVU1Hr1G088270.4	IMP dehydrogenase/GMP reductase			d	-	d
HORVU3Hr1G005500.6	Transcription factor bHLH35			u	u	u
HORVU2Hr1G118100.2	Heavy metal transport/detoxification superfamily protein			u	-	d
HORVU3Hr1G030460.1	Mitochondrial substrate carrier family protein			u	-	u
HORVU2Hr1G001320.4	Protein NRT1/ PTR FAMILY 8.5			u	u	u
HORVU7Hr1G116160.1	Cytochrome P450 superfamily protein			d	-	d
HORVU3Hr1G092070.2	-			u	u	u
HORVU5Hr1G102530.2	Hfr-2-like protein			u	u	u
HORVU7Hr1G042480.1	aluminum-activated malate transporter 9			u	-	u
HORVU3Hr1G025920.2	Cytochrome P450 superfamily protein			u	-	u
HORVU5Hr1G063620.1	Early light-induced protein 1, chloroplastic			u	-	u
HORVU3Hr1G013390.1	Serine/threonine-protein kinase			u	-	d
HORVU3Hr1G021890.1	undescribed protein			d	-	d

Gene	Description			
HORVU4Hr1G078410.2	Homeobox-leucine zipper protein family	u	u	u
HORVU2Hr1G044650.1	receptor kinase 1	u	-	d
HORVU7Hr1G069580.1	unknown function	u	u	u
WA1614-95 ∩ Esterel				
HORVU3Hr1G081060.4	Methionine--tRNA ligase	d	d	d
HORVU5Hr1G034830.3	WRKY family transcription factor	-	u	d
HORVU5Hr1G073760.2	dihydroflavonol 4-reductase-like1	d	d	d
HORVU6Hr1G003270.10	UDP-Glycosyltransferase superfamily protein	-	d	d
HORVU2Hr1G036590.4	sugar transporter 9	-	u	d
HORVU3Hr1G093100.1	Bifunctional inhibitor/lipid-transfer protein/seed storage 2S albumin superfamily protein	-	u	d
HORVU7Hr1G108820.3	unknown function	-	u	d
HORVU3Hr1G096190.7	Protein kinase family protein	u	u	d
HORVU1Hr1G092440.3	P-loop containing nucleoside triphosphate hydrolases superfamily protein	-	d	u
HORVU3Hr1G108900.3	LORELEI-LIKE-GPI-ANCHORED PROTEIN 1	u	u	d
HORVU5Hr1G005290.1	Thaumatin-like protein	u	u	d
HORVU3Hr1G097950.2	Glutathione S-transferase family protein	-	u	d
HORVU1Hr1G074840.1	unknown function	-	u	d
HORVU5Hr1G117910.3	ferredoxin 3	-	u	d
HORVU3Hr1G078550.2	Basic-leucine zipper (bZIP) transcription factor family protein	-	d	d
HORVU5Hr1G042750.1	unknown function	-	u	d
HORVU4Hr1G031840.1	vacuolar iron transporter 1	u	u	u
HORVU5Hr1G060370.2	vacuolar iron transporter 1	u	u	u
HORVU5Hr1G016650.1	-	u	u	u
HORVU2Hr1G081540.1	unknown function	-	u	d
HORVU5Hr1G098640.1	receptor kinase 2	d	u	d

Gene ID	Description		Reference			
HORVU7Hr1G043030.10	HD1	HvCO1	Griffiths *et al.*, 2003	-	u	u
HORVU2Hr1G125230.1	Receptor-like protein kinase			d	u	d
HORVU7Hr1G074660.3	Transmembrane amino acid transporter family protein			-	u	d
HORVU5Hr1G014290.2	Auxin-responsive protein IAA31			u	u	u
HORVU4Hr1G070600.3	BEST Arabidopsis thaliana protein match is: RPM1 interacting protein 13 .			-	d	d
HORVU5Hr1G014060.1	calmodulin-like 11			-	u	d
HORVU2Hr1G075820.2	undescribed protein			-	u	d
HORVU5Hr1G109190.1	germin-like protein 4			-	u	d
HORVU6Hr1G021780.2	Disease resistance protein			-	u	d
HORVU6Hr1G076110.1	Auxin efflux carrier family protein	HvPIN1	Pankin *et al.*, 2018	-	u	u
HORVU2Hr1G044680.2	receptor kinase 1			-	u	d
HORVU1Hr1G009130.1	unknown function			-	u	d
HORVU5Hr1G078100.19	Disease resistance protein			-	u	d
HORVU1Hr1G019770.3	Protein kinase superfamily protein			-	u	d
HORVU4Hr1G010080.6	Growth-regulating factor 6			u	u	u
HORVU3Hr1G033740.2	WRKY family transcription factor			-	u	d
HORVU7Hr1G010740.1	Protein kinase family protein			-	u	d
HORVU6Hr1G093740.5	Receptor-like protein kinase			-	u	d
HORVU7Hr1G085120.2	Aldehyde dehydrogenase family 2 member C4			-	d	u
HORVU2Hr1G089020.1	Disease resistance protein			-	u	d
HORVU4Hr1G063980.6	Senescence/dehydration-associated protein-related			u	u	u
Price ∩ WA1614-95						
HORVU2Hr1G082500.5	undescribed protein			d	d	-
HORVU3Hr1G054120.2	XH/XS domain-containing protein			d	d	d
HORVU4Hr1G071000.1	Polyol transporter 5			d	d	-
HORVU2Hr1G080770.4	receptor-like kinase 902			u	u	-
HORVU7Hr1G030210.2	Jacalin-like lectin domain containing protein			u	u	u

HORVU4Hr1G086050.2	12-oxophytodienoate reductase 2	HvOPR1	Pankin *et al.*, 2018	d	d	d
HORVU3Hr1G062900.2	O-acyltransferase (WSD1-like) family protein			u	u	-
HORVU3Hr1G070620.18	Auxin-responsive protein IAA6			u	u	-
HORVU3Hr1G117590.2	23 kDa jasmonate-induced protein			u	u	u
HORVU3Hr1G091160.1	undescribed protein			u	u	-
HORVU6Hr1G090600.6	Glutathione S-transferase family protein			d	d	-
HORVU1Hr1G044770.1	Epoxide hydrolase 1			u	u	-
HORVU3Hr1G019150.1	Zinc finger protein 235			u	u	u
HORVU3Hr1G019180.2	Zinc finger protein 235			u	u	u
HORVU3Hr1G109010.17	receptor kinase 2			u	u	d
HORVU7Hr1G033520.1	receptor-like protein kinase 1			u	u	d
HORVU4Hr1G005690.1	undescribed protein			u	u	-
HORVU6Hr1G054910.7	Transcription factor bHLH128			u	u	-
HORVU0Hr1G020580.1	undescribed protein			u	u	d
HORVU3Hr1G022210.2	Lipoxygenase			u	u	-
HORVU4Hr1G052490.5	myb domain protein 112			u	u	-
HORVU6Hr1G000070.1	Rhodanese-like domain-containing protein 17			d	d	-
HORVU6Hr1G002330.8	MADS-box transcription factor TaAGL1	HvAGL14	Campoli *et al.*, 2013	u	u	u
HORVU1Hr1G070780.2	unknown function			d	d	-
HORVU3Hr1G117550.1	Jasmonate induced protein			u	u	-
HORVU7Hr1G076480.2	Non-lysosomal glucosylceramidase			d	d	-
HORVU3Hr1G117570.4	23 kDa jasmonate-induced protein			u	u	-
HORVU6Hr1G079700.5	nitrate reductase 1			u	u	-
HORVU2Hr1G016070.6	Disease resistance RPP13-like protein 4			d	d	-
HORVU2Hr1G116670.1	Cytochrome P450 superfamily protein			d	d	-
HORVU3Hr1G117630.1	Jasmonate induced protein			u	u	u
HORVU5Hr1G029580.1	undescribed protein			d	d	-

HORVU3Hr1G077220.8	Serine/threonine-protein kinase			u	u	-
HORVU1Hr1G063720.6	WD repeat-containing protein 86			d	d	-
HORVU2Hr1G019900.1	flowering promoting factor 1			d	d	-
HORVU5Hr1G084230.1	Aquaporin-like superfamily protein			d	d	-
HORVU0Hr1G030020.2	undescribed protein			d	d	-
HORVU1Hr1G015480.1	undescribed protein			u	u	-
HORVU2Hr1G043900.1	Xylanase inhibitor protein 1			u	u	-
HORVU2Hr1G113790.1	undescribed protein			u	u	-
HORVU3Hr1G017930.1	DCD (Development and Cell Death) domain protein			d	d	d
HORVU3Hr1G052490.1	5'-methylthioadenosine/S-adenosylhomocysteine nucleosidase			u	u	-
HORVU3Hr1G087720.1	RING/U-box superfamily protein			u	u	-
HORVU4Hr1G079230.1	Aquaporin-like superfamily protein			u	u	u
HORVU3Hr1G062920.1	Chromosome 3B, genomic scaffold, cultivar Chinese Spring			u	u	-
HORVU1Hr1G054190.1	unknown function			d	d	-
HORVU5Hr1G075310.1	Chromosome 3B, genomic scaffold, cultivar Chinese Spring			d	d	-
HORVU2Hr1G097940.2	homeobox-leucine zipper protein 4			d	d	-
HORVU4Hr1G062940.1	Calcium-binding EF-hand family protein			d	d	-
HORVU6Hr1G064740.1	Transmembrane amino acid transporter family protein			d	d	-
HORVU6Hr1G077300.1	MADS-box transcription factor 22	HvBM10	Schmitz *et al.*, 2000, Campoli *et al.*, 2013, Pankin *et al.*, 2018	u	u	u
HORVU7Hr1G111960.3	terpene synthase 10			d	d	-
HORVU4Hr1G059790.1	Phosphatidylinositol-4-phosphate 5-kinase 2			u	u	-
HORVU2Hr1G080580.11	unknown protein			d	d	-

HORVU2Hr1G082490.1	undescribed protein			d	d	-
HORVU3Hr1G014780.6	shikimate kinase like 1			d	d	-
HORVU6Hr1G051650.2	Oxygen-evolving enhancer protein 3-1, chloroplastic			d	d	-
HORVU5Hr1G080860.9	UDP-glucose 4-epimerase 3			d	d	d
HORVU2Hr1G103880.2	Kelch-like protein 17			u	u	-
HORVU3Hr1G030990.1	-			u	u	-
HORVU3Hr1G000350.4	Protein kinase superfamily protein			d	d	-
HORVU7Hr1G054190.14	Threonylcarbamoyl-AMP synthase			d	d	-
HORVU6Hr1G018520.4	Prolyl endopeptidase			d	d	-
HORVU7Hr1G122470.1	sulfotransferase 4A			u	u	-
HORVU3Hr1G076790.3	Protein ULTRAPETALA 1			d	d	-
HORVU4Hr1G090780.6	Disease resistance-responsive (dirigent-like protein) family protein			u	u	-
HORVU5Hr1G096260.2	UDP-Glycosyltransferase superfamily protein			d	d	-
HORVU6Hr1G000090.3	sulfurtransferase protein 16			d	d	-
HORVU7Hr1G003100.2	EYES ABSENT homolog			d	d	-
HORVU6Hr1G017010.1	Glyoxylate/hydroxypyruvate reductase B			d	d	-
HORVU2Hr1G034420.2	WRKY DNA-binding protein 3			u	u	u
HORVU2Hr1G078510.3	lipoxygenase 3			u	u	u
HORVU3Hr1G114900.1	11S seed storage protein			u	u	u
HORVU7Hr1G101590.4	Cytochrome P450 superfamily protein			u	u	-
HORVU5Hr1G001730.3	Leucine-rich receptor-like protein kinase family protein			u	u	u
HORVU6Hr1G016070.3	Sodium Bile acid symporter family			d	d	-
HORVU5Hr1G080300.1	Dehydration-responsive element-binding protein 1B	HvCBF4A	Hill *et al.*, 2018	u	u	-
HORVU1Hr1G074180.1	U-box domain-containing protein			u	u	-
HORVU2Hr1G003600.6	Disease resistance protein			u	u	-
HORVU4Hr1G021950.13	Signal recognition particle 54 kDa protein, chloroplastic			d	d	d

● ● ●

HORVU4Hr1G085100.1	dihydroflavonol 4-reductase-like1			d	d	d
HORVU7Hr1G051260.3	3-hydroxy-3-methylglutaryl-coenzyme A reductase 3			u	u	u
HORVU3Hr1G117580.1	Jasmonate induced protein			u	u	-
HORVU4Hr1G068680.7	B3 domain-containing protein			d	d	d
HORVU5Hr1G093850.2	Phototropic-responsive NPH3 family protein			u	u	u
HORVU6Hr1G012170.1	terpene synthase 14			d	d	-
HORVU6Hr1G068760.5	Inorganic pyrophosphatase	HvPPa4	von Korff *et al.*, 2009	d	d	-
HORVU3Hr1G095090.1	MADS-box transcription factor family protein			u	u	-
HORVU2Hr1G099820.2	Cold-responsive protein Wcor15-A			u	u	-
HORVU4Hr1G051400.3	thioredoxin F2			d	d	d
HORVU7Hr1G039810.1	WD-40 repeat family protein			u	u	-
HORVU6Hr1G094460.4	Mitochondrial intermediate peptidase			d	d	-
HORVU6Hr1G062190.1	HXXXD-type acyl-transferase family protein			u	u	u
HORVU3Hr1G003410.1	tryptophan synthase alpha chain			d	d	-
HORVU1Hr1G036700.1	undescribed protein			d	d	-
HORVU2Hr1G016750.17	serine/threonine protein kinase 1			d	d	-
HORVU2Hr1G124510.1	Vacuolar iron transporter homolog 5			u	u	u
HORVU1Hr1G053510.1	GRAS family transcription factor			u	u	u
HORVU4Hr1G009060.1	pfkB-like carbohydrate kinase family protein			d	d	-
HORVU1Hr1G083500.1	Gag-pol polyprotein			d	d	N/A
HORVU2Hr1G013170.1	2-oxoglutarate dehydrogenase, E1 component			d	d	d
HORVU0Hr1G038220.1	Early light-induced protein 1, chloroplastic			u	u	u
HORVU2Hr1G113850.1	undescribed protein			u	u	-

•••

Gene	Description	Name	Reference			
HORVU7Hr1G115260.1	UDP-Glycosyltransferase superfamily protein			u	u	u
HORVU2Hr1G068590.1	undescribed protein			u	u	-
HORVU3Hr1G023740.1	ankyrin repeat family protein			d	d	-
HORVU7Hr1G043040.4	Peroxidase superfamily protein	HvCO1	Griffiths *et al.*, 2003	u	u	-
HORVU3Hr1G095880.1	NAC domain protein,			u	u	-
HORVU7Hr1G024210.4	P-loop containing nucleoside triphosphate hydrolases superfamily protein			d	d	-
HORVU4Hr1G060200.1	RNA polymerase sigma-C factor			d	d	-
HORVU2Hr1G105240.1	purine permease 11			d	d	-
HORVU2Hr1G105340.1	purine permease 11			d	d	-
HORVU2Hr1G069610.4	unknown function			d	d	-
HORVU4Hr1G087250.1	HXXXD-type acyl-transferase family protein			u	u	-
HORVU5Hr1G059210.1	undescribed protein			d	d	-
HORVU3Hr1G070880.7	Histidine-containing phosphotransfer protein 4			u	u	-
HORVU6Hr1G031150.1	undescribed protein			d	d	d
HORVU5Hr1G093150.8	Homeobox-leucine zipper protein HOX32			u	u	u
HORVU7Hr1G081510.1	DnaJ/Hsp40 cysteine-rich domain superfamily protein			d	d	-
HORVU3Hr1G117610.1	23 kDa jasmonate-induced protein			u	u	-
HORVU5Hr1G105960.1	undescribed protein			u	u	-
HORVU3Hr1G045240.1	undescribed protein			u	u	-
HORVU5Hr1G061250.11	Baculoviral IAP repeat-containing protein 7-B			u	u	-
HORVU7Hr1G052920.1	undescribed protein			d	d	-
HORVU3Hr1G003110.2	Glycosyltransferase			u	u	-

Legend		
	u	Upregulated in fluorescent with q.value < 0.01
	d	Downregulated in Fluorescent with q.val < 0.01
Legend	#N/D	No transcript
	u; d	Up or down regulated with q value < 0.05 and >0.01
	-	Not significant

References

Campoli C, Pankin A, Drosse B, Casao CM, Davis SJ, Von Korff M. 2013. *HvLUX1* is a candidate gene underlying the early maturity 10 locus in barley: Phylogeny, diversity, and interactions with the circadian clock and photoperiodic pathways. New Phytologist **199**, 1045–1059.

Griffiths S, Dunford RP, Coupland G, Laurie DA. 2003. The Evolution of *CONSTANS*-Like Gene Families in Barley, Rice, and Arabidopsis. Plant Physiology **131**, 1855–1867.

Hill CB, Angessa TT, McFawn L-A, *et al.* 2018. Hybridisation-based target enrichment of phenology genes to dissect the genetic basis of yield and adaptation in barley. Plant Biotechnology Journal **17**, 932–944.

Pankin A, Altmüller J, Becker C, von Korff M. 2018. Targeted resequencing reveals genomic signatures of barley domestication. New Phytologist **218**, 1247–1259.

Schmitz J, Franzen R, Ngyuen TH, Garcia-Maroto F, Pozzi C, Salamini F, Rohde W. 2000. Cloning, mapping and expression analysis of barley MADS-box genes. Plant Molecular Biology **42**, 899–913.

Von Korff M, Radovic S, Choumane W, *et al.* 2009. Asymmetric allele-specific expression in relation to developmental variation and drought stress in barley hybrids. The Plant Journal **59**, 14–26.
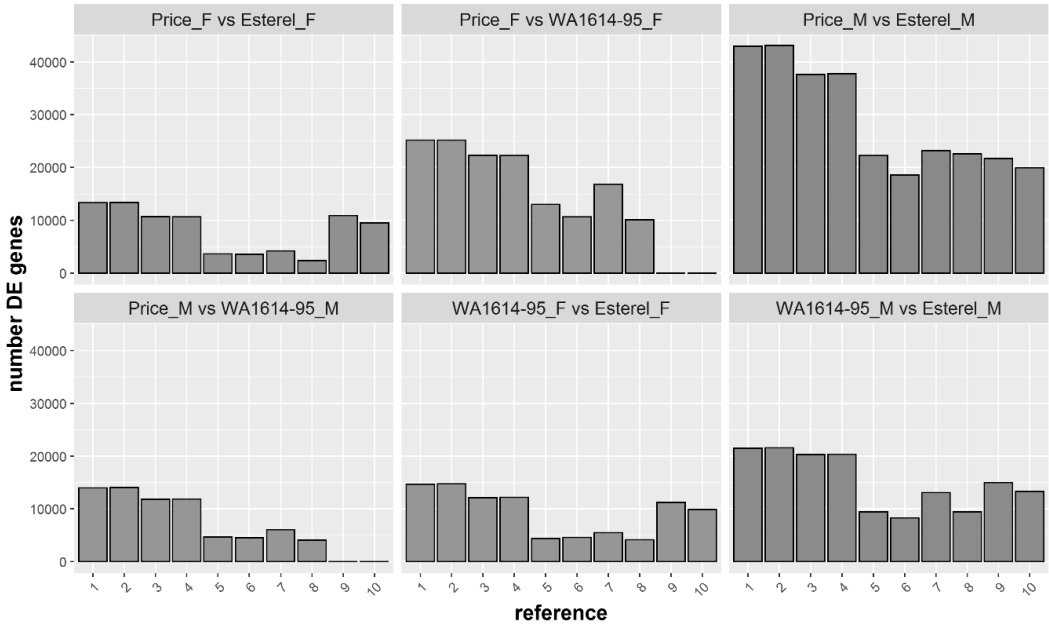
Figure S 5.1. Number of differentially expressed genes (DE) in each of the comparisons tested (q-value <0.05).

Each histogram represents a complete DE experiment, where each bar is the number of genes for each comparison.X-axis denotes the different references used: 1, reference-guided assembly; 2 nd 9, unigenes from reference-guided assembly; 3, *de novo* assembly; 4 and 10, unigenes from *de novo* assembly; 5, Zangqin320 (Tibetan) transcripts; 6, Morex transcripts; 7, Morex CDS sequences; 8, Haruna Nijo transcripts. Codes 1-8 represent number of DE genes using different references and obtained through the Kallisto/Sleuth procedure, and codes 9 and 10 through the RSEM//DESeq procedure.
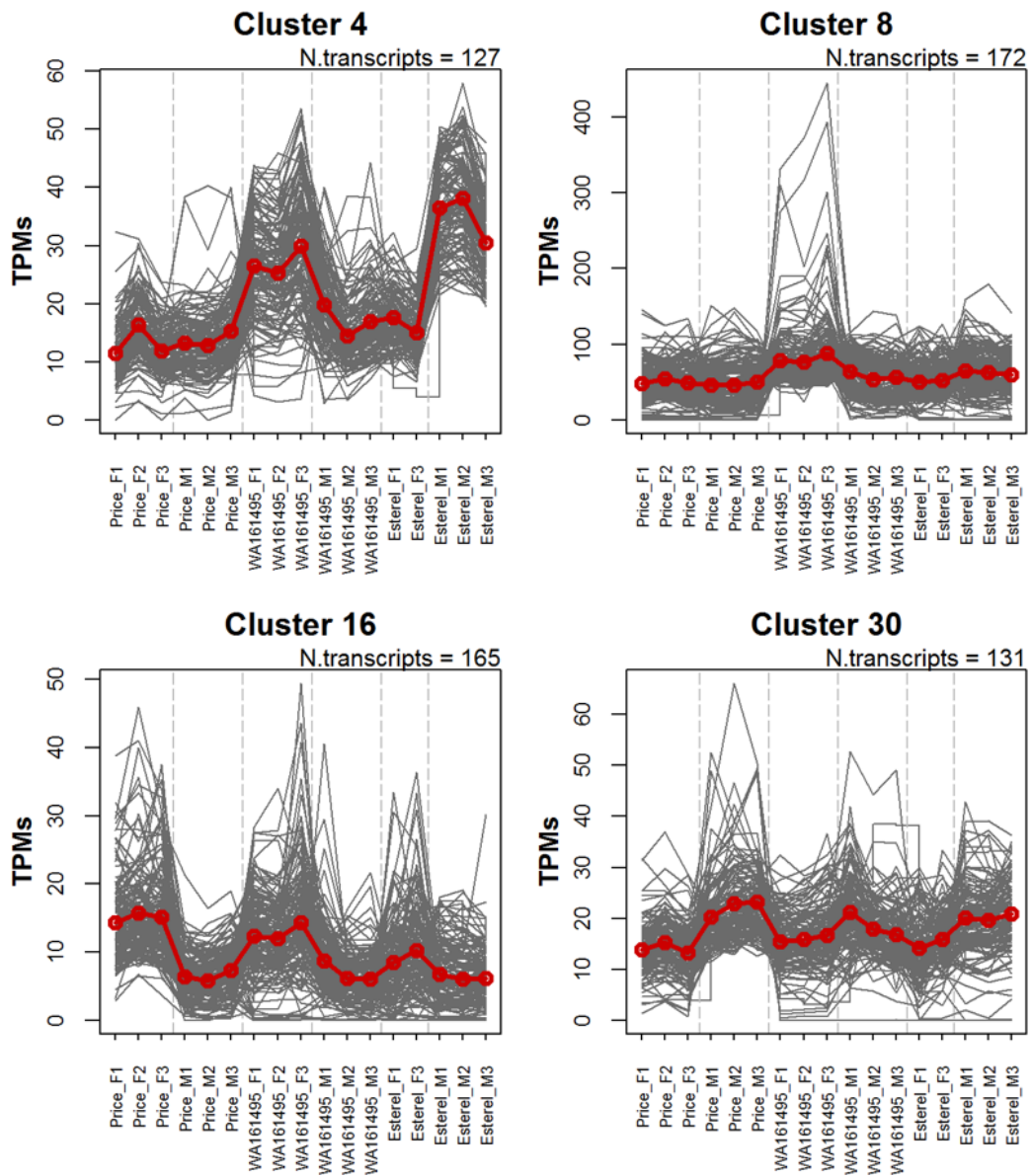
Figure S 5.2. Example of clusters of DE genes under fluorescent (F) and metal halide (M) conditions.
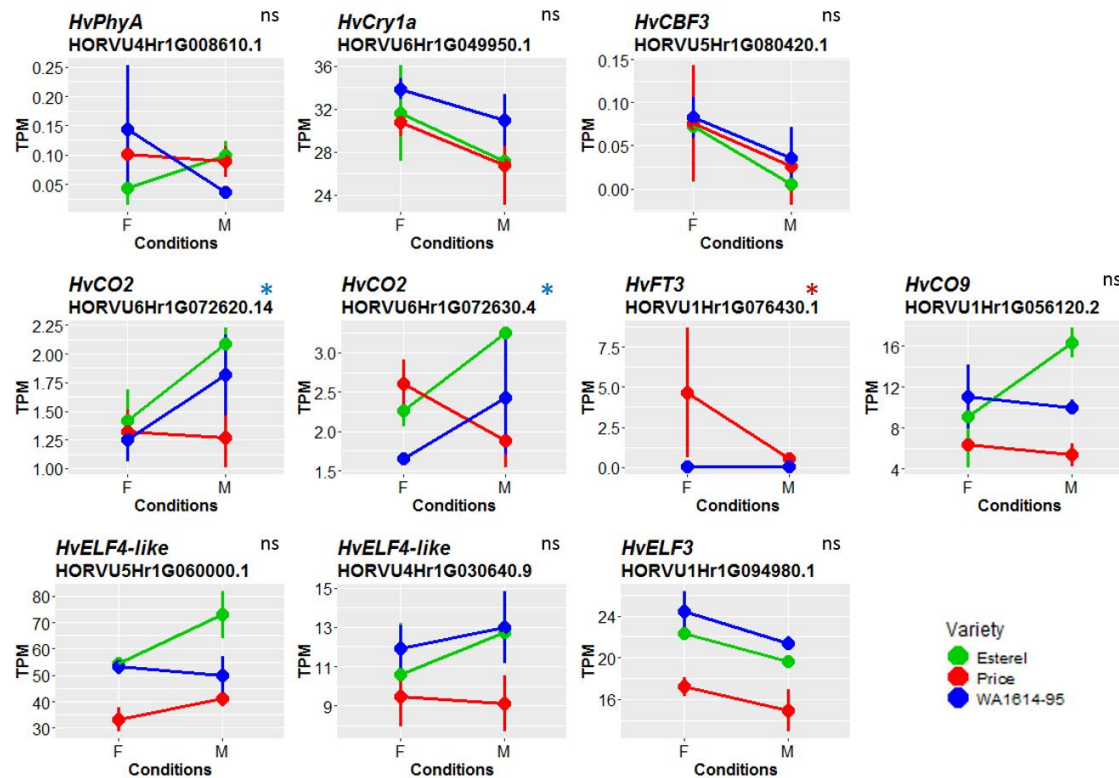
Figure S 5.3. Selection of flowering related DE genes (photoreceptors, circadian clock and development, q-value < 0.05). Genes are separated in two groups: upregulated (left) and downregulated (right) under fluorescent conditions. F, fluorescent conditions; M, metal halide conditions. *, differences between treatments are significant at q value < 0.05: two asterisks, significant at q<0.01; ns, not significant.

Chapter

6
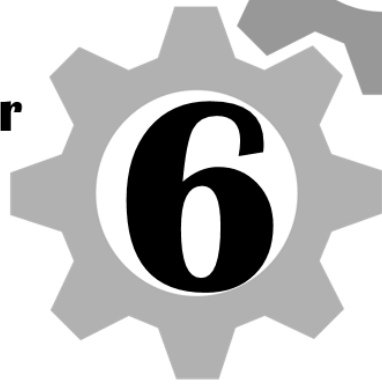
GENERAL DISCUSSION

Chapter 6. General Discussion

In crops, the time of transition from vegetative to reproductive phase is particularly relevant for yielding effectively. Plants perceive changes in the environment, getting information about the surrounding conditions, which are essential for their development. The main objective of this thesis was to get a deeper knowledge about the effect of **light and temperature** on the genetic control of flowering time in barley. The developmental responses to modifying light conditions were characterized, attending to two aspects of light: duration (**photoperiod**) and quality (**spectrum**). The responses observed might provide information about the adaptive strategies to changing conditions. In this sense, expression of the vernalization and photoperiod genes was studied in relation to the developmental responses seen under changing and/or sub-optimal environments. The effect of not satisfying a vernalization requirement in winter barleys was studied in Chapter 2. The next chapters were focused in the responses to shifting among day-lengths and light spectra, maintaining a constant temperature. The specific objectives have been discussed in each chapter. Hence, in this section, the aim is to provide an overview of the interactions found, putting the results obtained under a common perspective.

6.1. Light and temperature effects on genetic control of flowering

The mechanisms of monitoring environmental changes and adjusting growth to seasonal cues, such as cold or warm temperatures, are essential for determining whether plants are suitable for a particular region, avoid frost damage and improve yield (Xu and Chong, 2018). In winter cereals, the perception of cold is critical, to enable flowering timely. Two main genes control the vernalization response in winter barley: the promoter of flowering *HvVRN1,* and the repressor, *HvVRN2* (Trevaskis *et al.*, 2003; Yan *et al.*, 2004). Both interact with the floral pathway

integrator *HvFT1* (Yan *et al.*, 2006). Cold induces *HvVRN1*, which then represses *HvVRN2*, allowing the expression of the flowering integrator *HvFT1*, under long days. In absence of cold, long days promote *HvVRN2* expression, repressing *HvFT1*, and delaying flowering until plants have been vernalized (Trevaskis *et al.*, 2006; Hemming *et al.*, 2008). The studies carried out in this thesis combined a series of favourable and non-favourable conditions for exploring the relationship between temperature, day-length, and light quality, and also the role of the genes responsible of LD (*PPD-H1*) and SD (*HvFT3,* syn. *PPD-H2*) sensitivities (Laurie *et al.*, 1995). Several recurrent relations between the vernalization and photoperiod genes were observed in the different experiments of this thesis (i.e. *HvVRN1* − *HvVRN2*, *HvVRN1* − *HvFT3*, *HvVRN1* − *PPD-H1* and *HvVRN2* − *HvFT3*), and they are discussed in detail in this section.

The epistatic relation between *HvVRN1* and *HvVRN2*, at the core of the vernalization response, is well-known (Szucs *et al.*, 2007; Distelfeld *et al.*, 2009). The VRN1 protein directly regulates the expression of *HvVRN2*, and *HvFT1*, binding to the promoter of those genes (Deng *et al.*, 2015*a*). The balance between *HvVRN1* and *HvVRN2* expression might be essential in the control of flowering. Under non-optimal conditions, absence of cold treatment and long days, *HvVRN2* was induced, concurrently with the down-regulation of *HvVRN1* and *HvFT1*, and delayed development.

The results of Chapter 2, analysing the effect of vernalization, photoperiod and development, showed that *HvVRN2* was expressed across all the sampling dates, without vernalization. Expression was low until particular induction of *HvVRN2* expression was detected when day-length reached 12 h 30 min, approximately. This result, together with the circadian control of *HvVRN2*, observed in Chapter 3, already described in clock (*Hvelf3*) mutants (Faure *et al.*, 2012; Turner *et al.*, 2013), indicates that the mechanism that governs the induction of *HvVRN2* is complex,

involving endogenous and environmental signals through the interaction of other players. Specifically in cereals, it had been reported that day-length was relevant in the activation of the clock (Deng *et al.*, 2015*b*; Pearce *et al.*, 2017).

Flowering is associated with light- or age-dependent induction of *HvVRN1* and *HvFT1*, and in winter barleys, cold signals are required. In Chapter 2, growing the plants without vernalization, one of the genes that differed between the two cultivars studied was the "short photoperiod gene" *PPD-H2* (*HvFT3*). It was hypothesized that this gene could contribute to the different adaptation of the two cultivars studied, Hispanic and Barberousse, already evident in field studies (Igartua *et al.*, 1999; Mansour *et al.*, 2018). The relation of this gene with *HvVRN1*, *HvVRN2* and *HvFT1* was explored under different conditions and varied with age and light cues. In plants that had not satisfied their cold needs, it seemed that age or cold induction was needed for inducing *HvFT3*, having a positive effect on the acceleration of flowering, even in long days (Chapter 2). In plants with spring alleles in *HvVRN1* (Chapter 3) or vernalized winter types growing in less-inductive conditions (fluorescent bulbs in Chapter 4), *HvFT3* was expressed, possibly accelerating the initiation of spikelet primordia (Mulki *et al.*, 2018). Current breeding strategies must keep in mind the allelic variants of the vernalization and photoperiod genes to develop new varieties targeted to specific regions. Casao *et al.* (2011) described that *HvFT3* was predominant in winter cultivars from southern latitudes, whereas the proportion of cultivars with the recessive (null) allele was greater at higher latitudes. In Mediterranean conditions, the presence of *HvFT3* and strong vernalization requiring *HvVRN1* alleles has supposed an advantage in autumn sowings with temperate winters. The new results from our study, however, indicate that some vernalization clearly promotes the expression of *HvFT3*, linking the photoperiod and vernalization pathways in a previously unknown manner.

The positive correlation between *HvVRN1* and *PPD-H1* expression was relevant and not described previously. This finding contrasts with those reported for wheat *PPD-1* NILs, or a panel of varieties of bread wheat, in which no effect of *PPD-1* on *VRN1* was observed (Kitagawa *et al.*, 2012; Chen *et al.*, 2018). The relation between *PPD-H1* and *HvVRN1* occurred in experiments that involved day-length and light quality shifts. In spring barleys with the *PPD-H1* dominant allele, the expression of *HvVRN1* was constitutive, cycling in LD, and was associated with an acceleration of the development (Chapter 3). We proposed that *PPD-H1* might induce an effective rhythmicity of *HvVRN1*. Results of Liu *et al.* (2018) in rice, a short-day plant, indicate that overexpression of *OsPRR37* (the *PPD-1* rice-homologue), weakened the transcriptomic rhythms and altered the phases of rhythmic genes, delaying flowering time. Likewise, induced *VRN1* levels were detected in wheat lines mutated in the clock gene *LUX* (Nishiura *et al.*, 2018). This positive relation between clock and vernalization pathways agrees with the gene expression results obtained under different light quality treatments (Chapters 4 and 5).

PPD-H1 is the central gene controlling the response to photoperiod, being related to the expression of other actors in the photoperiod pathway. In barley, the expression of *PPD-H1* has been linked to the control of *HvVRN2* and *HvCO2* (Mulki and von Korff, 2016). These authors suggested the presence of a feedback loop between *HvVRN2* and *PPD-H1*, in which *PPD-H1* promotes *HvVRN2* before winter. In general, *PPD-H1* seems to be crucial in the integration of light and cold cues, whose regulation mechanism deserves further studies. This relation might be important in the design of ideotypes better adapted for future climatic conditions.

Variation of the activity of these genes is not completely understood, although it seems that the control of photoperiod and vernalization pathways can help in the adaptation process of cereals and grasses to different seasons, climates and

geographical regions. New insights about the role of other genes in these pathways will be important for breeding.

6.2.   New players in the flowering time control

In this work, we have used cultivated varieties, or isolines derived from varieties, with a known allelic combination of the major flowering time genes in barley, but with uncharacterized variation across their genome. On one hand, this fact made difficult to draw conclusions, as different genetic backgrounds will obscure the results, and they will not be as clear-cut as in studies based on induced mutants. On the other hand, it is a more close-to-nature approach that leads to obtaining meaningful results for a true agronomic scenario. We have found some lesser-known genes, i.e. related to the conditions experienced under fluorescent light. RNA-seq analysis revealed that there were several players relevant in light quality responses, which had been connected with cold and development in other studies.

In the generally accepted models for flowering time pathways, there are many uncertainties that have to be solved, including the identification of additional factors beyond the interaction *VRN1-VRN2* in vernalization control (Bouché *et al.*, 2017). Additional genes might be acting as regulators of *VRN2* (Chen and Dubcovsky, 2012; Sharma *et al.*, 2017), as other repressors of flowering have been proposed to interact with *VRN1*. Cuesta-Marcos *et al.* (2008) showed that facultative lines, with winter allele of *VRN1* and lacking the repressor *VRN2*, flowered later than spring types and proposed that other repressors could interact with *VRN1*. The MADS-box gene *HvVRT-2* (*VEGETATIVE TO REPRODUCTIVE TRANSITION-2*) was a possible candidate (Kane *et al.*, 2005). In this thesis, *HvVRT-2* was upregulated in the three genotypes, in the less-inductive light-quality conditions, with stronger effect in the facultative line. Similar results were observed for the MYB family transcription factor *HvRVE7*-like (*EARLY PHYTOCHROME RESPONSIVE*

1/REVEILLE7). Other MADS-box genes appeared to be important in the acceleration of flowering observed under metal halide conditions, such as the paralogues of *HvVRN1*, *HvBM3* (Barley MADS-box3), *HvBM8* and *HvBM10*. These results agree with other high throughput transcriptome studies in barley (Greenup *et al.*, 2011; Cuesta-Marcos *et al.*, 2015; Digel *et al.*, 2015; Ejaz and von Korff, 2017; Mulki *et al.*, 2018).

In Chapter 2, the comparison between two winter cultivars grown under non-inductive conditions showed that *HvVRN2* was probably not the only gene delaying flowering in LD. An interesting candidate to share this function is the orthologue of *FLOWERING LOCUS C*, *HvODDSOC2* (*HvOS2*), already identified as a player in the vernalization process in barley and other grasses (Greenup *et al.*, 2010; Ruelens *et al.*, 2013; Sharma *et al.*, 2017). In *Brachypodium distachion*, Sharma *et al.* (2017) proposed that high levels of *OS2* before a cold treatment would result in longer periods to complete the vernalization needs, clearly linking its expression levels to the scale of the vernalization response. In our work, *HvOS2* expression was also consistent with a role in delaying development in absence of cold, in SD, and in fluorescent light conditions (Chapters 3, 4 and 5). The relation between *HvVRN1* and *HvOS2* is antagonistic, as seen for *HvVRN2* (Deng *et al.*, 2015*a*). Sequencing of *HvOS2* showed natural variation in coding and non-coding regions (variants at intron 1 and VRN1-regulatory sites, Chapter 2), that might explain the different behaviours of flowering time through different regulation. Other authors have proposed novel ideas implicating epigenetic mechanisms for the adaptation of cereal varieties to different environments, based on the following observations: (1) the presence of single nucleotide polymorphisms in a regulatory site within the first intron of wheat *VRN-A1*, (Kippes *et al.*, 2018); (2) vernalization is associated with histone modifications at *VRN1* or *OS2* (*FLC*) regulating their active (inactive) states and manipulating winter-memory (Oliver *et al.*, 2009; Sharma *et al.*, 2017); and (3) the vernalization mechanism involves crosstalk between phosphorylation and *O-*

GlcNAcylation modification of key proteins, and epigenetic modifications of the key gene *VRN1* in wheat (Xu and Chong, 2018). Searching for variation in the regulatory region of *HvVRN1* (intron 1) and the polymorphisms here found in *HvOS2* might be of interest in the future development of winter barleys with a gradient of responses to cold.

Clock genes and signalling genes, such as phytochromes and cryptochromes have been essential stablishing the rhythmicity of the flowering time genes, and inducing rapid responses to light changes. Mutations of cereal clock and clock output genes, such as *ELF3* (Faure *et al.*, 2012; Zakhrabekova *et al.*, 2012), *LUX* (Mizuno *et al.*, 2012; Campoli *et al.*, 2013; Gawroński *et al.*, 2014), *PPD-1* (Turner *et al.*, 2005; Campoli *et al.*, 2012) or photoreceptors such as *PhyC* (Nishida *et al.*, 2013; Chen *et al.*, 2014; Pankin *et al.*, 2014), all influence *HvFT1* expression and alter flowering time. In our work (Chapter 3), changes in the expression patterns of clock genes occurred concomitantly with *PPD-H1*-dependent changes in *HvFT1* expression (Chapter 3), although this was not evident under different light quality conditions (Chapter 5). In this last case, the clock seemed to be mainly affected by changes in *HvPhyB* and *HvCry2*. Allelic variants of these photoreceptors are of interest as they might function as latitudinal drivers of adaptation, as already reported in genome wide association studies in Arabidopsis (Samis *et al.*, 2008; Ferrero-Serrano and Assmann, 2019).

6.3.   Molecular mechanisms involved in adaptation of barley to climate change

Future climate conditions will bring increasing temperatures, more frequent extreme weather events and, possibly, shifts in weeds, pests and disease pressures that will impact crop productivity (Jaggard *et al.*, 2010; Porter *et al.*, 2014). The specific impacts will depend on the region, although sign of deteriorating agroclimatic conditions seem to be widespread and will surely need to be tackled

with different approaches (Trnka *et al.*, 2011). Large changes in timing of flowering for cereals have been detected in Northern Europe in recent years, predicting an advancement of flowering and maturation of 1-3 weeks (Olesen *et al.*, 2012). Winter cropping (i.e., with autumn sowings) in this area could become more widespread than currently, benefiting from longer physiologically effective growing seasons and higher winter temperatures (Porter *et al.*, 2014). Crop modelling studies have determined that barley ideotypes, for future Boreal and Mediterranean climatic zones in Europe, should have appropriate vernalization and photoperiod responses finely tuned to the needs of each specific region (Tao *et al.*, 2017). These future cereal ideotypes may be different from the current cultivars, and new formats will have to be explored. One future avenue for plant breeding will be to use elite germplasm coming from regions that have experienced the foreseen conditions (Atlin *et al.*, 2017). For example, transferring cultivars adapted to Mediterranean conditions, which possess a strategy based on scape to drought, to more northern latitudes. To achieve that goal, the responses to photoperiod should be modified accordingly to avoid yield penalties (Dawson *et al.*, 2015). For this reason, comprehensive studies on the effect of photoperiod on major flowering genes are called for.

Photoperiod insensitivity has been associated with spring cultivars cultivated in Northern latitudes (Turner *et al.*, 2005; Jones *et al.*, 2008), which are sown after winter and do not accelerate flowering in LD. Here, we observed that a *ppd-H1* insensitive NIL built on a common genetic background, was associated with higher expression of *HvFT3*, *HvOS2* and *HvVRN2* in LD, compared to the *PPD-H1* NIL. Expression of some of these genes might delay development leading to flowering beyond what is agronomically viable, or could protect against late frosts. Normally, spring lines carry the non-functional *HvVRN2* allele, although less is known of the allelic variants for *HvOS2*. The selection of the variants will depend on the breeding target. What seems clear is that the effect of *HvFT3* was relevant in the less-

inductive conditions, especially in the acceleration and success of winter barley's flowering with less than optimum cold period, even when plants were sown later than agronomically viable.

The role of *PPD-H1* in adaptation might be consequence of the ability to trigger changes in the rhythmicity of the flowering time genes, and its effect on the clock genes. In this thesis, when clock genes were studied, most of them were not affected by the allelic variant at *PPD-H1*, but the response of *HvTOC1* to day-length cues was. Recent advances suggest that *PRR*s have very different and specific roles, as the stabilization of CO (Hayama *et al.*, 2017) and the coordination of environmental cues and plant growth through the control of the cell cycle rhythmicity, as *TOC1* in *Arabidopsis thaliana* (Fung-Uceda *et al.*, 2018). Hence, both might be responsible of the coordination of clock and development.

For understanding plant adaptation, it must be kept in mind that light spectrum and the entrainment signals of the clock vary with latitude, climate and seasonality. In *Arabidopsis*, variation across latitudes might be explained by a synchronization with the environment provided by the rhythmicity of the clock (Rees *et al.*, 2019), providing fitness advantage to the organisms. Crop productivity could be improved with increasing understanding of circadian rhythms, i.e. manipulating circadian clock in photoperiod response might increase the latitudinal range over which some crops can be grown (Hubbard and Dodd, 2016). Similarly, the different responses found between barley varieties in Chapter 4 highlight that some kind of adaptation could underly the diversity found in sensitivity to light quality. The biological meaning of this natural diversity could be related to the responsiveness to day-length in different latitudes. The onset of twilight, especially during the evening, is associated with a significant drop in the R:FR ratio from about 1.1 (during the day stays constant) to about 0.6–0.7 (Linkosalo and Lechowicz, 2006). Thus, it is possible that longer twilight periods of autumn, as occurs in northern latitudes,

serve as signal for the plant to be protected against frost (Franklin, 2009). It has been highlighted the role of light quality in the regulation of gene expression during cold acclimation in *Arabidopsis* (Franklin, 2009) and in cereals (Novák *et al.*, 2016). Thus, plants from different origins might have evolved differently to adapt to those twilight periods, which could be sensed as changes in spectrum composition. Phytochromes and cryptochromes are related to light quality responses, and also connect with the circadian clock, being also regulated by it (Fankhauser and Staiger, 2002). This suggests that a tight connection between both pathways would be relevant for fine-tuning the crop growth under specific conditions (Pocock, 2017). Although it is not evident at this moment, developmental-dependent responsiveness to light spectra might bear an agricultural and ecological significance that should be taken into account by breeders, particularly when moving materials between different latitudes and different agroecological zones.

The responses to the different light attributes complement the information that plants have of their surroundings. How phenology is connected with these responses is still unclear. It seems that, to be successful, the plants must manage complex interactions, involving signals from several pathways, that suppose a final balance between flowering promoters and repressors. In this thesis, the main aim has been to provide a wider perspective of how specific environmental factors affect the development and time of flowering thought the interaction with the vernalization and flowering time genes. A better knowledge of this specific responses will help in the development of better-suited varieties.

6.4.   References

Atlin GN, Cairns JE, Das B. 2017. Rapid breeding and varietal replacement are critical to adaptation of cropping systems in the developing world to climate change. Global Food Security **12**, 31–37.

Bouché F, Woods D, Amasino RM. 2017. Winter Memory throughout the Plant Kingdom: Different Paths to Flowering. Plant Physiology **173**, 27–35.

Campoli C, Pankin A, Drosse B, Casao CM, Davis SJ, Von Korff M. 2013. *HvLUX1* is a candidate gene underlying the *early maturity 10* locus in barley: Phylogeny, diversity, and interactions with the circadian clock and photoperiodic pathways. New Phytologist **199**, 1045–1059.

Campoli C, Shtaya M, Davis SJ, von Korff M. 2012. Expression conservation within the circadian clock of a monocot: natural variation at barley *Ppd-H1* affects circadian expression of flowering time genes, but not clock orthologs. BMC Plant Biology **12**, 97.

Casao MC, Karsai I, Igartua E, Gracia MP, Veisz O, Casas AM. 2011. Adaptation of barley to mild winters: A role for *PPDH2*. BMC Plant Biology **11**, 164.

Chen A, Dubcovsky J. 2012. Wheat TILLING Mutants Show That the Vernalization Gene *VRN1* Down-Regulates the Flowering Repressor *VRN2* in Leaves but Is Not Essential for Flowering. PLoS Genetics **8**, e1003134.

Chen A, Li C, Hu W, Lau MY, Lin H, Rockwell NC, Martin SS, Jernstedt JA, Lagarias JC, Dubcovsky J. 2014. PHYTOCHROME C plays a major role in the acceleration of wheat flowering under long-day photoperiod. Proceedings of the National Academy of Sciences of the United States of America **111**, 10037–10044.

Chen S, Wang J, Deng G, Chen L, Cheng X, Xu H, Zhan K. 2018. Interactive effects of multiple vernalization (*Vrn-1*)- and photoperiod (*Ppd-1*)-related genes on the growth habit of bread wheat and their association with heading and flowering time. BMC Plant Biology **18**, 374.

Cuesta-Marcos A, Igartua E, Ciudad FJ, *et al*. 2008. Heading date QTL in a spring × winter barley cross evaluated in Mediterranean environments. Molecular Breeding **21**, 455–471.

Cuesta-Marcos A, Muñoz-Amatrián M, Filichkin T, Karsai I, Trevaskis B, Yasuda S, Hayes P, Sato K. 2015. The Relationships between Development and Low Temperature Tolerance in Barley Near Isogenic Lines Differing for Flowering Behavior. Plant and Cell Physiology **56**, 2312–2324.

Dawson IK, Russell J, Powell W, Steffenson B, Thomas WTB, Waugh R. 2015. Barley: a translational model for adaptation to climate change. New Phytologist **206**, 913–931.

Deng W, Casao MC, Wang P, Sato K, Hayes PM, Finnegan EJ, Trevaskis B. 2015*a*. Direct links between the vernalization response and other key traits of cereal crops. Nature Communications **6**, 5882.

Deng W, Clausen J, Boden S, Oliver SN, Casao MC, Ford B, Anderssen RS, Trevaskis B. 2015*b*. Dawn and Dusk Set States of the Circadian Oscillator in Sprouting Barley (*Hordeum vulgare*) Seedlings. PloS ONE **10**, e0129781.

Digel B, Pankin A, von Korff M. 2015. Global transcriptome profiling of developing leaf and shoot apices reveals distinct genetic and environmental control of floral transition and inflorescence development in barley. The Plant Cell **27**, 2318–2334.

Distelfeld A, Li C, Dubcovsky J. 2009. Regulation of flowering in temperate cereals. Current Opinion in Plant Biology **12**, 178–184.

Ejaz M, von Korff M. 2017. The Genetic Control of Reproductive Development under High Ambient Temperature. Plant Physiology **173**, 294–306.

Fankhauser C, Staiger D. 2002. Photoreceptors in *Arabidopsis thaliana*: light perception, signal transduction and entrainment of the endogenous clock. Planta **216**, 1–16.

Faure S, Turner AS, Gruszka D, Christodoulou V, Davis SJ, von Korff M, Laurie DA. 2012. Mutation at the circadian clock gene *EARLY MATURITY 8* adapts domesticated barley (*Hordeum vulgare*) to short growing seasons. Proceedings of the National Academy of Sciences of the United States of America **109**, 8328–8333.

Ferrero-Serrano Á, Assmann SM. 2019. Phenotypic and genome-wide association with the local environment of Arabidopsis. Nature Ecology & Evolution **3**, 274–285.

Franklin KA. 2009. Light and temperature signal crosstalk in plant development. Current Opinion in Plant Biology **12**, 63–68.

Fung-Uceda J, Lee K, Seo PJ, Polyn S, De Veylder L, Mas P. 2018. The Circadian Clock Sets the Time of DNA Replication Licensing to Regulate Growth in Arabidopsis. Developmental Cell **45**, 101-113.

Gawroński P, Ariyadasa R, Himmelbach A, *et al*. 2014. A distorted circadian clock causes early flowering and temperature-dependent variation in spike development in the Eps-3Am mutant of einkorn wheat. Genetics **196**, 1253–1261.

Greenup AG, Sasani S, Oliver SN, Talbot MJ, Dennis ES, Hemming MN, Trevaskis B. 2010. *ODDSOC2* is a MADS Box Floral Repressor that Is Down-Regulated by Vernalization in Temperate Cereals. Plant Physiology **153**, 1062–1073.

Greenup AG, Sasani S, Oliver SN, Walford SA, Millar AA, Trevaskis B. 2011. Transcriptome analysis of the vernalization response in barley (*Hordeum vulgare*) seedlings. PLoS ONE **6**, e17900.

Hayama R, Sarid-Krebs L, Richter R, Fernández V, Jang S, Coupland G. 2017. PSEUDO RESPONSE REGULATORs stabilize CONSTANS protein to promote flowering in response to day length. The EMBO Journal **36**, 904–918.

Hemming MN, Peacock WJ, Dennis ES, Trevaskis B. 2008. Low-temperature and day-length cues are integrated to regulate FLOWERING LOCUS T in barley. Plant Physiology **147**, 355–366.

Hubbard K, Dodd A. 2016. Rhythms of Life: The Plant Circadian Clock. The Plant Cell

● ● ●

28, 1–10.

Igartua E, Casas AM, Ciudad F, Montoya JL, Romagosa I. 1999. RFLP markers associated with major genes controlling heading date evaluated in a barley germ plasm pool. Heredity **83**, 551–559.

Jaggard KW, Qi A, Ober S. 2010. Possible changes to arable crop yields by 2050. Philosophical Transactions of the Royal Society B: Biological Sciences **365**, 2835–2851.

Jones H, Leigh FJ, Mackay I, Bower MA, Smith LMJ, Charles MP, Jones G, Jones MK, Brown TA, Powell W. 2008. Population-based resequencing reveals that the flowering time adaptation of cultivated barley originated east of the fertile crescent. Molecular Biology and Evolution **25**, 2211–2219.

Kane NA, Danyluk J, Tardif G, Ouellet F, Laliberté J-F, Limin AE, Fowler DB, Sarhan F. 2005. *TaVRT-2*, a Member of the *StMADS-11* Clade of Flowering Repressors, Is Regulated by Vernalization and Photoperiod in Wheat. Plant Physiology **138**, 2354–2363.

Kippes N, Guedira M, Lin L, Alvarez MA, Brown GL, Dubcovsky J. 2018. Single nucleotide polymorphisms in a regulatory site of *VRN-A1* first intron are associated with differences in vernalization requirement in winter wheat. Molecular Genetics and Genomics **293**, 1231–1243.

Kitagawa S, Shimada S, Murai K. 2012. Effect of *Ppd-1* on the expression of flowering-time genes in vegetative and reproductive growth stages of wheat. Genes & Genetic Systems **87**, 161–168.

Laurie DA, Pratchett N, Snape JW, Bezant JH. 1995. RFLP mapping of five major genes and eight quantitative trait loci controlling flowering time in a winter × spring barley (*Hordeum vulgare* L.) cross. Genome **38**, 575–585.

Linkosalo T, Lechowicz MJ. 2006. Twilight far-red treatment advances leaf bud burst of silver birch (*Betula pendula*). Tree Physiology **26**, 1249–56.

Liu C, Qu X, Zhou Y, Song G, Abiri N, Xiao Y, Liang F, Jiang D, Hu Z, Yang D. 2018. *OsPRR37* confers an expanded regulation of the diurnal rhythms of the transcriptome and photoperiodic flowering pathways in rice. Plant Cell and Environment **41**, 630–645.

Mansour E, Moustafa ESA, El-Naggar NZA, Abdelsalam A, Igartua E. 2018. Grain yield stability of high-yielding barley genotypes under Egyptian conditions for enhancing resilience to climate change. Crop and Pasture Science **69**, 681–690.

Mizuno N, Nitta M, Sato K, Nasuda S. 2012. A wheat homologue of *PHYTOCLOCK 1* is a candidate gene conferring the early heading phenotype to einkorn wheat. Genes & Genetic Systems **87**, 357–367.

Mulki MA, Bi X, von Korff M. 2018. FLOWERING LOCUS T3 Controls Spikelet Initiation But Not Floral Development. Plant Physiology **178**, 1170–1186.

Mulki MA, von Korff M. 2016. *CONSTANS* Controls Floral Repression by Up-Regulating *VERNALIZATION2* (*VRN-H2*) in Barley. Plant Physiology **170**, 325–337.

Nishida H, Ishihara D, Ishii M, *et al.* 2013. *Phytochrome C* is a key factor controlling long-day flowering in barley. Plant Physiology **163**, 804–814.

Nishiura A, Kitagawa S, Matsumura M, Kazama Y, Abe T, Mizuno N, Nasuda S, Murai K. 2018. An early-flowering einkorn wheat mutant with deletions of *PHYTOCLOCK 1/LUX ARRHYTHMO* and *VERNALIZATION 2* exhibits a high level of *VERNALIZATION 1* expression induced by vernalization. Journal of Plant Physiology **222**, 28–38.

Novák A, Boldizsár Á, Ádám É, Kozma-Bognár L, Majláth I, Båga M, Tóth B, Chibbar R, Galiba G. 2016. Light-quality and temperature-dependent *CBF14* gene expression modulates freezing tolerance in cereals. Journal of Experimental Botany **67**, 1285–1295.

Olesen JE, Børgesen CD, Elsgaard L, *et al.* 2012. Changes in time of sowing, flowering and maturity of cereals in Europe under climate change. Food Additives & Contaminants: Part A **29**, 1527–1542.

Oliver SN, Finnegan EJ, Dennis ES, Peacock WJ, Trevaskis B. 2009. Vernalization-induced flowering in cereals is associated with changes in histone methylation at the *VERNALIZATION1* gene. Proceedings of the National Academy of Sciences of the United States of America **106**, 8386–8391.

Pankin A, Campoli C, Dong X, *et al.* 2014. Mapping-by-sequencing identifies *HvPHYTOCHROME C* as a candidate gene for the *early maturity 5* locus modulating the circadian clock and photoperiodic flowering in barley. Genetics **198**, 383–396.

Pearce S, Shaw LM, Lin H, Cotter JD, Li C, Dubcovsky J. 2017. Night-Break Experiments Shed Light on the Photoperiod1-Mediated Flowering. Plant Physiology **174**, 1139–1150.

Pocock T. 2017. Influence of Light-Emitting Diodes (LEDs) on Light Sensing and Signaling Networks in Plants. In: Dutta Gupta S, ed. Light Emitting Diodes for Agriculture: Smart Lighting. Singapore: Springer Singapore, 37–58.

Porter JR, Xie AJ, Challinor K, Howden SM, Iqbal MM, Lobell DB, Travasso MI. 2014. Food Security and Food Production Systems. In: Field CB, Barros VR, Dokken DJ, et al., eds. Climate Change 2014: Impacts, Adaptation, and Vulnerability. Part A: Global and Sectoral Aspects. Contribution of Working Group II to the Fifth Assessment Report of the Intergovernmental Panel on Climate Change. Cambridge, United Kingdom and New York, NY, USA: Cambridge University Press, 485–533.

Rees H, Joynson R, Brown JKM, Hall A. 2019. Circadian diversity in Swedish *Arabidopsis* accessions is associated with naturally occurring genetic variation in *COR28*. bioRxiv 665455.

Ruelens P, de Maagd RA, Proost S, Theißen G, Geuten K, Kaufmann K. 2013. FLOWERING LOCUS C in monocots and the tandem origin of angiosperm-specific MADS-box genes. Nature Communications **4**, 2280.

Samis KE, Heath KD, Stinchcombe JR. 2008. Discordant longitudinal clines in

flowering time and *phytochrome C* in *Arabidopsis thaliana*. Evolution **62**, 2971–2983.

Sharma N, Ruelens P, Dhauw M, Maggen T, Dochy N, Torfs S, Kaufmann K, Rohde A, Geuten K. 2017. A Flowering Locus C Homolog Is a Vernalization-Regulated Repressor in *Brachypodium* and Is Cold-Regulated in Wheat. Plant Physiology **173**, 1301–1315.

Szucs P, Skinner JS, Karsai I, Cuesta-Marcos A, Haggard KG, Corey AE, Chen THH, Hayes PM. 2007. Validation of the *VRN-H2/VRN-H1* epistatic model in barley reveals that intron length variation in *VRN-H1* may account for a continuum of vernalization sensitivity. Molecular Genetics and Genomics **277**, 249–261.

Tao F, Rötter RP, Palosuo T, *et al.* 2017. Designing future barley ideotypes using a crop model ensemble. European Journal of Agronomy **82**, 144–162.

Trevaskis B, Bagnall DJ, Ellis MH, Peacock WJ, Dennis ES. 2003. MADS box genes control vernalization-induced flowering in cereals. Proceedings of the National Academy of Sciences of the United States of America **100**, 13099–13104.

Trevaskis B, Hemming MN, Peacock WJ, Dennis ES. 2006. *HvVRN2* responds to daylength, whereas *HvVRN1* is regulated by vernalization and developmental status. Plant Physiology **140**, 1397–1405.

Trnka M, Olesen JE, Kersebaum KC, *et al.* 2011. Agroclimatic conditions in Europe under climate change. Global Change Biology **17**, 2298–2318.

Turner A, Beales J, Faure S, Dunford RP, Laurie DA. 2005. The Pseudo-Response Regulator *Ppd-H1* Provides Adaptation to Photoperiod in Barley. Science **310**, 1031–1034.

Turner AS, Faure S, Zhang Y, Laurie DA. 2013. The effect of day-neutral mutations in barley and wheat on the interaction between photoperiod and vernalization. Theoretical and Applied Genetics **126**, 2267–2277.

Xu S, Chong K. 2018. Remembering winter through vernalisation. Nature Plants **4**, 997–1009.

Yan L, Fu D, Li C, Blechl A, Tranquilli G, Bonafede M, Sanchez A, Valarik M, Yasuda S, Dubcovsky J. 2006. The wheat and barley vernalization gene *VRN3* is an orthologue of *FT*. Proceedings of the National Academy of Sciences of the United States of America **103**, 19581–19586.

Yan L, Loukoianov A, Blechl A, Tranquilli G, Ramakrishna W, SanMiguel P, Bennetzen JL, Echenique V, Dubcovsky J. 2004. The wheat *VRN2* gene is a flowering repressor down-regulated by vernalization. Science **303**, 1640–1644.

Zakhrabekova S, Gough SP, Braumann I, *et al.* 2012. Induced mutations in circadian clock regulator Mat-a^m facilitated short-season adaptation and range extension in cultivated barley. Proceedings of the National Academy of Sciences of the United States of America **109**, 4326–4331.

Chapter 7

CONCLUSSION

Chapter 7. Conclusions

1) Under increasing natural photoperiods and lack of vernalization, *HvVRN2* is always induced, even at sowings with short photoperiods, which was not expected. Its expression increases sharply when day-length reaches 12 h 30 min, approximately.

2) In winter barley lines, the presence of the *HvFT3* gene is relevant in the reduction of time to flowering without vernalization. Its induction under short days (12h) is promoted by a combination of a cold vernalizing period and plant age. Also, *HvOS2* seems to play a flowering repressor role in barley. It is probably part of the vernalization process, and the sequence polymorphisms found in this study could justify differential vernalization sensitivities within winter barleys. Further, its expression interacts with the photoperiod pathway in spring barleys. These hypotheses need confirmation and open new avenues for further research on this gene in barley breeding.

3) When plants are subjected to photoperiod transitions at dusk, expression of the clock genes changes rapidly. Allelic variation in *PPD-H1* did not affect the oscillation of most of the clock genes but the response of the member of the core oscillator *HvTOC1* was dependent on the *PPD-H1* allele, being reflected in other clock output genes.

4) Barley development was under the influence of light spectra, being time to first node appearance and the period from that moment until the onset of stem elongation, the most affected phases. There exists variability in the sensitivity to light quality among cultivars, as manifested by changes in the expression of key flowering time genes, and other transcription factors, with underlying differences in the induction of phytochromes and cryptochromes.

5) The interaction between *PPD-H1* and *HvVRN1* remains unexplored. The correlation between the expression of these genes in shift experiments involving different day-lengths and spectral conditions indicates a relationship between their pathways, which could be relevant for adaptation of barley to future conditions.